LEABHARLANN CHOLÁISTE NA TRÍONÓIDE, BAILE ÁTHA CLIATH | TRINITY COLLEGE LIBRARY DUBLIN
Ollscoil Átha Cliath | The University of Dublin

Terms and Conditions of Use of Digitised Theses from Trinity College Library Dublin

Copyright statement

All material supplied by Trinity College Library is protected by copyright (under the Copyright and Related Rights Act, 2000 as amended) and other relevant Intellectual Property Rights. By accessing and using a Digitised Thesis from Trinity College Library you acknowledge that all Intellectual Property Rights in any Works supplied are the sole and exclusive property of the copyright and/or other IPR holder. Specific copyright holders may not be explicitly identified. Use of materials from other sources within a thesis should not be construed as a claim over them.

A non-exclusive, non-transferable licence is hereby granted to those using or reproducing, in whole or in part, the material for valid purposes, providing the copyright owners are acknowledged using the normal conventions. Where specific permission to use material is required, this is identified and such permission must be sought from the copyright holder or agency cited.

Liability statement

By using a Digitised Thesis, I accept that Trinity College Dublin bears no legal responsibility for the accuracy, legality or comprehensiveness of materials contained within the thesis, and that Trinity College Dublin accepts no liability for indirect, consequential, or incidental, damages or losses arising from use of the thesis for whatever reason. Information located in a thesis may be subject to specific use constraints, details of which may not be explicitly described. It is the responsibility of potential and actual users to be aware of such constraints and to abide by them. By making use of material from a digitised thesis, you accept these copyright and disclaimer provisions. Where it is brought to the attention of Trinity College Library that there may be a breach of copyright or other restraint, it is the policy to withdraw or take down access to a thesis while the issue is being resolved.

Access Agreement

By using a Digitised Thesis from Trinity College Library you are bound by the following Terms & Conditions. Please read them carefully.

I have read and I understand the following statement: All material supplied via a Digitised Thesis from Trinity College Library is protected by copyright and other intellectual property rights, and duplication or sale of all or part of any of a thesis is not permitted, except that material may be duplicated by you for your research use or for educational purposes in electronic or print form providing the copyright owners are acknowledged using the normal conventions. You must obtain permission for any other use. Electronic or print copies may not be offered, whether for sale or otherwise to anyone. This copy has been supplied on the understanding that it is copyright material and that no quotation from the thesis may be published without proper acknowledgement.

Synthesis, Characterization and Activity Evaluation of Novel Spiropyran-Based Ion Sensors

By

Manuel Natali



A thesis submitted to the University of Dublin, Trinity College for the degree of Doctor of Philosophy

School of Chemistry

March 2011

University of Dublin

Trinity College

TRINITY COLLEGE
19 JUL 2011
LIBRARY DUBLIN
THESIS
9114

Declaration

This thesis is submitted by the undersigned to the University of Dublin, Trinity College for the examination of Doctorate of Philosophy. Except as otherwise stated, this thesis is entirely my own work and has not been submitted as an exercise for a degree to any other university. I agree that the library may lend or copy this thesis freely on request.

Summary

Photochromism indicates a reversible transformation of a single chemical species induced in one or both directions by electromagnetic radiation between two states having different absorption spectra. Photochromic compound have been of great interest because of their unique properties. Indeed they have been employed in supramolecular assemblies such as polymers, liquid crystals, light-sensitive eyewear, information recording, optical memory, and molecular devices. Chemical modification of photochromic compounds has opened in the last decade new possibilities for developing systems that may be suitable for other purposes such as chemical sensing. This can be applied to countless analytes. In this research we focused on the synthesis of spiropyran based photochromic compounds designed for the selective and reversible detection of transition metal cations.

Chapter 1 provides an overview of the concept of photochromism and the most important classes of photochromic compounds. Additionally, the most important examples of chemical sensors based on well known photochromic compounds will be treated. The aims of this project are included in this chapter.

Chapter 2 contains the results of our research including the design of our molecules, the synthesis, preliminary studies on the effect of solvent and pH on their photochromism, and the studies on their binding abilities. Thirteen molecules will be presented in this section. They are organized in four groups depending on the substituents present on their structures.

Chapter 3 details the conclusions of this work and also gives a future outlook for our research.

Finally, Chapter 4 provides a full description of the experimental procedures.

Overall, we believe that this research should contribute to further development of photoresponsive compounds for selective metal ion detection.

Acknowledgements

Firstly I would like to sincerely thank my supervisor Dr Silvia Giordani for giving me the opportunity to work in this group, for Miami, where I had such a great time (except for some small accident with Miami cops, cheap mopeds and Clerks of Court...what doesn't kill ya, makes you stronger) , for her hospitality and support during this three years.

To Silvia's group both past and present for their support and friendship during these years: Elisa, Laura, Dania, Kevin, Sonia, Antoin, Jackie, Pintu, Lyn, David, Stephanie, Ilona, Antonello, Eoghan, and Fergus.

I would also like to thank Prof. Thorfinnur Gunnlaugsson and his group, Dr. Isabel Rozas, Padraic, Amila, Aoife, Sergio, Fernando, and Giuseppe La Spina, Buddhie Lankage for the precious help during the first few months of my PhD.

Thanks to Prof. Francisco Raymo and his crew in Miami: Stefania, Ibrahim, Erhan, Janet, and Mutlu. I wish to thank also Prof. Massimiliano Lamberto for saving me and my performant moped in many difficult situations....unfortunatelly the moped couldn't make it.

Thanks to Dr. Paula Colavita, to my internal examiner Dr. Eoin Scanlan and their groups for the fruitful scientific conversations.

To Dr. Manuel Ruether, Dr. John O'Brien, Dr. Martin Feeney, and Dr. Bernard Jean-Denis for their help on NMR and Mass Spec.

Thanks to my external examiner A.P. De Silva, the greatest man and scientist I have ever met.

Thanks to Prof. John Boland and his group, in particular to Ronan, Dorotee, David and to Prof. Martin Hegner's group.

I am grateful to Prof. Christer Aakeroy for his collaboration.

Thanks to Rohit "Ruoppolo" Mishra for being one of my best friends....punk!

Thanks to Dr Kevin "Flavinio" Flavin "Da Wavin" for his friendship and wisdom, and to his future wife Dr Ana "Banana", cause there is always a great woman beside a great man.

Thanks to Dania "Movida", more shoes for her!

Thanks to Dr Niall "What's the story" Kinahan for his friendship, his patience with Elisa, and his love for motors...and boats.

Thanks to the good fellows Mauro Mantega and Sandip Bhattacharya...God save India and the Bottarga!

Cheers to Ruggggggero, the best remedy for bad mood.

To Alessandro Piccinini for being so good in Organic Chemistry.

To the Salamata's fellowship: Simone, Giovanni and Elena, Guido, Adriele, and Andrea.

To Daniela Dei Agnoli and the great time spent together.

A special grazie to my special friends Dr Laura "Dinero" Soldi and Dr Stefano "Il Ghera" Gherardi. To Stefano for having always the right answers and to Laura for having the right questions....and for being so big-hearted, funny...and weird!

Alla mia famiglia: mamma, papa', Miky, Paolo, Carola e nonna Gina per supportarmi sempre in tutte le mie scelte.

Alla famiglia Del Canto: Ale, Jo, Adele, Tacco e nonna Attilia per essere le persone splendide che sono...non go voia de sbilanciarme troppo in complimenti...chiaro?!

Thanks finally to the most important person in my life, Elisa, to whom this thesis is dedicated. Grazie per l'amore e la fiducia che mi hai sempre dimostrato, per avermi seguito in questa avventura, per le parole di incoraggiamento nelle situazioni difficili. Grazie per compensare i miei difetti (innumerevoli), per combattere sempre il mio estremo pessimismo (e fastidio), per riuscire a sedare il mio temperamento rude con la tua dolcezza (di tanto in tanto vaffanculo alle tue frecciatine). Grazie per essere la mia compagna, spero di riuscire a darti il futuro che meriti.

THAT'S ALL FOLKS, BIG TIME!

Table of Contents

Chapter 1: Introduction

1.1 Photochromism 2

1.2 Photochromic Compounds 4

1.2.1 Diazastilbenes 4

1.2.2 Anils 5

1.2.3 Fulgides 6

1.2.4 Diarylethenes 7

1.2.5 Dihydroindolizines 8

1.2.6 Spirooxazines 9

1.2.7 Spiropyrans 11

1.2.8 Chromenes 13

1.3 Photoswitchable Molecular Ligands 14

1.3.1 Photoswitchable Receptors Based on Azobenzenes 15

1.3.2 Photoswitchable Receptors Based on Fulgides 17

1.3.3 Photoswitchable Receptors Based on Diarylethenes 19

1.3.4 Photoswitchable Receptors Based on Dihydroindolizines 25

1.3.5 Photoswitchable Receptors Based on Chromenes 27

1.3.6 Photoswitchable Receptors Based on Spirooxazines 30

1.3.7 Photoswitchable Receptors Based on Spiropyrans 35

1.4 Conclusions 55

1.5 Aims of the project 55

References 58

Chapter 2: Results and Discussion

2.1 Design 64

2.1.1 Substituents R_1 in 1-position 64

2.1.2 Substituents R_2 in 8'-position 65

2.1.3 Substituents R_3 in 6'-position 66

2.1.4 Structures of the Chelating Spiropyrans 66

2.2 Synthesis 68

2.3 Acidochromism and Solvatochromism 72

2.3.1 Solvatochromic Effects 72

2.3.2 Acidochromic Effects 77

2.3.3 Conclusions 82

2.4 Metal Binding Studies 83

2.4.1 Binding Studies on Compounds of Group 1 83

2.4.2 Conclusions on Group 1 89

2.4.3 Binding Studies on Compounds of Group 2 89

2.4.4 UV-vis Absorption Studies on Metal Complexes 90

2.4.5 Reversibility of the complex formation 96

2.4.6 ^{1}H NMR Analysis on the Zinc Complexes of SP4 and SP7 96

2.4.7 The Effect of Counter Ions: Complexes' Composition Studies 100

2.4.8 The Effect of Different Counter Ions on the Absorption 102

2.4.9 Emission Measurements and Zinc Detection Limit 106

2.4.10 Single-crystal X-ray Diffraction 107

2.4.11 MALDI-TOF Mass Spectrometry 109

2.4.12 Conclusions on Group 2 112

2.4.13 Binding Studies on Compounds of Group 3 113

2.4.14 UV-vis Absorption Studies 114

2.4.15 Reversibility of the Spiropyrans-Copper Interactions 118

2.4.16 Mass Spectroscopy Analysis 119

2.4.17 Purification and Identification of SP-dimers 120

2.4.18 SP Dimers' Photoswitchability and Response to Cu(II) 129

2.4.19 Possible Mechanism of Dimerization 133

2.4.20 Conclusions on Group 3 137

2.4.21 Binding Studies on Compounds of Compounds of Group 4 138

2.4.22 Zinc Detection and Known Zinc Sensors 139

2.4.23 A Novel Spiropyran Based Photoswitchable Zinc (II) Receptor 143

2.4.24 Binding Studies 144

2.4.25 Emission Studies 148

2.4.26 ^{1}H-NMR Studies 150

2.4.27 Conclusions on Group 4 151

References 153

Chapter 3: Conclusions and Future Work

3.1 Conclusions 156

3.2 Future Work 156

References 158

Chapter 4: Experimental

4.1 General 160

4.2 UV-vis Absorption and Emission Studies 160

4.3 ^{1}H-NMR studies 161

4.4 Mass Spectrometry 161

4.5 Compounds 162

List of Publications

Del Canto, E.; Flavin, K.; Natali, M.; Perova, T.; Giordani, S. *Carbon* **2010**, *48*, 2815-2824.

Aakeroy, C. B.; Hurley, E. P.; Desper, J.; Natali, M.; Douglawi, A.; Giordani, S. *CrystEngComm* **2010**, *12*, 1027-1033.

Natali, M.; Soldi, L.; Giordani, S. *Tetrahedron* **2010**, *66*, 7612-7617.

Natali, M.; Aakeroy, C. B.; Desper, J.; Giordani, S. *Dalton Transactions* **2010**, *39*, 8269-8277.

List of Figures, Schemes and Tables

Chapter 1: Introduction

Figure 1.1 Typical absorbance patterns in a normal photochromic process.

Scheme 1.1 Conversion of *E*-Diazastilbene **1a** into and *Z*-Diazastilbene **1b** *via cis-trans* isomerization driven by irradiation.

Scheme 1.2 Tautomerism of photochromic 2-chloro-N-salicylideneaniline **2a** to its keto form **2b** modulated by UV and visible irradiation.

Scheme 1.3 Tautomerism of photochromic 5-chloro-N-salicylideneaniline **2a** to its keto form **2b** modulated by UV and visible irradiation.

Scheme 1.4 Photochromic cyclization of fulgide **4a** to its corresponding dihydronaphthalene **4b** modulated by UV and visible irradiation.

Scheme 1.5 Photochromic cyclization of diarylethenes **5a** and **6a** to their corresponding closed-ring forms **5b** and **6b** modulated by UV and visible irradiation.

Scheme 1.6 Reversible photochromic conversion of dihydroindolizine **7a** to its corresponding betaine **7b** by UV irradiation.

Scheme 1.7 Reversible photochromic conversion of spirooxazine **8a** to its corresponding merocyanine **8b** by UV irradiation. The reverse cyclization is actuated by either visible light or thermal fading of **8b**.

Figure 1.2 Absorption changes of **9a** (20 μM, DCM) with 365 nm light irradiation (periods: 0, 10, 20 s).

Figure 1.3 Absorption spectra of solutions of **10** (dotted line, 5.1 x 10^{-4}M in trimethylpentane, 77 K), **11** (dashed line, 5.1 x 10^{-4}M in trimethylpentane, 77 K) and **12** (continuous line, 1.7 x 10^{-4}M in trimethylpentane, 77 K).

Figure 1.4 Absorption spectra of an ethanol solution of **13a** before (continuous line) and after irradiation with UV light (dashed line). The broad band with maximum at 530 nm indicates the formation of the merocyanine **13b**.

Scheme 1.8 Photochromic isomerization reported by Moorthy and co-workers of chromene **14a** to its corresponding quinoidal form **14b** modulated by UV and visible irradiation or thermally.

Scheme 1.9 Reversible cation binding and release by compound **15a** actuated by UV and visible irradiation respectively. UV light produce *trans-cis* isomerization of **15a** into **15b** which is able to bind $M^+ = K^+$, Na^+ and Rb^+. The cation release is effected by visible light irradiation that converts **15b** into **15a**.

Scheme 1.10 *Trans-cis* isomerization of **16a** into **16b** by UV light irradiation UV light with consecutive binding of a metal cation $M^+ = Na^+$, K^+, Li^+, Rb^+ and Me_4N^+.

Scheme 1.11 Reversible *cis-trans* photoisomerization of **17a** into **17b** by UV and visible irradiation.

Scheme 1.12 Reversible *cis-trans* and *trans-cis* photoisomerization of **18a** into **18b** by UV and visible irradiation/storage in the dark respectively.

Scheme 1.13 Photoisomerization of fulgenates **19a**, **20a** and **21a**, into their corresponding closed isomers **19b**, **20b** and **21b** driven by UV irradiation.

Scheme 1.14 Benzo-18-crown-6 indolylfulgide **22** and benzo-15-crown-5-modified fulgide **23** synthesized by Guo *et al.*

Scheme 1.15 Photoresponsive tweezers based on crown ether functionalized diarylethenes synthesized by Takeshita and collaborators.

Scheme 1.16 Photochromism of crown ether modified diarylethenes synthesized by Kawai.

Figure 1.5 Schematic representation of the photoconversion of **29a** and **30a** into **29b** and **30b**. Fluorescence spectra of **30a** before and after irradiation with UV light (λ_{exc} = 365 nm).

Figure 1.6 Schematic representation of the interaction between **30a** and Zn^{2+}. Fluorescence spectra of **30a** before (**A**) and after addition of Zn^{2+} (**B**) (λ_{exc} = 365 nm).

Scheme 1.17 Schematic representation of the cation release/uptake by compound **31a** after its photoisomerization to the closed form **31b** driven by irradiation with UV and visible light.

Scheme 1.18 Interconversion between **32a** and **32b** controlled by UV and visible irradiation and formation of adducts **32c** and **32d** after addition of F^-.

Figure 1.7 Schematic representation of the switchable interaction between **33a** and D-Glucose. CD spectra change upon addition of D-Glucose (7×10^{-4} M) to a solution of **33a** (1.4×10^{-5} M) in EtOH-tris-HCl (pH 7.8).

Scheme 1.19 Interconversion between **34a** and **35a** controlled by UV irradiation and thermal fading of **34b** and **35b** to their corresponding starting materials.

Scheme 1.20 Dihydroindolizines **36** and **37** beating crown ether moieties as cation ligand sites.

Scheme 1.21 Ca^{2+} uptake and release by photoisomerization of compound **38a** to **38b** and *vice versa*.

Scheme 1.22 Uptake and release Pb^{2+} by the two isomers **39a** and **39b**.

Scheme 1.23 Modulation of the uptake and release of a cation by photoconversion triggered by UV irradiation of chromene **40a** to the corresponding merocyanine **40b**.

Scheme 1.24 Chromenes **41** and **42** synthesized by Glebov and co-workers.

Scheme 1.25 Representative metal ligation by a common spirooxazine *via* phenolate-imine bidentate chelator.

Scheme 1.26 Isomerization of compounds **43a** and **44a** to their corresponding isomers **43b** and **44b** followed by chelation of bivalent cations M^{2+}= Cu^{2+}, Ca^{2+}, or Pb^{2+}.

Scheme 1.27 Structures of photochromic and ionochromic spiroindolinonaphthoxazines **45** and **46**.

Scheme 1.28 Structures of photochromic crown-ether functionalized spirooxazine **47-52** and equilibrium between the hypothetical different complexes involved in the chelation by compound **51**.

Scheme 1.29 Structures of photochromic spironaphthoxazines **53**, **54**, and **55** functionalized on the indolic part of the molecule with monoaza crown ether rings with different cavity sizes suitable for alkali metal cations recognition.

Scheme 1.30 Structures of photochromic spironaphthoxazines **56**, and **57** functionalized with aza-15(18)-crown-5(6)-ether moieties at 8' position of naphthalene fragment.

Figure 1.8 **a)** Structure changes of **58a** after irradiation with UV light (**58b**) and addition of CN^- (**58b-CN**$^-$); **b)** absorption spectra of 1 (20 μM) measured with 50 equiv of respective anions (as a *n*-Bu_4N^+ salt) in a water/MeCN mixture (1/1 v/v; CHES 100 mM, pH 9.3) under UV irradiation (334 nm) at 25 °C. The spectra were obtained after stirring the solution containing 1 and each anion for 30 min with UV irradiation. The red spectrum is obtained without anion in the dark; **c)** photograph of the solutions (A) without anion (dark), (B) without anion, (C) F^-, (D) Cl^-, (E) Br^-, (F) I^-, (G) AcO^-, (H) $H_2PO_4^-$, (I) HSO_4^-, (J) ClO_4^-, (K) NO_3^-, (L) SCN^-, and (M) CN^-.

Scheme 1.31 Photochromism and chelation of M^{n+}=Fe^{3+} or Cu^{2+} effected by the different isomers **59a** and **59b**

Scheme 1.32 Quinolinospiropyranindolines **60-63** bearing different substituents on the indolic nitrogen and 6' position of the quinolinospiropyran moiety.

Scheme 1.33 Photoisomerization of spiropyrans **64-69** bearing different substituents on the indolic nitrogen and 5 position of the indolic half followed by complexation of a metal cation M^{2+}= Mg^{2+}, Zn^{2+}, Ni^{2+}, Cu^{2+}, Hg^{2+}, and Pd^{2+}. The complexes have stoichiometry spiropyran-metal 2:1.

Scheme 1.34 Structures of photochromic spiropyrans **70-73** functionalized on the indolic part of the molecule with monoaza crown ether rings with different cavity sizes suitable for alkali metal cations recognition.

Figure 1.9 Partial 'H NMR spectra (500 MHz) of **75** in CD_3CN **(a)** before addition of SrI_2, **(b)** 30min after the addition, and **(c)** after 3 h.

Scheme 1.35 Spiropyran based MRI contrast agent described by Tu.

Scheme 1.36 Structures of photochromic bis(spiropyrans) **81** and **82** used in the metal cation active transport through liquid membrane.

Figure 1.10 Mechanisms at boundary phase between source, membrane and receiving phases for transport of Li^+ through liquid membrane containing compound **82**.

Scheme 1.37 Structures of photochromic bis(spiropyrans) **83-86** reported by Liu and collaborators.

Scheme 1.38 Alkaline earth cations selective sensor synthesized by Yagi and co-workers. The picture shows the hypothetical stucture of the complex with a alkaline-earth metal cation M^{2+}.

Scheme 1.39 Calcium and magnesium selective sensor **89** linking two spiropyran units *via* alkylic tether attached to the indolic nitrogen.

Figure 1.11 **(a)** Sketches of equilibrium reactions of compound **90a** and its corresponding isomers **90b** and **90c** in the presence of lanthanide ions M^{3+}; **(b)** UV-vis spectra of **90a** (40 mM) in the presence of and without metal ions (20 mM) in acetonitrile under dark conditions for 48 h. The selectivity toward lanthanides is obvious as the absorption maxima shift to shorter wavelengths and undergo dramatic intensity increases.

Figure 1.12 Schematic representation of the isomerization of compound **91a** to its open merocyanine **91b** with chelation of Cu^{2+}. The plot indicates time history of the sensing membrane responses to different concentrations of Cu^{2+}. Fluorescence intensity was recorded at 603 nm (λ_{exc}=556 nm).

Figure 1.15 The absorbance changes, A/A_0, of ethanol/water solutions 1:1 of **91a** (gray, 540 nm) and **92** (black, 453 nm) upon addition of 5.0×10^{-5} M metal ions (x-axis markers), separately.

Figure 1.14 Color changes of an ethanol/water solution containing **91a** and Hg^{2+} in the presence of different amino acids: 1) no amino acid, 2) Gly, 3) Leu, 4) His, 5) Glu, 6) Asp, 7) Met, 8) Cys, 9) Hcy, and 10) GSH (glutathione).

Figure 1.15 The absorbance ratio changes A_{400}/A_{530}, of **92a**, **93**, and **94a** in the ethanol–water solution upon additions of selected metal ions in the presence of Cys.

Figure 1.16 Mechanism of the chelation of zinc followed by the coordination of a pyrophosphate anion. The plot shows the changes in the fluorescence intensity of **94a** at 560 nm with respect to that at 620 nm in the ethanol aqueous solution (pH 7.4) upon addition of different concentrations of anions (λ_{exc}=522 nm). The values of F_{560nm}/F_{620nm} underwent an increase only i the presence of PPi proving the selectivity toward this anion.

Figure 1.17 Confocal microscope images of human acute T cell leukaemia (A) without spiropyran, (B) incubated with 100 μM **96** for 3 h. The fluorescence visible in (B) is given by the formation of a complex between **96** and glutathione.

Figure 1.18 Coordination mechanism of **97a** with a guanosine **G** derivative to for the complex **97b**. Absorption spectra of a solution containing **97a** and **G** in the absence and in the presence of other nucleosides cytidine (**C**), uridine (**U**), thymidine (**T**), and adenosine (**A**).

Figure 1.19 Electronic absorption spectra of **98a** ($3.0x\ 10^{-2}$ mM) in the presence of the lipophilic nucleosides guanosine (**G**), guanosine-guanosine (**GG**), thymidine-thymidine (**TT**), and adenosine-adenosine (**AA**) derivatives ($3.0x\ 10^{-2}$ mM) in CH_2Cl_2 at 25 °C.

Chapter 2: Results and Discussion

Scheme 2.1 Generic spiropyran structure with generic groups R_1, R_2, and R_3 in positions 1-, 8'-, and 6'- respectively.

Scheme 2.2 Structures of the designed spiropyrans.

Scheme 2.3 Synthesis mechanism for a generic spiropyran.

Scheme 2.4 Synthesis of 3-((dimethylamino)methyl)-2-hydroxy-5-methylbenzaldehyde **99**.

Scheme 2.5 Synthesis of spiropyrans **SP1**, **SP4**, and **SP8**.

Scheme 2.6 Synthesis of spiropyrans **SP2**, **SP6**, and **SP10** followed by hydrolysis in basic condition to afford **SP3**, **SP7**, and **SP11**.

Scheme 2.7 Synthesis of spiropyrans **SP5** and **SP9**.

Scheme 2.8 Synthesis of spiropyrans **SP12** and **SP13**.

Figure 2.1 UV-vis absorption spectra of **SP6** ($1.0x10^{-4}$ M) after irradiation with UV 254 nm light in acetonitrile (**a**) and methanol (**b**).

Figure 2.2 UV-vis absorption spectra of **SP5** ($1.0x10^{-4}$ M) after irradiation with UV 254 nm light in acetonitrile (**a**) and methanol (**b**).

Figure 2.3 UV-vis absorption spectra of **SP10** ($1.0x10^{-4}$ M) after irradiation with UV 254 nm light in acetonitrile (**a**) and methanol (**b**).

Figure 2.4 UV-vis absorption spectra of **SP2** ($1.0x10^{-4}$ M) after irradiation with UV 254 nm light in acetonitrile (**a**) and methanol (**b**).

Figure 2.5 The switching cycle associated with the three states **SP6**, **MC6**, and **MCH6**; (**a**) the absorption spectra of a solution at thermal equilibrium of **SP6** ($1.0x10^{-4}$ M, CH_3CN) (**black**) and of the same solution after the consecutive irradiation with ultraviolet light for 1 min (**grey**), addition of one equivalent of trifluoroacetic acid (**dotted curve**) and irradiation with visible light for 1 min (**green**); (**b**) absorption spectra of a solution of **SP6** ($1.0x10^{-4}$ M, CH_3CN) (**black**) after addition of 1 eq of TFA over a period of 40 min. (**dotted curves**), and after addition of 1 eq of triethylamine.

Figure 2.6 Absorption spectra of a methanol solution at thermal equilibrium of **SP6** ($1.0x10^{-4}$ M) before (**black**) and after addition of one equivalent of trifluoroacetic acid (**dotted curve**) followed by addition of 1 eq of triethylamine (**grey**).

Figure 2.7 Switching cycle associated with the three states **SP10**, **MC10**, and **MCH10** controlled only by pH variations; absorption spectra of a methanol solution at thermal equilibrium of **SP6** ($1.0x10^{-4}$ M) before (**black**) and after addition of one equivalent of trifluoroacetic acid (**dotted curve**) followed by addition of 1 eq of triethylamine (**grey**).

Figure 2.8 Absorption spectra of acetonitrile solutions at thermal equilibrium of **SP7** (**a**) ($1.0x10^{-4}$ M) and **SP11** (**b**) ($1.0x10^{-4}$ M) before (**black curves**) and after addition of one equivalent of trifluoroacetic acid (**dotted curves**).

Figure 2.9 (**a**) and (**b**) are the absorption spectra of **SP1** solutions ($1.0x10^{-4}$ M, acetonitrile) before and after the addition of 1 eq of different metal perchlorates and chlorides; (**c**) picture of the same solutions containing equimolar amount of **SP1** and the tested metal salts.

Figure 2.10 (**a**) and (**b**) are the absorption spectra of **SP2** solutions ($1.0x10^{-4}$ M, acetonitrile) before and after the addition of 1 eq of different metal

perchlorates and chlorides; (**c**) picture of the same solutions containing equimolar amount of **SP2** and the tested metal salts.

Figure 2.11 (**a**) and (**b**) are the absorption spectra of **SP3** solutions ($1.0x10^{-4}$ M, acetonitrile) before and after the addition of 1 eq of different metal perchlorates and chlorides; (**c**) picture of the same solutions containing equimolar amount of **SP3** and the tested metal salts.

Table 2.1 Absorption maxima of complexes with spiropyrans of group 1.

Figure 2.12 (**a**) Absorption spectra of a **SP2** solution ($1.0x10^{-4}$ M, acetonitrile) before (black) and after (grey) the addition of 1 eq $Zn(ClO_4)_2$ and after irradiation with visible light for 10 min (dotted curve); (**b**) absorption spectra of a **SP3** solution ($1.0x10^{-4}$ M, acetonitrile) before (black) and after (grey) the addition of 1 eq $Zn(ClO_4)_2$ and after irradiation with visible light for 10 min (dotted curve).

Figure 2.13 (**a**) and (**b**) are the absorption spectra of **SP4** solutions ($1.0x10^{-4}$ M, acetonitrile) before and after the addition of 1 eq of different metal perchlorates and chlorides; (**c**) picture of the same solutions containing equimolar amount of **SP4** and the tested metal salts.

Figure 2.14 (**a**) and (**b**) are the absorption spectra of **SP5** solutions ($1.0x10^{-4}$ M, acetonitrile) before and after the addition of 1 eq of different metal perchlorates and chlorides; (**c**) picture of the same solutions containing equimolar amount of **SP5** and the tested metal salts.

Figure 2.15 (**a**) and (**b**) are the absorption spectra of **SP6** solutions ($1.0x10^{-4}$ M, acetonitrile) before and after the addition of 1 eq of different metal perchlorates and chlorides; (**c**) picture of the same solutions containing equimolar amount of **SP6** and the tested metal salts.

Figure 2.16 (**a**) and (**b**) are the absorption spectra of **SP7** solutions ($1.0x10^{-4}$ M, acetonitrile) before and after the addition of 1 eq of different metal perchlorates and chlorides; (**c**) picture of the same solutions containing equimolar amount of **SP7** and the tested metal salts.

Table 2.2 Absorption maxima of complexes with spiropyrans of group 2.

Figure 2.17 Reversible interconversion between spiropyran and the open merocyanine-metal complex. (**a**) Absorption spectra of (black) **SP5** ($1.0x10^{-4}$ M, acetonitrile, 293K), after the addition of 1 equivalent of $Ni(ClO_4)_2$ (grey) and after the irradiation with visible light for 60s (dotted curve); (**b**) Absorption spectra of (black) **SP7** ($1.0x10^{-4}$ M, acetonitrile, 293K), after the addition of 1 equivalent of $ZnCl_2$ (grey) and after the irradiation with visible light for 60s (dotted curve); insets (**a**) and (**b**) are sequential cycles of conversion between **SP** and **MCM** controlled by visible light in the presence of $Ni(ClO_4)_2$ and $ZnCl_2$ respectively.

Figure 2.18 ^{1}H-NMR partial spectra of 1 ($2x10^{-2}$ M in CD_3CN, 293K) prior to (**SP4**) and after the addition of 1eq of $ZnCl_2$ (**MCZn4**).

Figure 2.19 ^{1}H-NMR partial spectra of 1 ($2x10^{-2}$ M in CD_3CN, 293K) prior to (**SP7**) and after the addition of 1eq of $ZnCl_2$ (**MCZn7**).

Figure 2.20 Job's analysis of (**a**) **SP7**-Zn^{2+} complex ([**SP**]+[Zn^{2+}] = $3.0x10^{-5}$ M, acetonitrile, 293 K) and (**b**) **SP7**-Cu^{2+} complex ([**SP7**]+[Cu^{2+}] = $3.0x10^{-5}$ M, acetonitrile, 293 K). Each analysis was carried out three times and the data were plotted as the average of the different series.

Figure 2.21 The absorption spectra of solutions of SP (1.0×10^{-4} M, acetonitrile, 293 K) after 20 min from the addition of 0.2, 0.4, 0.6, 0.8 and 1 equivalent of $ZnCl_2$; (Inset) Plot of $(A_\infty - A_x)/(A_x - A_0)$ against $1/[C]$.

Figure 2.22 Absorption spectra of **SP7** (1.0×10^{-4} M, acetonitrile, 293 K) after increasing the concentration of $Zn(ClO_4)_2$; (Inset) Absorption intensities at 492 nm of the same solution of **SP7**. The plateau of the maximum absorption intensity at 492 nm is reached after the addition of 0.3 eq of the zinc perchlorate.

Figure 2.23 The increase in absorption at 422 nm of a solution of **SP7** ($1.0x10^{-4}$ M, acetonitrile, 293K) after the addition of 1 equivalent of $Cu(ClO_4)_2$; (Inset) Plot of $(A_\infty - A_t)/(A_\infty - A_0)$ versus time.

Figure 2.24 Absorption spectra of a solution of **SP7** ($1.0x10^{-4}$ M, acetonitrile, 293 K) after the addition of more than 1 equivalent of $Cu(ClO_4)_2$; the formation of a new species is observable at 486 nm as the concentration of copper is higher than 1 equivalent.

Figure 2.25 Emission spectra of a **SP7** solution ($1.0x10^{-5}$ M, acetonitrile, 293K) before (black), after the addition of 1 equivalent of $ZnCl_2$ (red) and after the addition of 1 equivalent of $CuCl_2$ (blue), λ_{exc} = 481 nm; (Picture) coloration of a **SP7** solution ($1.0x10^{-5}$ M, acetonitrile, 293K) after addition of $ZnCl_2$.

Figure 2.26 Emission spectra of a **SP7** solution ($1.0x10^{-5}$ M, acetonitrile, 293 K) after varying the concentration of $Zn(ClO_4)_2$, λ_{exc} = 481 nm; (Inset) counterion effect on the emission response of a solution of **SP7**.

Figure 2.27 An extended core of metal ions (Zn^{2+} ions in pink, chloride ions in green) surrounded by a hydrophobic cladding.

Figure 2.28 MALDI-TOF mass spectrum of an acetonitrile solution of **SP7** containing (**a**) $[Zn(ClO_4)_2]=[\mathbf{SP7}]=1x10^{-3}M$ and (**b**) $[ZnCl_2]=[\mathbf{SP7}]=1x10^{-3}M$.

Figure 2.29 MALDI-TOF mass spectrum of acetonitrile solutions of **SP7** containing (**a**) $[CuCl_2]=[\mathbf{SP7}]=1x10^{-3}M$ and (**b**) $[Cu(ClO_4)_2]=[\mathbf{SP7}]=1x10^{-3}M$.

Figure 2.30 Absorption spectra of **SP8** (**a**), **SP9** (**b**), **SP10** (**c**), and **SP11** (**d**) ($1.0x10^{-4}$ M, acetonitrile, 293 K) before and after the addition of 1 eq of different metal perchlorates and chlorides.

Figure 2.31 Absorption spectra of **SP8** (**a**) and **SP9** (**b**) (1.0×10^{-4} M, acetonitrile, 293 K) after increasing the concentration of $Cu(ClO_4)_2$.

Figure 2.32 Absorption spectra of **SP10** (**a**) and **SP11** (**b**) (1.0×10^{-4} M, acetonitrile, 293 K) after increasing the concentration of $Cu(ClO_4)_2$.

Figure 2.33 Absorption spectra of **SP8** (**a**), **SP9** (**b**), **SP10**(**c**), and **SP11** (**d**) ($1.0x10^{-4}$ M, acetonitrile, 293 K) before (black curves), after the addition of 1 eq of copper perchlorates (grey curves), and irradiation with visible light for 10 min (dotted curves).

Figure 2.34 MALDI-TOF mass spectrum of acetonitrile solutions of **SP8** (**a**) and **SP9** (**b**) containing $[Cu(ClO_4)_2]=[\mathbf{SP}]=1x10^{-3}M$.

Figure 2.35 MALDI-TOF mass spectrum of acetonitrile solutions of **SP10** (**a**) and **SP11** (**b**) containing $[Cu(ClO_4)_2]=[\mathbf{SP}]=1x10^{-3}M$

Figure 2.36 (**a**) ^1H-NMR and (**b**) ^1H-^1H COSY NMR partial spectra of **2SP8** ($1x10^{-2}$ M in CD_3CN, 293K).

Figure 2.37 (**a**) ^1H-NMR and (**b**) ^1H-^1H COSY NMR partial spectra of **2SP10** ($1x10^{-2}$ M in CD_3CN, 293K).

Figure 2.38 (**a**) ^1H-NMR and (**b**) ^1H-^1H COSY NMR partial spectra of **2SP9** ($1x10^{-2}$ M in CD_3CN, 293K).

Figure 2.39 (**a**) UV-vis spectra of a solution of **2SP8** ($2.5x10^{-6}$ M in acetonitrile, 293K) before (black curve) and after (dotted curve) irradiation with UV light; (**b**) UV-vis absorption spectra of **2SP8** ($2.5x10^{-6}$ M, acetonitrile, 293 K) after increasing the concentration (0.4-3 equivalents) of $Cu(ClO_4)_2$.

Figure 2.40 (**a**) UV-vis spectra of a solution of **2SP10** ($2.5x10^{-5}$ M in acetonitrile, 293K) before (black curve) and after (dotted curve) irradiation with UV light; (**b**) UV-vis absorption spectra of **2SP10** ($2.5x10^{-5}$ M, acetonitrile, 293 K) after increasing the concentration (0.1-1 equivalents) of $Cu(ClO_4)_2$.

Figure 2.41 (**a**) UV-vis spectra of a solution of **2SP8** ($2.5x10^{-6}$ M in acetonitrile, 293K) in the presence of 3 equivalents of $Cu(ClO_4)_2$ before (black curve) and after (dotted curve) irradiation with visible light; (**b**)) UV-vis spectra of a solution of **2SP10** ($2.5x10^{-5}$ M in acetonitrile, 293K) in the presence of 1 equivalent of $Cu(ClO_4)_2$ before (black curve) and after (dotted curve) irradiation with visible light.

Scheme 2.9 Mechanism of dimerization of our spiropyrans.

Scheme 2.10 Mechanism of dimerization of our spiropyrans *via* radical formation.

Figure 2.42 Relative fluorescence intensity responses of **108** to various metal ions. Dark grey bars represent emission without Zn(II) for a particular metal ion. Light grey bars represent the emissions upon addition of Zn(II) to respective metal ion. The first bar shows the response to Zn(II) in the absence of any competitive ions.

Figure 2.43 Fluorescence spectrum of **111** in the presence of various metal ions in 0.1 M HEPES buffer at pH 7 (λ_{exc}=300 nm).

Scheme 2.11 Selective zinc (II) sensor synthesized by Dessingou and co-workers.

Scheme 2.12 Selective zinc (II) sensor synthesized by Lippard and co-workers.

Figure 2.44 Reversible interconversion between the closed spiropyran **SP13** and a hypothetical merocyanine-zinc complex **MCZn13**. Absorption spectra of **SP13** ($1.0x10^{-4}$ M, acetonitrile, 293 K) (black line) before, (grey line) after the addition of 1 equiv of $Zn(ClO_4)_2$ and (dotted line) after the subsequent irradiation with visible light for 1 min; (Inset) sequential cycles of conversion between **SP13** and **MCZn13** controlled by visible light.

Figure 2.45 Absorption spectra of spiropyran **SP13** ($1.0x10^{-4}$ M, acetonitrile, 293 K) (**a**) and spiropyran **SP12** ($1.0x10^{-4}$ M, acetonitrile, 293 K) (**b**) after 20 min from the addition of 1 equiv of different metal perchlorates and chlorides.

Figure 2.46 Absorption intensity at 504 nm of solutions of spiropyran **SP13** ($1.0x10^{-4}$ M, acetonitrile, 293 K) before and after the addition of 1 equiv of $Zn(ClO_4)_2$, $Cu(ClO_4)_2$, $Ni(ClO_4)_2$, $Co(ClO_4)_2$, $Mn(ClO4)_2$, $Cd(ClO_4)_2$, $Fe(ClO_4)_2$, Mg(ClO4)2, $CaCl_2$, NaCl and KCl.

Figure 2.47 Absorbance intensity responses of **SP13** ($1.0x10^{-4}$ M, acetonitrile, 293 K) to various metal ion. Grey bars represent the absorption of **SP13** at 504 nm in the presence of 1 equiv of a selected metal ion. Black bars represent the absorption of **SP13** at 504 nm in the presence of a binary mixture of Zn(II) and a competitive metal ion (1 equiv each).

Figure 2.48 Emission spectra of a solution of **SP13** ($1.0x10^{-5}$ M, acetonitrile, 293 K, λ_{exc}=492 nm) before (black) and after the addition of 1 equiv of $Zn(ClO_4)_2$ (red). The picture shows the spiropyran solutions in the absence and in the presence of zinc.

Figure 2.49 Absorption intensities at 504 nm of a solution of spiropyran **SP13** ($1.0x10^{-4}$ M, acetonitrile, 293 K) after increasing the concentration of $Zn(ClO_4)_2$; (Inset) Job's analysis of **MCZn13** complex ($[SP]+[Zn^{2+}]$ = $3.0x10^{-5}$ M, acetonitrile, 293 K).

Figure 2.50 The absorption spectra of a solution of **SP13** ($1.0x10^{-4}$ M, acetonitrile, 293 K) after 20 minutes from the addition of 0.1, 0.2, 0.3, 0.4, 0.5, 0.6, 0.7, 0.8, 0.9, 1, 1.5, 2 equivalent of ($Zn(ClO_4)_2$; (Inset) Plot of $(A_\infty - A_x)/(A_x - A_0)$ against 1/[C], binding constant $k = 1.6x10^4$ M^{-1}.

Figure 2.51 ^{1}H-NMR partial spectra of 1 ($2x10^{-2}$ M in acetonitrile, 293 K) prior to (**SP13**) and after the addition of 1 eq of $ZnCl_2$ (**MCZn13**).

Table 2.3 ^{1}H-NMR spectroscopy data (400 MHz, CD_3CN, 298 K) for **SP13** before (**SP13**) and after the aditon in mixture with **MCZn13** (1 equiv of Zn).

CHAPTER 1

INTRODUCTION

1.1. Photochromism

The term photochromism was coined in 1955 by Hirshberg and it indicates a reversible transformation of a single chemical species induced in one or both directions by electromagnetic radiation between two states having different absorption spectra.[1] Reversibility of the process is the criterion which establishes the main difference between photochromism and photochemistry. In the latter, reactions might be irreversible.

In all photoprocesses, a starting material called an educt, is converted to a product by means of UV, visible or IR irradiation. The back reaction can occur thermally or photochemically; the terms T-type and P-type are used, respectively, to discriminate between the two pathways. Moreover, when the educt absorbs at a shorter wavelength than the product, a normal photochromism is involved. When the absorption wavelength is larger for the educt, the process is called inverse photochromism.[2]

In Figure 1.1 the typical patterns of the absorbance prior to, and after irradiation of a photochromic compound are shown. The formation of the product P is induced by irradiation at an appropriate wavelength of the educt A. The conversion of P to the original state takes place following either a P-type or a T-type path.

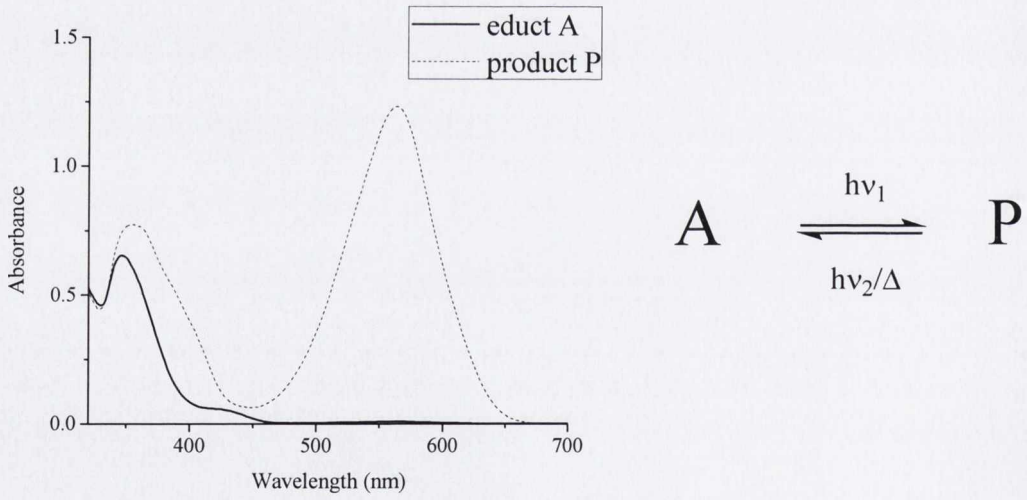


Figure 1.1 Typical absorbance patterns in a normal photochromic process.

Generally, the photoinduced and reversible change in the absorbance of a photochromic compound is the result of unimolecular reactions. In particular, ring-closing and ring-opening steps, *cis-trans* and *trans-cis* isomerizations and intramolecular proton-transfer processes may be invoked. In all instances the associated transformations produce dramatic changes in one or more properties of the compound such as the emissive behaviour, the ability to absorb visible radiation, the dipole moment and the polarizability of the molecule. As a consequence the macroscopic properties such as the refractive index, the colour, the phase partitioning may change.[3]

Several properties of photochromics are important for their use. These include:

- **Quantum Yield:** it describes the efficiency of the photochromic change with respect to the amount of light absorbed;
- **Fatigue Resistance:** that refers the loss of reversibility of the photoreaction. Several causes might trigger this process such as photodegradation, photobleaching, photooxidation, and other side reactions. All of them are strongly dependent on the conditions of the sample and the activating light;
- **Number of cycles:** in well defined experimental condition it indicates the number of cycles Educt-Product-Educt that a system can undergo;
- **Cyclizability (Z_{50}):** it estimates the number of cycles allowed before reducing the absorbance to ½ of the initial value;
- **Photostationary State:** it indicates the ratio of the two different state of a photochromic system after excitation with any given wavelength. In a perfect system, there would exist wavelengths that can provide 1:0 and 0:1 ratios of the isomers, but in real systems this is not possible, since the active absorbance bands always overlap to some extent;
- **Half life ($t_{1/2}$):** it is the time necessary for the absorbance of the product to decrease to 50% of its initial value during one cycle;
- **Solubility and Polarity:** they are often charged in one or more state, leading to very high polarity and possible large changes in polarity. They also generally contain large conjugated systems that limit their solubility.

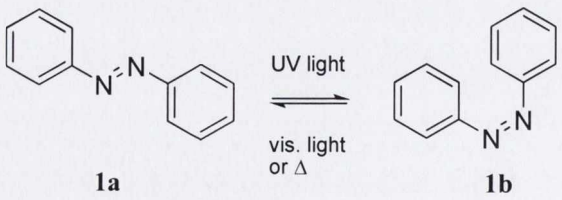
1.2. Photochromic Compounds

The intriguing nature of existing in two different states that may be switched by means of irradiation has led the scientific community to consider photochromic compound as the next candidates to be utilized in photonic devices. In particular, due to their unique properties, they have been extensively employed in supramolecular assemblies such as polymers,[4] liquid crystals,[5] light-sensitive eyewear, information recording and optical memory,[6] and molecular devices.[7]

Photochromes can be classified depending on the structure and, as a consequence, on the mechanism involved in the transformation. The most common mechanisms involved are usually *cis-trans* and *trans-cis* isomerizations, ring-closing and ring-opening steps and intramolecular proton-transfer. In this chapter, I will report the most significative and studied photochromic compounds classified on the basis of their conversion mechanisms.

1.2.1 Diazastilbenes

The first example are *Diazastilbenes* whose photochromic properties are due by a *cis-trans* isomerization mechanism. These compounds differ from Stilbenes because of a N-N double bond instead of a C-C double bond. They have relatively simple structures that undergo *cis-trans* isomerization in solution if irradiated with light of an appropriate wavelength.



1a **1b**

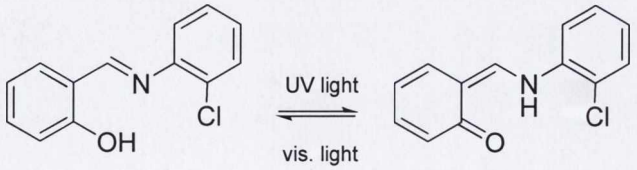
Scheme 1.1 Conversion of *E*-Diazastilbene **1a** into and *Z*-Diazastilbene **1b** *via cis-trans* isomerization driven by irradiation.

The isomerization step consists of a 180° rotation about their N-N double bond that produce two chemical species, the *Z* and *E* isomers, that have different absorption

spectra. In particular the *E* isomer is converted into the *Z* by means of UV irradiation in the range of 360-370 nm, where the first absorbs mainly. Since the *cis* isomer absorbs in the visible region at 430-440 nm, irradiation with visible light in this region will trigger the reversion to the *trans* isomer.[8] The same result may be achieved thermally.[9] The example of diazastilbene **1a** and its corresponding photogenerated isomer **1b** is shown in Scheme 1.1. Since their appealing properties, Diazastilbene may be used as tools for triggering reversibly the properties of different materials. The geometrical transformations of diazastilbenes incorporated in polymers may result in dramatic changes of the material properties such as swelling,[10] wettability,[11] viscosity[12] and solubility.[13]

1.2.2 Anils

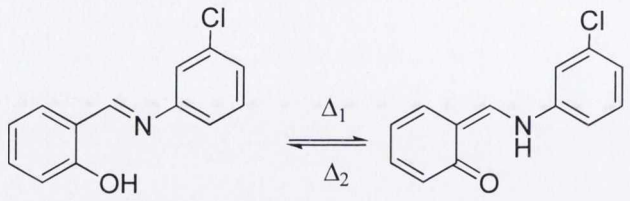
Another well studied photoisomerization mechanism is the tautomerism of *Anils*. In their early work Cohen and co-workers classified these compound in photochromic and thermochromic Anils.[14] Depending on the substituents on the molecular skeleton it is possible to observe two completely distinct behaviours. For instance, salicyldene-2-chloroaniline **2a** is photochromic in the solid state. While heat does not affect its absorption at 380 nm, UV-light produces at an intense band in the visible region in the range of 480-520 nm. This phenomenon is due to tautomerism of the proton on the OH group in **2a** to the nitrogen. Thus a *trans*-keto NH form is generated and it is responsible of the absorption in the visible region. The reverse process occurs upon irradiation with visible light (Scheme 1.2).



2a **2b**

Scheme 1.2 Tautomerism of photochromic 2-chloro-N-salicylideneaniline **2a** to its keto form **2b** modulated by UV and visible irradiation.

Anil **3a** differs from **2a** because of the position of the chlorine which is moved from *ortho* in **2a** to *meta* in **3a**. This small structure rearrangement produces dramatic changes in the responses to photostimuli. Compound **3a** is in fact thermochromic and does not respond to UV irradiation. The tautomer **3b** is stable at -49°C while **3a** is the main species at -159°C (Scheme 1.3). Thus the interconversion between the two tautomers is achieved by increasing and decreasing the temperature.



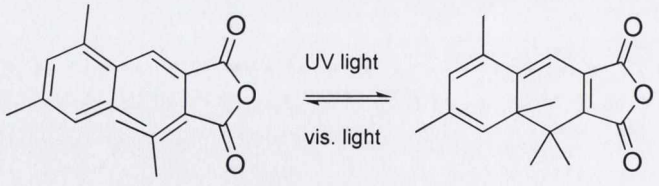
T = -159°C T = - 49°C

3a **3b**

Scheme 1.3 Tautomerism of photochromic 5-chloro-N-salicylideneaniline **2a** to its keto form **2b** modulated by UV and visible irradiation.

1.2.3 Fulgides

The oldest known photochromic organic compounds are *Fulgides*. Their remarkable fatigue resistance and the possibility to modify their photochromic properties by tailoring their structures has attracted interest both academically and commercially.[15] Their structure consist in a cyclic anhydride with two *exo*-methylenes. To be photochromic, one of the two methylenes has to be attached to an aromatic ring.



4a **4b**

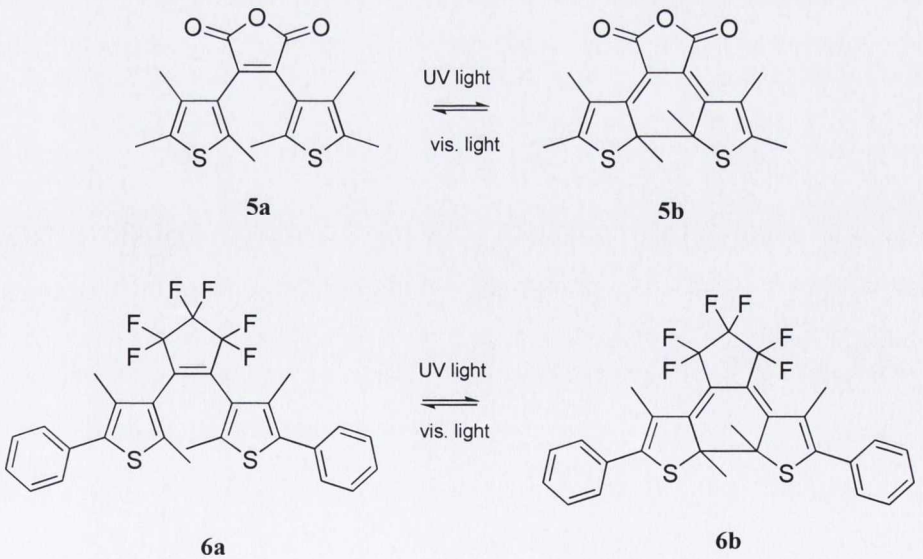
Scheme 1.4 Photochromic cyclization of fulgide **4a** to its corresponding dihydronaphtalene **4b** modulated by UV and visible irradiation.

Thus, the resulting 1,3,5-hexatriene undergoes a 6π-electocyclization that afford a dihydronaphtalene.

Fulgide **4a** absorbs UV irradiation at 360 nm and undergoes cyclization that produces compound **4b**. The latter is a dihydronaphtalene which absorbs in the visible region and can be reverted back to **4a** upon irradiation with white light (Scheme 1.4).[16] Due to their intrinsic properties they have found applications in non-linear optical switching[17] and optical recording memories.[18,19]

1.2.4 Diarylethenes

Although stilbene is known to undergo *cis-trans* photoisomerization upon ultraviolet irradiation, reversible cyclization reactions in the absence of oxygen to dihydrophenanthrene have been reported.[20] By replacing the phenyl rings of stilbene with thiophene rings and introducing a pentatomic ring that prohibits the *cis-trans* isomerization of the ethylene, a photochromic compound that undergoes cyclization to produce a thermally stable dihydro-type product is generated.[21,22] This class of compounds is the well known family of *Diarylethenes.* Two examples of thermally stable diarylethenes are shown in Scheme 1.5. A benzene solution of the diarylmaleic anhydride **5a** absorbs light



5a **5b**

6a **6b**

Scheme 1.5 Photochromic cyclization of diarylethenes **5a** and **6a** to their corresponding closed-ring forms **5b** and **6b** modulated by UV and visible irradiation.

in the range of 300-400 nm. After irradiation with UV light the solution turns into red and its absorption undergoes a bathochromic shift to 550 nm due to the formation of the photoproduct **5b**. The process is fully reversible and it is triggered by visible irradiation that converts **5b** into **5a**.[23] Closed-ring diarylperfluorocyclopentene **6b** is photogenerated by irradiation with UV light of a benzene solution of its open-ring analogue **6a**. In this instance the reverse pathway that produce the reversion of **6b** into **6a** is driven by visible irradiation as well.[24] Both compounds **5a** and **6a** can convert into their corresponding ring-closed analogues following P-type pathways. Indeed, the photogenerated species do not show any thermochromism as they are stable even at 80°C for weeks.

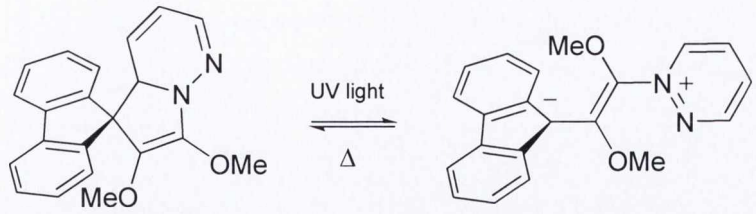
The high photochromic performances of diarylethenes like thermal irreversibility, fast response to photostimuli, fatigue resistance and photoswitchability in both solution and solid state satisfy the requirements for their application in optoelectronic devices such as memories and switches.[25]

1.2.5 Dihydroindolizines

The photochromism of *dihydroindolizines* or DHIs was first reported by Hauck and Durr in 1979.[26] The photochromic behaviour is based on a reversible pyroline opening upon UV irradiation that converts a colourless closed form into a betaine. The closed form is regenerated by thermal path and involves the 1,5-electrocyclization of the betaine.

Scheme 1.6 shows the photochromic reaction of dihydroindolizine **7a** and its corresponding betaine **7b**.[27] Depending on the substituent present on the molecular skeleton, the cyclization rate of betaine may be modulated from milliseconds to several weeks.[28,29]

Owing to their features they have been considered as suitable materials for ophthalmic lenses, data storage photoswitches, dental filling materials,[27,28] IR-sensitive photoswitchable materials,[29] and DNA markers.[30]



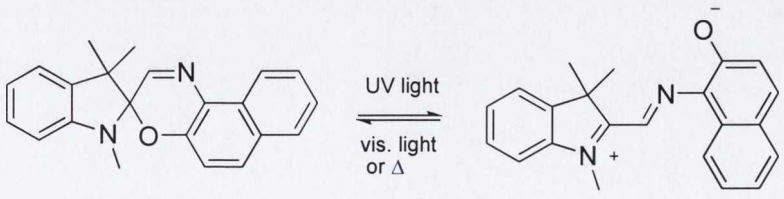
7a **7b**

Scheme 1.6 Reversible photochromic conversion of dihydroindolizine **7a** to its corresponding betaine **7b** by UV irradiation.

1.2.6 Spirooxazines

The term spirooxazine denotes a molecule containing an oxazine ring where the carbon in 3-position is involved in a spiro linkage. The photoinduced cleavage of the bond between the spiro carbon and the oxazine oxygen produces a change valence-bond structure and conformation of the molecule. The resulting new species that absorbs light at a different wavelength and, as a consequence, is coloured.

The photochromism of spirooxazine **8a** (Scheme 1.7) was first reported by Fox.[31] A solution of **8a** is colourless in toluene at room temperature but becomes blue upon irradiation with UV light. The colour change is due by conversion of the closed spiro compound into the open merocyanine **8b** which absorbs light in the visible region. This phenomenon takes place because of the cleavage of the C-O bond of the spirocarbon followed by a *cis-trans* isomerization that produce the fully conjugated merocyanine. Usually the decoloration of the open form takes place by thermal fading whose rate may



8a **8b**

Scheme 1.7 Reversible photochromic conversion of spirooxazine **8a** to its corresponding merocyanine **8b** by UV irradiation. The reverse cyclization is actuated by either visible light o thermal fading of **8b**.

be modulated by increasing or decreasing the temperature.

Figure 1.2 shows the typical patterns in the absorption spectra of a solution of the spirooxazine **9a** synthesized recently by Guo and Chen.[32] This analogue bears a dimethylamino substituent in 7' position on its benzopyran moiety. A dichloromethane solution of **9a** absorbs mainly in the UV region with a broad band in the range of 250-400 nm. After irradiation with 365 nm light a new band with maximum intensity at 607 nm appears in the visible region. This new absorption is indicative of the formation of **9b**.

Spirooxazines photochromism in polymeric matrices is well established.[33] Since their capability of switching between the open and closed form both in solution and if included in polymers they have been considered perfect candidates for application in ophthalmology. Indeed, they were first used in Orgaver™ sunglasses and in PHOTOLITE™ photochromic lenses in the early 1980's.

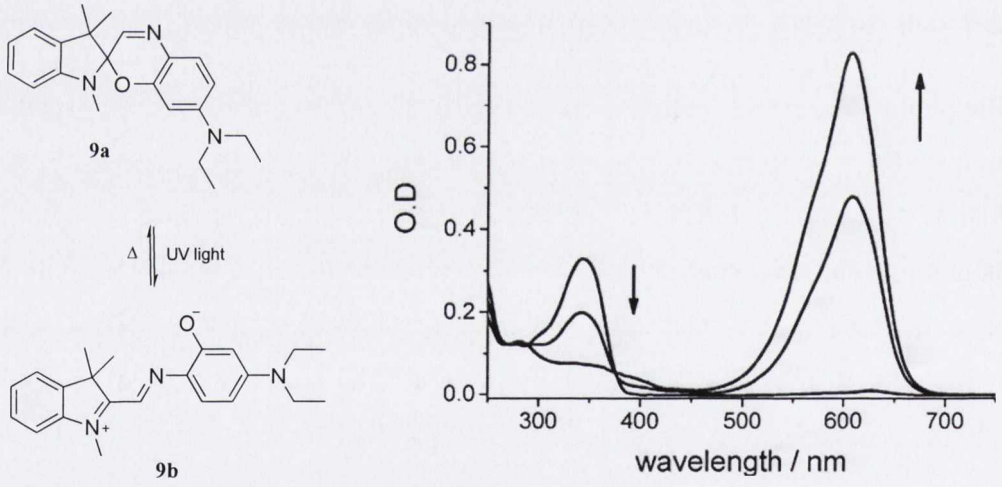


Figure 1.2 Absorption changes of **9a** (20 μM, DCM) with 365 nm light irradiation (periods: 0, 10, 20 s).[32]

Current research on spirooxazine has delved into the investigation of their photochromic behaviour for application in data storage processes and nonlinear optical phenomena.[34]

1.2.7 Spiropyrans

Nowadays, many different compounds have been shown to exhibit photochromism. Among them the class of spiropyrans has been probably the most extensively studied over the past several decades owing to the profitable applications they could be used for. Already in his early work Hirshberg envisaged the suitability of such compounds as photochemical erasable memory.[35] Well-known photochromic compounds, spiropyrans or spirochromenes are characterized by the presence of two heterocyclic parts linked to each other through a tetrahedral carbon atom. The two halves of the molecule are located on two perpendicular planes. The benzopyran moiety is a common motif present in most of the molecules.

The absorption spectra usually range in the UV region between 200-400 nm. The spirocarbon atom should disrupt the conjugation between the two halves of the molecule. Thus the contribution of the two different halves are expected in the spiropyran spectra. Tyer and Becker[36] studied the absorption of spiropyran **12** and compared it to model compounds **10** and **11** that represent good approximations of the indolic and the benzopyran moieties of the parent spiropyran. A solution of **10** in 3-methylpentane at room temperature (dotted line in figure 1.3) gives two absorption

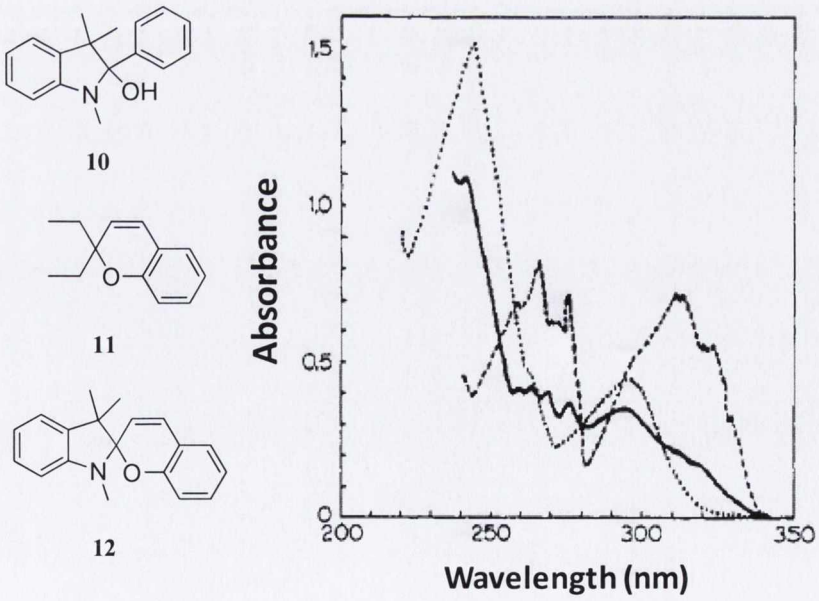


Figure 1.3 Absorption spectra of solutions of **10** (dotted line, 5.1 x 10^{-4}M in trimethylpentane, 77 K), **11** (dashed line, 5.1 x 10^{-4}M in trimethylpentane, 77 K) and **12** (continuous line, 1.7 x 10^{-4}M in trimethylpentane, 77 K).[36]

bands with maxima at 244 and 295 nm. In the same conditions, model compound **11** absorbs in the UV region with maxima at 265, 311 and 313 nm (dashed line in figure 1.3). The absorption maxima of the parent **12** can be clearly seen although the indoline and the benzopyran moiety transitions are mixed for some extent in the 265 and 310 regions. In particular Tyer and Becker assigned the absorption maxima at 265, 324 and 312 nm (continuous line in figure 1.3) to the benzopyran half of **12**, while absorption maxima at 243 and 296 nm were given to the contribution of the indolic moiety.

Absorption in the 200-400 nm range produces the cleavage of the bond that involves the spirocarbon and the oxygen atom generating a new zwitterionic species. The latter, called merocyanine, undergoes a *cis-trans* isomerization of the double bond in the pyran ring to produce a more stable product. There is no disruption of the molecule aromatic system and the absorption of the open form is dramatically redshifted to the visible region with respect to the closed spiropyran. The reversion of the closed form takes place either under thermal condition or by photochemical path. In the latter visible light at a larger wavelength or continuous UV irradiation can be utilized.[37] The absorption spectra of an ethanol solution of spiropyran **13a** before and after irradiation with UV light is shown in figure 1.4. This spiropyran absorbs in the region 230-300 nm with a sharp maximum at 248 nm. After irradiation with UV light the appearance of a broad band between 480 and 600 nm indicates the formation of the open merocyanine **13b**.[2]

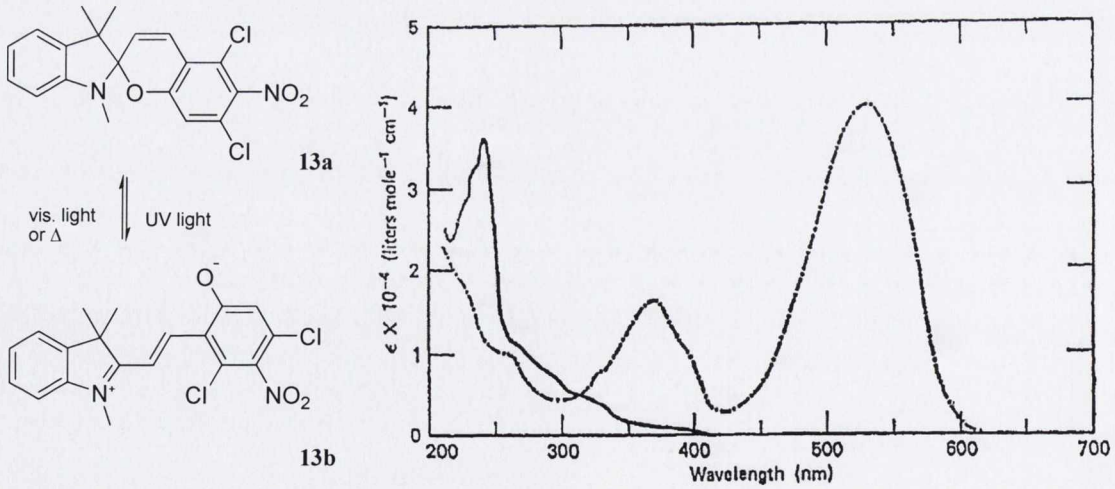


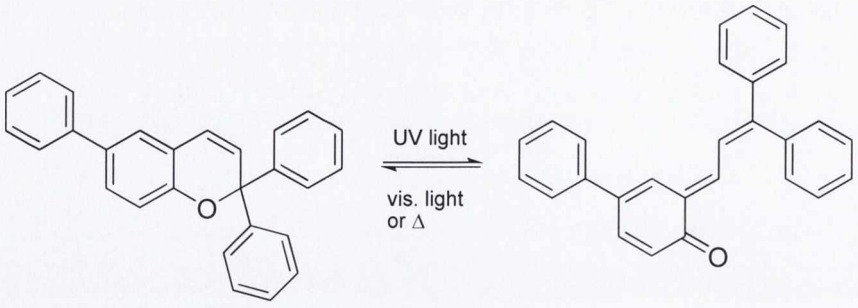
Figure 1.4 Absorption spectra of an ethanol solution of **13a** before (continuous line) and after irradiation with UV light (dashed line). The broad band with maximum at 530 nm indicates the formation of the merocyanine **13b**.[31]

As most of the known photochromic compounds, spiropyrans can undergo photodegradation. It occurs partially by oxidation and the identified products are carbon monoxide, carbon dioxide, substituted derivatives of salicylaldehyde, oxindole and polycondensates which decrease the functionality and the lifetime of the photochromic system.[38] Atmospheric oxygen facilitates this photodegradation by radical processes.[39] There is no systematic basis for describing spiropyrans photochromic behaviour. It is dependent on several factors such as:

- the structure: depending on the substituents and their position different results can be achieved;[40-44]
- the medium: the polarity of the solvent plays a fundamental role in stabilizing either the closed or the open form: the higher the medium polarity, the longer the merocyanine lifetime. Solid supports incorporating spirochromenes might respond to photostimuli in different manner depending on the matrix composition;[45]
- temperature and absorption range also play a crucial role.[46]

1.2.8 Chromenes

Benzo and naphthopyran have general structures where a benzopyran or a naphthopyran ring is attached through a tetrahedral carbon to two groups that are not jointed to form spiro heterocyclic ring like in the parent compounds spiropyrans and spirooxazines. The mechanism for the photochromism of these compounds is similar to that for the oxazines involving opening of the pyran ring. These molecules, upon UV irradiation, yield open metastable photoproducts, having the structure of *o*-quinone-allides which are the coloured forms due to the increased electronic delocalization. Photoproducts reconvert to the starting material either thermally or photochemically by irradiation with light at higher wavelengths.[47,48] In scheme 1.8 the photoisomerization of chromene **14a**, recently synthesized by Moorthy and co-workers, to its quinonic form **14b** *via* irradiation with UV light is depicted. The photoproduct is reverted back to the tetrahedral form by means of either irradiation with visible light or thermal fading. They have also reported the facile synthesis of arylchromenes with wide-ranging spectrokinetic properties.[49] These molecules have found their main application in the industry as photochromic compounds for ophthalmic lenses.[50]



14a **14b**

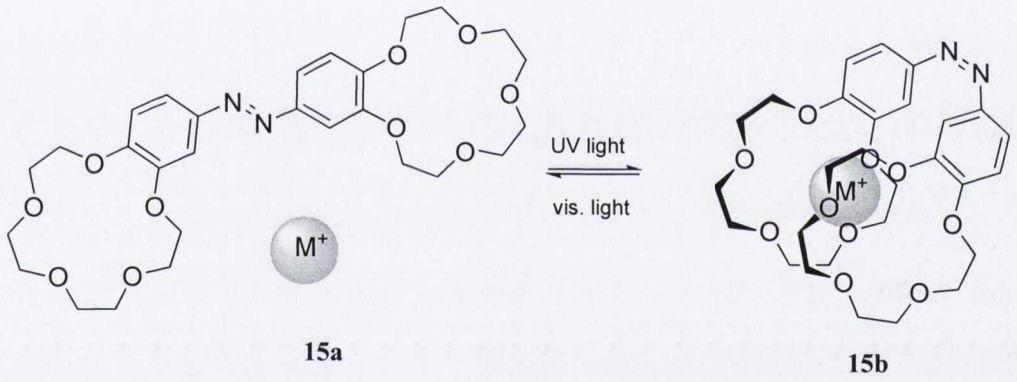
Scheme 1.8 Photochromic isomerization reported by Moorthy and co-workers of chromene **14a** to its corresponding quinoidal form **14b** modulated by UV and visible irradiation or thermally.

1.3 Photoswitchable Molecular Ligands

The reversible interconversion between distinct forms driven by light has attracted attention for potential application in the field of optoelectronic devices such as memories and switches. Of different molecular processes that trigger photochromic phenomena in the afore mentioned compounds, electrocyclic reactions and *cis-trans* isomerizations produce the most dramatic changes in the molecular structure and as a consequence in the physical properties of the involved species. Chemical modification of photochromic compounds offers new possibilities for developing systems that may be suitable for other purposes. Indeed, the incorporation of one or more specific sites for the interaction with other molecular species into a photochromic molecule may afford a system that optically respond to the presence of a guest. In particular, functionalization with an ionophore generates receptors for cations where the uptake and release of the cationic species can be controlled by irradiation with light at different wavelengths. Additionally the presence of a cation is always accompanied by an optical signal that allows its detection. This new approach for chemical sensing has been extensively studied and many of the known photochromic compounds have been modified for these purposes. In this chapter I survey studies on reversible molecular receptors based on the widely known photochromic compounds.

1.3.1 Photoswitchable Receptors Based on Azobenzenes

Several examples of azobenzenes (or diazastilbenes) modified in order to obtain photoswitchable ion receptors have been synthesized. Shinkai and co-workers reported on the light-driven membrane transport of K^+, Na^+ and Rb^+ cations mediated by the azobis(benzo-15-crown-5) **15a**.[51] This derivative of the well known diazastilbene **1** previously mentioned bears two crown ethers, one on each benzene ring. Crown ethers are known for their capability of complexing alkali, alkaline earth, heavy and other metals and/or ammonium ions.[52,53] In the presence of K^+, Na^+ and Rb^+ the *trans* isomer **15a** undergoes *trans-cis* isomerization that afford the cis isomer **15b**. Owing to the reduced distance between the two crown ethers, this isomer is able to bind the metal cations working as tweezers. The cationic guest release is effected by means of irradiation with visible light that produces the conversion of **15b** into **15a** (scheme 1.9).

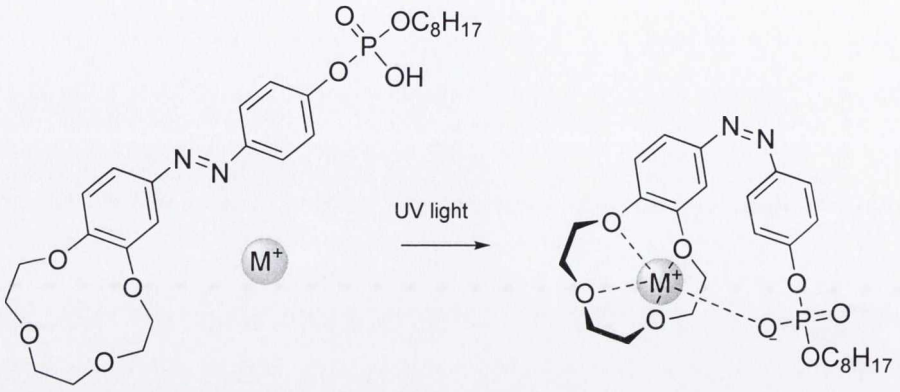


15a **15b**

Scheme 1.9 Reversible cation binding and release by compound **15a** actuated by UV and visible irradiation respectively. UV light produce *trans-cis* isomerization of **15a** into **15b** which is able to bind M^+= K^+, Na^+ and Rb^+. The cation release is effected by visible light irradiation that converts **15b** into **15a**.

A similar approach was used by Akabori and co-workers to investigate the cation extraction ability of the diazastilbene analogue **16a** (scheme 1.10) from an aqueous solution containing monovalent cations like Na^+, K^+, Li^+, Rb^+ and Me_4N^+.[54] They found that irradiation with UV light of a solution containing **16a** increase the amount of cation extracted by the compound. This phenomena was explained as the result of the *cis-trans* photoisomerization of **16a** into **16b** that decreases the distance between the binding sites

present on the molecule: a crown ether and an alkyl phosphoric acid. Thus the photochromic compound can act as tweezers able to grab a cation.

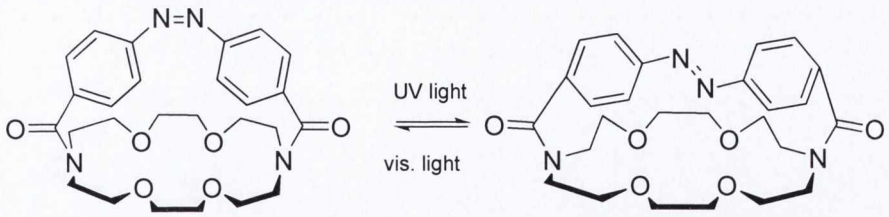


16a **16b**

Scheme 1.10 *Trans-cis* isomerization of **16a** into **16b** by UV light irradiation UV light with consecutive binding of a metal cation M^+= Na^+, K^+, Li^+, Rb^+ and Me_4N^+.

The azobenzene-bridged crown ether **17a** was synthesized by Shinkai and collaborators.[55] In this analogue the diazastibene phenyl rings are linked to the same crown ether. The photoisomerization of the diaza compound from *cis* to *trans* produces a stretching of the bonded macro cycle. Thus the inner area of the crown ether can be modified by means of irradiation with light at different wavelength driving its selectivity toward cations with different size. For instance they found that the *cis* isomer **17a** has a wider inner area with respect to its *trans* analogue **17b** as a consequence of the more compact and constrained geometry of the *cis* form (scheme 1.11). Thus the *cis* isomer should prefer large cations while the *trans* analogue should prefer smaller ones. The result of the solvent extraction efficiency of a series of monovalent cations with **17a** was in the order of $K^+ > Na^+ > Rb^+ > Li^+$ and Cs^+. The corresponding *trans* analogue **17b** extracted the same cations in the order of $K^+ > Na^+ > Li^+ > Rb^+$ and Cs^+. Large alkali metal ions such as Rb^+ and Cs^+ are hardly extracted by the *trans* isomer while small cations like Li^+ are not extracted by the *cis* isomer.

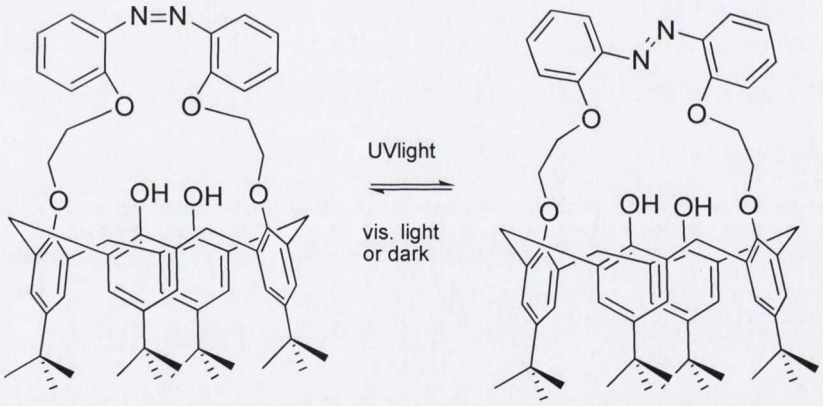
Pipoosananakaton and collaborators synthesized new derivatives of *p-tert*-butylcalix[4]arenes capped with a diazastilbene.[56] Compound **18a** shown in scheme



17a **17b**

Scheme 1.11 Reversible *cis-trans* photoisomerization of **17a** into **17b** by UV and visible irradiation.

1.12 is one of these derivatives. They interestingly found that the stable isomer is the *cis* one, due to the rigidity of the calixarene ionophore. After irradiation with UV light, a mixture of *cis* and *trans* **18b** isomers were obtained. The *trans* form reverts back to *cis* conformation both upon irradiation with visible irradiation or thermal fading after storage in the dark. Complexation analysis with sodium and potassium salts showed that Na^+ preferred to bind the *cis* form **18a** while K^+ preferred to bind the *trans* isomer **18b**.

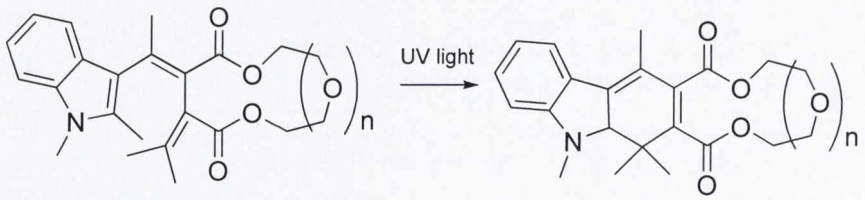


18a **18b**

Scheme 1.12 Reversible *cis-trans* and *trans-cis* photoisomerization of **18a** into **18b** by UV and visible irradiation/storage in the dark respectively.

1.3.2 Photoswitchable Receptors Based on Fulgides

Thermal decoloration of fulgides is a forbidden path. The transformation between the two isomers is fully controlled by UV and visible irradiation.[57] Despite these appealing



19a n=2
20a n=3
21a n=4

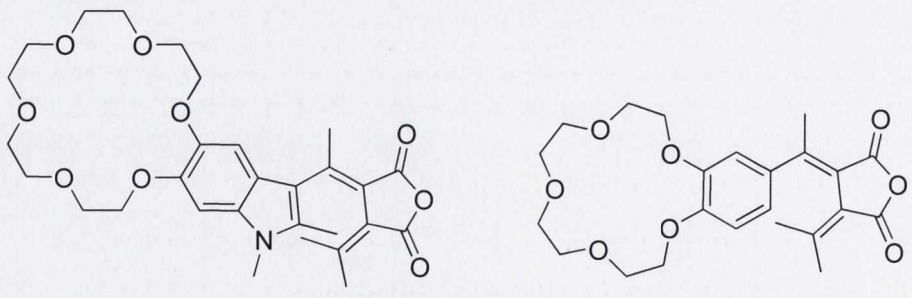
19b n=2
20b n=3
21b n=4

Scheme 1.13 Photoisomerization of fulgenates **19a**, **20a** and **21a**, into their corresponding closed isomers **19b**, **20b** and **21b** driven by UV irradiation.

features, just a few examples of fulgides bearing an ionophore suitable for ion sensing were found in literature.

Yokoyama and co-workers reported the photochromism of three fulgenates bridged with tri- (**19a**), tetra- (**20a**), and pentaethyleneglycoles (**21a**) as binding sites and they studied the interactions with Li^+, Na^+ and K^+ of their colourless and coloured forms.[58] Compound **19a** and its closed isomer **19b** did not bind cations effectively because of the small size of their ionophore. The association constant for Na^+ was large for **20a** and that for K^+ was large for **21a**. The photoisomerization of **20a** and **21a** into their corresponding closed forms **20b** and **21b** produced a drop in the affinities for sodium and potassium. This phenomena were given by the higher flexibility of the open isomers that guarantees a better interaction with the cations. The fulgenates synthesized by Yokoyama are depicted in scheme 1.13.

Guo and co-workers synthesized the two fulgides **22** and **23** (scheme1.14) bearing a



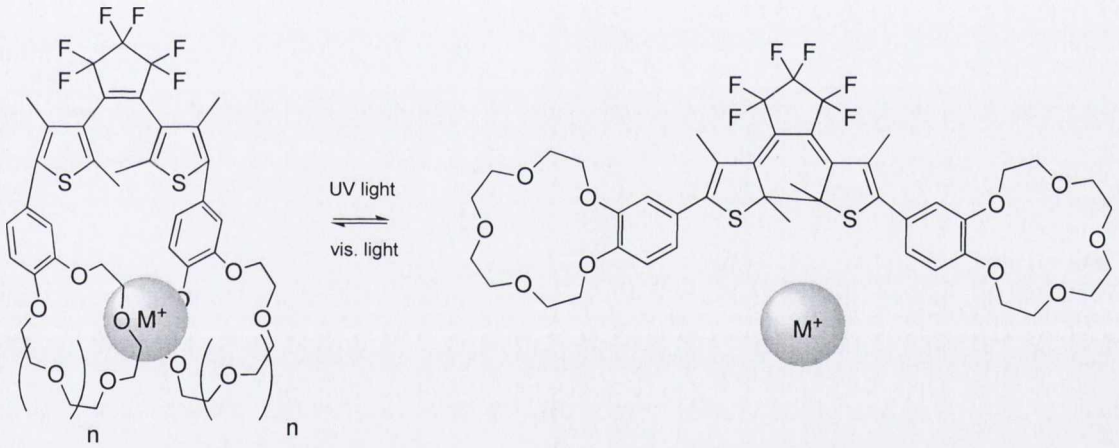
22 **23**

Scheme 1.14 Benzo-18-crown-6 indolylfulgide **22** and benzo-15-crown-5-modified fulgide **23** synthesized by Guo *et al.*

benzo-18-crown-6 moiety as ionophore.[59] The interactions with alkali and alkaline earth metal cations were studied. The decoloration rate of the closed isomers of the two derivatives evidently decreases upon selective cation binding. A hypsochromic shift of the absorption of the open and closed forms by up to 50 nm was also observed upon complexes formation.

1.3.3 Photoswitchable Receptors Based on Diarylethenes

Switching of host-guest interactions by photoirradiation potentially enables to carry out active transportation of guest molecules or simply to detect certain chemical species. The photochromic properties of diarylethenes can also be exploited for such purposes as their switching unit may be modified with appropriate functional groups suitable for interacting with a chemical guest.



24a n=0
25a n=1
26a n=2

24b n=0
25b n=1
26b n=2

Scheme 1.15 Photoresponsive tweezers based on crown ether functionalized diarylethenes synthesized by Takeshita and collaborators.

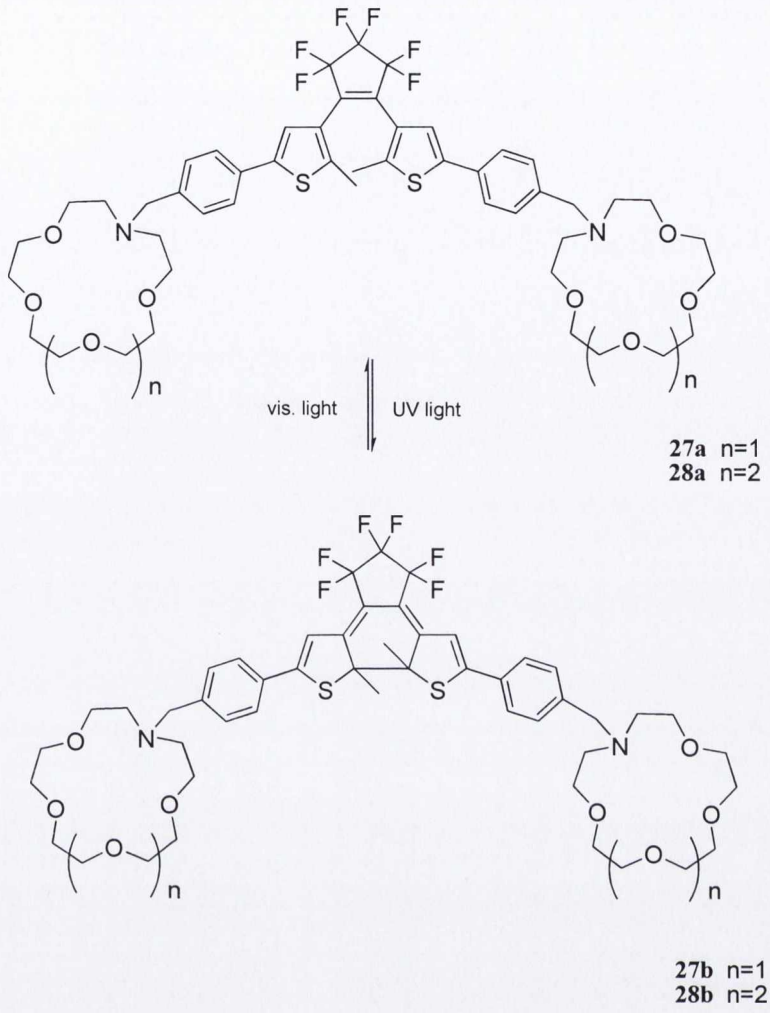
Takeshita and co-workers reported in several publications the chelation of different metal cations by means of the modified diarylethenes **24a**, **25a** and **26a** where two crown ether units with different inner area were introduced in the molecular skeleton.[60-62] When the crown moieties are parallel to each other in the open forms, they are able to capture in a tweezer like manner a large metal cation. The photoisomerization to the

closed isomers **24b**, **25b** and **26b** carried out by irradiation with UV light (330 ± 70 nm) forces the two crown units to separate from each other, impeding the metal chelation. Thus, if the switchable unit is open and chelating a metal cation, by irradiation with UV light the cation should be released. Irradiation with light at wavelengths higher than 450 nm, triggers the reverse process of ring opening. Thus, following structural rearrangement that brings the crown ether moieties in close proximity, the re-uptake of the metal cation would take place (scheme 1.15).

The same authors studied the two-phases solvent extraction of alkali metal picrates by the three compounds mentioned above. An estimate of the amount of cations extracted by the diarylethenes was given by the absorption decrease of picrates in the aqueous phase. They noticed that compound **25a** bearing a benzo-15-crown-5 ether extracted 50% of potassium and rubidium picrates from the aqueous phase. After irradiation with UV light the amount of the same picrates extracted fell to 20%. A similar result was observed for the extraction of caesium picrate extracted by compound **26a** bearing a benzo-18-crown-6 ether which decreased dramatically after photoconversion to the closed isomer **26b** by irradiation with light at 330 nm. Compound **24a** possesses the smallest ionophores in the series and its extractability was studied as well but the photoeffect was not remarkable.

Kawai synthesized a novel series of diarylethenes (compounds **27a**, **28a** and their corresponding photoproducts **27b** and **28b** depicted in scheme 1.16) bearing two crown ether units linked to the switchable core via methylenic bridges.[63] This approach affords structures that are similar to those synthesized by Takeshita but with a slightly increased flexibility of the ionophores. The phase extraction of lithium, sodium, potassium, caesium and rubidium picrates was studied and both the photoisomers **27a** and **28a** showed good capability of extracting all the cations with marked preference for K^+ while no extraction of Li^+ was observed.

Hu and co-workers developed two new diarylethene **29a** and **30a** with terpyridine units (tpy) attached via a phenylene linker to the thiophene rings.[64] This compound showed good photochromic properties. First of all, the tpy residues are fluorescent. If the switchable unit is in its open form and intense fluorescent band with maximum intensity at 467 and 458 nm are visible upon excitation at 365 nm. Irradiation with UV light triggers the ring closure of the diarilethene units affording the isomers **29b** and



Scheme 1.16 Photochromism of crown ether modified diarylethenes synthesized by Kawai.

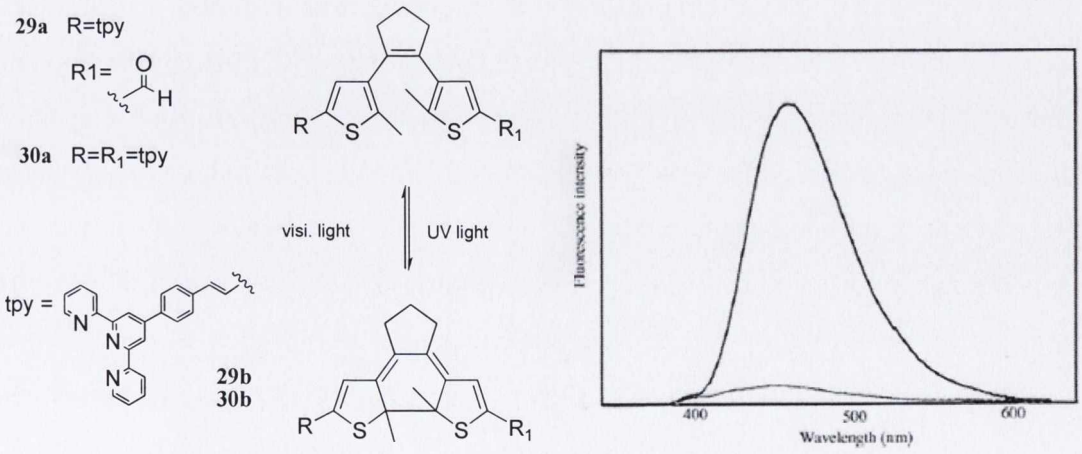


Figure 1.5 Schematic representation of the photoconversion of **29a** and **30a** into **29b** and **30b**. Fluorescence spectra of **30a** before and after irradiation with UV light (λ_{exc} = 365 nm).[64]

30b. As a consequence of the efficient energy transfer from the terpyridine units to the aromatic system of the closed switch, emissions undergo a drastic quench (figure 1.5).

The presence of Mn^{2+}, Co^{2+}, Ni^{2+}, Cu^{2+}, Zn^{2+}, Pb^{2+} caused changes to the spectral properties of the ligands. It is worth to notice that the presence of zinc in a solution containing the open form **30a** caused a dramatic redshift of 100 nm in the emission maximum due to the ligation of the metal cation to the tpy units (figure 1.6). Thus, this analogue may be considered a potential candidate for zinc sensing.

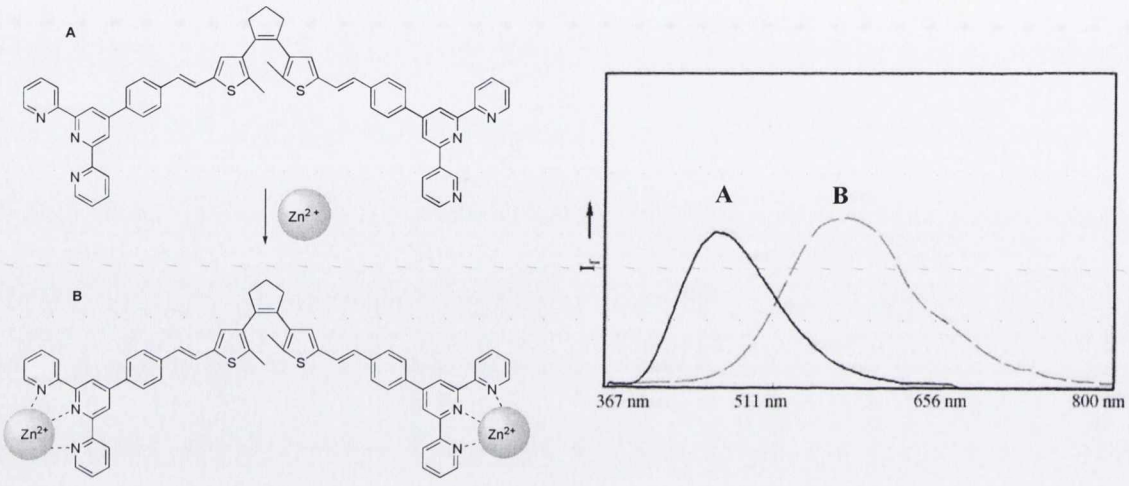
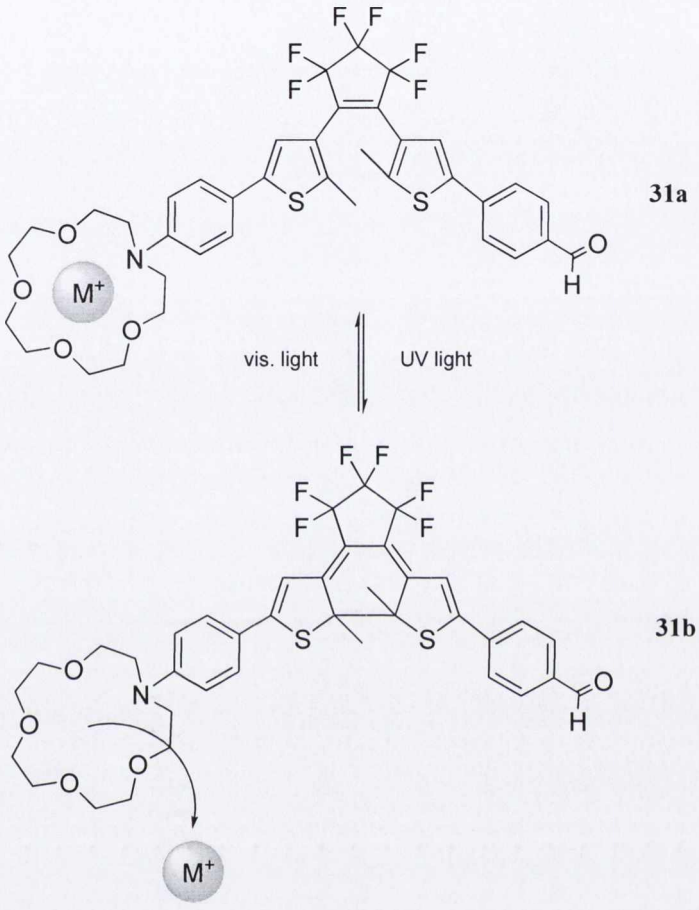


Figure 1.6 Schematic representation of the interaction between **30a** and Zn^{2+}. Fluorescence spectra of **30a** before (**A**) and after addition of Zn^{2+} (**B**) (λ_{exc} = 365 nm).[64]

A stunning example of metal binding ability tuned by switching between the open and closed isomers of a functionalized diarylethene was reported by Malval and collaborators.[65] The two thiophene rings of the molecular switch **31a** are functionalized with a chelating crown ether and an electron withdrawing formyl group respectively. Ligation of Ag^{+}, Na^{+} and Ca^{2+} by photogenerated closed isomer **31b** gave a decrease of four order of magnitude in the binding affinities for these metals with respect to the complexation by the open isomer **31a** (scheme 1.17). The lowered binding ability is the result of a decrease of the electronic density in the crown ether of the closed form due by the communication through an extended aromatic system between the ionophore and the electron withdrawing formyl group on the other thiophene ring. If the diarylethene is open, the conjugation through the molecule skeleton is disrupted and the electronic effect of the formyl group is not allowed to take place. Thus, the higher

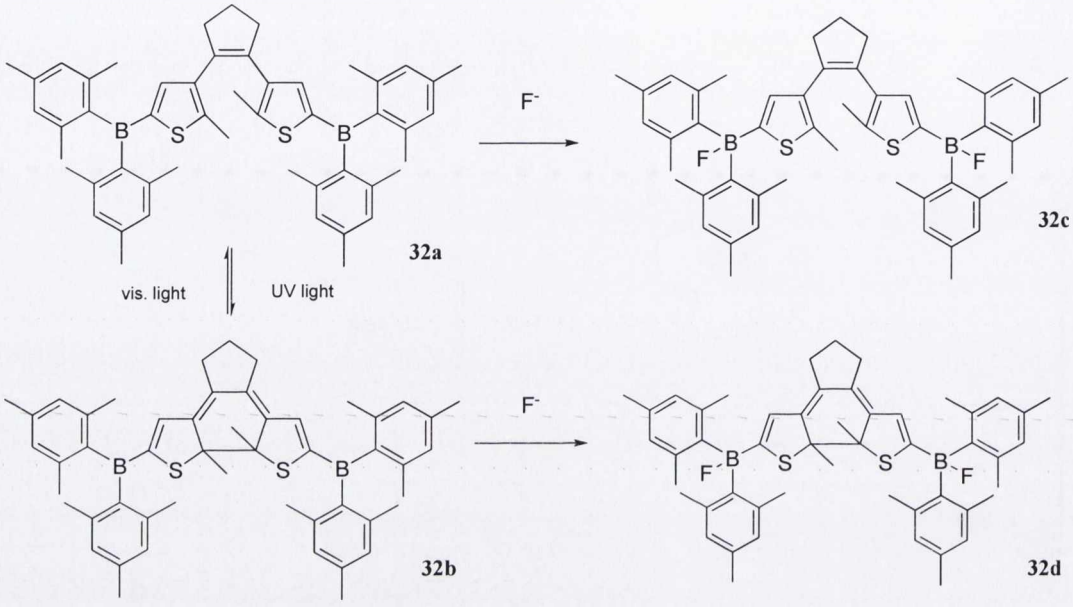
electronic density of the ionophore in the open form results in a better interaction with a cationic guest. In this way the uptake/release of metal cations may be effected by switching the photochromic core of this system with UV and visible light.



Scheme 1.17 Schematic representation of the cation release/uptake by compound **31a** after its photoisomerization to the closed form **31b** driven by irradiation with UV and visible light.

Zhou and co-workers reported the synthesis of the organoboron based diarylethene **32a** and studied its selective interaction with fluoride anions.[66] They observed that this compound, functionalized with two dimesitylboryl residues on the thiophenic rings, responded to UV irradiation with the appearance of a new absorption band at 655 nm indicating the formation of the closed isomer **32b**. As shown in scheme 1.18, the conversion was reversible upon irradiation with visible light and the starting material was readily regenerated under these conditions. Additionally, both isomers responded to

the presence of F^- with dramatic shifts in their absorption spectra indicating the formation of two adducts **32c** and **32d**. The most dramatic absorption change was observed after the addition of F^- to a THF solution of **32a** whose absorption maximum blueshifted from 655 to 490 nm due to the formation of **32d**.



Scheme 1.18 Interconversion between **32a** and **32b** controlled by UV and visible irradiation and formation of adducts **32c** and **32d** after addition of F^-.

Switching of host-guest interactions between a diarylethene functionalized with two boronic acid units and saccharides has been reported.[67] Derivative **33a** undergoes reversible photoisomerization upon UV irradiation to the corresponding closed ring isomer **33b**. As expected, the latter could be converted back to the starting material by means of visible light. The open form could exist in two conformations, parallel and anti-parallel, which exchanges rapidly at room temperature. In the parallel conformer, the two thiophene rings and the two boronic acid groups present on them face each other in a tweezer like fashion. Thus, the two boronic moieties may form linkages with a saccaride, generating a chiral complex which is CD active and whose chirality is due by the sugar configuration. Indeed, after addition of D-Glucose to an ethanolic solution of **33a**, a drastic increase of the $\Delta\varepsilon$ at 224 nm indicative of the diarylethene-saccharide complex formation was observed (figure 1.7). This value decrease of 60% after

irradiation of the same solution with UV light. This phenomenon is the result of the ring closure of the diarylethene which separate the two boronic functionalities and impedes the interaction with the glucose molecule. The 100% of the Δε value is restored after irradiation with visible light.

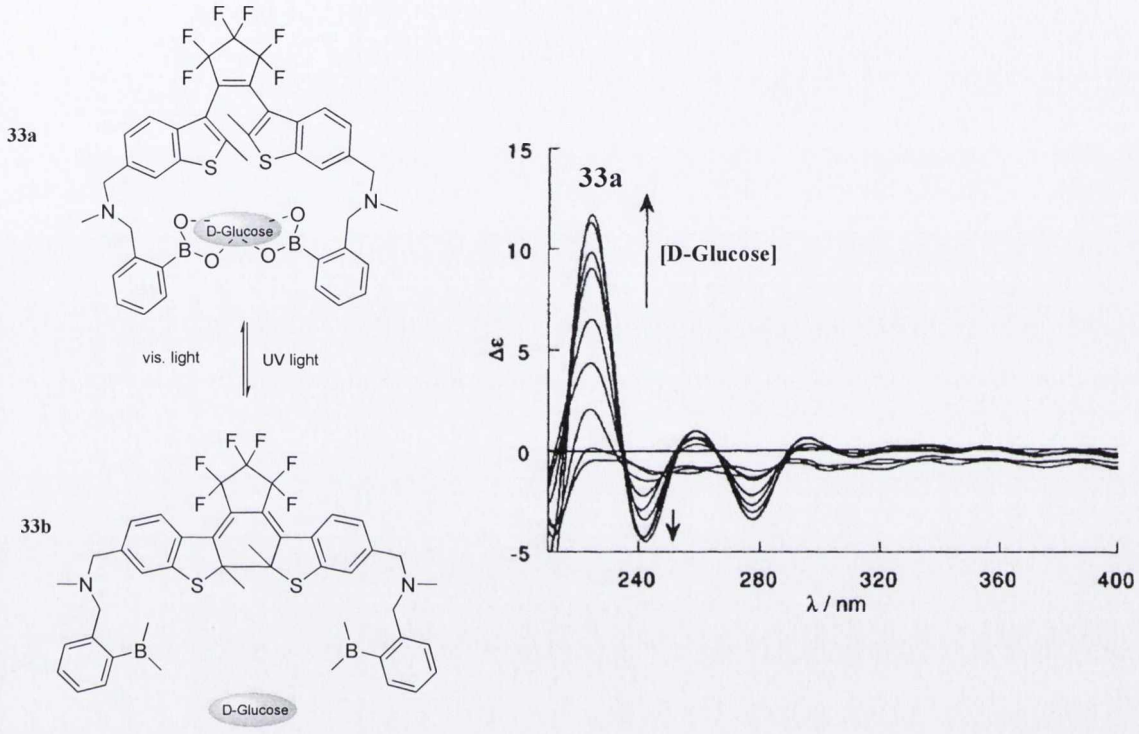
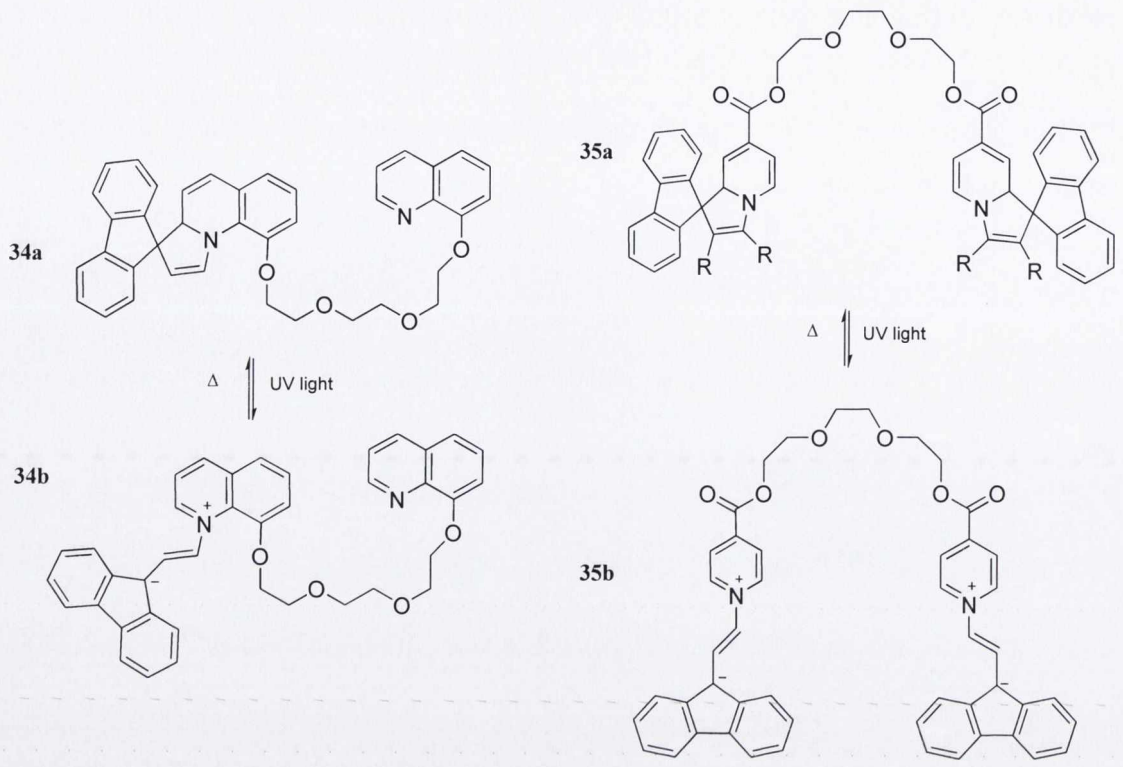


Figure 1.7 Schematic representation of the switchable interaction between **33a** and D-Glucose. CD spectra change upon addition of D-Glucose (7×10^{-4} M) to a solution of **33a** (1.4×10^{-5} M) in EtOH-tris-HCl (pH 7.8).[67]

1.3.4 Photoswitchable Receptors Based on Dihydroindolizines

Transformation of dihydroindolizines to their corresponding betaines is actuated by UV irradiation while the reverse process is driven by irradiation with visible light or thermally. A new approach for tuning physical properties of DHIs *via* host-guest interactions has been reported and involves the complex formation in crown, calixarene and ether containing molecular switches.[68-70]

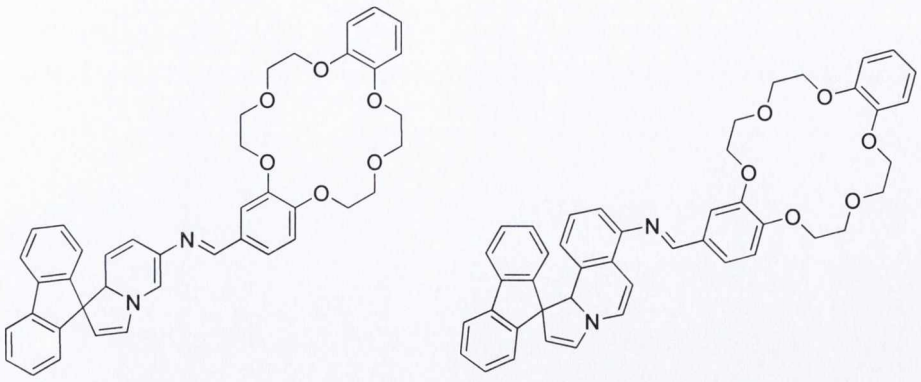
Two example are molecules **34a** and **35a** reported Dürr.[70] In both of them a dihydroindolizine core is attached through a polyethyleneglycol linker, the ionophore, to a quinoline and to an additional indolizine unit. Photoinduced ring opening by means



Scheme 1.19 Interconversion between **34a** and **35a** controlled by UV irradiation and thermal fading of **34b** and **35b** to their corresponding starting materials.

of UV light causes the formation of the betaine isomers **34b** and **35b** which revert back thermally (scheme1.19). Complexation of alkaline cations by the different isomers produces only small changes in the spectral properties of these molecules due to the high flexibility of the ionophore.

More remarkable changes were observed for compounds **36** and **37** containing crown ether units as ligands (scheme 1.20).[68] Compound **37** and the corresponding betaine responded to the addition of alkali and alkaline earth metal cations with bathochromic shifts in their UV spectra. Emission spectra underwent an intensity increase on metal guests addition and the conversion rate between the closed and open isomers changed depending on the cation added. In particular, alkali metal cation decelerate the ring opening and closing while alkaline earth accelerate the process.



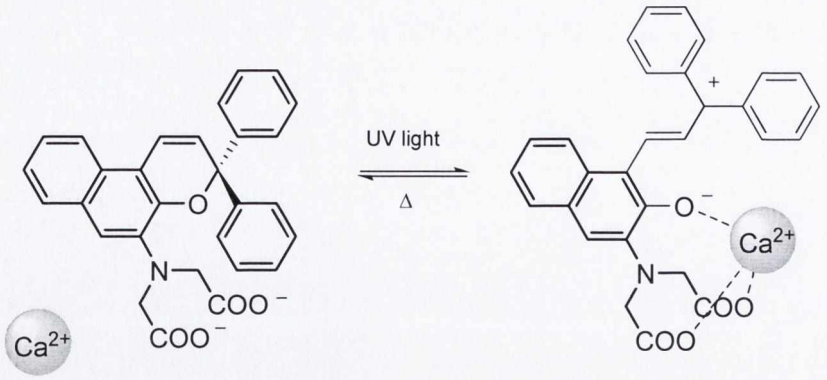
36 37

Scheme 1.20 Dihydroindolizines **36** and **37** beating crown ether moieties as cation ligand sites.

1.3.5 Photoswitchable Receptors Based on Chromenes

Irradiation of a chromene colourless form with UV light leads to the cleavage of a C-O bond, resulting in coloured isomeric ring-opened forms which revert to the original form predominantly through thermal processes. Open forms are zwitterionic species where the anion is a phenolate. Such an electronically rich oxygen atom represents the starting point to tailor a system that incorporates other functionalities capable to act in synergy with the phenolate itself to bind an ionic guest. Since the phenolate is the result of the photoinduced process of ring opening of a chromene, the metal chelation by such a system should be fully reversible and controlled by light. An example of this concept was reported by Kumar recently.[71] Molecule **38a** is a 3*H*-naphtho[2,1-*b*]pyran with an iminodiacetic acid substituent in 5 position. The photoinduced ring opening by continuous UV irradiation generates the isomer **38b** which exhibits higher affinity for Ca^{2+} than the closed form. The absorption maxima of the open form redshifted of 20 nm in the presence of calcium and a decrease of the thermal closure rate due to stabilization of the merocyanine coordinating the cation was observed. The cation release takes place when the irradiation ceases. Scheme 1.21 shows calcium uptake and release by the two isomers of compound **38**.

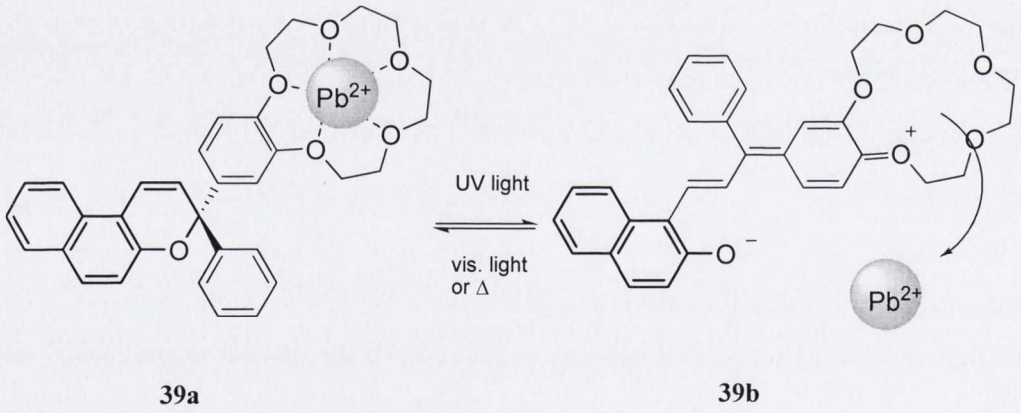
A different mechanism of uptake/release of Pb^{2+} is involved in the photoinduced chelation by compound **39**.[72] The electron density of the crown ether ring fused to one of the two phenyl groups of its isomer **39a** can be reduced by photoinduced ring



38a **38b**

Scheme 1.21 Ca^{2+} uptake and release by photoisomerization of compound **38a** to **38b** and *vice versa*.

opening by UV irradiation. The carbocation of the open form is consequently stabilized by electron donation from the crown ether. As a result, less electrons are available for coordinating a Pb^{2+} cation. Thus, while **39a** binds the guest in the cyclic ether, the photoinduced isomerization destabilizes the metal complex determining the metal liberation (scheme 1.22).

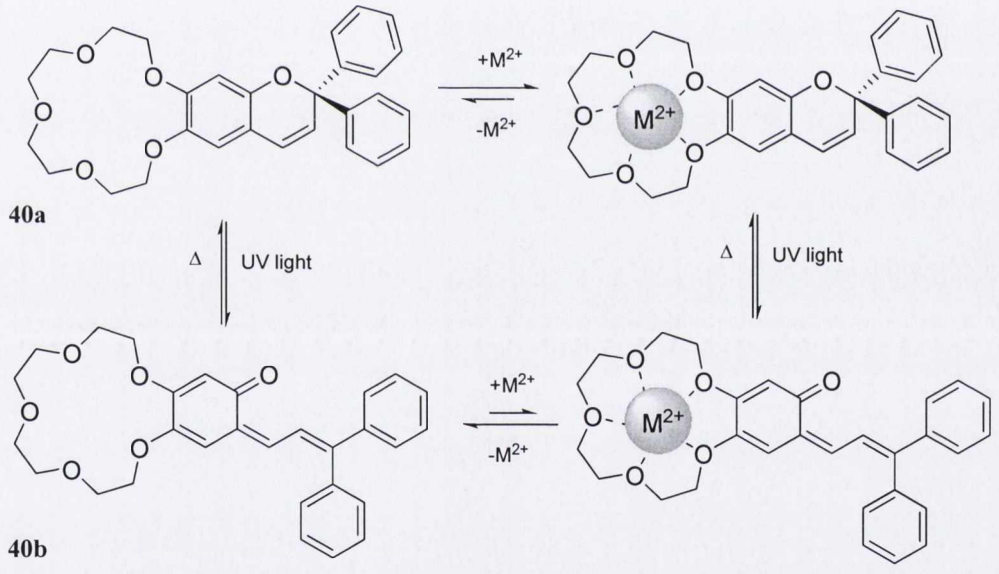


39a **39b**

Scheme 1.22 Uptake and release Pb^{2+} by the two isomers **39a** and **39b**.

The analogous effect of metal complex destabilization is achieved as well if the macrocyclic function is fused to benzopyran half of the molecular skeleton.[73] In this example, the chelation Mg^{2+}, Ba^{2+}, and Pb^{2+} by the two isomers **40a** and **40b** was extensively studied. Metal chelation produced slight shifts of the closed form absorption

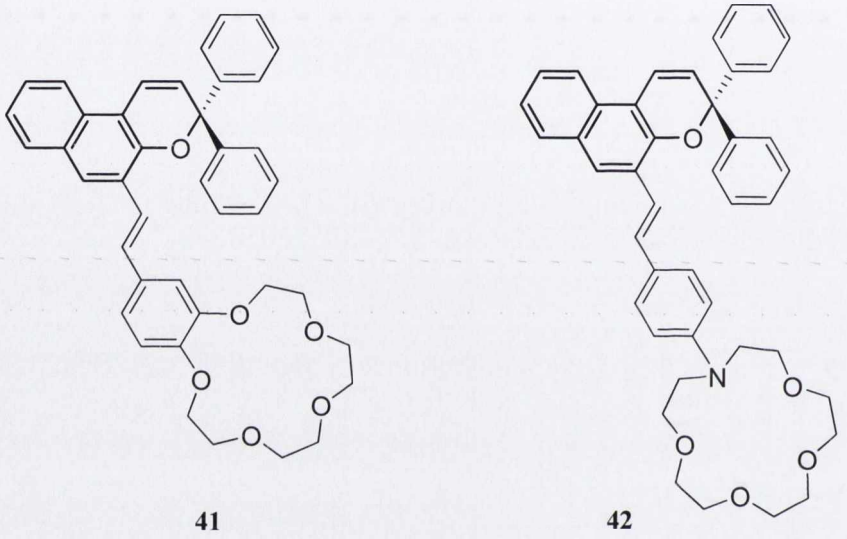
maxima without triggering ring opening photoisomerization. Complexes chromene-metal with stoichiometry 1:1 and 2:1 were observed depending on the cation radius. Generally smaller atoms tend to form 1:1 complexes while larger ones are coordinated by two crown ether moieties from two different molecule in a sandwich like fashion. Irradiation of acetonitrile solutions of ligand free **40a** resulted in the appearance of a new absorption band in the visible region which was attributed to the open photomerocyanine **40b**. The latter reverts back to its closed form following thermal path. Addition of metal to a chromene solution produced two significant effect on the ligand kinetic properties. The photomerocyanines appeared to have lower affinity to metal ions with respect to the corresponding closed isomers leading to partial destabilization of complexes. In parallel, complexation caused destabilization of the open forms resulting in a decrease of the coloured species lifetimes. Scheme 1.23 shows a representation of the equilibria involved in this processes.



Scheme 1.23 Modulation of the uptake and release of a cation by photoconversion triggered by UV irradiation of chromene **40a** to the corresponding merocyanine **40b**.

Glebov and collaborators introduced on a photochromic chromene scaffold a styryl fragment bearing crown ether ionophores. The corresponding molecules **41** and **42** are depicted in scheme 1.24. The styryl group offers a second photon switchable chromophore that undergoes cis-trans isomerization upon UV irradiation. Both photochromic effects, cis-trans isomerization of the styryl unit and ring opening and

closure of the chromene core driven by light were observed via UV-visible absorption spectroscopy. The inclusion of a Mg^{2+} cation in the ionophoric cavities did not produce any change to the photoinduced response to UV and visible irradiation by the molecules. This is due to the fact that the rate constant of complexes formation is less than the rate constant of their transformation to the open form. Additionally, the phenolate is too distant from the coordination site and this would not affect the chromene unit switchability.

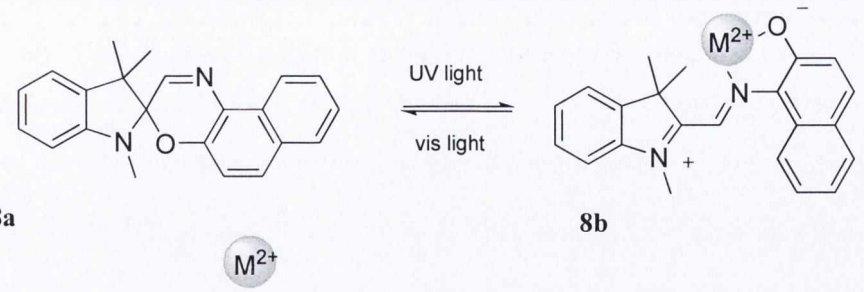


41 **42**

Scheme 1.24 Chromenes **41** and **42** synthesized by Glebov and co-workers.

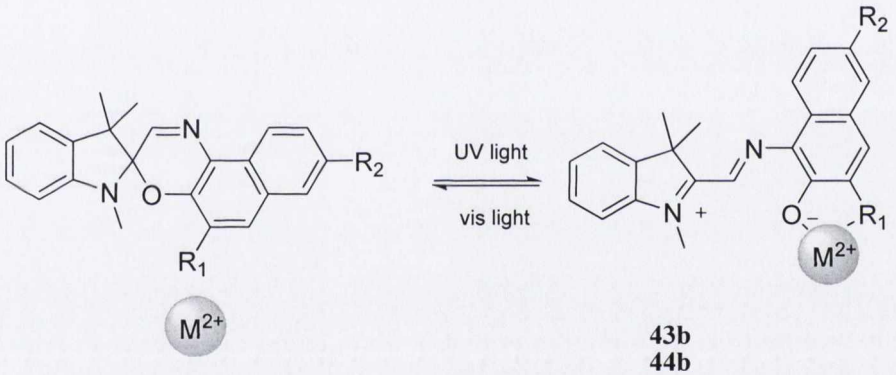
1.3.6 Photoswitchable Receptors Based on Spirooxazines

The chemical structures of spirooxazines are closely related to those of spiropyrans and chromenes as well as the mechanism of their photochromic reactions. In the same fashion of chromenes, heterocyclic cleavage of spirooxazines generate a metastable merocyanine. This species is a zwitterion whose negative charge is due to a phenolate anion site through which certain (d- and f-element) metal ions can bind, giving rise to a new absorption band in the visible spectrum.[74] A plausible mechanism for this chelation process is reported in scheme 1.25 and shows the reversible chelation of a hypothetical bivalent cation by the two isomers **8a** and **8b**, both previously reported. The azomethinic N and the phenoxide O may function as a bidentate chelator.



Scheme 1.25 Representative metal ligation by a common spirooxazine *via* phenolate-imine bidentate chelator.

More common strategies to produce a regenerable spirooxazine-based ligand are based on functionalization with suitable ionophoric groups. Generally, this additional coordinating groups are placed in a strategic position where they can easily interact with the phenolate and eventually cage a metal guest.

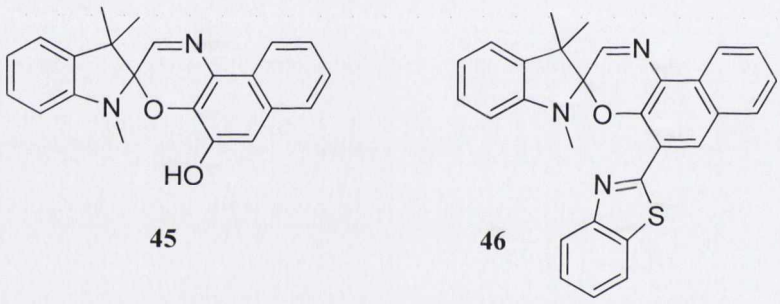


Scheme 1.26 Isomerization of compounds **43a** and **44a** to their corresponding isomers **43b** and **44b** followed by chelation of bivalent cations M^{2+}= Cu^{2+}, Ca^{2+}, or Pb^{2+}.

In 1989, Tamaki and Ichimura [75] first and other authors later,[76] reported that derivatives of spironaphthoxazine like **43a** and **44a** (scheme 1.26), with a coordinating group near the O atom of the naphthoxazine moiety could be transformed into the coloured merocyanine on UV irradiation and subsequently chelate to certain bivalent metal ions. Aqueous solutions of **43a** and **44a** respond to UV light with the typical conversion to the open merocyanine **43b** and **44b** which revert back to the closed forms *via* either P or T process. To generate complexes with Cu^{2+}, Ca^{2+}, and Pb^{2+}, irradiation

with UV light is necessary to produce the open forms. Thus, both the ester or methoxy groups and the phenolate anion can grab a cation together. The complex formation is detected as a slight blue shift of the open forms' peak maxima and significant retardation of the thermal decolouration rate in the dark. Metal release can be achieved through irradiation with visible light. The only presence of metals in the dark does not affect spirooxazines' spectra.

Both photoinduced and spontaneous ionochromism were observed for molecules **45**, that bear a hydroxy group in the 5'-position of its naphthoxazine half (scheme 1.27).[77] Chelation of Al^{3+}, Fe^{2+}, or Cu^{2+} by the open photomerocyanine was obtained under steady irradiation of spiroindolinonaphthoxazines with UV light. This induces a slight hypsochromic shift of its visible absorption band and increases the lifetime of this form, slowing down its thermal bleaching in the dark.

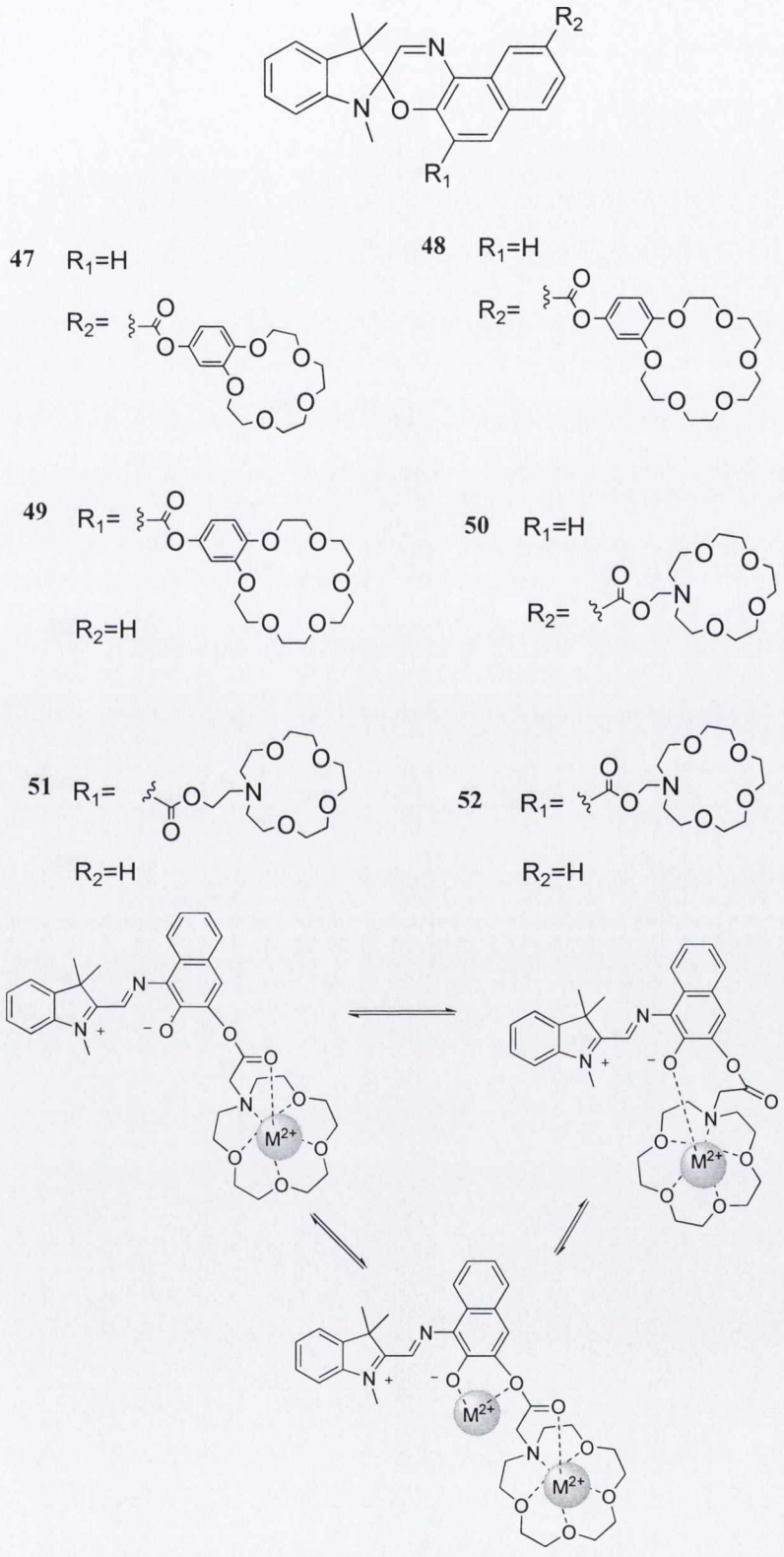


45 **46**

Scheme 1.27 Structures of photochromic and ionochromic spiroindolinonaphthoxazines **45** and **46**.

Complexation with the same metal cations allows the spiroindolinonaphthoxazine to isomerize to its open coloured form even under dark conditions giving a complex spectroscopically identical to the photoinduced product. In the same manner, coordination of Zn^{2+}, Co^{2+}, or Ni^{2+} by compound **46**, containing benzothiazolyl substituent in the naphthooxazine moiety as a potential chelating functional group (scheme 1.27), was achieved *via* photostimulation with UV light that triggers the isomerization to the corresponding open merocyanine. Additionally this derivative responded to the presence of cations even under dark conditions giving a complex spectroscopically identical to the photoinduced product. As a result of the coordination,

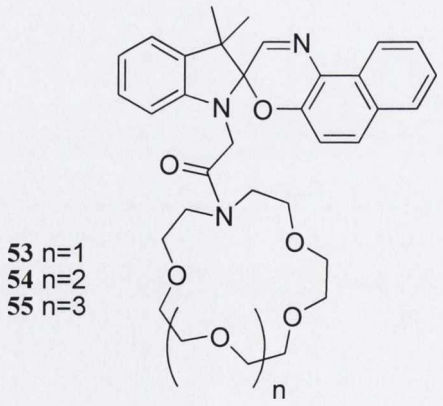
the thermal fading rate of the open form resulted dramatically decreased with respect to that of a solution containing only the photochromic compound.



Scheme 1.28 Structures of photochromic crown-ether functionalized spirooxazine **47-52** and equilibrium between the hypothetical different complexes involved in the chelation by compound **51**.

The synthesis and evaluation of the complexation ability of new spirooxazines containing benzo-15(18)-crown-5(6) and aza-15-crown-5 moieties in either 5' or 9' position (compounds **47-52**, scheme 1.28) have been reported.[78-81] The two ionophores differ from each other because of their rigidity which is higher in the first case. This constraint plays an important role in the metal coordination of bivalent cations. Indeed, compounds **47-49** can coordinate a metal cation relying only on the macrocyclic ether while the additional coordination by the phenolate oxygen of the open form does not take place.[78,79] Differently, compounds **50-52** containing an aza-15-crown-5 ionophore with a more flexible linker follows competitive routes in the coordination process.[80,81] Comparative studies were carried on spectral properties of crown-ether- containing and crown-ether-free analogues and it was found that the phenolate anion of the open forms of compound **51** and **52**, bearing the heterocyclic moiety in position 9', can coordinate both free metal cations and those already linked to an adjacent crown ether unit. A representation of this equilibrium between different metal complexes (in this case for compound **52**) is depicted in scheme 1.28.

The indolic nitrogen of a spirooxazine offers an additional site suitable for anchoring an ionophoric group. Thus the recognition site can rely on the synergy given by the near phenolate of the open form. A novel series of spironaphthoxazines, **53**, **54**, and **55** in scheme 1.29, functionalized with a monoaza crown ether ring on the indolic nitrogen have been reported.[82] Substantially, these three compounds differ from each other because of the their crown cavity size. They responded to the presence of alkali cations

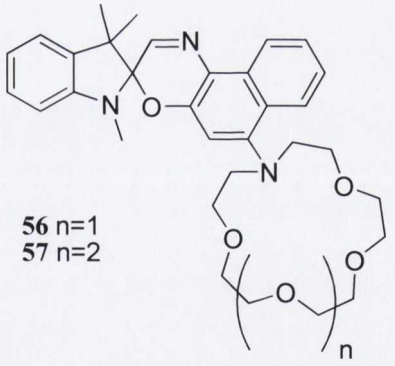


53 n=1
54 n=2
55 n=3

Scheme 1.29 Structures of photochromic spironaphthoxazines **53**, **54**, and **55** functionalized on the indolic part of the molecule with monoaza crown ether rings with different cavity sizes suitable for alkali metal cations recognition.

with the pyran ring opening and subsequent chelation of the tested cations. A comparative NMR study between these compounds and their spiropyran analogues bearing the same ionophores was carried out and it revealed that the affinity for metals of the spirooxazines is lower than that of spiropyrans. This is probably due by the fact that the open coloured forms of spironaphthoxazines are thought to exist also in their neutral keto forms, so that stabilization by an alkali-metal cation might not be essential.

The photochromic properties and ionochromism of two spironaphthoxazines conjugated with aza-15(18)-crown-5(6)-ether moieties at 8' position of naphthalene fragment were studied.[83] Upon addition of Li^+ and alkaline earth metal cations to solutions of **56** and **57** (scheme 1.30), blueshifts of the UV absorption bands of the closed forms and redshifts of the visible absorption bands of the open ones were observed. This phenomenon is due by the cation trapping in the crown ether cavity. The result of metal coordination is a dramatic increase of the open merocyanines lifetime. The photoinduced isomerization to their open form causes the decrease of the cation binding affinities.



56 n=1
57 n=2

Scheme 1.30 Structures of photochromic spironaphthoxazines **56**, and **57** functionalized with aza-15(18)-crown-5(6)-ether moieties at 8' position of naphthalene fragment.

1.3.7 Photoswitchable Receptors Based on Spiropyrans

The closed and open isomers of a spiropyrans are different chemical species that can undergo different reactions. This represents the basis for several applications in chemical sensing. Two reactive functions present in the coloured form but not in the colourless one are the phenolate anion and the positively charged indolium. The first

has been the most exploited so far as its electron donating properties allow the interaction with electronically poor species like transition metal cations. However, the indolium ion of the merocyanine **58b**, produced by irradiation with UV light of a solution of **58a**, has been reported to react selectively, sensitively, and reversibly with cyanide *via* nucleophilic addition (figure 1.8a).[84] The formation of the spiropyran-CN^- adduct **58b-CN^-** is detected in a water/acetonitrile solution, after UV irradiation, as the solution turned from pink to yellow and the appearance of an intense absorption band was observed in the visible region with maximum intensity at 421 nm (figure 1.8b and 1.8c). The cyanide detection is selective also in mixture with F^-, Cl^-, Br^-, I^-, AcO^-, $H_2PO_4^-$, HSO_4^-, ClO_4^-, NO_3^-, and SCN^- and it is fully reversible if the solution containing the adduct is irradiated with visible light.

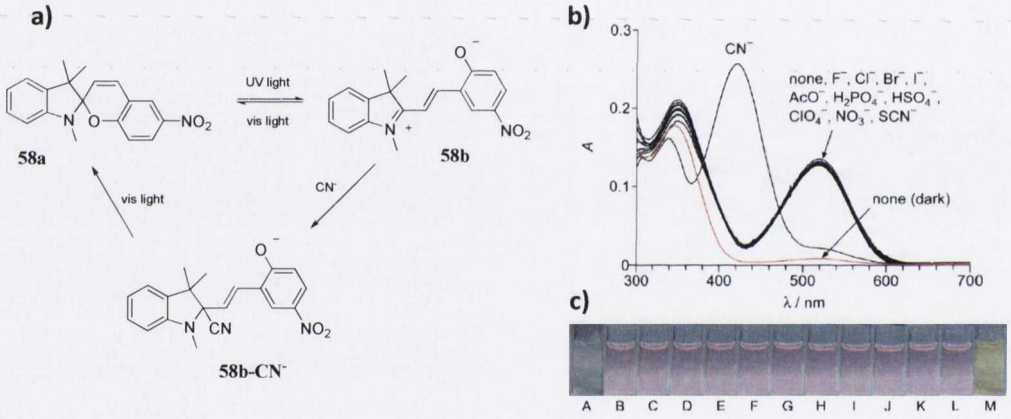
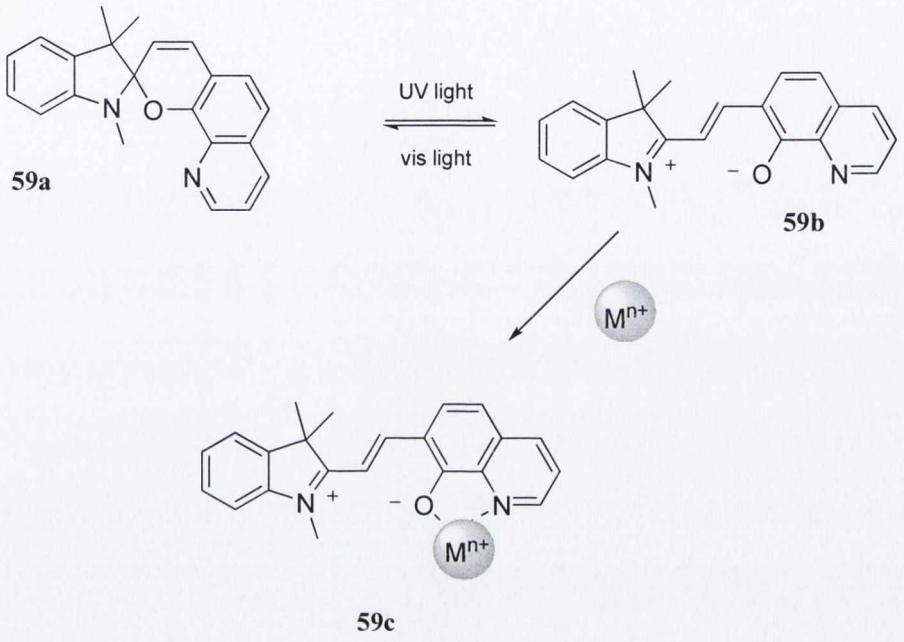


Figure 1.8 **a)** Structure changes of **58a** after irradiation with UV light (**58b**) and addition of CN^- (**58b-CN^-**); **b)** absorption spectra of 1 (20 μM) measured with 50 equiv of respective anions (as a *n*-Bu_4N^+ salt) in a water/MeCN mixture (1/1 v/v; CHES 100 mM, pH 9.3) under UV irradiation (334 nm) at 25 °C. The spectra were obtained after stirring the solution containing 1 and each anion for 30 min with UV irradiation. The red spectrum is obtained without anion in the dark; **c)** photograph of the solutions (A) without anion (dark), (B) without anion, (C) F^-, (D) Cl^-, (E) Br^-, (F) I^-, (G) AcO^-, (H) $H_2PO_4^-$, (I) HSO_4^-, (J) ClO_4^-, (K) NO_3^-, (L) SCN^-, and (M) CN^-.[84]

As afore mentioned, the phenolate anion in conjunction with another appropriate group can give a chelating moiety. The synthesis and ionochromism of various quinolinospiropyranindolines have been extensively studied. The photoisomerization of such systems generate a reactive oxine function which can operate as ligand for a multitude of metal cations. The first example was reported by Phillips and his co-workers that noticed the deep red-purple coloration of a colourless solution of

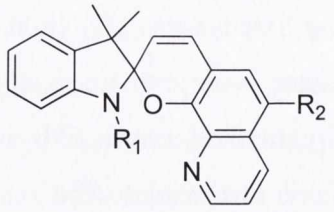
compound **59a**, few seconds after being irradiated with UV light and subsequent treatment with Cu^{2+} or Fe^{3+}.[85] These phenomena were explained as the result of the metal coordination by the photochemically generated oxine **59b** which exhibit its coordinating properties by forming the deeply coloured chelate **59c**.



Scheme 1.31 Photochromism and chelation of M^{n+}=Fe^{3+} or Cu^{2+} effected by the different isomers **59a** and **59b**.

The addition of a strong electron withdrawing group in *para* position with respect to the benzopyran oxygen, allows the delocalization of the electronic density of the phenolate anion. Thus the metal complexes are strongly destabilized and the metal can be ejected by photoisomerization to the closed form induced by visible light irradiation. Collins and collaborators reported their studies on zinc (II) release by the open form of spiropyran **60** (scheme 1.32), modified with a nitro group in 6' position, in aqueous environment.[86] They pointed out the fact that the cation release can be induced only if the molecule presents a strong electron withdrawing group opposite to the phenoxy oxygen.

Compounds **61-63** have the same skeleton of compound **60** but a chlorine as substituent in 6' position of the quinolinospiropyran half and different alkylic chains on the indolic nitrogen.[87] Their photochromic behaviour was investigated *via* UV-vis



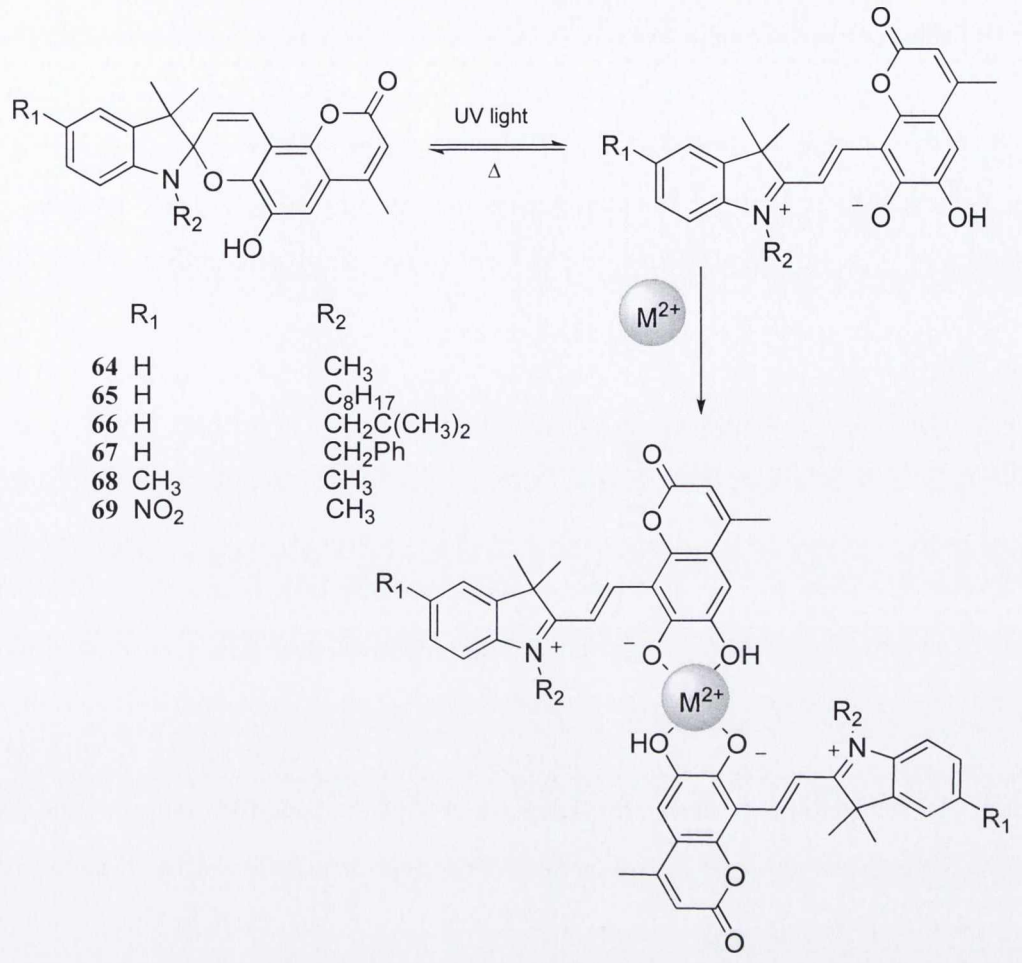
	R_1	R_2
60	CH_3	NO_2
61	CH_3	Cl
62	$(CH_2)_2OH$	Cl
63	$(CH_2)_2COOH$	Cl

Scheme 1.32 Quinolinospiropyranindolines **60-63** bearing different substituents on the indolic nitrogen and 6' position of the quinolinospiropyran moiety.

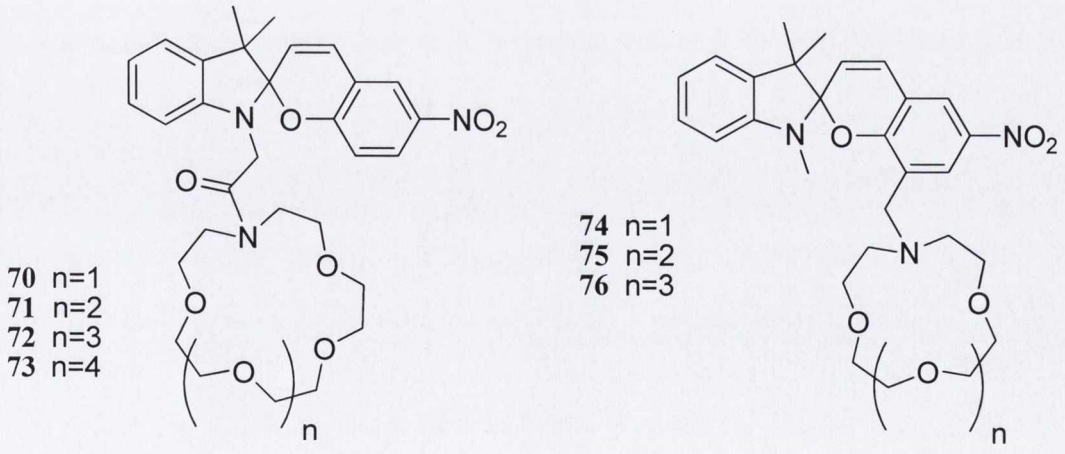
spectroscopy and the most stable merocyanine was that generated from irradiation of **61** with UV light. On the other hand, compounds **62** and **63** responded to the presence of zinc (II) and copper (II) with the formation of more stable complexes than those formed by compound **61**. This is due by the presence of the OH group on **62** and the COOH group on **63** which offer additional binding sites for the metal coordination.

Chelation of Mg^{2+}, Zn^{2+}, Ni^{2+}, Cu^{2+}, Hg^{2+}, and Pd^{2+} by spiropyrans **64-69** (scheme 1.33) has been reported.[88] The hydroxy group adjacent to the benzopyran oxygen is a common motif present in all the compounds belonging to this series. Once the spiropyrans isomerise to their open form, the hydroxy group is accessible for the coordination of a metal along with the vicinal phenolate. Different functional groups were chosen for R_1 and R_2. The presence of a strong electron withdrawing group like NO_2 in R_1 (compound **69**), reduced dramatically the merocyanine lifetime while an electron donating group like a methyl (compound **68**) stabilizes the open form in a metal free solution. The interactions of spiropyrans with the tested metal cations were examined via UV-vis absorption resulted in the appearance of intense absorption band in the visible regions, blueshifted with respect to those of the free metal merocyanines. Additionally all the complexes were found to have stoichiometry spiropyran-metal 2:1, which is plausible if two dyes in their open form cage the metal to form a quadridentate complex. The hypothetical structure of such a complex is depicted in scheme 1.33.

A new class of host molecules whose optical properties are markedly perturbed by the presence of cations, is that of crown ring bearing spiropyrans. Inouye and his collaborators reported on the ionochromism of spiropyrans **70-73** functionalized with different size monoaza crown ethers to their indolic nitrogen (scheme 1.34).[89] The ionophoric group is suitable for interacting with alkali metal cations whose presence



Scheme 1.33 Photoisomerization of spiropyrans **64-69** bearing different substituents on the indolic nitrogen and 5 position of the indolic half followed by complexation of a metal cation M^{2+}= Mg^{2+}, Zn^{2+}, Ni^{2+}, Cu^{2+}, Hg^{2+}, and Pd^{2+}. The complexes have stoichiometry spiropyran-metal 2:1.



Scheme 1.34 Structures of photochromic spiropyrans **70-73** functionalized on the indolic part of the molecule with monoaza crown ether rings with different cavity sizes suitable for alkali metal cations recognition.

gave rise to strong absorption band in the visible region, redshifted with respect to those of metal free solutions of spiropyrans, which absorbs in the UV region. The selective chelation of Li^+ was observed for compounds **70** and **71**, while **72** preferred Na^+. No changes in the absorption spectrum of **73** were observed upon addition of any alkali-metal due to the large cavity of the monoaza crown ether appendix which impedes a proper interaction with the metal guest. Analogously, spirobenzopyran derivatives having a monoazacrown moiety such as 12-crown-4 (**74**), 15-crown-5 (**75**) and 18-crown-6 (**76**) at 8'-position have been reported.[90] Binding of alkali metal ions such as Li^+, Na^+, and K^+ by their crown rings leads to isomerization of spirobenzopyrans in the dark. NMR spectroscopy carried out on the complexes containing the NMR active isotopes ^7Li and ^{23}Na suggested that cations, most significantly Li^+, coordinated by the crown moiety in the merocyanine isomer are subject to intramolecular interaction with the merocyanine phenoxide anion. The additional-binding-site effect is stopped on exposure to visible light as the cation-bound merocyanine readily reverts to its closed form, releasing the metal ions to some extent. Alternate irradiation with UV and visible light causes isomerization of the crowned spirobenzopyrans even in the presence of alkali metal ions, which in turn provides a tool for controlling their cation-complexing capability.

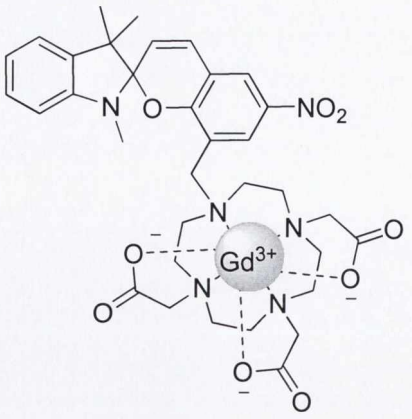
Inouye and collaborators reported the synthesis and the alkaline-earth selective chelation by spiropyran based cryptands with a diazacrown ether bridge that connect the two halves of the spirochromene backbone.[91] The crown ring cavity was varied in size. The addition of alkaline earth metal cation to acetonitrile solutions of compounds **77**, **78**, and **79** resulted in the appearance of broad absorption bands in the visible region whose maxima depended on the metal coordinated by the cryptand. The isomerization of compound **78** stimulated by the presence of Sr^{2+} was investigated via ^1H-NMR spectroscopy at 500 MHz in acetonitrile. Figure 1.9 shows the partial ^1H-NMR spectra of **78** as a function of time, before and after the addition of Sr^{2+}. The typical shifts of the closed form (figure 1.9a) underwent dramatic change after the addition of the metal (fig 1.9b) and reached a stable equilibrium after 3 hours from the addition (fig 1.9c).

A spiropyran based MRI (magnetic resonance imaging) contrast agent was described by Tu and his collaborators.[92] The molecule **80** is functionalized with an azacrown ether ring in 8'-position of its benzopyran part (scheme 1.35). The ionophore present three carboxylated appendixes which can cage a Gd^{3+}. At ground state, the complex exist in

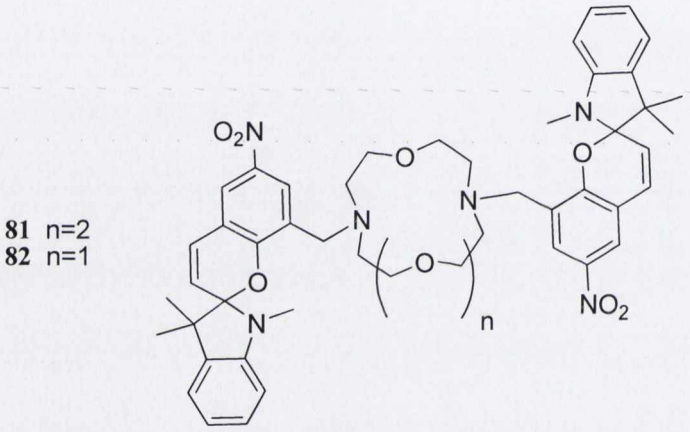


Figure 1.9 Partial 'H NMR spectra (500 MHz) of **75** in CD_3CN **(a)** before addition of SrI_2, **(b)** 30min after the addition, and **(c)** after 3 h.[91]

the open merocyanine form with the gadolinium coordinated by the crown ether and the phenoxy group of the photochromic unit. Irradiation with visible light produced the spiropyran ring closure accompanied by a relaxivity decrease of 18% while UV light restored the open merocyanine and the normal relaxivity. Addition of NADH to the complex caused a drop of relaxivity of 26% but this time the event was irreversible. Such a unique response to NADH offers the possibility to investigate non-invasively metabolic activities and cell signalling *in vivo*.



Scheme 1.35 Spiropyran based MRI contrast agent described by Tu.



Scheme 1.36 Structures of photochromic bis(spiropyrans) **81** and **82** used in the metal cation active transport through liquid membrane.

The behaviour of crowned bis(spirobenzopyran) **81** was investigated in solution and compared with the corresponding derivative with only one photochromic unit.[93-95] The complexation of bivalent and trivalent metal ions like especially Ca^{2+} and La^{3+}, by the macrocyclic ionophore promotes isomerization of the spirobenzopyran units to their corresponding merocyanines. The resulting metal complex is stabilized by intramolecular interactions between the crown-complexed cation and the two phenoxide anions. ^{1}H-NMR spectroscopy was carried out on the lithium-merocyanine complex generated from **81**. The results indicate that, upon complexation with Li^{+}, one of the two spirobenzopyran units in compound **81** isomerizes to the its open form. The

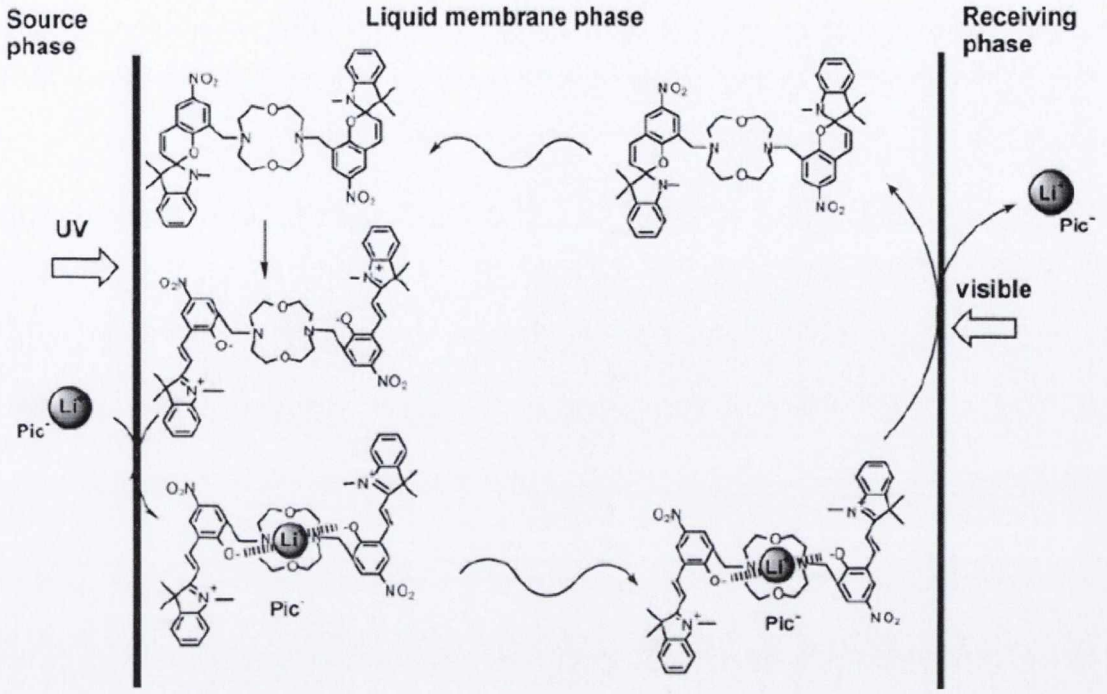


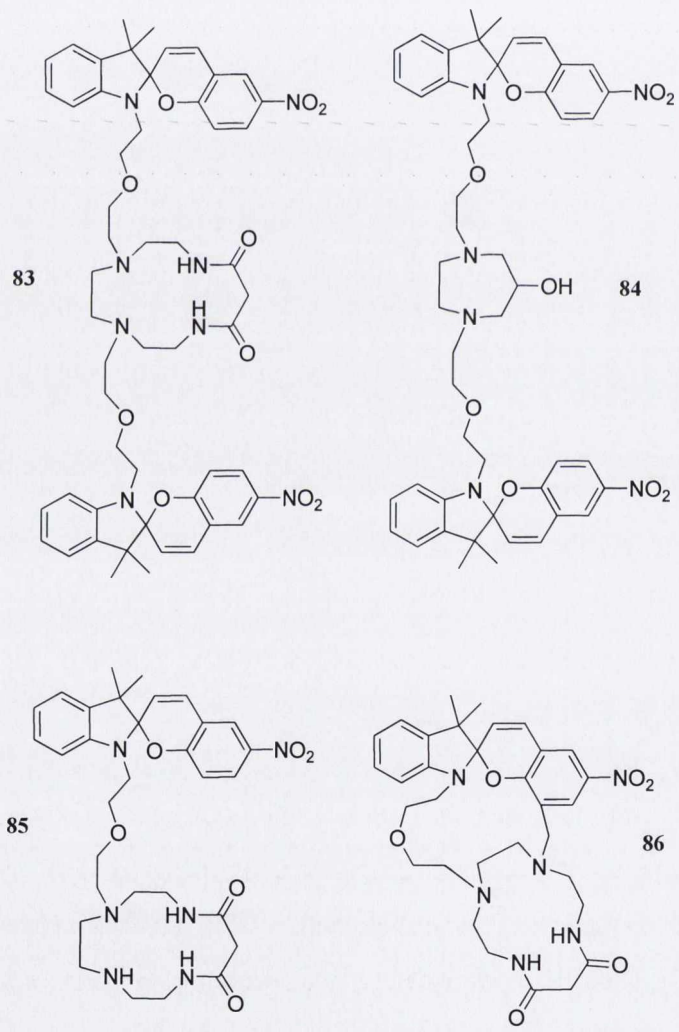
Figure 1.10 Mechanisms at boundary phase between source, membrane and receiving phases for transport of Li^+ through liquid membrane containing compound **82**.[96]

complexation of divalent and trivalent metal cations by **81** forces the second unit to isomerise and complete the whole binding cage around the metal guest.

An interesting application of the reversible ionophoric properties of spiropyran **81** and its corresponding derivative **82** (scheme 1.36) bearing a smaller crown ether bridge between the two spirochromene units, was reported more recently by the same authors. The metal ion transport using liquid membranes was investigated.[96] The transport was performed on a U-shaped glass cell with three distinctive phases. A source phase containing water solutions of alkali metals, an organic phase containing the crown ether modified spiropyrans and a receiving phase containing aqueous tetramethylammonium hydroxide. The transport of the alkali metal from the source phase to the receiving aqueous phase through the spiropyran liquid membrane was accelerated by UV-light irradiation and retarded under visible light exposure. When the visible light is on, the spiropyran units exist in their closed form and the interaction between the crown moiety and the metals is the only one likely to take place. Irradiation with UV light improves the interaction with the metal guests because of the additional binding sites on the open merocyanines. Thus the cation extraction from the source phase and the release in the

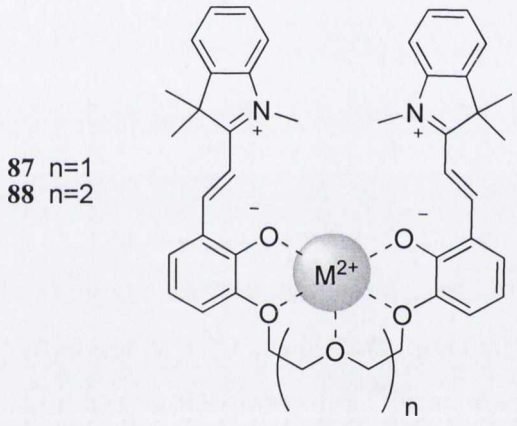
receiving phase is largely accelerated. A schematic overview on the transport of lithium picrate through a liquid membrane containing compound **82** effected by sequential switching of UV-visible light is depicted in figure 1.10.

Bis(spiropyrans) containing azacrown fragments **83** and **84** and their corresponding derivative possessing one photochromic unity, **85** and **86**, were reported by Liu and co-workers (structures **83-86** are reported in scheme 1.37).[97] They showed the capability to recognize transition metal cations like Cu^{2+}, Co^{2+}, and Ni^{2+} owing to isomerization to their corresponding merocyanines. High selectivity for Co^{2+} was observed for all compounds while compound **86** responded selectively to Cu^{2+}.



Scheme 1.37 Structures of photochromic bis(spiropyrans) **83-86** reported by Liu and collaborators.

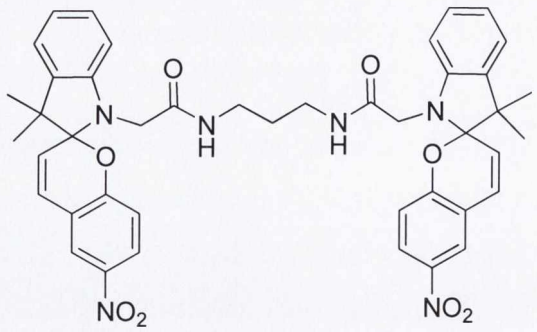
Another example of coordination of metal cations through the cooperation of two spiropyrans was provided by Yagi and co-workers.[98] They synthesized a series of chemosensors selective toward alkaline-earth metal ions. Such molecules consist of two spiropyrans linked to each other through an oligoether chain attached on position 8' of each photochrome. Compounds **87** and **88**,displayed in scheme 1.38, are two examples. They observed that the podands were able to coordinate selectively alkaline earth metal cations and the chelation involved both the merocyanine generated by the presence of the cation (scheme 1.38). This was confirmed by ^{1}HNMR analysis which showed signals consistent with the open form with no trace of the closed form. In addition the signals of the spacer were shifted indicating that it participated in the chelation. By modifying its length a higher selectivity toward cations with larger radii is achievable.[98]



Scheme 1.38 Alkaline earth cations selective sensor synthesized by Yagi and co-workers. The picture shows the hypothetical structure of the complex with a alkaline-earth metal cation M^{2+}.

In a similar manner, the selective binding of calcium and magnesium was achieved by linking two spiropyran units *via* alkylic tether attached to the indolic nitrogen of each photochrome.[99] Bis-benzospiropyranindoline **89** chelating ability was investigated and compared to simple mono-spiropyrans. Kinetic binding constants were measured and moderately strong metal binding occurs in acetone solution when the bis-spiropyran is irradiated with light at 365 nm. This binding is eight times higher than the binding of the analogous mono-spiropyrans studied. The absorption maximum of the merocyanine form of the bis-spiropyran at 548 nm is strongly influenced by the metal.

89



Scheme 1.39 Calcium and magnesium selective sensor **89** linking two spiropyran units *via* alkylic tether attached to the indolic nitrogen.

Absorbance maxima blue-shifts of 43 nm for Mg^{2+} and 22 nm for Ca^{2+} complexes were observed. Additionally, both metal complexes exhibited strong fluorescence with emission maxima at 586 nm (λ_{exc}=365 nm) for magnesium and 606 nm for calcium.

The selective coordinating properties towards lanthanide ions of the calix[4]arene derivate **90a** carrying two spirobenzopyran moieties were described by Liu and collaborators.[100] The two photochromic units are attached to the lower rim of a calixarene system via alkylic linkers. In the ground state, an acetonitrile solution contains **90a** and its corresponding isomer **90b** with the photochromic units isomerized to open merocyanines. ^{1}H-NMR analysis showed the equilibrium to be shifted toward **90b**, which absorbs in the visible region with maximum at 555 nm. Under dark conditions, addition of lanthanide ions resulted significant hypsochromic shifts from 68 to 84 nm accompanied by drastic intensity increase of absorption maxima in visible region. In these events, the authors hypothesized the lanthanides entrapment in the calixarene cavity followed by the metal coordination by the phenolic oxygen of the two open merocyanines. Thus the equilibrium between **90a** and **90b** is shifted toward a third new species **90c** (figure 1.11a). Addition of alkali metal cations (such as Na^+, K^+), alkali earth metal cations (such as Mg^{2+}, Ca^{2+}) or transition metal cations (such as Fe^{3+}, Cu^{2+}, Zn^{2+}) resulted in no visible changes in the UV-vis absorption spectra (figure 1.11b). Moreover, the lanthanide complexes exhibited strong fluorescence enhancement with respect to non coordinated lanthanide cations in solution. The complexes fluorescence was quenched after irradiation with visible light that caused the open merocyanines to isomerise to their corresponding closed form.

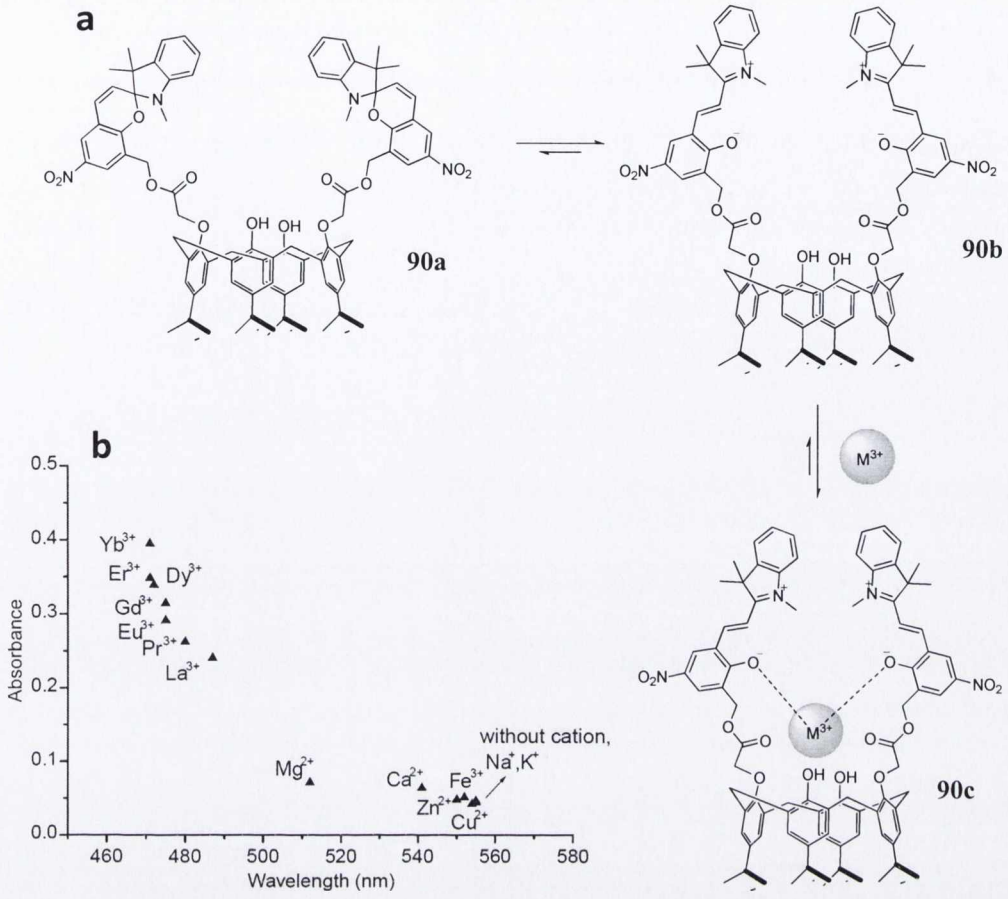


Figure 1.11 **(a)** Sketches of equilibrium reactions of compound **90a** and its corresponding isomers **90b** and **90c** in the presence of lanthanide ions M^{3+}; **(b)** UV-vis spectra of **90a** (40 mM) in the presence of and without metal ions (20 mM) in acetonitrile under dark conditions for 48 h. The selectivity toward lanthanides is obvious as the absorption maxima shift to shorter wavelengths and undergo dramatic intensity increases.[100]

A series of novel spiropyran functionalized to act as molecular receptors for a variety of hosts such as metal cations, aminoacids and glutathione was synthesized by Shao and his collaborators. These molecules possess outstanding properties despite the simplicity of their structures. The first example is spiropyran **91a** functionalized with a dimethylamino methyl substituent in the 8' position which forms a bidentate site with the phenolate oxygen of the open form **91b** that coordinates selectively Cu^{2+} (figure 1.12). While a metal free solution of **91a** does not absorb in the visible region, the coordination of copper (II) was detected as the appearance of a broad absorption band with maximum at 547 nm (spiropyran/metal ratio =2:1). The selective detection of copper (II) was performed by means of inner filter effect approach. The spiropyran was immobilized in a poly-(vinyl chloride) membrane with a fluorescent zinc meso-

tetraphenylporphyrin (Zntpp) fluorophore whose excitation band nicely overlaps with the absorption band of the **91b**. Thus, depending on the copper concentration, the porphyrin emission was quenched as the excitation light was competitively absorbed by the spiropyran metal complex. The detection was fully reversible as the liberation of copper ion from the complex was achieved by addition of EDTA to the complexed solution.[101] The plot in figure 1.12 shows the quenching of the membrane fluorescence after addition of increasing concentrations of Cu^{2+}.

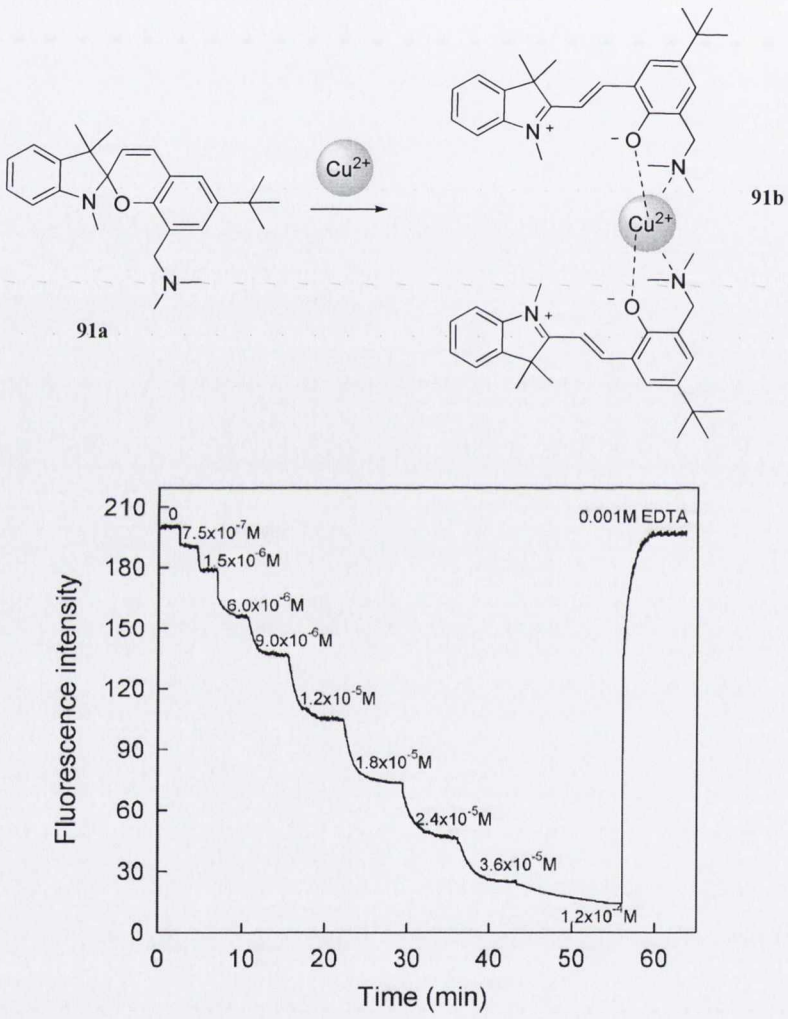


Figure 1.12 Schematic representation of the isomerization of compound **91a** to its open merocyanine **91b** with chelation of Cu^{2+}. The plot indicates time history of the sensing membrane responses to different concentrations of Cu^{2+}. Fluorescence intensity was recorded at 603 nm (λ_{exc}=556 nm).[101]

In the spiropyran derivative **92** , a morpholine functionality was covalently attached at the 8'-position instead of the dimethylamino group present on **91a**. The choice of this

new substituent improved both water solubility and absorbance response to the presence of Cu^{2+} ions. Indeed, compound **92** displayed extreme specificity toward Cu^{2+} in an aqueous solution even in the presence of a high concentration of competitive heavy metal ions. Additionally, the direct detection of Cu^{2+} in human serum in the presence these heavy metals was successfully performed. Such a response was not observed with derivative **91a**.[102] Figure 1.13 shows the photocolorability of the derivatives **91a** and **92** toward various metal ions defined as the absorption changes (A/A_0) at the wavelength of maximum absorption of spiropyran-metal complexes. Here A_0 and A are the absorbance of the photochromes in the absence of and the presence of a cation. The selectivity for Cu^{2+} of **92** is evident.

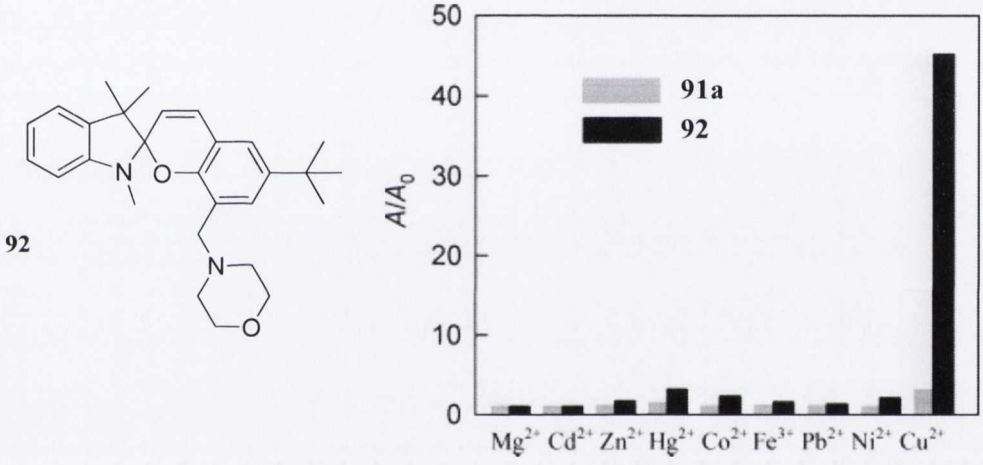


Figure 1.15 The absorbance changes, A/A_0, of ethanol/water solutions 1:1 of **91a** (gray, 540 nm) and **92** (black, 453 nm) upon addition of 5.0×10^{-5} M metal ions (x-axis markers), separately.[102]

In a different study, the same authors proposed a new method that allows simple and efficient recognition and quantification of cysteine (Cys) and homocysteine (Hcy) by spiropyran derivative **91a**.[103] The detection mechanism was proven by IR and ^{1}H-NMR techniques and it involves the cooperative ligation of either Cu^{2+} or Hg^{2+}, two merocyanines **91b** and two aminoacids linked to each other via disulfide bridge. The Cys and Hcy recognition was successful in aqueous media, at physiologic pH and it was selective over a series of different aminoacids. Figure 1.14 displays the mechanism

purposed by Shao for the cooperative ligation of the photochromic compound, Cys or Hcy, and either a copper or a mercury cation.

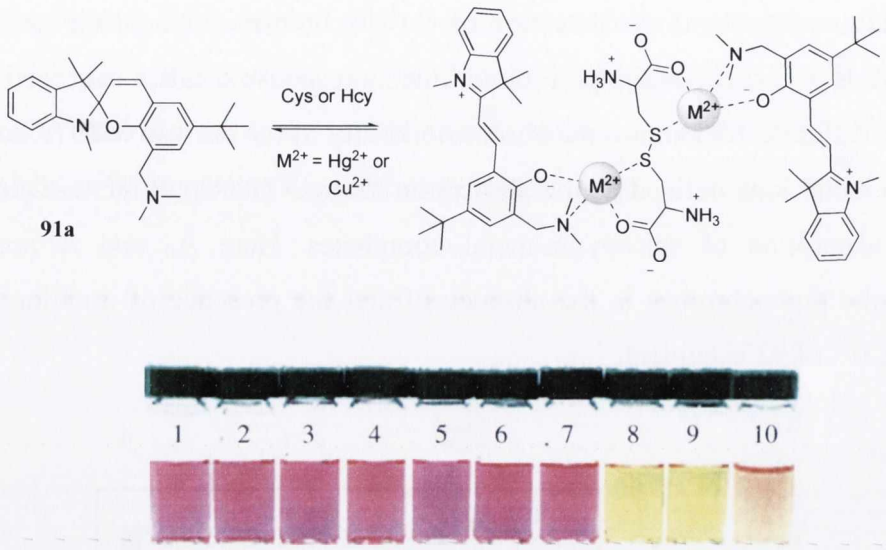


Figure 1.14 Color changes of an ethanol/water solution containing **91a** and Hg^{2+} in the presence of different amino acids: 1) no amino acid, 2) Gly, 3) Leu, 4) His, 5) Glu, 6) Asp, 7) Met, 8) Cys, 9) Hcy, and 10) GSH (glutathione).[103]

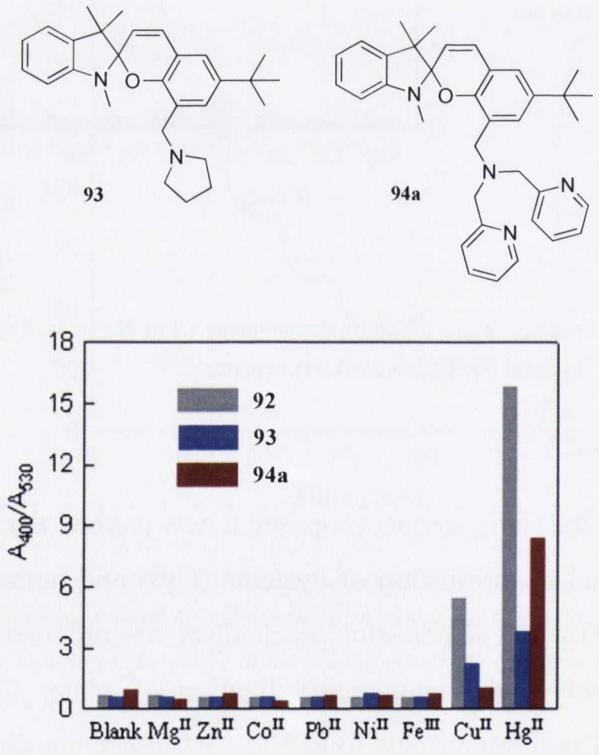


Figure 1.15 The absorbance ratio changes A_{400}/A_{530}, of **92a**, **93**, and **94a** in the ethanol–water solution upon additions of selected metal ions in the presence of Cys.[104]

The same approach of integrating a spiropyran molecule and an amino acid cooperatively to a metal center, could be used for optical sensing of Hg^{2+} ions in aqueous solution. The new spiropyran derivatives **93** and **94a** in figure 1.15 have been developed and their binding ability was tested over Mg^{2+}, Ca^{2+}, Mn^{2+}, Pb^{2+}, Fe^{3+}, Co^{2+}, Ni^{2+}, Zn^{2+}, and Hg^{2+} and compared with compound **92**. Considering the response sensitivity and the detection range in aqueous solutions containing 5% of ethanol, experimental conditions were optimized and the relative amount of Cys and spiropyran was set at 5:1. The histogram in figure 1.15 shows the sensors response to the tested metal cations as the ratio between two wavelengths, 530 nm and 400 nm, where the absorptions are notable for all spiropyrans. Interference was observed for the chelation of Hg^{2+} and Cu^{2+} by **92** and **93** while compound **94a** was fully selective for mercury.[104]

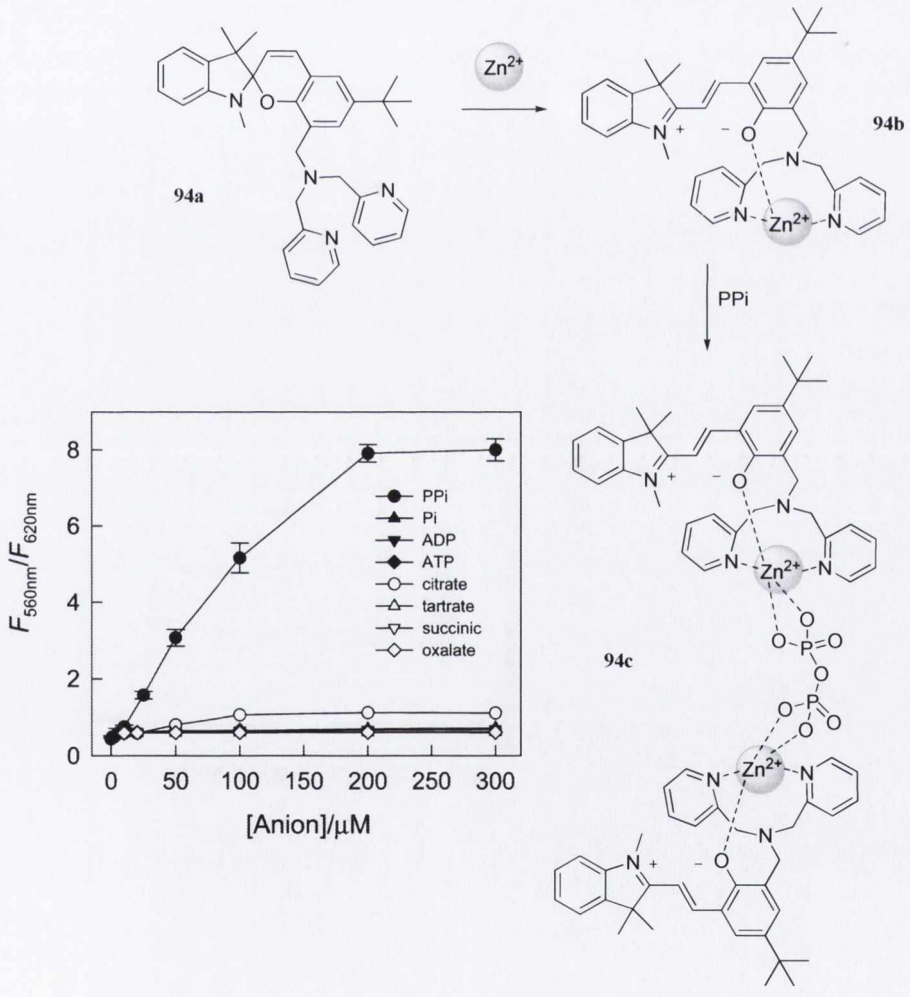


Figure 1.16 Mechanism of the chelation of zinc followed by the coordination of a pyrophosphate anion. The plot shows the changes in the fluorescence intensity of **94a** at 560 nm with respect to that at 620 nm in the ethanol aqueous solution (pH 7.4) upon addition of different concentrations of anions (λ_{exc}=522 nm). The values of F_{560nm}/F_{620nm} underwent an increase only i the presence of PPi proving the selectivity toward this anion.[105]

The Dpa substituent on **94a**, is known for its capability to form a complex with Zn^{2+} (**94b** in figure 1.16) in aqueous solutions. The authors found that the coordination between the two species encourages the ligation of a pyrophosphate anion (PPi) selectively (structure **94c**).[105] This phenomenon was studied extensively and the interaction mechanism was explained as the result of the coordination of a pyrophosphate by two spirochromene-zinc units (figure 1.16). The presence of PPi in an aqueous solution containing the **94c** complex was detected as a fluorescence intensity decrease at 630 nm concomitant to an increase at 530 nm. The fluorescent ratiometry plot in figure 1.16 shows the changes in the fluorescence intensity of **94** at 560 nm with respect to that at 620 nm in the presence of the different anion Pi, PPi, ADP, ATP, citrate, tartrate, succinate, and oxalate and the selectivity to PPi is obvious as it was the only detectable. Additionally, the PPi concentration in human urine was successfully determined.

Two novel bis(spiropyrans) **95** and **96**, incorporating two photochromes tethered to each other via either a piperazine or a binol linker, were synthesized aiming to the

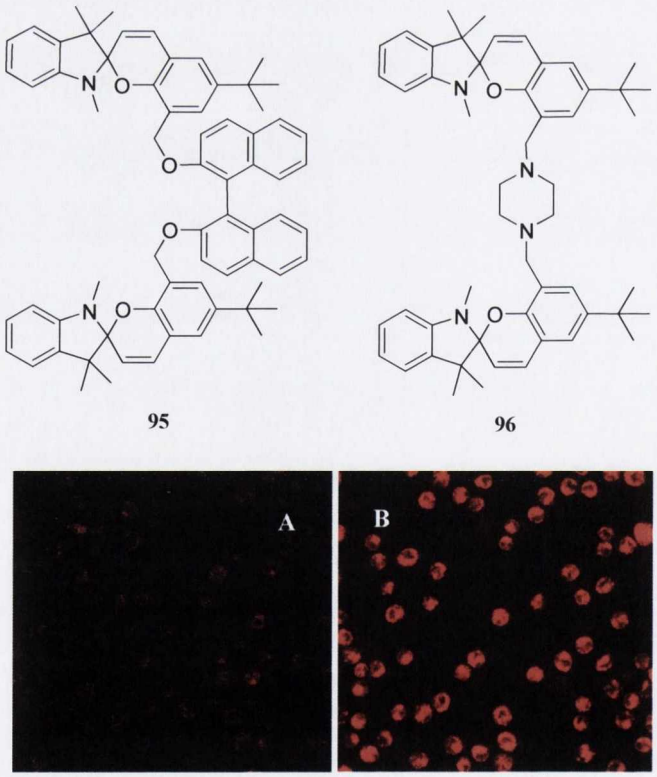


Figure 1.17 Confocal microscope images of human acute T cell leukaemia (A) without spiropyran, (B) incubated with 100 μM **96** for 3 h. The fluorescence visible in (B) is given by the formation of a complex between **96** and glutathione.[106]

detection of glutathione in living cells.[106] They represent an outstanding example of organic sensor with remarkable properties for *in vivo* applications. For both sensors, the molecular recognition is based on multipoint electrostatic interactions and structure complementarity between the opened merocyanine forms and a glutathione molecule (figure 1.17). Surprisingly the presence of thiolated aminoacids or other peptides did not interfere with the GSH interaction which indeed showed strong fluorescence emission. Confocal fluorescence microscopy experiments were carried out for compound **96** with human acute leukaemia T cells. The spiropyran was internalized in the cells and produces fluorescence enhancement by GSH complexation.

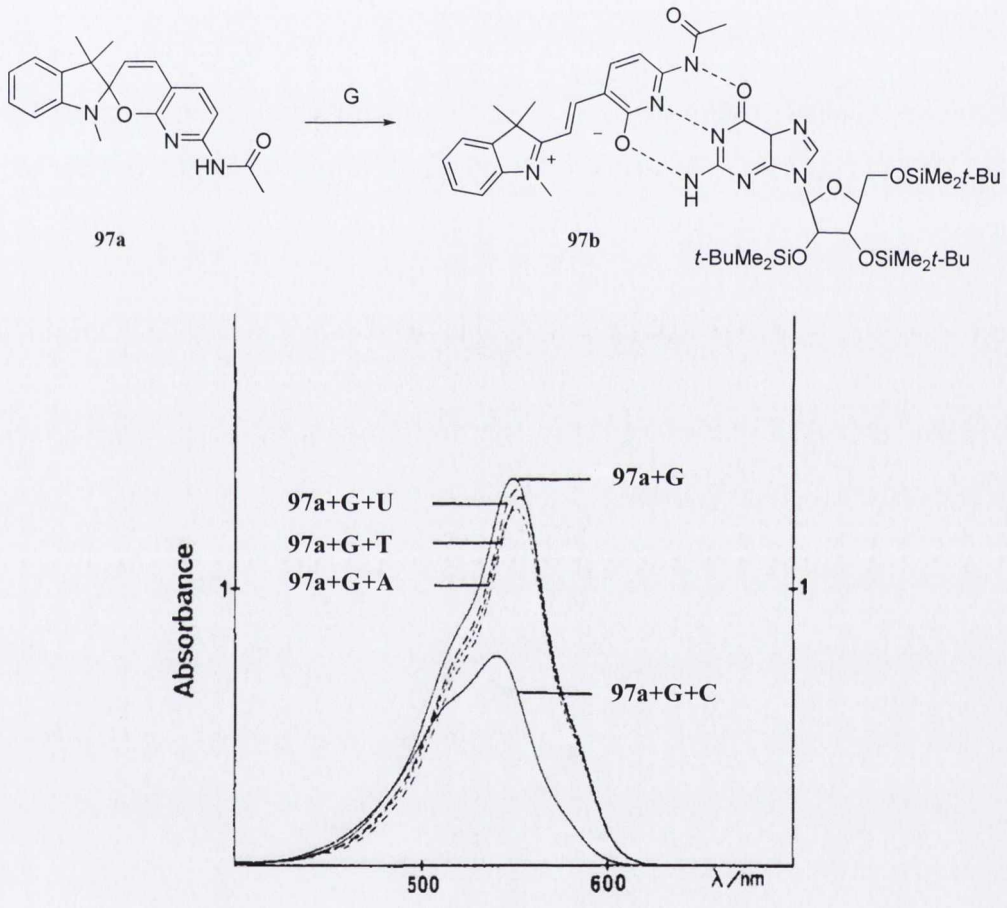


Figure 1.18 Coordination mechanism of **97a** with a guanosine **G** derivative to for the complex **97b**. Absorption spectra of a solution containing **97a** and **G** in the absence and in the presence of other nucleosides cytidine (**C**), uridine (**U**), thymidine (**T**), and adenosine (**A**).[107]

The first spiropyran based selective receptor for nucleosides was reported by Inouye and co-workers in the early nineties.[107] Compound **97a** can bind selectively a guanosine

relying on the triple hydrogen bond formation between the acetamidopyridone anion unit of its open form and the complementarity of the nucleoside structure (structure **97b** in figure 1.18). This interaction produced dramatic changes in the UV-vis absorption spectrum of **97a** with the appearance of a strong absorption band with maximum intensity at 550 nm. Despite the small interference with cytidine, the spiropyran selectivity was not affected by the presence of other nucleosides (plot in figure 1.18).

Later, the same authors reported on the synthesis and activity evaluation of the ferrocene-modified bis(spiropyridopyran) **98a**, aimed at the selective recognition of guanine–guanine (GG) dinucleoside derivatives.[108] They demonstrated the high selectivity of the receptor by means of ^{1}H-NMR and UV-vis absorption spectroscopies. In particular, upon addition of GG or G, a solution of **98a** turned into red and an intense absorption band appeared in the visible region with maximum intensity at 575 nm. No significant changes in the absorption spectra were observed in the presence of other nucleosides (absorption spectra in figure 1.19). The authors suggested that the inter-ring spacing of the two ferrocene rings is near to the spacing between the stacked base pairs and its restricted conformational flexibility allows the merocyanine units to interact

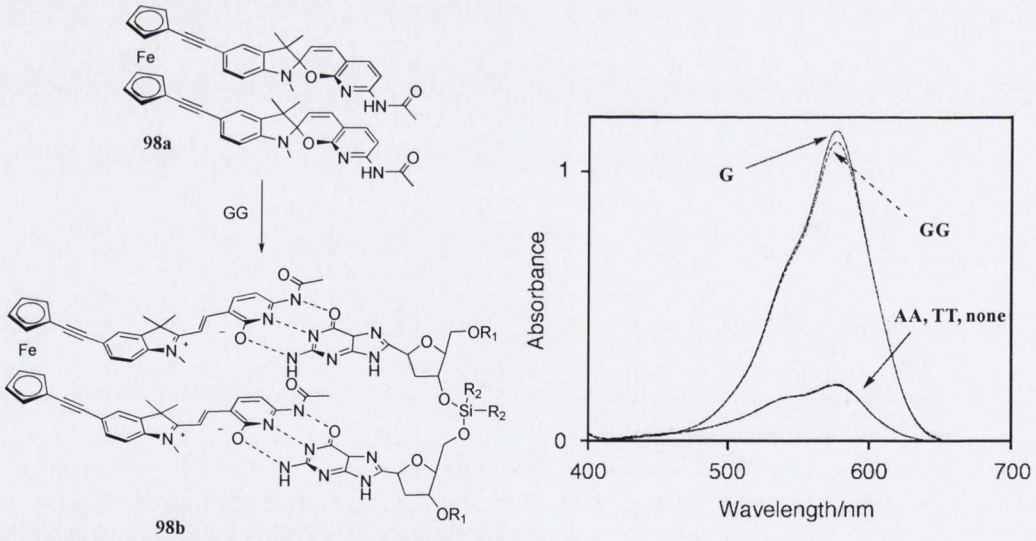


Figure 1.19 Electronic absorption spectra of **98a** (3.0×10^{-2} mM) in the presence of the lipophilic nucleosides guanosine (**G**), guanosine-guanosine (**GG**), thymidine-thymidine (**TT**), and adenosine-adenosine (**AA**) derivatives (3.0×10^{-2} mM) in CH_2Cl_2 at 25 °C.[108]

with the complementary guanine-guanine modules. The mechanism of interaction is depicted in figure 1.19.

1.4 Conclusions

Photochromic compounds are molecules which respond to electromagnetic radiation stimuli exhibiting macroscopic changes due to variation in their molecular structure. The transformation is reversible and the two generated species differ from each other because of their clearly different absorption spectra. The incorporation into a photochromic molecule of a functional group that can interact selectively with a substrate can afford a system that performs as an artificial signalling receptor. Several photochromic compounds possessing these features have been reported. These receptors were designed to enable molecular recognition information to be signalled as changes in their optical properties. Additionally, since the photochromic ability of the hosts was retained, the host-guest interactions are fully regulated at our will by means of optical stimulations. This approach allows to reach a new level of molecular sensing, with receptors that can bind selectively and reversibly a disparate multitude of chemical guests and allow to overcome the problem of a one-time use sensor.

1.5 Aims of the Project

The ever increasing concern on ecological issues such as the potential toxicity of metallic pollutants has lead to an active quest for sensitive and selective sensors in order to be able to monitor their presence and their concentration. At present, a wide variety of colorimetric and fluorescent probes for transition metal cations are available such as non-reusable "chemodosimeters", fluorochromic and colorimetric dyes for optodes. Although many reactions and various techniques have been developed for assaying transition metal cations, there is still plenty of room for improvement in term of selectivity, sensitivity, and performance with a new interaction mechanism. For this purpose, photochromic compounds are very appealing candidates for several reason. First, the possibility to modulate the complexation strength of the dye by a photoswitching event that is fully controllable *via* external light stimuli. Second,

considering that the recycling of the commonly used probes for transition metals is based on a simple equilibrium shift that can be obtained by extensive washings, photochromic compound allow to overcome this problem as the metal guest can be released upon irradiation with an appropriate light source. Photochromic spiropyrans in particular, have shown the most promising properties for such applications. They have the ability of reversibly switch between a strongly coloured merocyanine form by exposure to UV light, and a spirocyclic form upon irradiation with visible light. The two isomers present different physical and chemical properties and the equilibrium is also influenced by solvent, medium, and temperature. The cleavage of the C-O bond on the spiro carbon is the responsible for their photochromism and, at the same time, generates the negatively charged site of the merocyanine form, a phenate. This represent the starting point for the incorporation of suitable chelating substituents into the molecular skeleton, in the vicinity of the etheroxide group, in order to tailor a substance that optically responds the presence of metal ions in solution. In addition, since the strength of the binding of metal ions is sensitive to the ligand structure, the efficiency of the complexation by merocyanine form can be modulated by both electronic effects of the substituent on the molecular backbone and by modulating the accessibility of the binding site.

Nowadays, a huge number of ionochromic spiropyran based sensors for transition metal cations have been reported. However, the mechanisms that govern the interactions between the photochromic host and the metallic guests still need to be comprehensively understood. Additionally, among the huge number of spiropyran-based sensors reported in literature, many compounds have shown selectivity for groups of metals rather than full selectivity to single guests.

In order to fill these gaps, the overall goals of this project were:

- design of a new series of spirochromenes for metal sensing application. The choice of substituents was made in order to obtain:
    - a group of molecules functionalized with carboxylated chains that give more flexibility to the structure and allow a more stable interaction with the metal cation;

- a group of molecules with photo- and ionochromic behaviour due to the presence of a strong electron withdrawing group and a group with only ionochromic behaviour due to the presence of an electron donating group.
- a group of molecules with aromatic etherosubstituents to give more rigidity to the structure in order to increase the selectivity of the sensor.

- synthesis of a batch of precursors and the assembly of the final photochromic molecules;
- preliminary investigations of the effect of different solvents and pH on the molecules' switchability by means of UV-Vis absorption spectroscopy;
- evaluation of their activity as ion sensing molecules in the presence of biologically important transition metal cations by means of UV-Vis absorption spectroscopy;
- characterization of the complexes by using ^{1}H NMR, HRMS and X-Ray analysis in order to understand the role of the different substituents.

Reference List

(1) Hirshberg, Y.; Fischer, E. *Journal of Chemical Physics* **1955**, *23*, 1723-1723.
(2) Bertelson, R. C. *Photochromism* **1971**, (Ed.: Brown, G. H.), Wiley: New York.
(3) Garcia, A. A.; Cherian, S.; Park, J.; Gust, D.; Jahnke, F.; Rosario, R. *Journal of Physical Chemistry A* **2000**, *104*, 6103-6107.
(4) Wilson, A. E. J. *Physics in Technology* **1984**, *15*, 232-238.
(5) Guglielmetti, R. *Photochromism: Molecules and Systems* **1990**, (Ed.: Durr, H.; Bouas-Laurent, H.) Elsevier: Amsterdam.
(6) Tsivgoulis, G. M.; Lehn, J. M. *Angewandte Chemie-International Edition in English* **1995**, *34*, 1119-1122.
(7) Feringa, B. L. *Molecular Switches* **2001**, Wiley-VCH.
(8) Wyman, G. M. *Chemical Reviews* **1955**, *55*, 625-657.
(9) Rau, H. *Angewandte Chemie-International Edition in English* **1973**, *12*, 224-235.
(10) Ishihara, K.; Hamada, N.; Kato, S.; Shinohara, I. *Journal of Polymer Science Part A-Polymer Chemistry* **1984**, *22*, 121-128.
(11) Ishihara, K.; Hamada, N.; Kato, S.; Shinohara, I. *Journal of Polymer Science Part A-Polymer Chemistry* **1983**, *21*, 1551-1555.
(12) Irie, M.; Hirano, Y.; Hashimoto, S.; Hayashi, K. *Macromolecules* **1981**, *14*, 262-267.
(13) Mamada, A.; Tanaka, T.; Kungwatchakun, D.; Irie, M. *Macromolecules* **1990**, *23*, 1517-1519.
(14) Cohen, M. D.; Schmidt, G. M. J. *Journal of Physical Chemistry* **1962**, *66*, 2442-2444.
(15) Yokoyama, Y. *Chemical Reviews* **2000**, *100*, 1717-1739.
(16) Heller, H. G.; Megit, R. M. *Journal of the Chemical Society-Perkin Transactions 1* **1974**, 923-927.
(17) Atassi, Y.; Chauvin, J.; Delaire, J.; Delouis, J. F.; Fanton-maltey, I.; Nakatani, K. *Molecular Crystals and Liquid Crystals Science and Technology Section A-Molecular Crystals and Liquid Crystals* **1998**, *315*, 11-22.
(18) Matsui, F.; Taniguchi, H.; Yokoyama, Y.; Sugiyama, K.; Kurita, Y. *Chemistry Letters* **1994**, 1869-1872.
(19) Yu, L. H.; Ming, Y. F.; Fan, M. G.; Yu, H. T.; Ye, Q. Q. *Science in China Series B-Chemistry* **1996**, *39*, 1-6.
(20) Waldeck, D. H. *Chemical Reviews* **1991**, *91*, 415-436.
(21) Kellogg, R. M.; Groen, M. B.; Wynberg, H. *Journal of Organic Chemistry* **1967**, *32*, 3093-3100.
(22) Irie, M.; Mohri, M. *Journal of Organic Chemistry* **1988**, *53*, 803-808.
(23) Irie, M.; Sayo, K. *Journal of Physical Chemistry* **1992**, *96*, 7671-7674.
(24) Irie, M.; Sakemura, K.; Okinaka, M.; Uchida, K. *Journal of Organic Chemistry* **1995**, *60*, 8305-8309.
(25) Irie, M. *Chemical Reviews* **2000**, *100*, 1685-1716.
(26) Hauck, G.; Durr, H. *Angewandte Chemie-International Edition in English* **1979**, *18*, 945-946.
(27) Fromm, R.; Ahmed, S. A.; Hartmann, T.; Huch, V.; Abdel-Wahab, A. A.; Durr, H. *European Journal of Organic Chemistry* **2001**, 4077-4080.

(28) Tan, Y. S.; Ahmed, S. A.; Durr, H.; Huch, V.; Abdel-Wahab, A. *Chemical Communications* **2001**, 1246-1247.
(29) Weber, C.; Rustemeyer, F.; Durr, H. *Advanced Materials* **1998**, *10*, 1348-1351.
(30) Gogritchiani, E.; Hartmann, T.; Palm, B. S.; Samsoniya, S.; Durr, H. *Journal of Photochemistry and Photobiology B-Biology* **2002**, *67*, 18-22.
(31) Fox, M. A.; Voynick, T. A. *Journal of Organic Chemistry* **1981**, *46*, 1235-1239.
(32) Guo, K. P.; Chen, Y. *Journal of Materials Chemistry* **2009**, *19*, 5790-5793.
(33) Such, G.; Evans, R. A.; Yee, L. H.; Davis, T. P. *Journal of Macromolecular Science-Polymer Reviews* **2003**, *C43*, 547-579.
(34) Berkovic, G.; Krongauz, V.; Weiss, V. *Chemical Reviews* **2000**, *100*, 1741-1753.
(35) Hirshberg, Y. *Journal of the American Chemical Society* **1956**, *78*, 2304-2312.
(36) Tyer, N. W.; Becker, R. S. *J. Am. Chem. Soc.* **1970**, *92*, 1289-1294.
(37) Pimienta, V.; Lavabre, D.; Levy, G.; Samat, A.; Guglielmetti, R.; Micheau, J. C. *Journal of Physical Chemistry* **1996**, *100*, 4485-4490.
(38) Oda, H. *Dyes and Pigments* **1998**, *38*, 243-254.
(39) Malkin, Y. N.; Krasieva, T. B.; Kuzmin, V. A. *Journal of Photochemistry and Photobiology a-Chemistry* **1989**, *49*, 75-88.
(40) Vandewye P.; Hoefnage J.; Smets, G. *Tetrahedron* **1969**, *25*, 3251-3266.
(41) Berman, E.; Fox, R. E.; Thomson, F. D. *Journal of the American Chemical Society* **1959**, *81*, 5605-5608.
(42) Roxburgh, C. J.; Sammes, P. G. *Dyes and Pigments* **1995**, *27*, 63-69.
(43) Roxburgh, C. J.; Sammes, P. G. *Dyes and Pigments* **1995**, *28*, 317-325.
(44) Roxburgh, C. J.; Sammes, P. G.; Abdullah, A. *Dyes and Pigments* **2009**, *83*, 31-50.
(45) Rosario, R.; Gust, D.; Hayes, M.; Springer, J.; Garcia, A. A. *Langmuir* **2003**, *19*, 8801-8806.
(46) Chibisov, A. K.; Gorner, H. *Physical Chemistry Chemical Physics* **2001**, *3*, 424-431.
(47) Becker, R. S.; Michl, J. *Journal of the American Chemical Society* **1966**, *88*, 5931-5935.
(48) Kolc, J.; Becker, R. S. *Journal of Physical Chemistry* **1967**, *71*, 4045-4049.
(49) Moorthy, J. N.; Venkatakrishnan, P.; Samanta, S.; Kumar, D. K. *Organic Letters* **2007**, *9*, 919-922.
(50) Crano, J. C.; Flood, T.; Knowles, D.; Kumar, A.; VanGemert, B. *Pure and Applied Chemistry* **1996**, *68*, 1395-1398.
(51) Shinkai, S.; Shigematsu, K.; Sato, M.; Manabe, O. *Journal of the Chemical Society-Perkin Transactions 1* **1982**, 2735-2739.
(52) An, H. Y.; Bradshaw, J. S.; Izatt, R. M.; Yan, Z. M. *Chemical Reviews* **1994**, *94*, 939-991.
(53) Gokel, G. W.; Leevy, W. M.; Weber, M. E. *Chemical Reviews* **2004**, *104*, 2723-2750.
(54) Akabori, S.; Miura, Y.; Yotsumoto, N.; Uchida, K.; Kitano, M.; Habata, Y. *Journal of the Chemical Society-Perkin Transactions 1* **1995**, 2589-2594.
(55) Shinkai, S.; Nakaji, T.; Nishida, Y.; Ogawa, T.; Manabe, O. *Journal of the American Chemical Society* **1980**, *102*, 5860-5865.
(56) Pipoosananakaton, B.; Sukwattanasinitt, M.; Jaiboon, N.; Chaichit, N.; Tuntulani, T. *Tetrahedron Letters* **2000**, *41*, 9095-9100.
(57) Santiago, A.; Becker, R. S. *Journal of the American Chemical Society* **1968**, *90*, 3654-3658.

(58) Yokoyama, Y.; Ohmori, T.; Okuyama, T. *Molecular Crystals and Liquid Crystals* **2000**, *344*, 265-270.
(59) Guo, Z.; Wang, G.; Tang, Y.; Song, X. *Liebigs Annalen* **1997**, *1997*, 941-942.
(60) Takeshita, M.; Soong, C. F.; Irie, M. *Tetrahedron Letters* **1998**, *39*, 7717-7720.
(61) Takeshita, M.; Irie, M. *Tetrahedron Letters* **1998**, *39*, 613-616.
(62) Takeshita, M.; Irie, M. *Journal of Organic Chemistry* **1998**, *63*, 6643-6649.
(63) Kawai, S. H. *Tetrahedron Letters* **1998**, *39*, 4445-4448.
(64) Hu, H. Y.; Zhu, M. Z.; Meng, X. M.; Zhang, Z. P.; Wei, K.; Guo, Q. X. *Journal of Photochemistry and Photobiology a-Chemistry* **2007**, *189*, 307-313.
(65) Malval, J. P.; Gosse, I.; Morand, J. P.; Lapouyade, R. *Journal of the American Chemical Society* **2002**, *124*, 904-905.
(66) Zhou, Z. G.; Xiao, S. Z.; Xu, J.; Liu, Z. Q.; Shi, M.; Li, F. Y.; Yi, T.; Huang, C. H. *Org. Lett.* **2006**, *8*, 3911-3914.
(67) Takeshita, M.; Uchida, K.; Irie, M. *Chemical Communications* **1996**, 1807-1808.
(68) Durr, H.; Thome, A.; Kranz, C.; Kilburg, H.; Bossmann, S.; Braun, B.; Janzen, K. P.; Blasius, E. *Journal of Physical Organic Chemistry* **1992**, *5*, 689-698.
(69) Durr, H.; Kranz, C. *Molecular Crystals and Liquid Crystals Science and Technology Section A-Molecular Crystals and Liquid Crystals* **1994**, *246*, 135-138.
(70) Durr, H.; Kranz, C.; Kilburg, H. *Molecular Crystals and Liquid Crystals Science and Technology Section A-Molecular Crystals and Liquid Crystals* **1997**, *297*, 365-372.
(71) Kumar, S.; Hernandez, D.; Hoa, B.; Lee, Y.; Yang, J. S.; McCurdy, A. *Organic Letters* **2008**, *10*, 3761-3764.
(72) Stauffer, M. T.; Knowles, D. B.; Brennan, C.; Funderburk, L.; Lin, F. T.; Weber, S. G. *Chemical Communications* **1997**, 287-288.
(73) Paramonov, S.; Delbaere, S.; Fedorova, O.; Fedorov, Y.; Lokshin, V.; Samat, A.; Vermeersch, G. *Journal of Photochemistry and Photobiology a-Chemistry* **2010**, *209*, 111-120.
(74) Preigh, M. J.; Lin, F. T.; Ismail, K. Z.; Weber, S. G. *Journal of the Chemical Society-Chemical Communications* **1995**, 2091-2092.
(75) Tamaki, T.; Ichimura, K. *Journal of the Chemical Society-Chemical Communications* **1989**, 1477-1479.
(76) Zhou, J. W.; Zhao, F. Q.; Li, Y. T.; Zhang, F. S.; Song, X. Q. *Journal of Photochemistry and Photobiology a-Chemistry* **1995**, *92*, 193-199.
(77) Minkovska, S.; Fedieva, M.; Jeliazkova, B.; Deligeorgiev, T. *Polyhedron* **2004**, *23*, 3147-3153.
(78) Elmaloulibibout, M.; Lareginie, P.; Noussi, L.; Samat, A.; Guglielmetti, R. *Molecular Crystals and Liquid Crystals Science and Technology Section A-Molecular Crystals and Liquid Crystals* **1994**, *246*, 177-181.
(79) Nazarov, V. B.; Soldatenkova, V. A.; Alfimov, M. V.; Lareginie, P.; Samat, A.; Guglielmetti, R. *Russian Chemical Bulletin* **1996**, *45*, 2105-2108.
(80) Fedorova, O. A.; Gromov, S. P.; Strokach, Y. P.; Pershina, Y. V.; Sergeev, S. A.; Barachevskii, V. A.; Pepe, G.; Samat, A.; Guglielmetti, R.; Alfimov, M. A. *Russian Chemical Bulletin* **1999**, *48*, 1950-1959.
(81) Fedorova, O. A.; Gromov, S. P.; Pershina, Y. V.; Sergeev, S. S.; Strokach, Y. P.; Barachevsky, V. A.; Alfimov, M. V.; Pepe, G.; Samat, A.; Guglielmetti, R. *Journal of the Chemical Society-Perkin Transactions 2* **2000**, 563-570.
(82) Inouye, M.; Ueno, M.; Tsuchiya, K.; Nakayama, N.; Konishi, T.; Kitao, T. *Journal of Organic Chemistry* **1992**, *57*, 5377-5383.

(83) Fedorova, O. A.; Strokach, Y. P.; Gromov, S. P.; Koshkin, A. V.; Valova, T. M.; Alfimov, M. V.; Feofanov, A. V.; Alaverdian, I. S.; Lokshin, V. A.; Samat, A.; Guglielmetti, R.; Girling, R. B.; Moore, J. N.; Hester, R. E. *New Journal of Chemistry* **2002**, *26*, 1137-1145.
(84) Shiraishi, Y.; Adachi, K.; Itoh, M.; Hirai, T. *Organic Letters* **2009**, *11*, 3482-3485.
(85) Phillips, J. P.; Mueller, A.; Przystal, F. *Journal of the American Chemical Society* **1965**, *87*, 4020.
(86) Collins, G. E.; Choi, L. S.; Ewing, K. J.; Michelet, V.; Bowen, C. M.; Winkler, J. D. *Chemical Communications* **1999**, 321-322.
(87) Chernyshev, A. V.; Metelitsa, A. V.; Gaeva, E. B.; Voloshin, N. A.; Borodkin, G. S.; Minkin, V. I. *Journal of Physical Organic Chemistry* **2007**, *20*, 908-916.
(88) Nikolaeva, O. G.; Tsukanov, A. V.; Shepelenko, E. N.; Lukyanov, B. S.; Metelitsa, A. V.; Kostyrina, O. Y.; Dubonosov, A. D.; Bren, V. A.; Minkin, V. I. *International Journal of Photoenergy* **2009**.
(89) Inouye, M.; Ueno, M.; Kitao, T.; Tsuchiya, K. *Journal of the American Chemical Society* **1990**, *112*, 8977-8979.
(90) Kimura, K.; Yamashita, T.; Yokoyama, M. *Journal of the Chemical Society-Perkin Transactions 2* **1992**, 613-619.
(91) Inouye, M.; Noguchi, Y.; Isagawa, K. *Angewandte Chemie-International Edition in English* **1994**, *33*, 1163-1166.
(92) Tu, C. Q.; Osborne, E. A.; Louie, A. Y. *Tetrahedron* **2009**, *65*, 1241-1246.
(93) Kimura, K.; Teranishi, T.; Yokoyama, M.; Yajima, S.; Miyake, S.; Sakamoto, H.; Tanaka, M. *Journal of the Chemical Society-Perkin Transactions 2* **1999**, 199-204.
(94) Teranishi, T.; Yokoyama, M.; Sakamoto, H.; Kimura, K. *Molecular Crystals and Liquid Crystals* **2000**, *344*, 271-276.
(95) Nakamura, M.; Fujioka, T.; Sakamoto, H.; Kimura, K. *New Journal of Chemistry* **2002**, *26*, 554-559.
(96) Sakamoto, H.; Takagaki, H.; Nakamura, M.; Kimura, K. *Analytical Chemistry* **2005**, *77*, 1999-2006.
(97) Liu, S. H. *Molecular Crystals and Liquid Crystals* **2004**, *419*, 97-101.
(98) Yagi, S.; Nakamura, S.; Watanabe, D.; Nakazumi, H. *Dyes and Pigments* **2009**, *80*, 98-105.
(99) Filley, J.; Ibrahim, M. A.; Nimlos, M. R.; Watt, A. S.; Blake, D. M. *Journal of Photochemistry and Photobiology a-Chemistry* **1998**, *117*, 193-198.
(100) Liu, Z. L.; Jiang, L.; Liang, Z.; Gao, Y. H. *Tetrahedron* **2006**, *62*, 3214-3220.
(101) Shao, N.; Zhang, Y.; Cheung, S. M.; Yang, R. H.; Chan, W. H.; Mo, T.; Li, K. A.; Liu, F. *Analytical Chemistry* **2005**, *77*, 7294-7303.
(102) Shao, N.; Jin, J. Y.; Wang, H.; Zhang, Y.; Yang, R. H.; Chan, W. H. *Analytical Chemistry* **2008**, *80*, 3466-3475.
(103) Shao, N.; Jin, J. Y.; Cheung, S. M.; Yang, R. H.; Chan, W. H.; Mo, T. *Angewandte Chemie-International Edition* **2006**, *45*, 4944-4948.
(104) Shao, N.; Gao, X.; Wang, H.; Yang, R. H.; Chan, W. H. *Analytica Chimica Acta* **2009**, *655*, 1-7.
(105) Shao, N.; Wang, H.; Gao, X. D.; Yang, R. H.; Chan, W. H. *Analytical Chemistry* **2010**, *82*, 4628-4636.
(106) Shao, N.; Jin, J. Y.; Wang, H.; Zheng, J.; Yang, R. H.; Chan, W. H.; Abliz, Z. *Journal of the American Chemical Society* **2010**, *132*, 725-736.

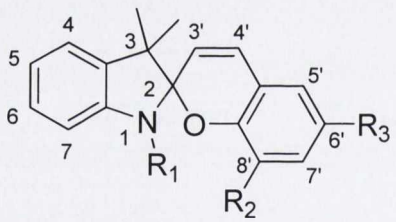
(107) Inouye, M.; Kim, K.; Kitao, T. *Journal of the American Chemical Society* **1992**, *114*, 778-780.
(108) Takase, M.; Inouye, M. *Chemical Communications* **2001**, 2432-2433.

CHAPTER 2

DISCUSSION

2.1 Design

To achieve the required selectivity towards a specific metal-ion, it is necessary to complement the optical properties of the spiropyran backbone with appropriate functional groups that, collectively, provide a binding site that matches the specific coordination requirements of the targeted ion. Our design brings together elements that can facilitate metal-ion binding and promote photoinduced control of the metal ligation. The possibilities of modification applicable to the molecule skeleton are several. Variation of the substituents utilized and their position in the molecule are the main strategies used to tailor a sensor which shows a certain degree of selectivity toward particular ions. Considering the backbone of a general spiropyran, like the one shown in scheme 2.1, one can identify three different positions that can be modified to obtain such systems. The indolic nitrogen is the 1-position, the aromatic carbon vicinal to the benzopyran oxygen is the 8'-position and the 6'-position corresponds to the carbon in *para* with respect to the benzopyran oxygen. Positions 1- and 8'- are usually functionalized with groups that participate directly to the cation coordination while 6'-position should bear an element that controls the cation binding constant *via* electronic effects. The choice of groups R_1, R_2, and R_3 in positions 1-, 8'-, and 6'- respectively will be herein explained.



Scheme 2.1 Generic spiropyran structure with generic groups R_1, R_2, and R_3 in positions 1-, 8'-, and 6'- respectively.

2.1.1 Substituents R_1 in 1-position

The negatively charged phenolic oxygen in the zwitterionic open form produces a moiety that can convert the neutral spiropyran into an efficient ligand for protons and metal ions. The indolic nitrogen offers a good functionalizable site on the molecule that would keep the group mounted on it in close proximity to the phenolic oxygen. Thus, if the chelating site in R_1 is sufficiently close to the phenolate, a bidentate system can be

generated. Several examples of *N*-modified spirochromenes for metal chelation applications are known and they have been mentioned in the previous chapter. For the functionalization of our spiropyrans we chose three different type of functional groups. First, a methyl substituent: in this case, no interaction with a metal cation can take place since the substituent does not bring any suitable chelating moiety. Thus, the metal ligation would depend essentially on the choice of the substituent on the benzopyran half of the molecule. Additionally, since the size of a methyl group is very small, we expected the sterical hindrance during the coordination event to be minimal. Second, in order to combine sufficient conformational flexibility with relatively strong coordinating moieties, we chose either an aliphatic chain with a hydroxy terminal group or ethyl ester and carboxylated chains as additional binding sites. The latter bears the strongest coordinating group of this series and the fact that the coordinating ability (and charge) of the carboxylic acid moiety can be modulated means that we have an additional tool for further fine-tuning the coordination chemistry of our ligand. Finally, we oriented the choice of the last substituent toward a methyl pyridinyl group. In this case, the pyridinyl nitrogen is a relatively good binding atom since its spare lone pair electrons and, at the same time, its aromatic structure and the short linker that connects it to the spiropyran backbone offer lower conformational flexibility. This gives rise to obvious restrictions in the cation coordination which depend mainly on its radius.

2.1.2 Substituents R_2 in 8'-position

Our primary goal was to improve the probes' sensitivity and selectivity for metal ions by introducing R_2 groups in 8'-position that can cooperate with the phenolate anion in the guest coordination. To achieve strong and highly specific binding to metal ion, the ion receptor domain of the spiropyran nucleuses was firstly designed by introducing a N-containing moiety like an dimethylaminomethyl substituent, already known for its binding properties towards groups d and f elements.[1,2] The second choice was oriented toward a methoxy group. This substituent has been a common motif in several spirochromenes aimed at metal coordination because it can cooperate with the phenolate anion of the open merocyanine in the chelation of cations.[3-6] In both cases, either the N, O^- or the OMe, O^- bidentate binding sites present in the molecule would generate great affinity toward transition metals. In the choice of the third type of substituent we

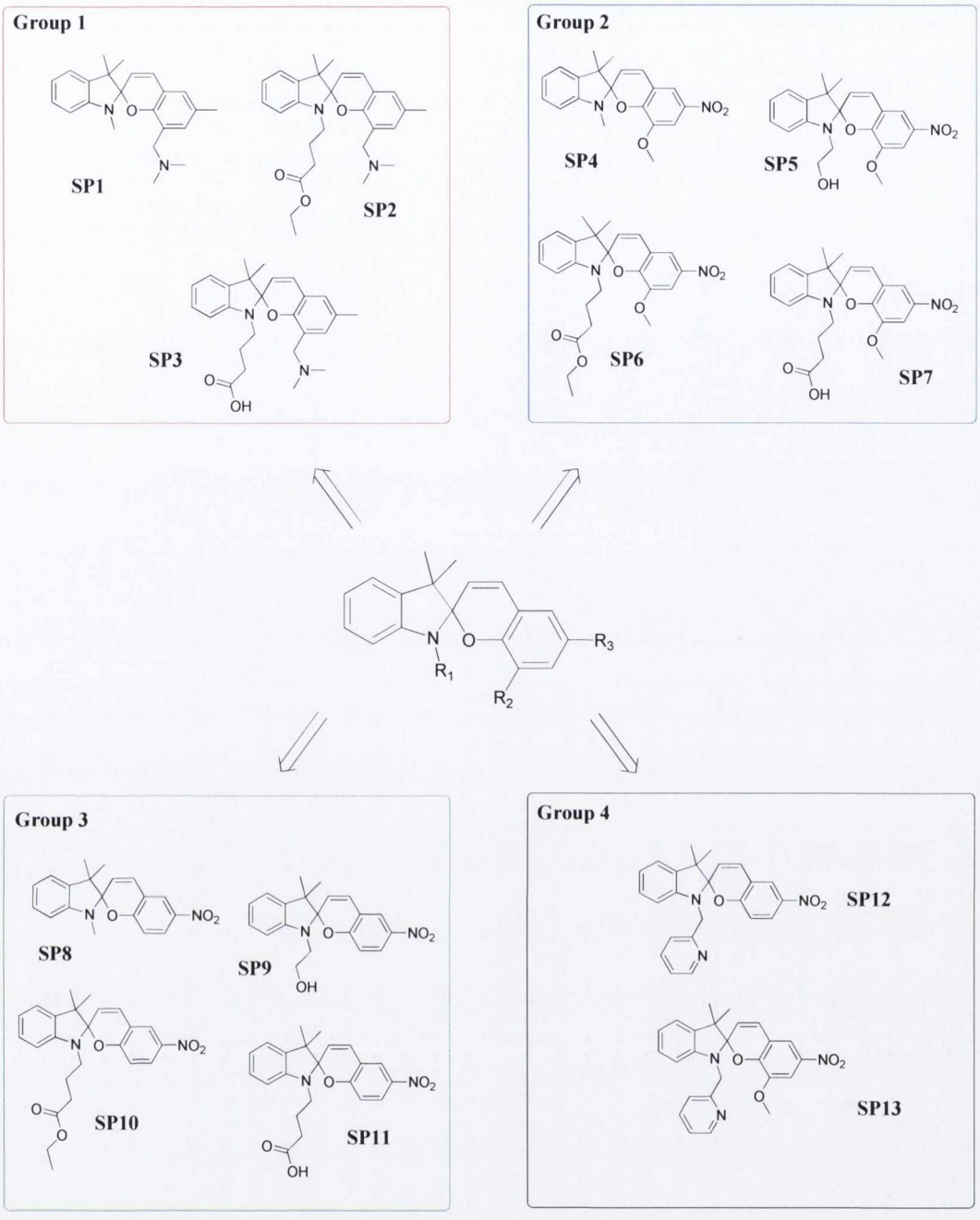
decided to produce structure capable to chelate a cation just relying on the interaction between the phenoxy group of the open merocyanines and the functional groups on the indolic nitrogen. Hence we opted to maintain a hydrogen atom in 8'-position next to the benzopyran oxygen. Thus, when a spiropyran is converted into its corresponding merocyanine because of the presence of a cation, the receptor domain that interact with the metal consists of a phenolate and a second binding site located on the other half of the molecule.

2.1.3 Substituents R_3 in 6'-position

Although 6'-position is considerably distant from the molecular region where the coordination of the metal takes place, so it could not participate to this event, it has been reported that the nature of R_3 substituents is a determining factor in stabilizing or destabilizing the spiropyran-metal complex. Indeed, a strong electron withdrawing group like a NO_2, can delocalize the negative charge of the phenolate anion. While this fact would stabilize enormously the open merocyanines with a drastic increase of their half-life with respect to molecules that do not bring such substituents,[7,8] the decrease of the oxygen electronic density would lead to a weaker interaction with a coordinated metal cation. Thus the photocontrol on the metal coordination is possible and the guest release can be performed by irradiating with visible light the spiropyran solution. On the other hand, the presence of an electron donating substituent in 8'-position would impede the stabilization of a photogenerated merocyanine but it would force the high electronic density around the phenolate anion to be available for being shared with an electron deficient cation. Thus, the metal release is unlikely to take place upon visible light irradiation because of the high stability of the resulting complex.[2,9,10]

2.1.4 Structures of the Chelating Spiropyrans

Once the substituents choice had been decided, we designed a library of spiropyrans modified with different combinations of functional groups. If we consider the substituent R_2 (8'-position) of the generic spiropyran in scheme 2.1 and maintain this group as a common motif but vary the other substituents, we can classify our molecules in four groups. Scheme 2.2 shows the structure of the different candidates we designed.



Scheme 2.2 Structures of the designed spiropyrans.

Group 1 contains molecules **SP1**, **SP2**, and **SP3** with a common dimethylaminomethyl substituent in 8'-position which has been reported to coordinate metal cations of groups d and f. The substituent in 6'-position is an electron donating methyl group that should increase the affinity for cations, impeding the photoinduced metal release. Substituents on the indolic nitrogen are a methyl group in **SP1**, an ethyl butyrate in **SP2**, and a butyric acid in **SP3**. The coordination of a metal by compound **SP1** should involve only the phenate of its corresponding merocyanine and the N of the

R_2 substituent while the interaction with a cation and compounds **SP2** and **SP3** would involve the additional ester and carboxy group of the alkyl chains in 1-position, enhancing the binding affinity of the two compounds for the guest.

Group 2 contains four derivatives that have a methoxy group in 8'-position and a nitro group in 6'-position. The methoxy affords an additional binding site that cooperates in the chelation with the adjacent phenolate when the molecule is in its open form. The presence of the nitro group would encourage the metal release upon irradiation with visible light. The indolic nitrogen is attached to methyl group which does not help the coordination in compound **SP4**, to a 2-hydroxyethyl group in **SP5**, an ethyl butyrate and a butyric acid in **SP6** and **SP7** respectively. The last three compounds can form tridentate complexes caging the cation between the methoxy, the phenolate and the terminal group on the alkylic chains on the indolic N.

Group 3 contains derivatives that differ from their analogues in group 2 because the methoxy group is substituted with a hydrogen. While compound **SP8** has only one binding site, the phenolate anion of its open isomer, compounds **SP9**, **SP10**, and **SP11** can count on the formation of a bidentate system where the cation is trapped between the phenolate and the functionalities of the indolic nitrogen tethers.

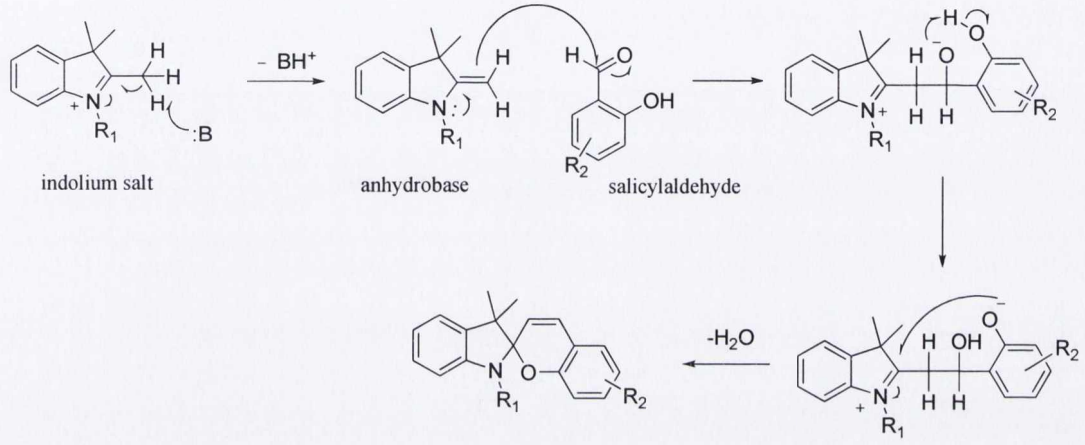
Group 4 contains two analogues where the nitro group in 6' position would lead to photoreversibility of the cation coordination, while the receptor site consists in a bidentate pyridine-phenolate system in **SP12** and a pyridine-phenoxy-methoxy triad in **SP13**.

2.2 Synthesis

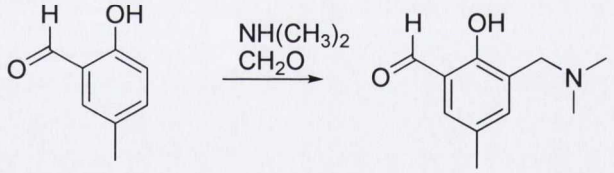
The general synthetic route of nitrogen containing spiropyrans consists in condensing an indolium salt in basic medium onto a substituted 2-hydroxy benzaldehyde. The reaction yield can be improved by adding a base like triethylamine or pyridine. The indolium salt undergoes a proton abstraction by basic attack (even NaOH if the molecular structure is compatible with strong basic condition) and it is readily converted into an anhydrobase which can be isolated or just implicitly obtained from the indolium precursor in basic medium. The anhydrobase reacts quickly with a substituted salicylaldehyde affording a spiropyran. The solvent is often ethanol but it could be a

different one if the substrates are reactive to alcoholic solvents. A general mechanism can be formulated as reported in Scheme 2.3.

The synthesis of 3-((dimethylamino)methyl)-2-hydroxy-5-methylbenzaldehyde **99**, which is the precursor for the synthesis of derivatives in group 1, was carried out *via* a Mannich reaction[1] starting from 5-methylalicylaldehyde which was reacted with formaldehyde and dimethylamine to afford the target molecule with a yield of 80% (scheme 2.4).



Scheme 2.3 Synthesis mechanism for a generic spiropyran.

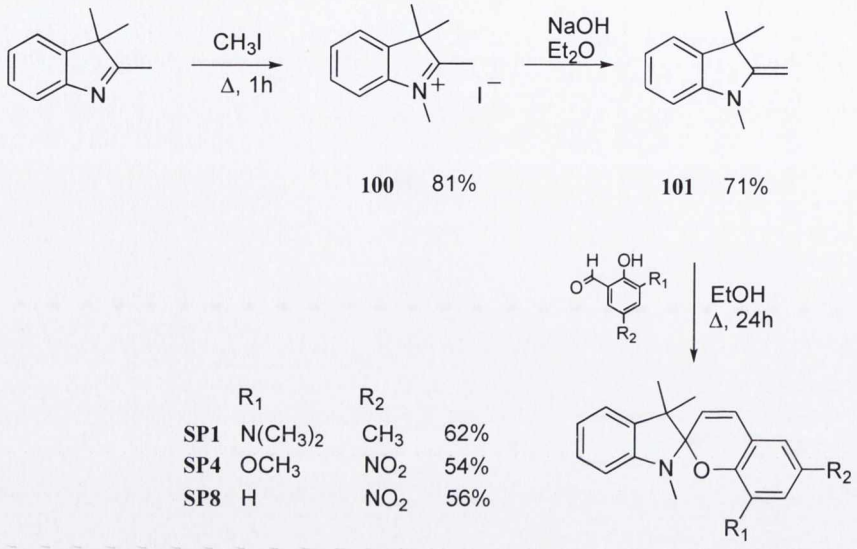


99 80%

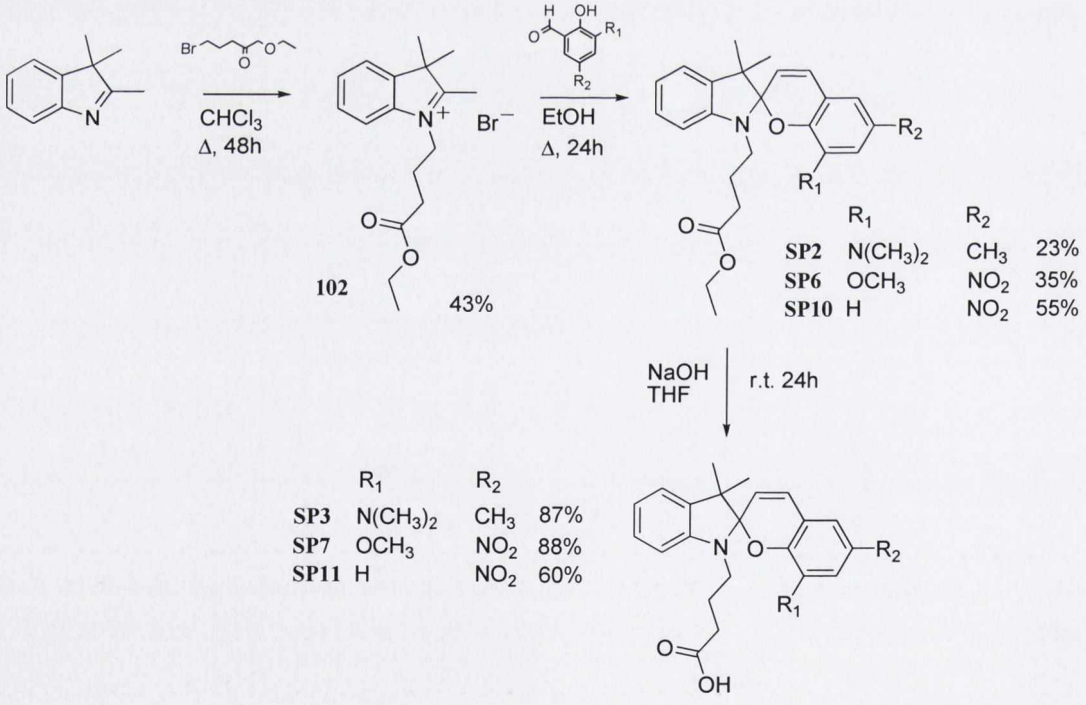
Scheme 2.4 Synthesis of 3-((dimethylamino)methyl)-2-hydroxy-5-methylbenzaldehyde **99**.

Spiropyrans bearing a methyl group on the indolic nitrogen were synthesized after making the indolium salt **100** that is the result of *N*-alkylation of 2,3,3-trimethyl-3*H*-indole according to known procedures.[11] Subsequent deprotonation of the quaternary salts by 2 N NaOH afforded the methylenebase **101** with 71% yield. Condensation in

EtOH with the appropriate salicylaldehydes afforded **SP1**, **SP4**, and **SP8** with yields of 62%, 54% and 56% respectively (Scheme 2.5).



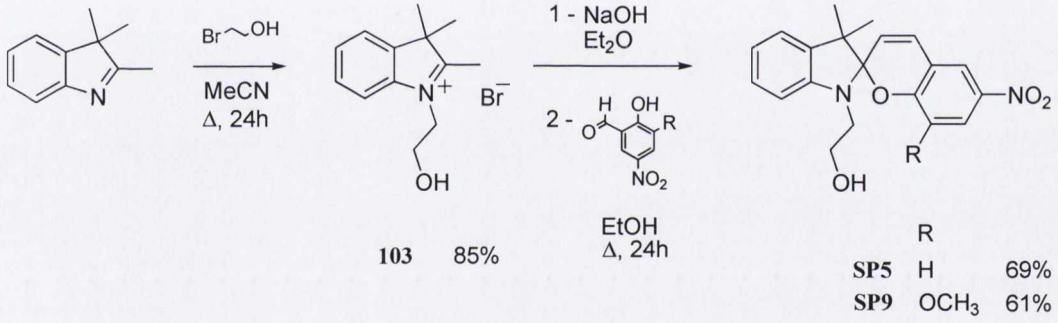
Scheme 2.5 Synthesis of spiropyrans **SP1**, **SP4**, and **SP8**.



Scheme 2.6 Synthesis of spiropyrans **SP2**, **SP6**, and **SP10** followed by hydrolysis in basic condition to afford **SP3**, **SP7**, and **SP11**.

Spiropyrans **SP2**, **SP6**, and **SP10** were synthesized in two steps starting from alkylation of commercially available 2,3,3-trimethyl-3*H*-indole with 4-bromobutyrate that produced the bromide salt **102** with yield of 43%. Reaction with the appropriate salicylaldehyde afforded the target molecules with yields respectively of 23%, 35% and 55%. Additional treatment with NaOH caused the hydrolysis of the ester groups of the three compounds affording the carboxylated analogues **SP3**, **SP7**, and **SP11** with yields of 87%, 88% and 60% respectively (Scheme 2.6).

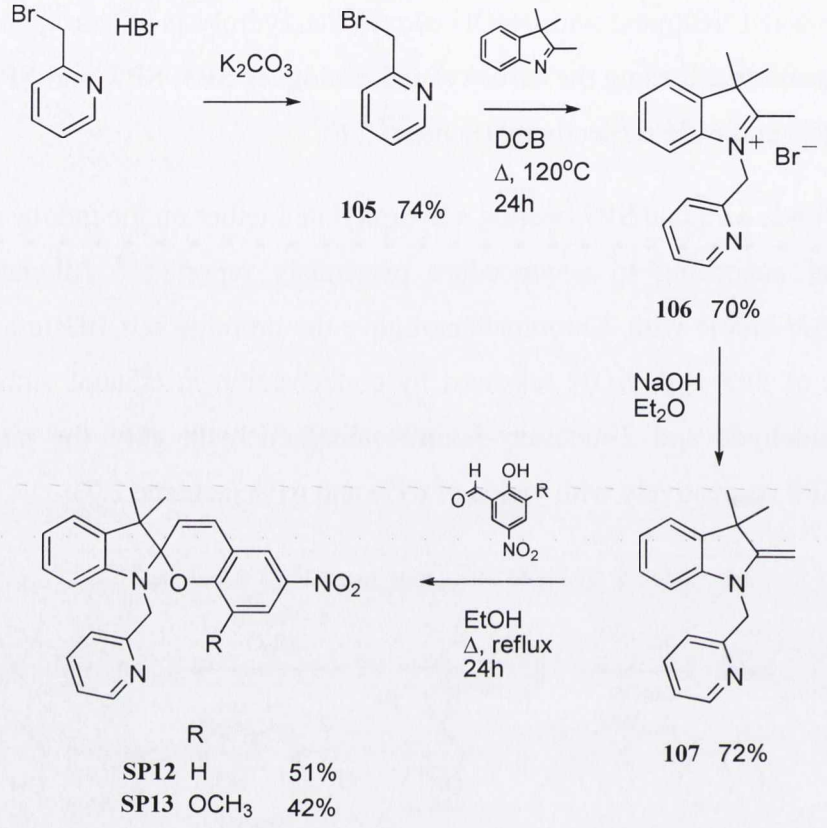
Compounds **SP5** and **SP9** bearing a hydroxylated tether on the indolic nitrogen, were synthesized according to a procedure previously reported.[12] Alkylation of 2,3,3-trimethyl-3*H*-indole with 2-bromoethanol gave the bromide salt **103** in a yield of 85%. Treatment of **103** with KOH followed by condensation in ethanol with 2-hydroxy-5-nitrobenzaldehyde and 2-methoxy-5-nitro salicylaldehyde gave the target molecules **SP5** and **SP9** respectively with yields of 69% and 61% (scheme 2.7).



Scheme 2.7 Synthesis of spiropyrans **SP5** and **SP9**.

The synthesis of the analogues **SP12** and **SP13** bearing a pyridine residue on the indole were synthesized similar conditions. The indolenine alkylation by 2-(bromomethyl)pyridine **105**, freshly prepared by treatment of its hydrobromide salt with K_2CO_3, took place in dichlorobenzene at 120°C affording the indolium salt **106**. Any attempt of purification of this compound failed so it was used as it was in the next synthetic step. First it was treated with in a strong alkaline medium to produce the anhydrobase **107** which was extracted from the mixture and reacted with two different salicylaldehydes. Reaction with 2-hydroxy-5-nitrobenzaldehyde in ethanol at reflux for 24 h afforded compound **SP12** while reaction in the same conditions with 2-methoxy-

5-nitro salicylaldehyde afforded compound **SP13**. Both final compounds were easily purified *via* flash chromatography on silica gel. Scheme 2.8 shows the forward synthetic route.



Scheme 2.8 Synthesis of spiropyrans **SP12** and **SP13**.

2.3 Acidochromism and Solvatochromism

2.3.1 Solvatochromic Effects

While traditionally the commonly employed external stimuli have been thermal and photochemical, modulation of the conversion between spiropyrans and merocyanine might be actuated *via* acid-base equilibrium.[12-14] To have a comprehensive overview on our molecules' behaviour, we examined the effect of medium, pH and substituents on the spiropyran-merocyanine conversion process; thus we carried out preliminary acidochromic, solvatochromic and photochromic UV-vis absorption studies on few compounds.

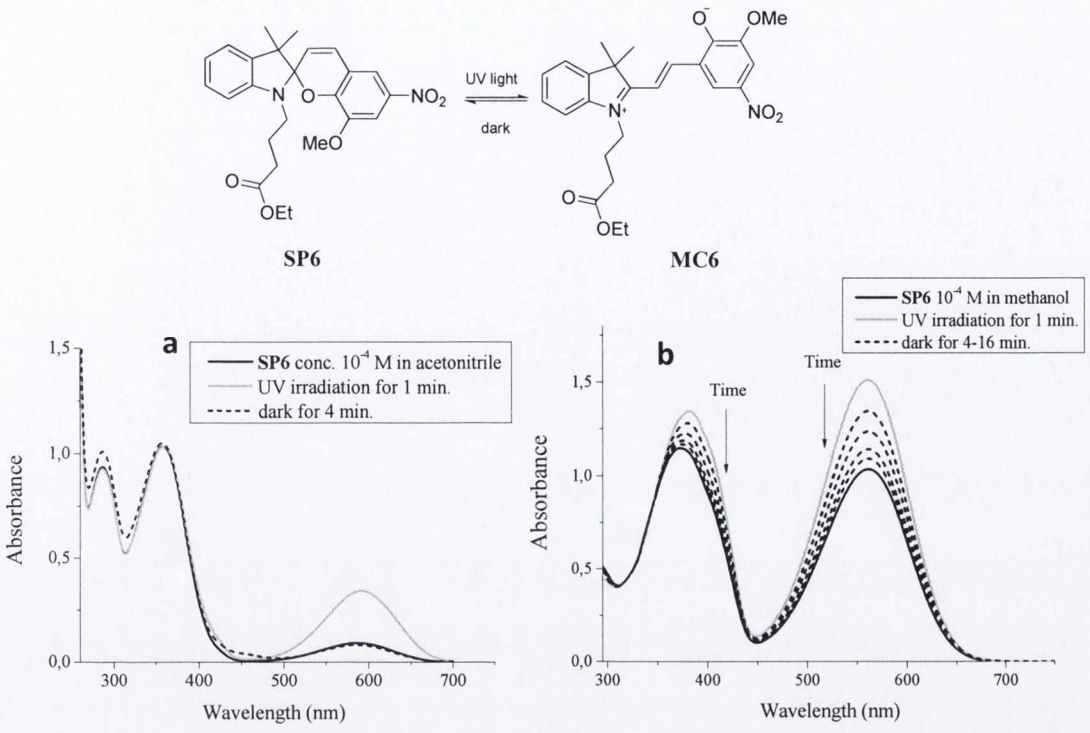


Figure 2.1 UV-vis absorption spectra of **SP6** ($1.0x10^{-4}$ M) after irradiation with UV 254 nm light in acetonitrile (**a**) and methanol (**b**).

Stock solutions for each spiropyran were prepared and stored in the dark to equilibrate overnight in acetonitrile and methanol with a concentration of $1x10^{-4}$ M. They were irradiated with a UV light source at a wavelength of 254 nm and the absorbance spectra for each of them were collected. In figure 2.1 the effect of two different solvent on the compound **SP6** is shown. After UV irradiation of both spiropyran solutions in acetonitrile and methanol two different spectra were produced. In acetonitrile the solution before irradiation was slightly pink and two peaks at 294 and 360 nm were observable for the closed spiropyran (black curve in figure 2.1a). A lower intensity peak was visible at 594 nm indicating a low concentration of the open merocyanine **MC6** in equilibrium with the closed form. After irradiation with UV light at 254 nm for 1 min the peak at 594 nm (grey curve in figure 2.1a) underwent a dramatic intensity increase due to the formation of the merocyanine. After storage in the dark the latter reverted back to the closed form in approximately 4 minutes (dotted curve in figure 2.1a). The methanolic solution of **SP6** was instead deeply blue coloured. The spectrum shows a high intensity peak at 560 nm for the zwitterionic **MC6** and a peak of the same intensity at 380 nm for the **SP6** (black curve, figure 2.1b). Hydrogen

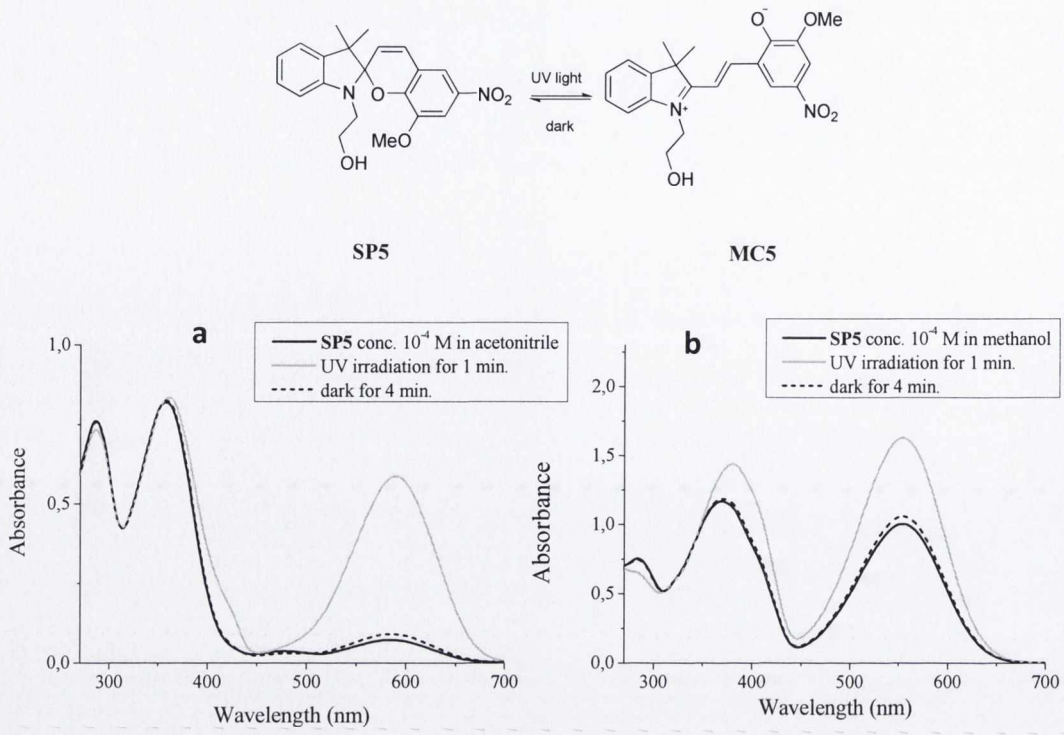


Figure 2.2 UV-vis absorption spectra of **SP5** ($1.0x10^{-4}$ M) after irradiation with UV 254 nm light in acetonitrile (**a**) and methanol (**b**).

bonding between the protic solvent and the phenolate stabilized the open form in such a way that a consistent amount of merocyanine was present at equilibrium with the closed form and irradiation with UV light produced little effects on the ground state absorption spectra (grey and dotted curves in figure 2.1b).

The substitution of the ethyl ester in 1-position of **SP6** with a 2-hydroxyethyl chain in compound **SP5** produced similar changes in the molecule UV-vis spectra. While **SP5** is the predominant species in an acetonitrile solution, as proven by its absorption bands at 285 and 358 nm (black curve in figure 2.2a), in methanol the appearance of a broad band at 554 nm indicates the remarkably high concentration of it open isomer **MC5** (black curve in figure 2.2a). Irradiation with UV light of the acetonitrile solution caused the isomerization of the spiropyran to merocyanine (grey curve in figure 2.2a) which faded thermally when stored in the dark in 4 minutes (dotted curve in figure 2.1a). In the alcoholic solution, the intensity increase of the two absorption bands at 368 nm and 554 nm was observed with an additional bathochromic shift of the maximum at 368 nm to 380 nm after irradiation with UV light (grey curve in figure 2.2b). The original spectrum was recovered after 4 minutes as a result of the strong stabilization of the

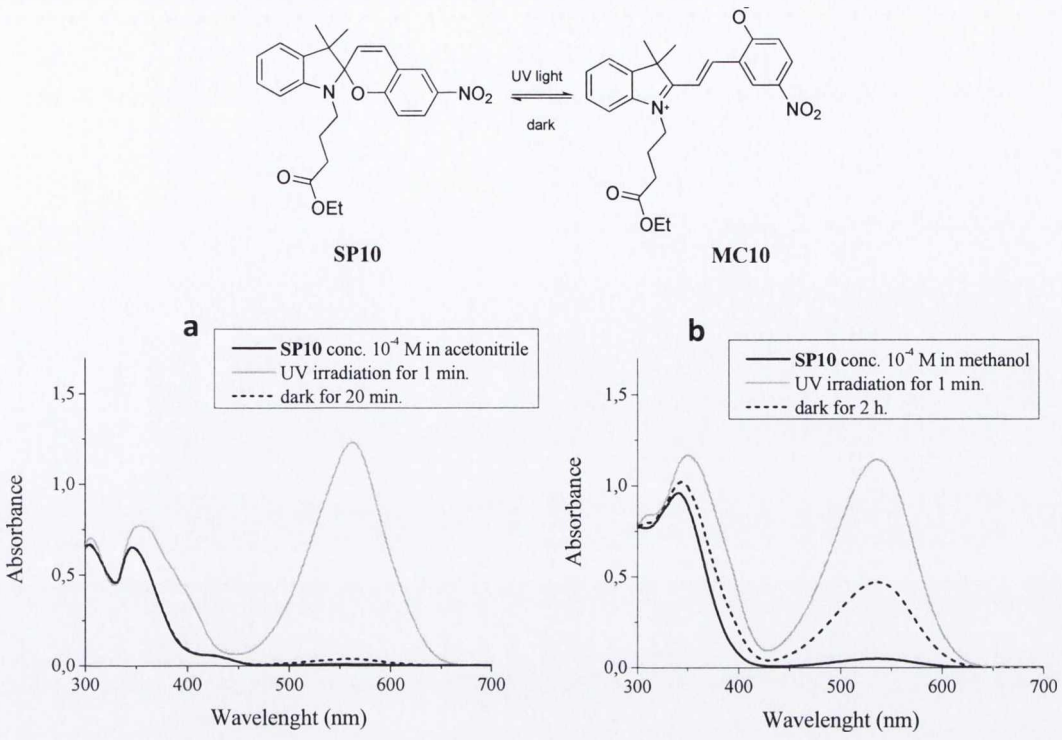


Figure 2.3 UV-vis absorption spectra of **SP10** ($1.0x10^{-4}$ M) after irradiation with UV 254 nm light in acetonitrile (**a**) and methanol (**b**).

merocyanine isomer effected by the hydrogen bonding with the solvent (dotted curve in figure 2.2b).

Considering spiropyran **SP6** and its methoxy free analogue **SP10** which bears the same functional group on the indolic nitrogen, the strong stabilization of merocyanine **MC10** arose as the result of the absence of an electron donating substituent vicinal to the benzopyran oxygen. While the thermal fading of **MC6** took place immediately after the UV source was switched off, the corresponding analogue **MC10** was detectable as a broad absorption band with maximum at 563 nm (grey curve in figure 2.3a) which disappeared after 20 minutes from the cessation of irradiation (dotted curve in figure 2.3a). It seems that the charge delocalization effect on the merocyanine isomer **MC6** actuated by the nitro group is contrasted by the methoxy group that forces a high electronic density on the phenolate oxygen. The strong stabilization effect on the open merocyanine **MC10** was more consistent if the solvent was methanol. In this instance, the thermal bleaching of a spiropyran solution (whose spectrum is the black curve in figure 2.3b) irradiated for just 1 minute (grey curve in figure 2.3b) needed several hours to be complete. The absorption maximum of **MC10** is blueshifted with respect to the

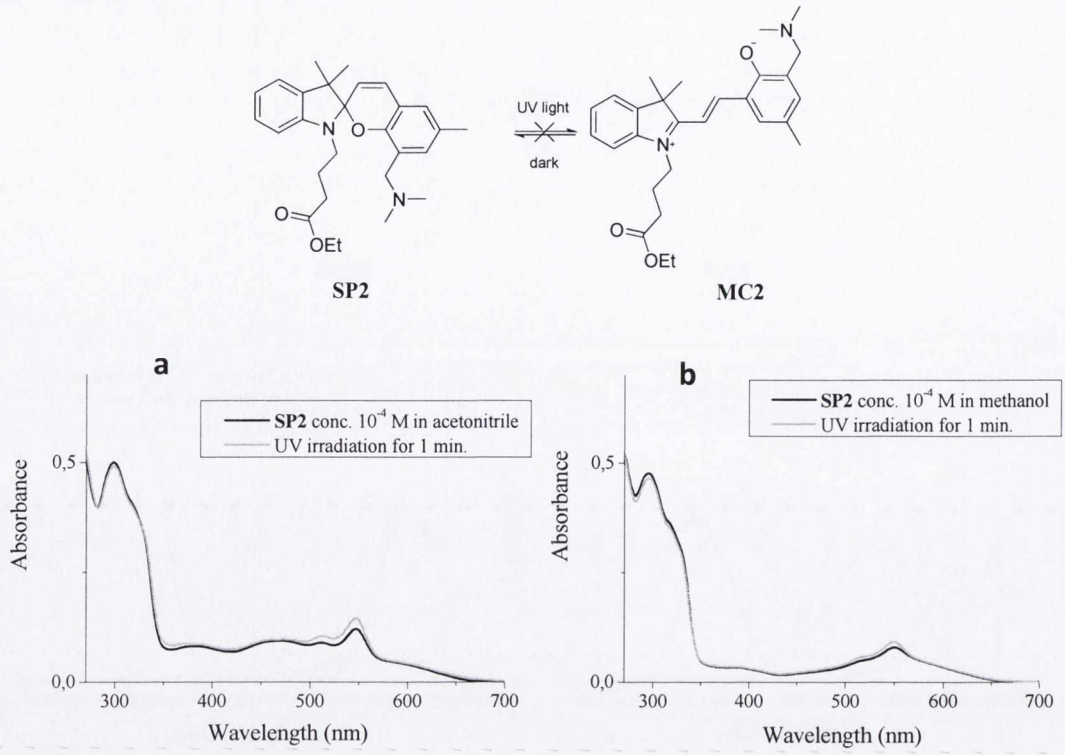


Figure 2.4 UV-vis absorption spectra of **SP2** ($1.0x10^{-4}$ M) after irradiation with UV 254 nm light in acetonitrile (**a**) and methanol (**b**).

value obtained in acetonitrile and takes 2 hours to decrease of 50% of its initial intensity value (dotted curve in figure 2.3b). Although hydrogen bonding produced a dramatic shift in the equilibrium between **SP6** and **MC6**, pushing it toward the open form, this effect was not observed for compound **SP10**. Indeed, the open form was barely detectable in a methanolic solution as a small absorption band with maximum at 536 nm (black curve in figure 2.3b). This can be explained as the solvation of both O^- and OMe in **SP6** that is forced to isomerise to merocyanine while such a phenomenon is not observable if the methoxy group is not present.

Compound **SP2** showed neither photochromic nor solvatochromic behaviour under the same experimental conditions. An acetonitrile solution of this spiropyran absorbs mainly in the ultraviolet region of the electromagnetic spectrum with a broad transition with maximum absorption at 300 nm and a shoulder at 325 nm. Small absorption bands, lower in intensity with respect to the absorptions in the UV region, were observed at 384, 466, 513, and 546 nm (black curve in figure 2.4a). Irradiation of the solution with 254 nm UV light did not produce any significant change in the spectrum (grey curve in figure 2.4a). When the same spiropyran was dissolved in methanol, the same transitions

were observed. The absorption maximum in the UV region blueshifted to 295 nm while the two maxima at 513 nm and 546 nm redshifted slightly to 516 nm and 513 nm respectively (black curve in figure 2.4b). Upon irradiation with UV light at 254 nm did not produce any change in the absorption spectrum of **SP2** (grey curve in figure 2.4b). Despite the presence of an amino group next to the benzopyran oxygen which could in principle interact with methanol molecules via hydrogen bonding and leading to the spiropyran ring opening with the consequent formation of its open form **ME2**, the equilibrium was strongly pushed toward the closed form. Indeed, excitation with UV light does not induce the cleavage of the C-O responsible for the spiropyran photochromism neither in acetonitrile nor in a protic solvent. As expected, the choice of a methyl group in 6'-position was effective in producing a non-photochromic molecule whose equilibrium between the open and close forms is not affected by the solvent polarity either.

2.3.2 Acidochromic Effects

The phenolate anion in the merocyanine form is subject to variation of pH as it can be protonated. Protonation of this site generate a new species whose absorption is dramatically different from the absorption of its corresponding merocyanine and spiropyran. In order to investigate the effect of variations in the acidity of the medium, few UV-vis absorption experiments were carried out. The absorption spectrum of a colourless acetonitrile solution of **SP6** absorbs in the UV region with two bands with maximum intensities at 294 and 360 nm (black curve in figure 2.5a). Irradiation with visible light caused the appearance of a band at 594 nm corresponding to the blue isomer **MC6** (grey curve in figure 2.5a). The absorption spectrum of the open merocyanine changed dramatically after the addition of 1 equivalent of trifluoroacetic acid (TFA). The solution turned yellow and the absorption band at 594 nm disappeared while a new absorption shoulder was visible in the range of 400-450 nm (dotted curve in figure 2.5a). The latter was attributed to the protonated merocyanine isomer **MCH6** that switched back to **SP6** under visible irradiation (red curve in figure 2.5a) with complete decoloration occurring in less than 2 min. The absorption spectrum of an acidified solution of **SP6** (1 eq of TFA) maintained in the dark changes over the course of ca. 40 min. The gradual formation of the protonated merocyanine **MCH6** produced

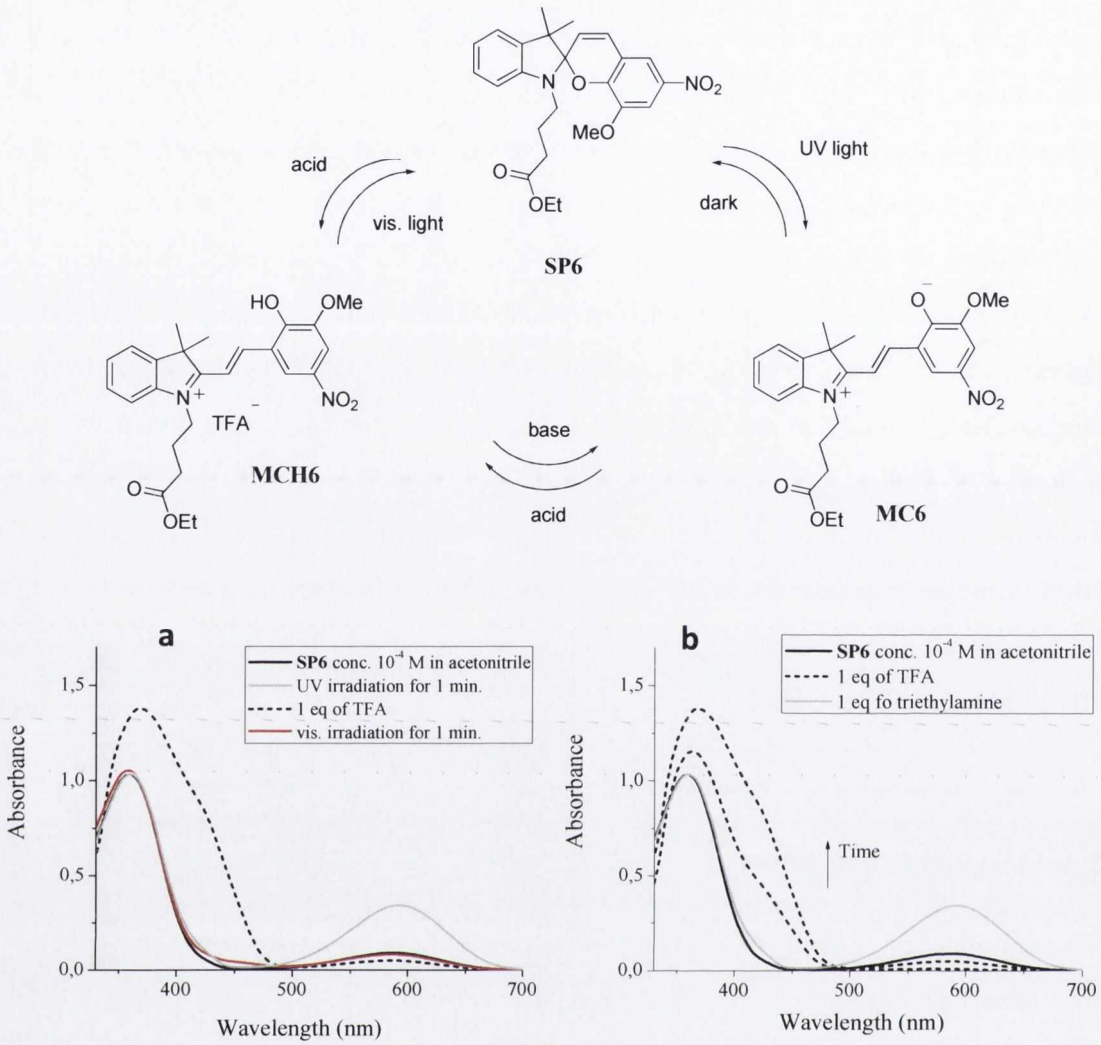


Figure 2.5 The switching cycle associated with the three states **SP6**, **MC6**, and **MCH6**; (**a**) the absorption spectra of a solution at thermal equilibrium of **SP6** ($1.0x10^{-4}$ M, CH_3CN) (**black**) and of the same solution after the consecutive irradiation with ultraviolet light for 1 min (**grey**), addition of one equivalent of trifluoroacetic acid (**dotted curve**) and irradiation with visible light for 1 min (**green**); (**b**) absorption spectra of a solution of **SP6** ($1.0x10^{-4}$ M, CH_3CN) (**black**) after addition of 1 eq of TFA over a period of 40 min. (**dotted curves**), and after addition of 1 eq of triethylamine (**grey curve**).

an increase in absorbance at 400-450 nm (dotted curves in figure 2.5b). The addition of triethylamine resulted in the deprotonation of **MCH6** to produce **MC6** (grey curve in figure 2.5b). Consistently, the characteristic absorption band of **MC6** can be observed at 594 nm immediately after the addition of base. However, **MC6** isomerizes to **SP6** in the dark and only the absorption bands of **SP6** can be detected after ca. 4 min from the addition of triethylamine.

Figure 2.6 shows the spectra of a solution of **SP6** in methanol. This contains a consistent amount of merocyanine in equilibrium with the closed form (figure 2.6). The intense absorption band with maximum at 560 nm, indicating **MC6**, disappeared immediately after the addition of 1 equivalent of TFA. Concomitantly, the appearance of a shoulder ranging between 420 nm and 450 nm indicated the formation of the protonated merocyanine **MCH6**. The absorption maximum at 380 nm underwent an intensity increase and a redshift to 385 nm. Addition of triethylamine restored the two absorption bands at 380 nm and 594 nm, higher in intensity with respect to their values before the addition of acid. The equilibrium was fully restored after 4 min from the addition of triethylamine.

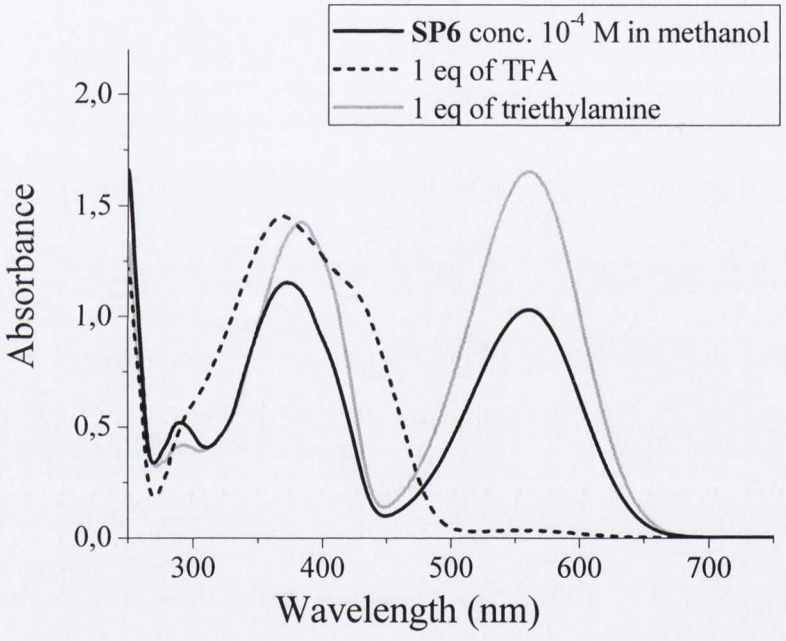


Figure 2.6 Absorption spectra of a methanol solution at thermal equilibrium of **SP6** (1.0×10^{-4} M) before (**black**) and after addition of one equivalent of trifluoroacetic acid (**dotted curve**) followed by addition of 1 eq of triethylamine (**grey**).

The absorption spectrum of a solution of spiropyran **SP10** at thermal equilibrium is consistently different from that of **SP6**. The absence of a methoxy group on the benzopyran moiety of **SP10** does not guarantee the stabilization of the open form by solvation. Thus the spirocyclic form is the predominant species in the ground state.

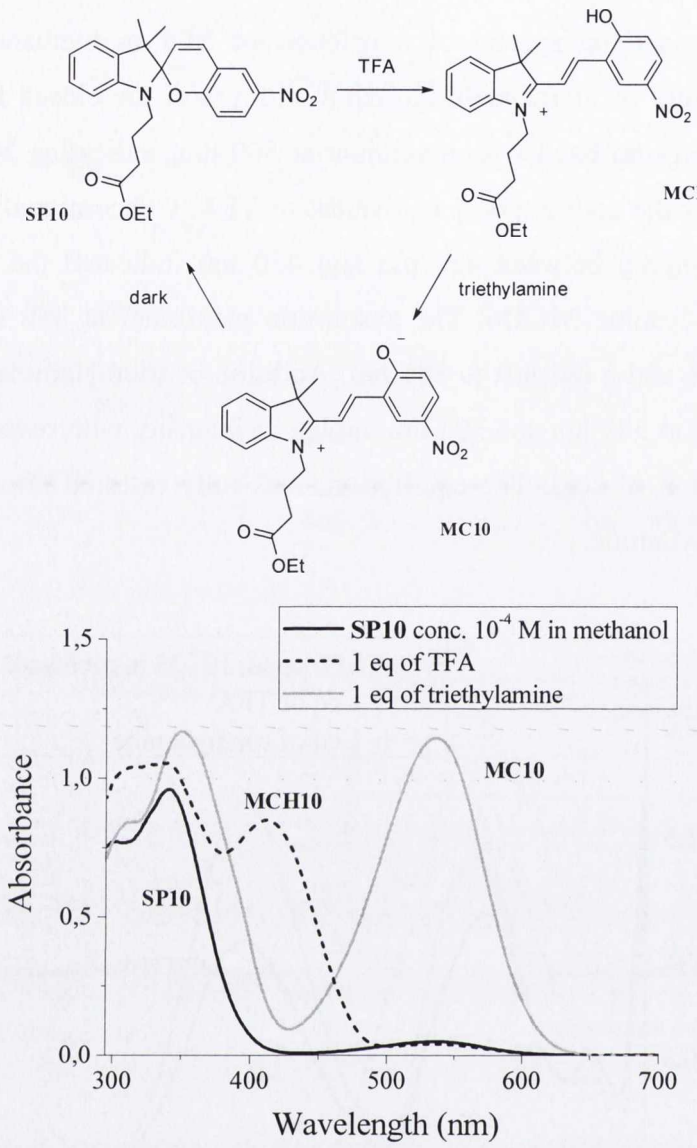


Figure 2.7 Switching cycle associated with the three states **SP10**, **MC10**, and **MCH10** controlled only by pH variations; absorption spectra of a methanol solution at thermal equilibrium of **SP10** ($1.0x10^{-4}$ M) before (**black**) and after addition of one equivalent of trifluoroacetic acid (**dotted curve**) followed by addition of 1 eq of triethylamine (**grey**).

Addition of trifluoroacetic acid to a methanolic spiropyran solution gave rise to a sharp peak at 413 nm that reached its maximum intensity after 50 min from the acidification of the solution (dotted curve in figure 2.7). This peak was attributed to the formation of the protonated species **MCH10**. The non protonated merocyanine **MC10** was obtained by treatment of the acidified solution with triethylamine as demonstrated by the disappearance of the **MCH10** absorption concomitantly with the appearance of a new absorption band in the visible region with maximum intensity at 560 nm (grey curve in

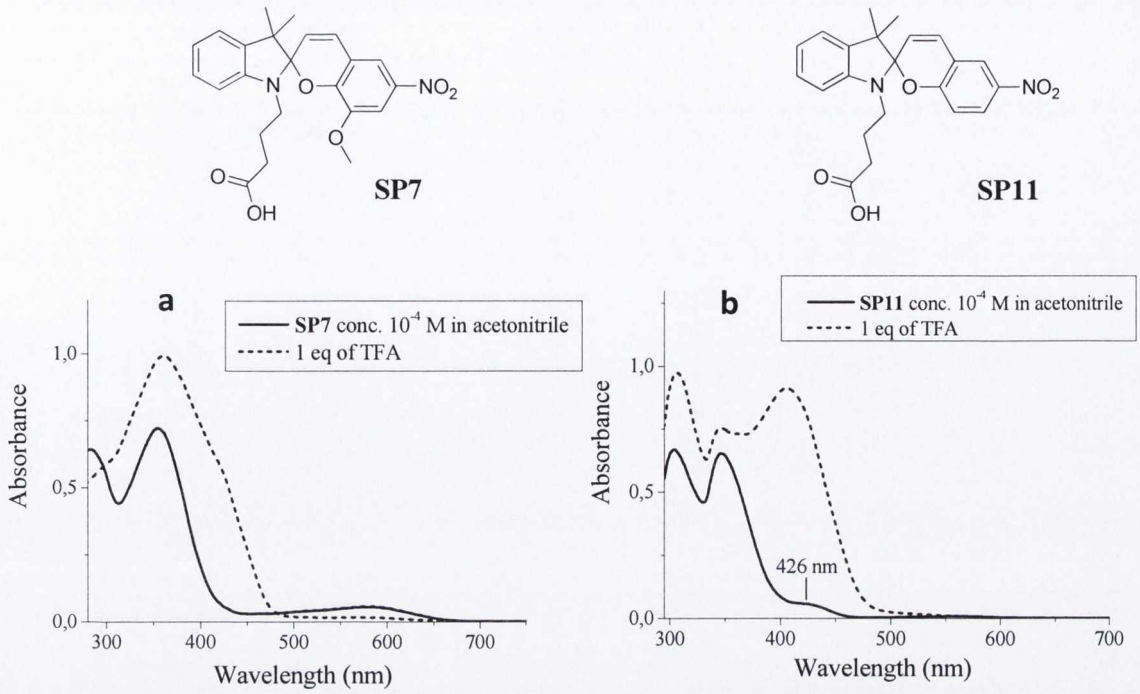


Figure 2.8 Absorption spectra of acetonitrile solutions at thermal equilibrium of **SP7** (**a**) ($1.0x10^{-4}$ M) and **SP11** (**b**) ($1.0x10^{-4}$ M) before (**black curves**) and after addition of one equivalent of trifluoroacetic acid (**dotted curves**).

figure 2.7). This band faded in 20 min when the solution was placed in the dark, and the **SP10** spectrum was completely recovered.

The acidochromic ring-opening process was performed in acetonitrile with the carboxylic acid derivatives **SP7** and **SP11**. A **SP7** solution absorbs in the ultraviolet region with maxima at 282 nm and 358 nm (black curve in figure 2.8a). After the addition of acid a certain time was required to allow **SP7** to be protonated and to reach a stable equilibrium in its open and protonated form. The new absorption band (420-440 nm, dotted curve in figure 2.8a) indicating this species reached its maximum intensity after 35 min. Spiropyran **SP11** has a similar absorption profile in acetonitrile. Additionally, a low intensity absorption band was observed in its ground state absorption spectrum with maximum at 426 nm (black curve in figure 2.8b). This band was explained as the result of intramolecular proton transfer from the aliphatic carboxy group to the merocyanine phenolate which is in thermal equilibrium with the closed isomer. Such a band was not observed in the spectra of **SP7**. Addition of acid to a solution of **SP11** caused a dramatic intensity increase of the peak at 426 nm with a

concomitant 20 nm blueshift over a period of 30 minutes confirming the formation of the protonated merocyanine (dotted curve in figure 2.8b).

2.3.3 Conclusions

The response of our molecules to pH and solvent variations were investigated. The choice of different substituents on the benzopyran half of the spirochromenes has profound influence on their behaviour in different solvents and at different pH. The presence of an electron donating group in 8'position and an electron withdrawing nitro group in 6'-position pushes the equilibrium toward the closed spirocyclic forms in a non protic solvent such as acetonitrile while, in a protic solvent like methanol, the open merocyanines are strongly stabilized. This phenomenon was explained as the result of hydrogen bonding between the protic solvent, the phenolate, and the methoxy in the open forms. The removal of the electron donating methoxy group shifts the SP-MC equilibrium toward the closed form in both protic and non protic solvents. However, excitation of spiropyrans with UV light produce open merocyanines whose half-lives were longer in both solvents than those of the corresponding analogues with the methoxy substituent in 8'-position. This is due by the delocalization of the phenolate negative charge on the nitro group in 6'-position in the methoxy free analogues while such an event is seemingly contrasted by the presence of the electron donating group. When the nitro group is substituted by an electron donating group and a dimethylaminomethyl group is placed in 8'-position, no responses to photostimuli were observed. Indeed the only species in solution were the closed spirocyclic forms regardless to solvents. The substituents on the indolic nitrogen seem to have no influence on the photochromism of the tested spiropyrans and on their ground state equilibrium SP-MC in both solvents. However, when a nitro group was present in 6'-position and a carboxylated chain on the indolic N, intramolecular proton transfer from the carboxy group to the phenolate anion was observed. The resulting protonated merocyanine was detectable at thermal equilibrium with its closed form. The effect of acidity changes in the spiropyran solutions were studied and low pH generates new chemical species namely protonated merocyanine. Their absorption spectra generally range in the visible region around 400-450 nm and differ dramatically from those of their corresponding merocyanines and spiropyrans. The proton removal can be actuated

by either irradiation with visible light, which triggers the reconversion to the spirocyclic form, or by addition of a base that produce the non protonated merocyanine which isomerizes to the closed form thermally.

2.4 Metal Binding Studies

In order to establish whether the combination of the different functional groups were, in fact, capable of offering selective metal-ion recognition, systematic binding studies were performed on our spiropyrans with eleven different metal cations. Biologically and environmentally relevant metal ions such as Zn(II), Cu(II), Ni(II), Co(II), Mn(II), Cd(II), Fe(II), Mg(II), Ca(II), Na(I) and K(I) were tested. The investigations were carried out via different spectroscopic techniques such as UV-vis absorption and emission spectroscopy, ^{1}H-NMR, ESI and MALDI-TOF HRMS, and X-ray crystallography.

2.4.1 Binding Studies on Compounds of Group 1

This group of spiropyrans was tailored to be non photochromic since the choice of the methyl group in 6'-position. Additionally, the affinity for metal cations should increase along the series with order **SP3**>**SP2**>**SP1** since the receptor site in **SP1** is formed by the dimethylaminomethyl group in 8'-position and the vicinal benzopyran oxygen while compounds **SP2** and **SP3** can count on two additional moieties represented by an ethyl ester and a carboxylic acid chain respectively. In order to verify this hypothesis we carried out UV-vis absorption studies on the metal coordination ability of our compounds. Acetonitrile solutions of **SP1**, **SP2**, and **SP3** were equilibrated overnight after the addition of 1 equivalent of a different metal to each solution. The metal used were $Zn(ClO_4)_2$, $Cu(ClO_4)_2$, $Ni(ClO_4)_2$, $Co(ClO_4)_2$, $Mn(ClO_4)_2$, $Cd(ClO_4)_2$, $Fe(ClO_4)_2$, $Mg(ClO_4)_2$, $Cr(ClO_4)_3$, $CaCl_2$, NaCl and KCl. The absorption spectra were then recorded.

Compound **SP1** absorbs in the ultraviolet region of the electromagnetic spectrum with a broad band of maximum intensity at 294 nm and a shoulder at 320 nm. No absorption bands were observed in the visible region. Addition of the different metal

cations caused intense absorptions in the visible region indicating the formation of spiropyran-metal complexes **MCM1** (figure 2.9). Particularly impressive were the responses to Cu(II), Ni(II), Fe(II), Co(II), and Cd(II). The presence of nickel and cobalt produced two similar absorption bands ranging in two different regions of the spectrum at 380-395 nm and 560-580 nm respectively (figure 2.9a). The spiropyran cadmium

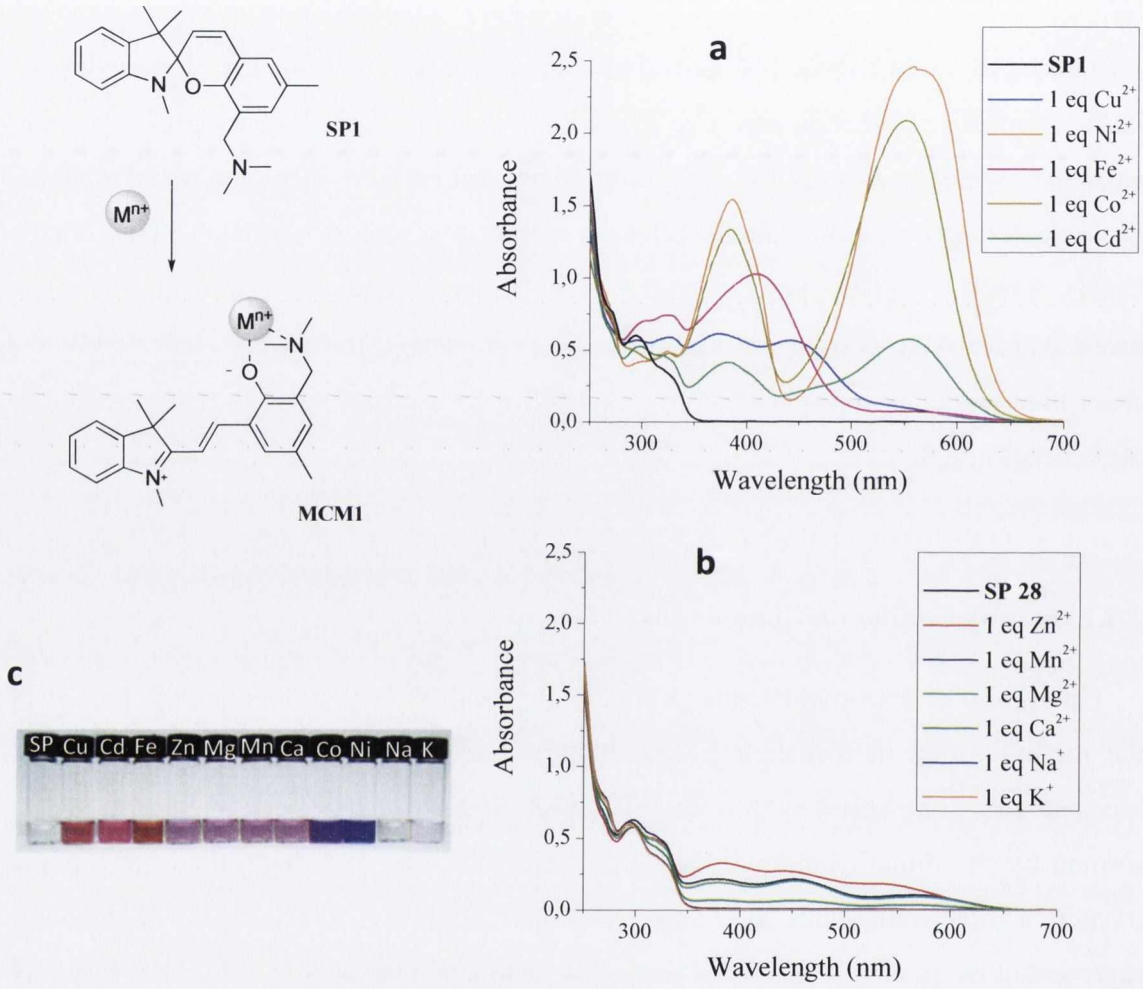


Figure 2.9 (**a**) and (**b**) are the absorption spectra of **SP1** solutions ($1.0x10^{-4}$ M, acetonitrile) before and after the addition of 1 eq of different metal perchlorates and chlorides; (**c**) picture of the same solutions containing equimolar amount of **SP1** and the tested metal salts.

complex absorbed as well visible light in these same regions but the intensities of the two maxima were one fifth of the intensities observed for the cobalt and nickel complexes (figure 2.9a). Copper and iron caused two different type of absorption spectra. The SP-Fe(II) complex was detected as a massively large absorption band that ranged between 350 nm and 500 nm with maximum intensity at 410 nm. Similarly, the

SP-Cu(II) complex absorbed light in the same range but two absorption maxima were observed at 374 nm and 444 nm respectively (figure 2.9a). Weak transitions were observed in the presence of zinc, manganese, magnesium, and calcium localized in three different regions of the visible spectrum around 375-390 nm, 450-460 nm, and 550-600 nm (figure 2.9b). The addition of sodium and potassium did not produce any relevant change in the spiropyran absorption spectrum (figure 2.9b). The picture in figure 2.9c displays the different solutions containing each spiropyran-metal complex analyzed.

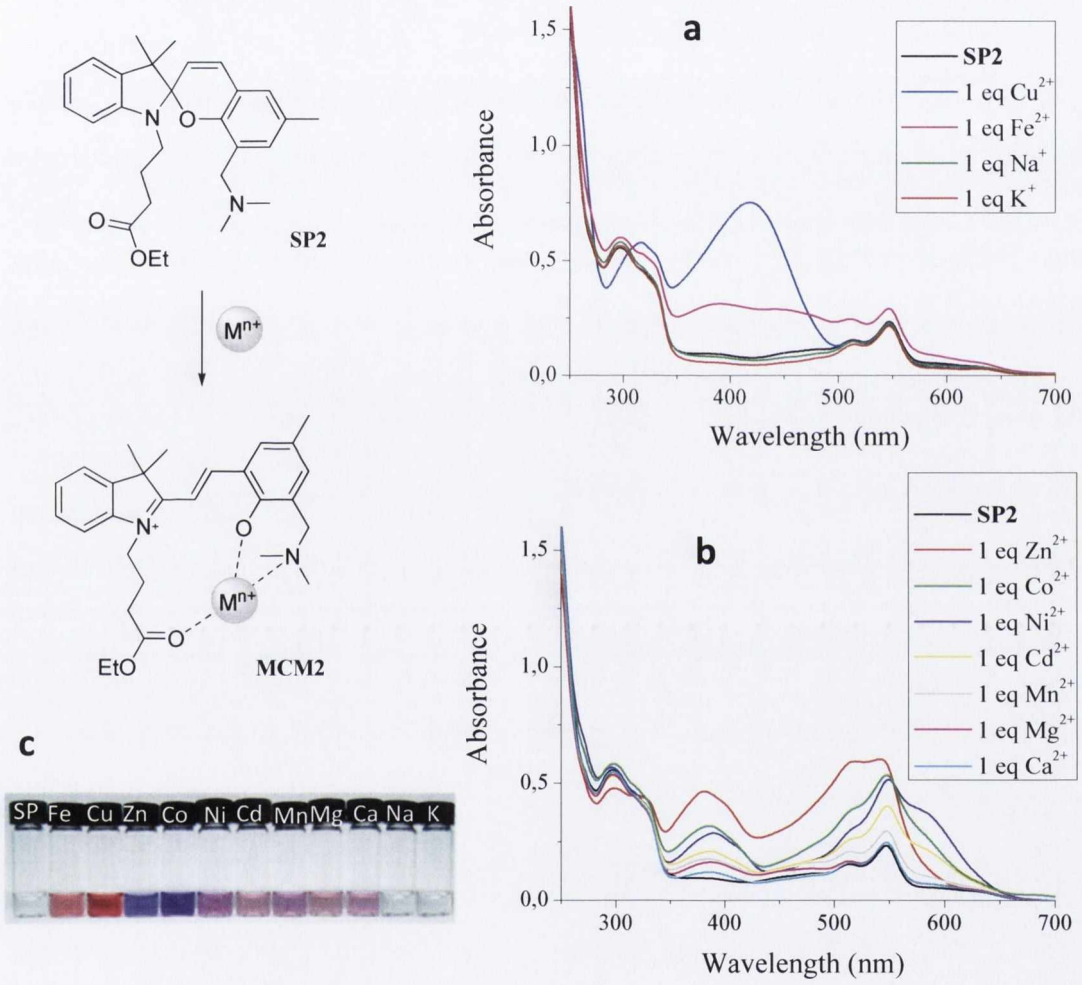


Figure 2.10 (**a**) and (**b**) are the absorption spectra of **SP2** solutions ($1.0x10^{-4}$ M, acetonitrile) before and after the addition of 1 eq of different metal perchlorates and chlorides; (**c**) picture of the same solutions containing equimolar amount of **SP2** and the tested metal salts.

Compound **SP2** absorbs in the ultraviolet region with a broad band of maximum intensity at 300 nm and a shoulder at 325 nm. In addition, low intensity absorption

bands were observed at 513, and 546 nm. Analogously to **SP1**, the addition of sodium and potassium chlorides to a **SP2** solution in acetonitrile did not produce significant changes to its spectrum (figure 2.10a). In the presence of copper a broad absorption band appeared in the visible region with maximum intensity localized at 417 nm (figure 2.10a). A lower intensity absorption band appeared upon addition of iron perchlorate. Although this band was flat an spread over the region between 350 nm and 500 nm, two maxima were identified at 387 nm and 445 nm (figure 2.10a). Both solutions containing copper and iron complexes with **SP2** were deeply orange-red coloured. Addition of zinc, cobalt, nickel, cadmium, manganese, magnesium, and calcium produced the same pattern of changes in **SP2** absorption spectra. All the solutions containing equimolar concentrations of spiropyran and metal salts turned from slightly pink into purple immediately after the addition of metals, indicating the formation of spiropyran-metal complexes structurally similar to **SPM2**, suggested in figure 2.10. The coordination of each metal should involve the three binding sites of the open form of **SP2**. The main absorption band observed were localized in the ranges of 380-390 nm and 540-550 nm. Both bands decreased in intensity and redshifted slightly along the series with order Zn>Co>Ni>Cd>Mn>Mg>Ca (figure 2.10b).

Compound **SP3** is the last in this group of molecules and its skeleton resembles that of **SP2** except for the terminal carboxy group on **SP3**. This substituent ensures higher affinity bindings for transition metal cations than the ethyl ester present on the other analogue. The spiropyran was tested with the same group of metal perchlorates and chlorides in acetonitrile and the absorption spectra of the resulting metal complexes are shown in figure 2.11a and 2.11b. The absorption intensity maximum of a metal free solution of **SP3** is localized at 293 nm (figure 2.11a and 2.11b). No transitions were observed at longer wavelength than 350 nm. The presence of sodium and potassium did not affect the spiropyran absorption similarly to the other two analogues afore mentioned (figure 2.11a). Upon addition of copper perchlorate a broad absorption band extending from 350 nm to 620 nm appeared (figure 2.11a). The maximum absorption was located at 385 nm. Two distinctive bands characterized instead the spiropyran-iron complex whose absorption maxima were located at 378 nm and 504 nm (figure 2.11a). The absorption of the remaining complexes were all located in the same two regions of the electromagnetic spectrum and all the solutions were all deeply purple (figure 2.11c). The first bands were all almost overlapped in intensity and position, ranging between

378 nm and 385 nm. The highest intensity band was recorded for the spiropyran-cobalt complex. The second absorption bands were localized at longer wavelengths between 533 nm, for the spiropyran-zinc complex and 571 nm for the spiropyran-nickel complex (figure 2.11b). This spiropyran responded to all metal cation tested with no preferences to some in particular. The most likely structure of these complexes would resemble the hypothetical one in figure 2.11 namely **MCM3** with a generic metal M^{n+} trapped by the triad phenoxy-dimethylamino-carboxy.

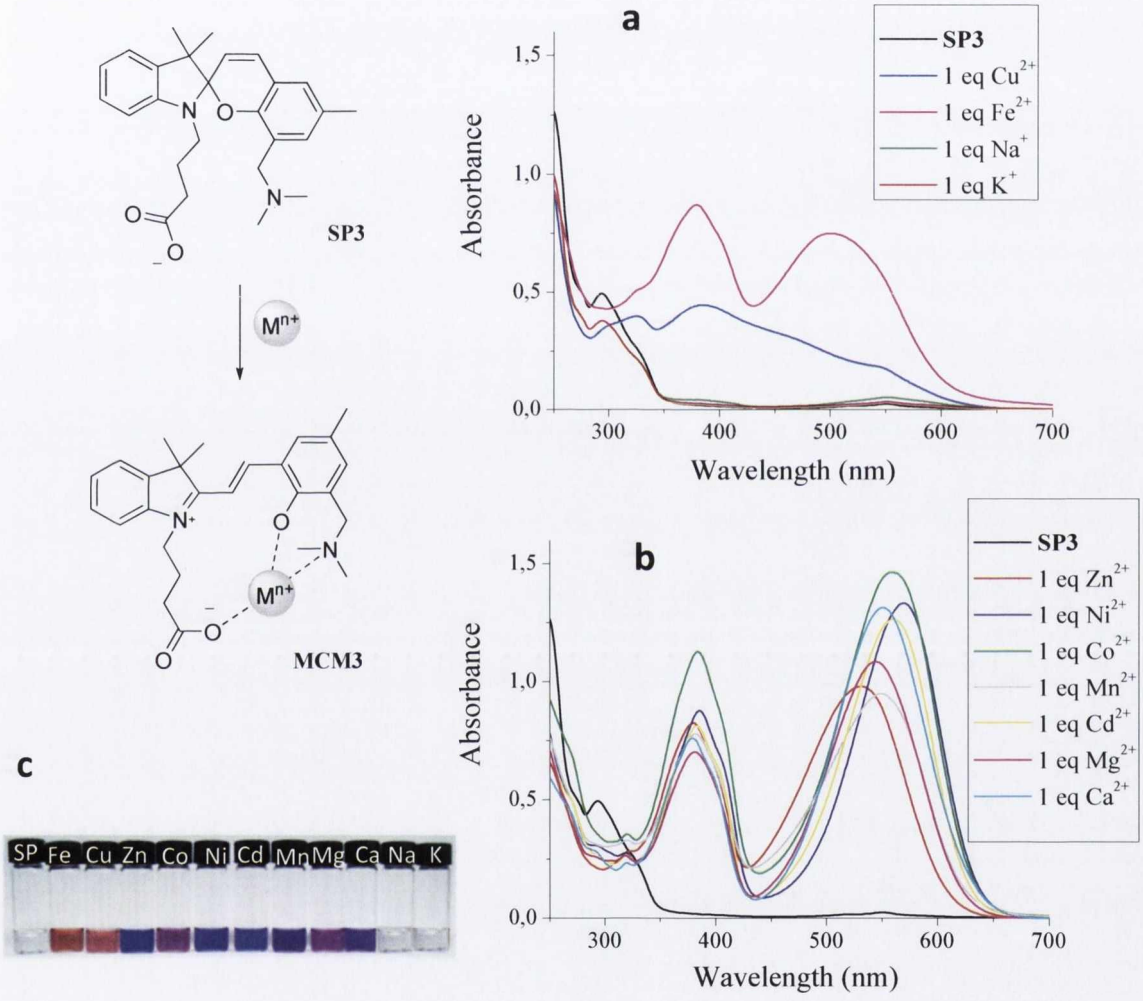


Figure 2.11 (**a**) and (**b**) are the absorption spectra of **SP3** solutions ($1.0x10^{-4}$ M, acetonitrile) before and after the addition of 1 eq of different metal perchlorates and chlorides; (**c**) picture of the same solutions containing equimolar amount of **SP3** and the tested metal salts.

Table 2.1 reports the absorption maxima of all metal complexes in this group of spiropyran.

Comp.	Cu λ max (nm)	Fe λ max (nm)	Zn λ max (nm)	Ni λ max (nm)	Co λ max (nm)	Mn λ max (nm)	Mg λ max (nm)	Cd λ max (nm)	Ca λ max (nm)
SP1	374/444	410	382/454/541	386/559	385/551	380/456/567	318/457/565	385/550	378/454/561
SP2	417	387/445	382/513/541	391/548	385/548	384/546	388/546	387/548	389/546
SP3	385	378/504	378/533	385/571	380/559	381/549	382/545	384/561	385/549

Table 2.1 Absorption maxima of complexes with spiropyrans of group 1.

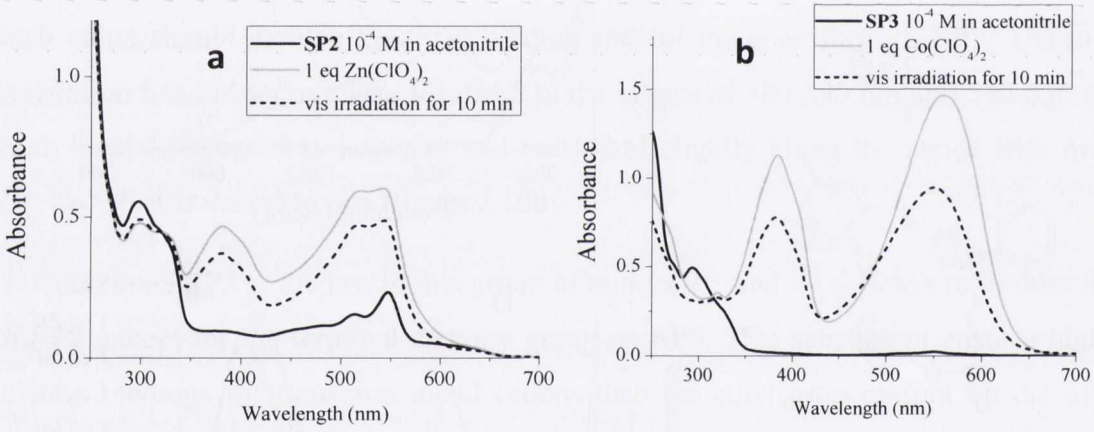


Figure 2.12 (**a**) Absorption spectra of a **SP2** solution ($1.0x10^{-4}$ M, acetonitrile) before (black) and after (grey) the addition of 1 eq $Zn(ClO_4)_2$ and after irradiation with visible light for 10 min (dotted curve); (**b**) absorption spectra of a **SP3** solution ($1.0x10^{-4}$ M, acetonitrile) before (black) and after (grey) the addition of 1 eq $Zn(ClO_4)_2$ and after irradiation with visible light for 10 min (dotted curve).

For spiropyran-metal complexes where the switchable molecule is also photochromic, the metal release should be effected by irradiation of the complex in solution with visible light. The trans-cis isomerization of the open merocyanine chelating the cation followed by the pyran ring closure with the reformation of the spiro C-O bond would be the event that triggers the metal release. Such a phenomenon can be followed by absorption spectroscopy and it is generally accompanied by the disappearance of the spiropyran-metal complex absorption with the concomitant

recovering of the spiropyran ground state absorption. The actual influence of the amino group present in the three derivatives **SP1**, **SP2**, and **SP3** was evaluated by UV-vis absorption spectroscopy studies. Few solutions containing spiropyran-metal complexes were irradiated with visible light for 10 minutes each and the corresponding absorption spectra were recorded. A couple of examples are shown in figure 2.12 a and b. Spiropyran **SP2** chelates zinc perchlorate in acetonitrile. The metal binding is accompanied by the appearance of one band of absorption with maxima at 380 nm and another band at longer wavelength with two maxima at 516 nm and 540 nm respectively. Upon irradiation with visible light all the absorption bands indicating the presence of the metal complex dropped to lower intensities with no significant shifts in their maxima but they did not disappear. This indicates only a partial displacement of the metal cation from the spiropyran receptor site. Analogously **SP3** responded to the addition of $Co(ClO_4)_2$ with two intense absorptions at 382 nm and 560 nm. Visible light irradiation affected poorly the metal complex spectra as the two bands fell in their intensities of the 30% of the original value indicating also in this instance only a partial release of the metal guest from the tridentate receptor site.

2.4.2 Conclusions on Group 1

In conclusion, the three spiropyran derivatives **SP1**, **SP2**, and **SP3** showed good abilities of metal bindings toward bivalent cations. In fact, no response was observed toward monovalent cations such as sodium and potassium. The choice of a electron donating group in 6'-position afforded cation receptors whose binding properties are negligibly affected by light and interact with good affinity with a good range of biologically important cations. However, selective response to particular cations were not observed as all the absorption spectra corresponding to the different metal complexes were overlapped for a consistent extent, impeding the actual discrimination between the metals.

2.4.3 Binding Studies on Compounds of Group 2

Spiropyran derivatives belonging to this group were designed to be both ionochromic and photochromic. Thus, coordination of metal cations should be detectable as the appearance of new absorption bands in the visible region of spiropyrans' spectra. In

addition the metal guests uptake-release should be modulated by visible light irradiation.

Compounds **SP4** and **SP5** have already been reported in literature for being metal ligands[3,4] but the number of metals tested was very limited. We wanted to widen the range of metals in order to improve the understanding of the mechanisms involved in the binding process and lead us in tailoring highly selective systems.

2.4.4 UV-vis Absorption Studies on Metal Complexes

The same experimental condition used for the spectroscopic analysis of compounds of group 1 were used with the members of group 2 as well. Spiropyran **SP4** is the only derivative in this series whose receptor site is a bidentate can form bidentate metal complexes with an hypothetical metal guest. An acetonitrile solution of **SP4** is colourless and absorbs in the UV region with maxima at 285 nm and 357 nm. Addition of equimolar amounts of two alkaline cations like sodium and potassium maintained the spiropyran spectrum unvaried (figure 2.13a) but dramatic changes were observed after the addition of copper (II) perchlorate and iron (II) perchlorate. In the copper complex, the two spirochromene absorption bands coalesced in a unique broad band with a maximum at 359 nm and a shoulder at 421 nm. The band extent covered a wide part of the ultraviolet-visible spectrum from 280 nm to almost 600 nm (figure 2.13a). This huge transition was attributed to the formation of a bidentate copper complex where the metal cation is bonded to the phenolate anion of the open merocyanine and the methoxy group adjacent to the phenolate oxygen. The presence of iron (II) perchlorate caused the same coalescence of the two spirochromene absorption bands but the resulting band maximum was slightly red shifted at 368 nm as well as the shoulder observed in the visible region, now localized at 477 nm (figure 2.13a). Completely different responses were observed upon formation of complexes with the remaining different cations. Addition of Zn(II), Ni(II), Co(II), Mn(II), Cd(II), Mg(II), and Ca(II) perchlorates caused the appearance of new absorption bands redshifted with respect to the ground state absorptions of **SP4**, ranging between 477 nm for the zinc complex and 520 nm for the calcium complex (figure 2.13b). The absorption maximum at 357 nm underwent dramatic intensity increases depending on the coordinating metal. The **SP4** absorption maximum at 285 nm decreased upon addition of metals and an isosbestic point was

observed in all the spectra at 303 nm, suggesting the presence of only two species in solution namely **SP4** and the corresponding metal complex **MCM4**, depicted in figure 2.13. All the solutions turned from colorless to deeply orange upon addition of all bivalent metal salts as shown in the picture of figure 2.13c.

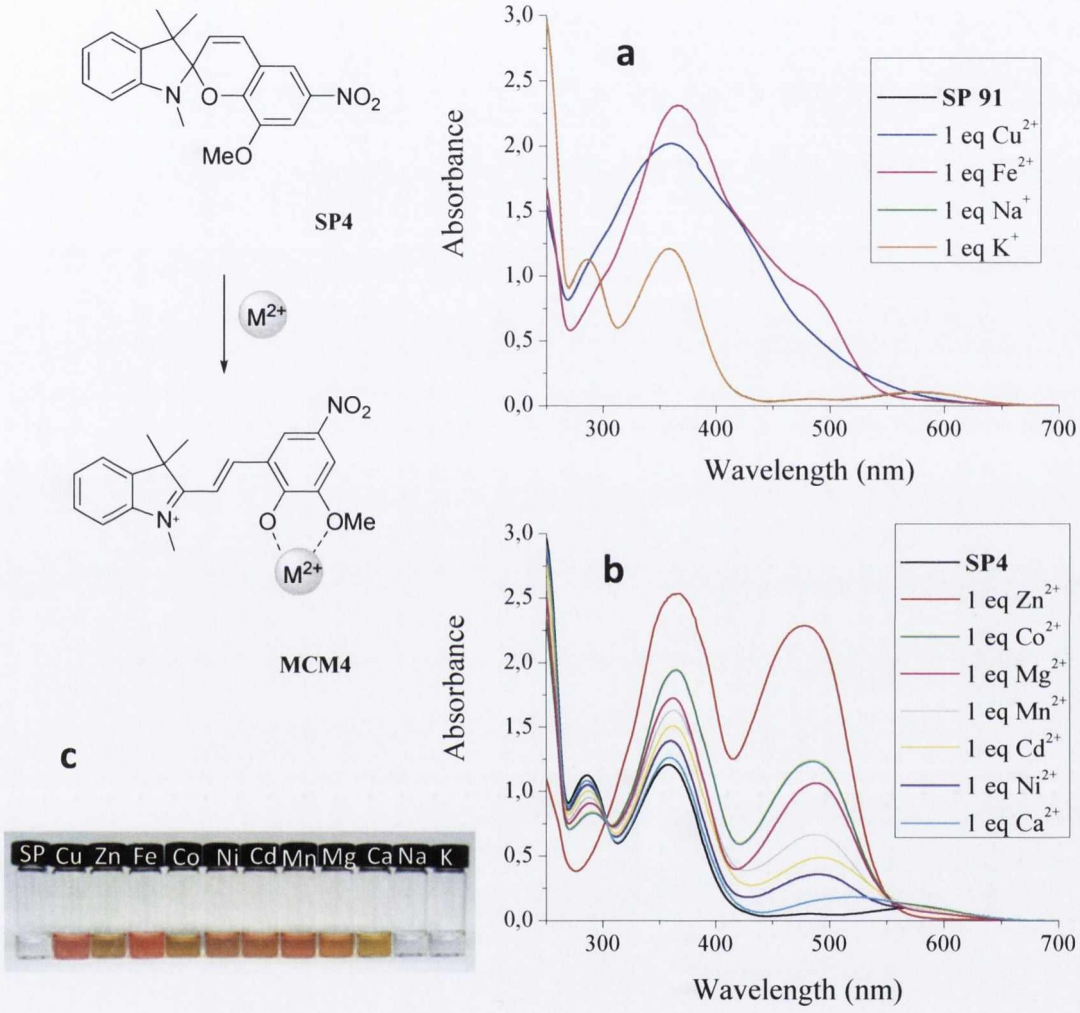


Figure 2.13 (**a**) and (**b**) are the absorption spectra of **SP4** solutions ($1.0x10^{-4}$ M, acetonitrile) before and after the addition of 1 eq of different metal perchlorates and chlorides; (**c**) picture of the same solutions containing equimolar amount of **SP4** and the tested metal salts.

Metal complex spectra of compound **SP5** are shown in figure 2.14 a and b. The short hydroxylated tether on the indolic nitrogen of this molecule offers an additional site for metal binding. When a complex is formed, in theory a metal would be caged in the tridentate system hydroxy-phenoxy-methoxy. The UV-visible spectroscopic analysis

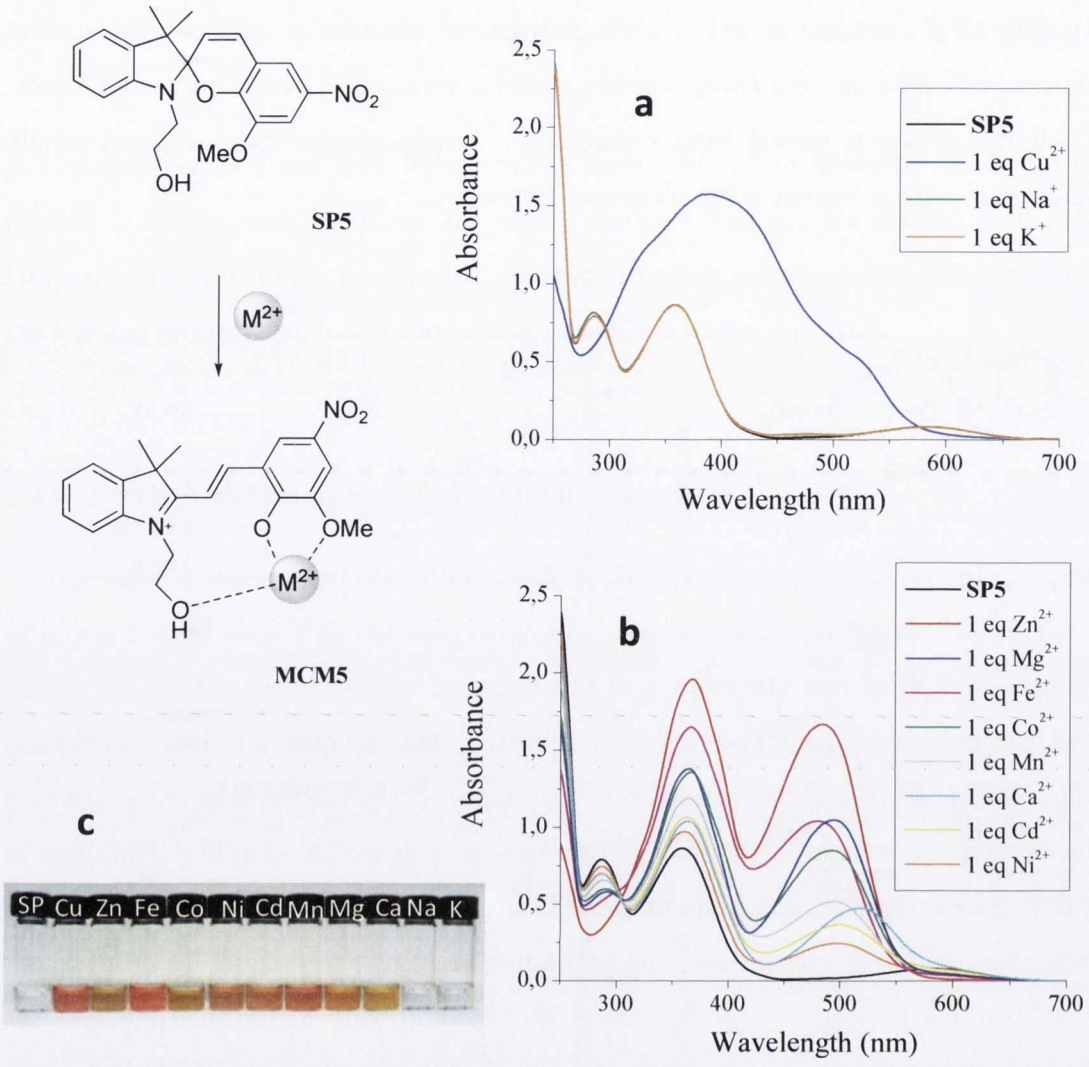


Figure 2.14 (**a**) and (**b**) are the absorption spectra of **SP5** solutions ($1.0x10^{-4}$ M, acetonitrile) before and after the addition of 1 eq of different metal perchlorates and chlorides; (**c**) picture of the same solutions containing equimolar amount of **SP5** and the tested metal salts.

proved the metal complexes are formed after addition of equimolar amount of Zn(II), Cu(II), Ni(II), Co(II), Mn(II), Cd(II), Fe(II), Mg(II), and Ca(II) but no response was observed upon addition of Na and K (figure 2.14a). While in the complexation of both copper and iron the spectra indicating the corresponding spiropyran-metal complexes differed significantly from those with the other bivalent cations, in this instance, only copper gave a different absorption profile while the **SP5**-Cu complex absorbed in the visible region with a band whose maximum was located at 478 nm (figure 2.14a). The **SP5**-Mg complex absorption at 494 nm had intensity similar to that observed for the iron complex. The **SP5**-Zn complex was the one whose characteristic absorption

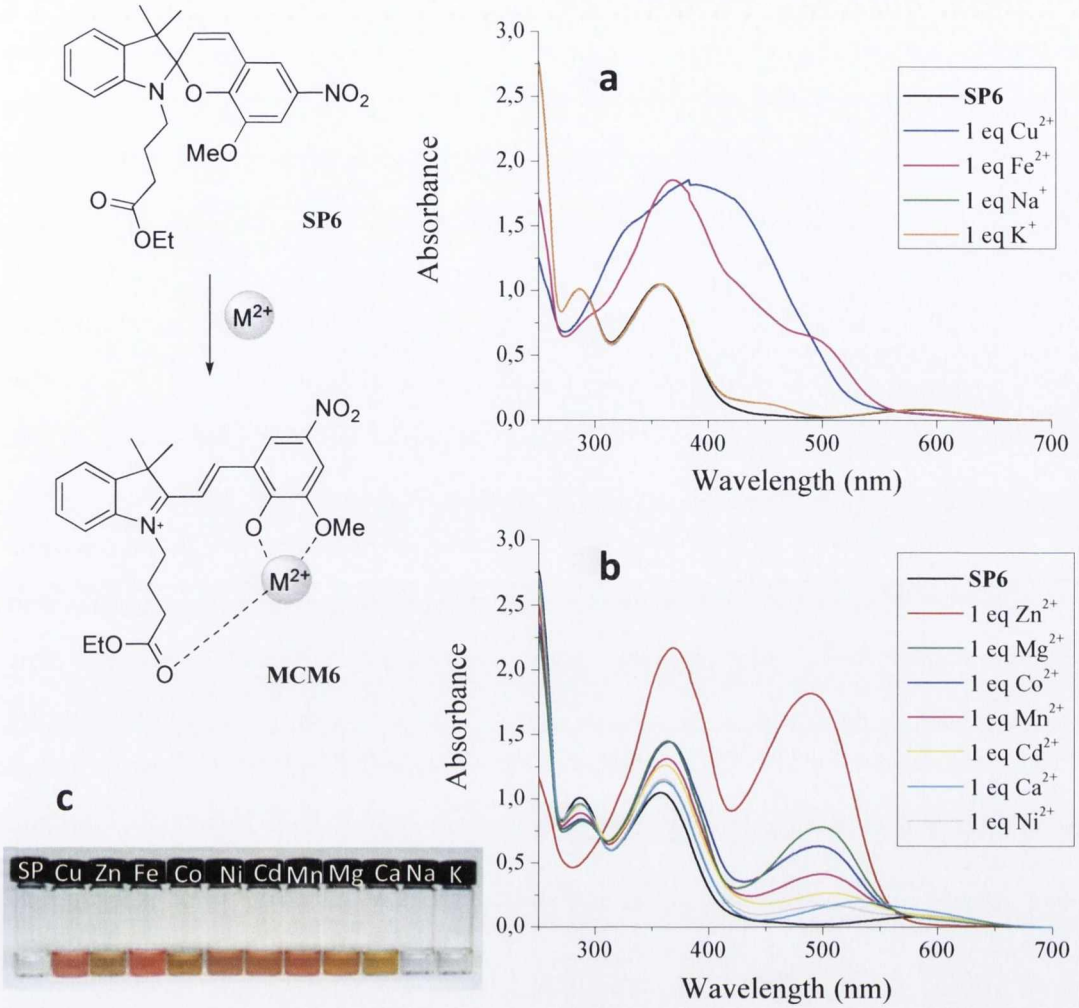


Figure 2.15 (**a**) and (**b**) are the absorption spectra of **SP6** solutions ($1.0x10^{-4}$ M, acetonitrile) before and after the addition of 1 eq of different metal perchlorates and chlorides; (**c**) picture of the same solutions containing equimolar amount of **SP6** and the tested metal salts.

intensity at 483 nm was the highest in the series. All the complexes absorbed light in the same region ranging between 478 nm, for the **SP5**-Fe complex, and 516 nm the **SP5**-Ca complex. Similarly to the results obtained for spiropyran **SP4**, an isosbestic point was observed also in all the spectra at 305 nm, indicating that two species are involved in the complexation, namely **SP5** and the bivalent metal complex **MCM5**. The absorption maxima values of all complexes are reported in table 2.2.

Spiropyran **SP6** is functionalized with an ethyl butyrate tether on the indolic nitrogen. The ester group offers a better binding moiety with respect to that of **SP5**. The absorption spectra of **SP6**-metal complexes resembles those of **SP4**. Coordination of copper and iron gave two absorptions significantly different from the patterns observed

for the other complexes. The copper complex gave a broad absorption with maximum intensity at 390 nm while the iron complex absorbs with maximum intensity at 365 nm. The absorption band is extended until 500 nm and shows smooth shoulder at 495 nm (figure 2.15a). Despite the dramatic difference between spectra of iron and copper complexes and the other metal chelates, all the solutions were characterized by deeply orange colorations (figure 2.15c). Interestingly, addition of sodium and potassium gave weak absorptions with maximum intensity at 455 nm, indicating little but still present interactions with the receptor site of this molecule (figure 2.15a). The spectra of the remaining metal complexes are featured in figure 2.13b. Their main absorptions range in the visible region between 489 nm and 539 nm (figure 2.15b). Weak interactions were observable between the spirochromene and calcium, magnesium, and cadmium. In addition the absorption band of calcium is the most redshifted in the series. The zinc complex absorption band has an intensity which is equal to the double or more than the intensities observed for the other complexes. An isosbestic point at 304 nm indicates that two species are involved in the process, namely the closed form **SP6** and the chelate **MCM6**. Table 2.2 reports the maximum intensities of the different **SP6** metal complexes.

The last spiropyran in this series is **SP7** bearing a carboxylic terminal group on the aliphatic chain attached to the indolic nitrogen. This functional group can form a tridentate system with both methoxy and phenolate of the open isomer to trap tightly a metal ion. Upon addition of the different metal we observed the similar patterns observed in the previous experiments. For instance, the responses to sodium and potassium were both negligible (figure 2.16a), while the copper and the iron complexes produced two absorption spectra that differed significantly from the absorption of other complexes (figure 2.16a). The typical broad absorption band for the copper complex had maximum intensity at 414 nm and a small shoulder was observed at 329 nm. Similarly, the iron complex absorbed in the same region but its maximum absorption was localized at 375 nm. In this case the zinc complex was not the one with the most intense absorption. In fact, its spectra resembles those of cobalt, cadmium, and manganese, ranging between 485 nm and 510 nm with very similar intensities (figure 2.16b). The lowest intensity absorption was found for the nickel complex, with maximum at 507 nm and the most intense absorption was that of the calcium complex, which was significantly shifted to longer wavelength, with maximum at 527 nm (figure

2.16b). The absorption maxima values of spiropyran-metal complexes in this series are reported in table 2.2 below.

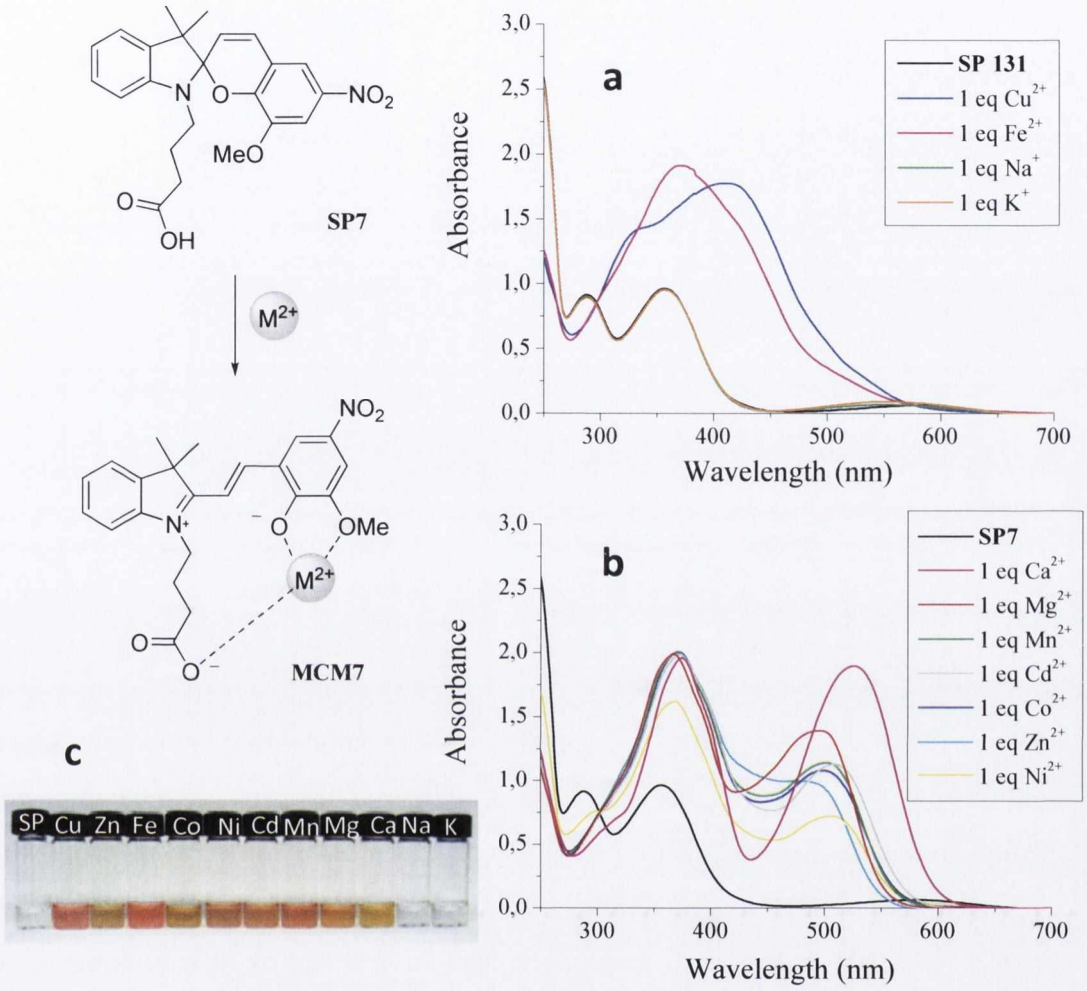


Figure 2.16 (**a**) and (**b**) are the absorption spectra of **SP7** solutions ($1.0x10^{-4}$ M, acetonitrile) before and after the addition of 1 eq of different metal perchlorates and chlorides; (**c**) picture of the same solutions containing equimolar amount of **SP7** and the tested metal salts.

All spiropyrans in this group responded to the presence of bivalent cations by forming stable complexes which absorbed light in the visible region of the electromagnetic spectrum. The same absorption patterns were observed in the coordination of copper and iron that gave wide absorptions, blueshifted with respect to those of the other complexes. The latter are in fact narrower with sharper peaks localized between 500 nm and 580 nm. Remarkably higher intensity peaks were generally observed for complexes with zinc. This is probably due by the cation size

which is more compatible with the bidentate phenolate-methoxy receptor. The wavelength values of absorption maxima for all spiropyran complexes are reported in table 2.2.

Comp.	Cu λ max (nm)	Fe λ max (nm)	Zn λ max (nm)	Ni λ max (nm)	Co λ max (nm)	Mn λ max (nm)	Mg λ max (nm)	Cd λ max (nm)	Ca λ max (nm)
SP4	359/421	368/477	477	491	485	486	486	494	520
SP5	389	478	483	500	491	493	494	500	516
SP6	390	365	489	506	497	501	497	510	539
SP7	414	329	492	509	497	500	496	510	525

Table 2.2 Absorption maxima of complexes with spiropyrans of group 2.

2.4.5 Reversibility of the complex formation

The complex formation reversibility was confirmed by additional experiments where the solutions containing spiropyrans and metals were irradiated with visible light. Upon irradiation the metals were fully released as the typical peaks of the complexes disappeared (figure 2.17a and 2.17b). The complexes formation were reversible as the peaks in the visible region re-appeared after storage in the dark. Thus the metal release was fully controllable and modulated by light, and several cycles of irradiation were possible and reproducible. Figure 2.17a shows the absorption spectra of compound **SP5** before and after the addition of cobalt. Once the solution reached the equilibrium, it was irradiated with visible light for 1 min. The peak indicating the spiropyran-cobalt clearly disappeared recovering perfectly the metal free spiropyran spectrum. The inset of the same figure shows the reproducibility of sequential irradiation cycles. The plot and the inset in figure 2.17b, display very similar results obtained for zinc complex with **SP7**.

2.4.6 ^{1}H NMR Analysis on the Zinc Complexes of SP4 and SP7

All spiropyrans belonging to group 2 were relatively responsive to the presence of zinc as indicated by the high intensity bands of spirochromene-zinc complexes. Tendentiously, red shifts are observed in the whole group of compounds going from

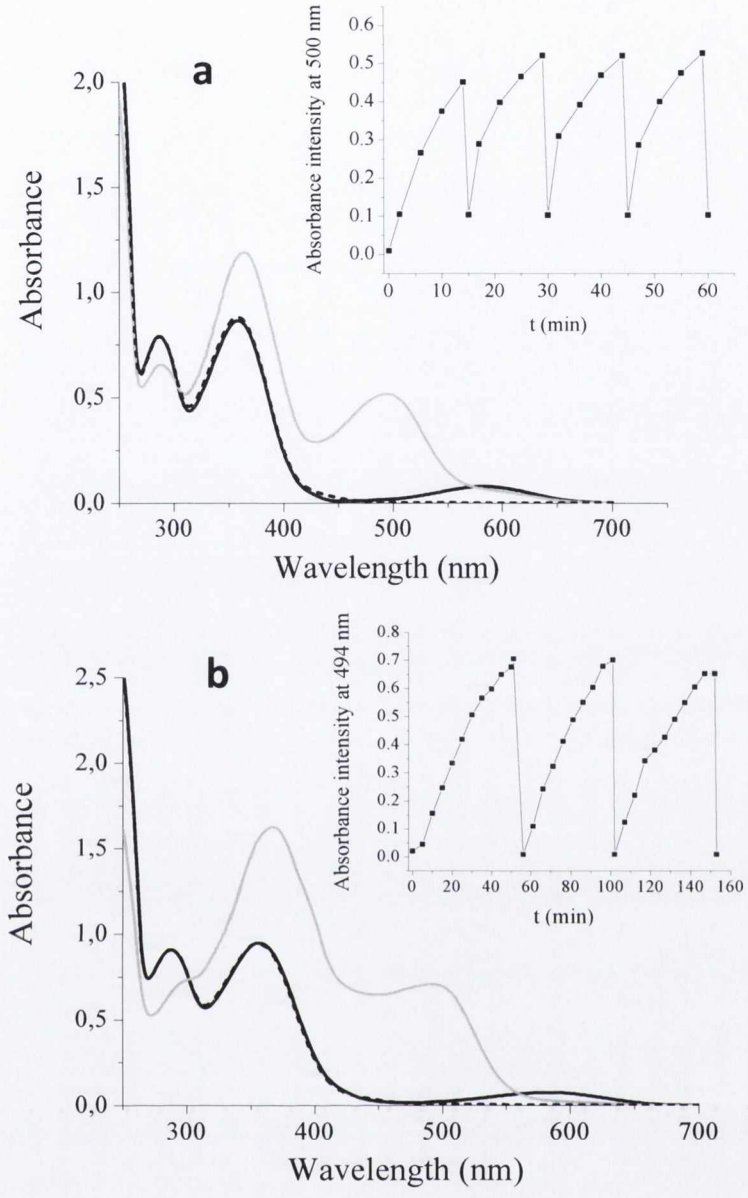


Figure 2.17 Reversible interconversion between spiropyran and the open merocyanine-metal complex. (**a**) Absorption spectra of (black) **SP5** ($1.0x10^{-4}$ M, acetonitrile, 293K), after the addition of 1 equivalent of $Co(ClO_4)_2$ (grey) and after the irradiation with visible light for 60s (dotted curve); (**b**) Absorption spectra of (black) **SP7** ($1.0x10^{-4}$ M, acetonitrile, 293K), after the addition of 1 equivalent of $ZnCl_2$ (grey) and after the irradiation with visible light for 60s (dotted curve); insets (**a**) and (**b**) are sequential cycles of conversion between **SP** and **MCM** controlled by visible light in the presence of $Ni(ClO_4)_2$ and $ZnCl_2$ respectively.

SP4 to **SP7** with a maximum value 15 nm observed between the absorption maxima at 477 nm of **SP4**-Zn complex and that at 492 nm of **SP7**-Zn complex. In order to gather more information about the chelation process we delved into the study of complexes **SP4**-Zn and **SP7**-Zn. The two compound differ from each other because of the chelating

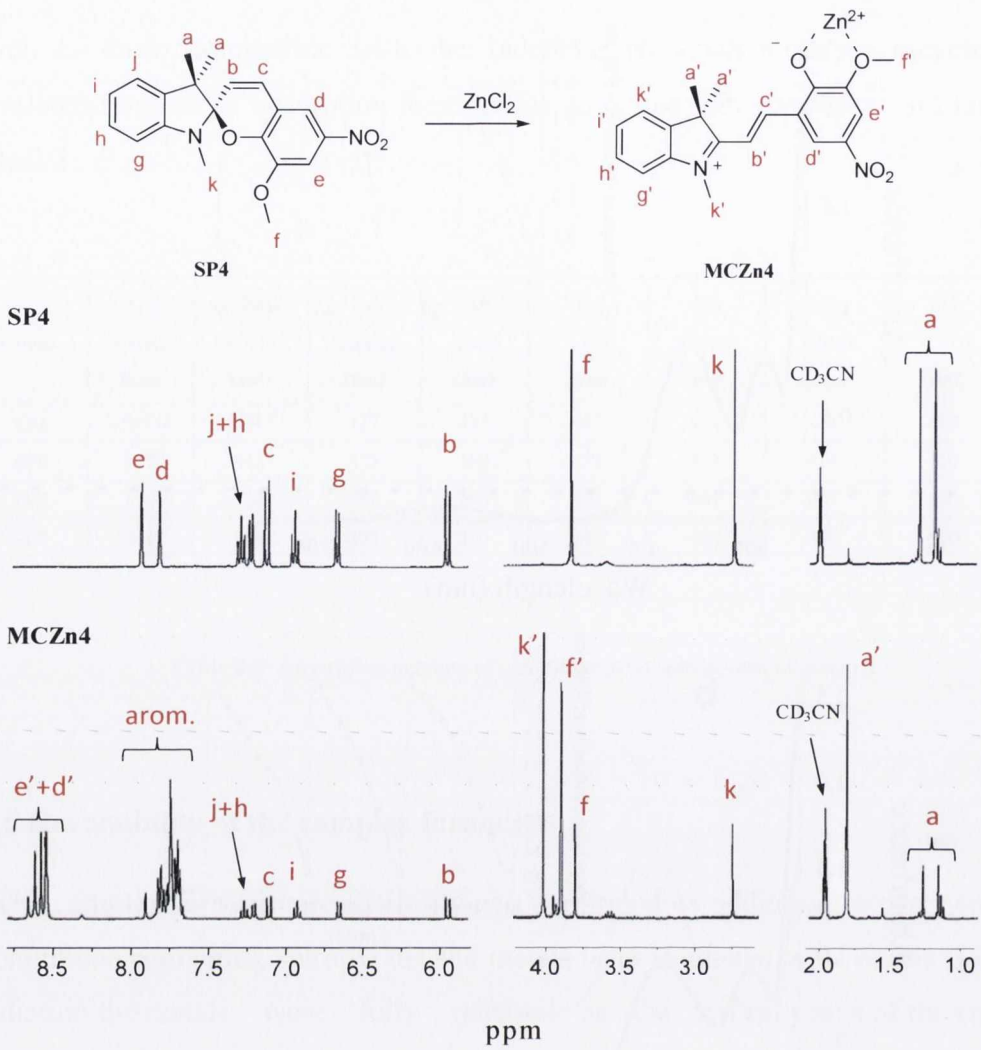


Figure 2.18 ^{1}H-NMR partial spectra of **SP4** ($2x10^{-2}$ M in deuterated acetonitrile, 293K) prior to and after the addition of 1eq of $ZnCl_2$ (**MCZn4**).

ability of the substituent on N and, as a consequence the coordination mechanism would be different as well. In **SP4** only the benzopyran moiety can participate at the metal binding while **SP7** can form a tridentate receptor.

The complexation of zinc was studied by ^{1}H-NMR (400MHz) in CD_3CN. In figure 2.18 the two NMR spectra of **SP4** before (**SP4**) and after the addition of 1 eq of $ZnCl_2$ (**MCZn4**) are reported. Chemical shifts of the two geminal methyl groups resulted in two singlets at 1.16 and 1.26 ppm (a) for a free ligand solution of **SP4**. The addition of the salt produced a six proton singlet shifted to 1.59 ppm (a') for the same *gem*-methyl groups which are magnetically equivalent in the *quasi*-planar merocyanine. The singlet of the N-methyl group (k) shifted downfield (k') from 2.75 to 3.89 because of the

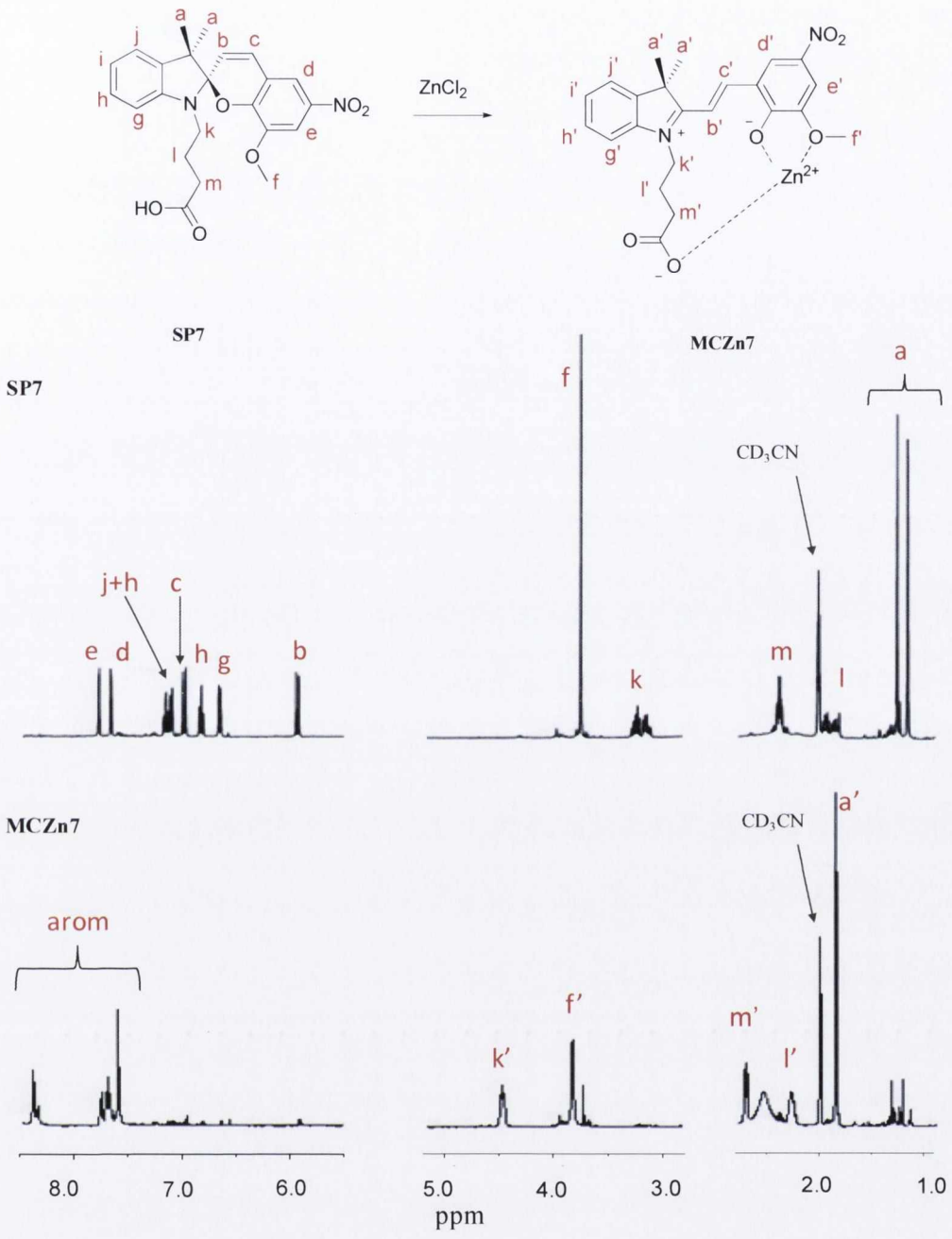


Figure 2.19 ^{1}H-NMR partial spectra of **SP7** ($2x10^{-2}$ M in acetonitrile, 293K) prior to and after the addition of 1eq of $ZnCl_2$ (**MCZn7**).

presence of a positive charge on the indolic nitrogen in the open form. The methoxy group in position 8 (f) shifted downfield also (f') from 3.79 ppm to and 4.02 ppm confirming the interaction with the metal cation. Two new groups of signals appeared in the range of 7.19-7.29 ppm and 8.51-8.69 ppm corresponding to the aromatic and the vinylic protons of the open form (arom.). The formation of the complex was not

complete as the signals for the spiropyran were still visible after the addition of Zn^{2+}. The molar ratio between **SP4** and **MCZn4** was calculated to be 1:8.

Figure 2.19 shows the comparison between the partial ^{1}H-NMR spectra of a solution of **SP7** prior to (**SP7**) and after the addition of 1 eq of $ZnCl_2$ (**MCZn7**). Once the thermal equilibrium was reached, the concentration of the closed form was negligible with respect to the open one. The presence of the free carboxylic group in this ligand on the indolic nitrogen was decisive in stabilizing the metal complex. The signals of the vinylic (b and c) and aromatic protons disappeared and two distinguishable group of signals appeared in the range of 7.61-7.82 ppm and 8.30-8.42 ppm. The typical shifts of the *gem* methyl groups (a) coalesced in a singlet at 1.83 ppm (a') due to the symmetry of the *quasi* planar merocyanine. Moreover, all the peaks corresponding to the aliphatic protons of the carboxylated chain moved downfield. Among them, the widest shift was observed for protons adjacent to the indolic nitrogen from 3.21 ppm (k) to 4.53 ppm (k') because of the effect of the positively charged N in the open form. The shifts to a lower field observed for the protons of the methoxy group (f-f') and the aliphatic protons adjacent to the acid group (l, l', m, m') confirmed the formation of the complex involving the triad carboxy, methoxy and phenolate.

2.4.7 The Effect of Counter Ions: Complexes' Composition Studies

Although most of the known spiropyran-based receptors are tailored to bind metal ions, very little has been reported about the importance of counterions on the coordination process and on the overall photochemical behaviour of spiropyrans.[15,16] In the long term we are interested in developing selective and rapid metal-ion sensors that can function in complex solutions with a range of potentially competing ligands. In this chapter, I will examine the complexation behaviour of the photoregenerable spiropyran **SP7** derivative in the presence of Zn(II) and Cu(II). In particular, I will analyse the effects that two different counterions, (Cl^-, $[ClO_4]^-$) have on complex stability, sensitivity, and kinetics of binding. Additionally, both solution- and solid-state methods to establish composition of the resulting spiropyran-metal complexes will be treated.

The spectroscopic determination of the complexes' composition was investigated by means of the isomolar solutions technique (Job's method).[1,17] The plots of the Job's

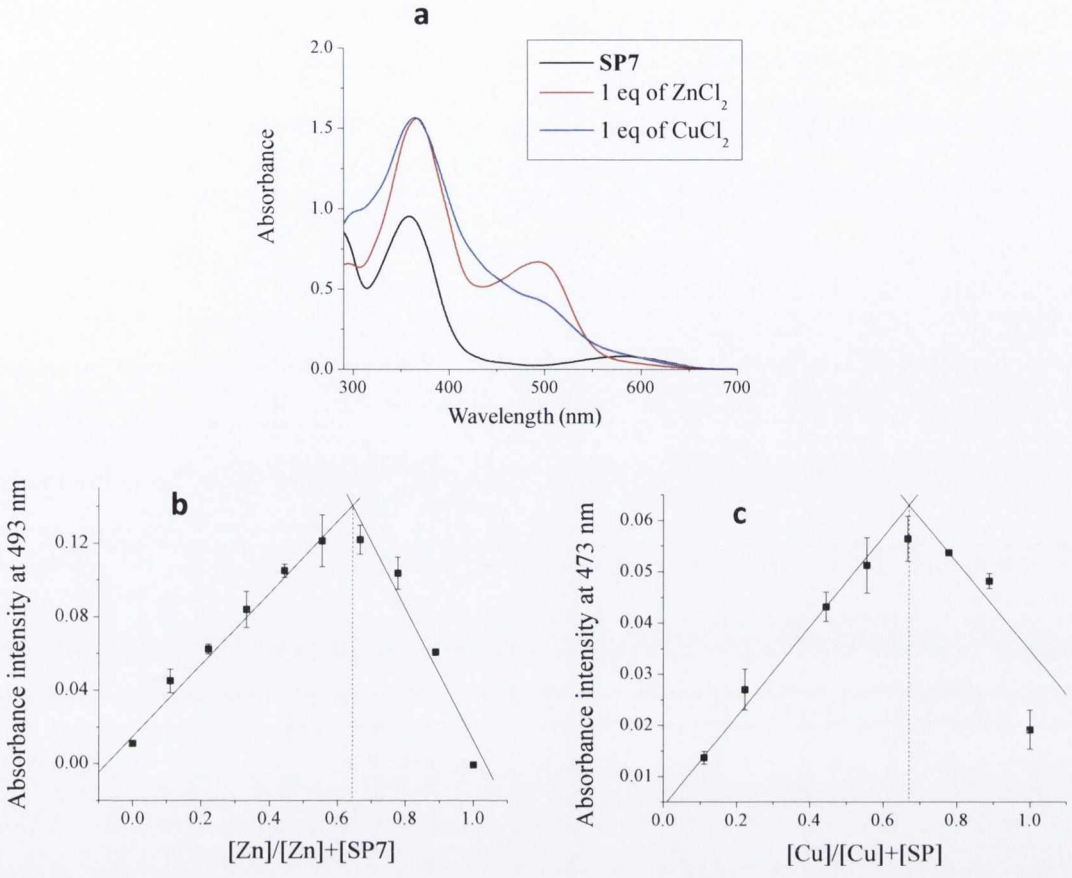


Figure 2.20 Job's analysis of (**a**) **SP7**-Zn^{2+} complex ([**SP**]+[Zn^{2+}] = $3.0x10^{-5}$ M, acetonitrile, 293 K) and (**b**) **SP7**-Cu^{2+} complex ([**SP7**]+[Cu^{2+}] = $3.0x10^{-5}$ M, acetonitrile, 293 K). Each analysis was carried out three times and the data were plotted as the average of the different series.

analysis of a the spiropyranzinc (II) chloride and spiropyran copper (II) chloride complexes are featured in figure 2.20b and 2. 20c. The plot in figure 2.20a shows the spectra of SP7 at equilibrium after the addition of 1 eq of $ZnCl_2$ and 1 eq of $CuCl_2$. The absorbance values for the Job's analysis were taken at the complexes' absorption maxima, 494 nm for zinc (II) and 447 nm, where the shoulder is located, for copper (II), and they were correlated to the composition of the isomolar solutions. As shown in the plots (figure 2.20a and 2.20b), in both cases the maxima correspond to the solutions of composition metal/spiropyran 2:1. The stoichiometry observed herein is different to those reported previously for overall charge neutral SP-based ligands. With such ligands, 1:2 or 1:1 stoichiometries (metal ion/SP) are observed.[18-20] The 2:1 stoichiometry that we obtain indicates that the dominating species in solution is most likely a dinuclear species which must therefore also incorporate three chloride ions to

achieve overall charge neutrality (the carboxylic acid group on the **SP7** is expected to be protonated). The exact geometry of this complex cannot be determined from the data in hand, but it is likely that several ligands act as bridges between the two zinc ions.

2.4.8 The Effect of Different Counter Ions on the Absorption

Although we designed this spiropyran to act as an efficient chelating ligand for metal ions, it is also important (for real-life applications) to establish what role, if any, different counterions may play in the coordination chemistry or photochemical behaviour of the ligand. To explore this, we carried out a series of experiment on chloride/perchlorate salts of Zn(II) and Cu(II), respectively, in order to establish how counterion characteristics relate to the sensitivity and complexation rate of the **SP7**, as well as to the composition of the complex. Binding constants K for the complexes were determined from the absorbance intensities recorded at different metal salts concentrations following the modified Benesi-Hildebrand equation $1/\Delta A = 1\Delta A_{max} + (1/K[C])(1/\Delta A_{max})$.[21] Here $\Delta A = A_x - A_0$ and $\Delta A_{max} = A_\infty - A_0$ where A_0, A_x and A_∞ are the intensities of the **MCM^{2+}7** complex at the wavelength considered in the absence of metals, at a certain concentration of metals and at a concentration of complete interaction respectively; K is the binding constant and $[C]$ is the concentration of metal. The K values were extrapolated from the slope of the plot $(A_\infty - A_x)/(A_x - A_0)$ against $1/[C]$. The most stable complex was obtained with copper perchlorate with a binding constant $K = 3.37 \times 10^4$ M^{-1}. Changing the counterion from perchlorate to chloride the affinity of the molecule to copper decreases of an order of magnitude with a value $K = 2.04 \times 10^3$ M^{-1}. The same effect was observed by changing the counterion of zinc but it was not as dramatic as it was for copper. The binding values of 2.68×10^4 M^{-1} and 1.29×10^4 M^{-1} were found for the spiropyran-$Zn(ClO_4)_2$ and spiropyran-$ZnCl_2$ complexes respectively. In figure 2.21 the absorption spectra of solutions of **SP7** containing different concentrations of $ZnCl_2$ are shown. The inset of figure 2.21 is the plot of the Benesi-Hildebrand equation for the spiropyran-$ZnCl_2$ complex. Although the binding constant was higher for copper perchlorate, **SP7** showed a surprisingly high sensitivity to the presence of $Zn(ClO_4)_2$. For all the complexes, the maximum value of absorption intensity was reached after the addition of 1 equivalent of metal cation while only 0.3

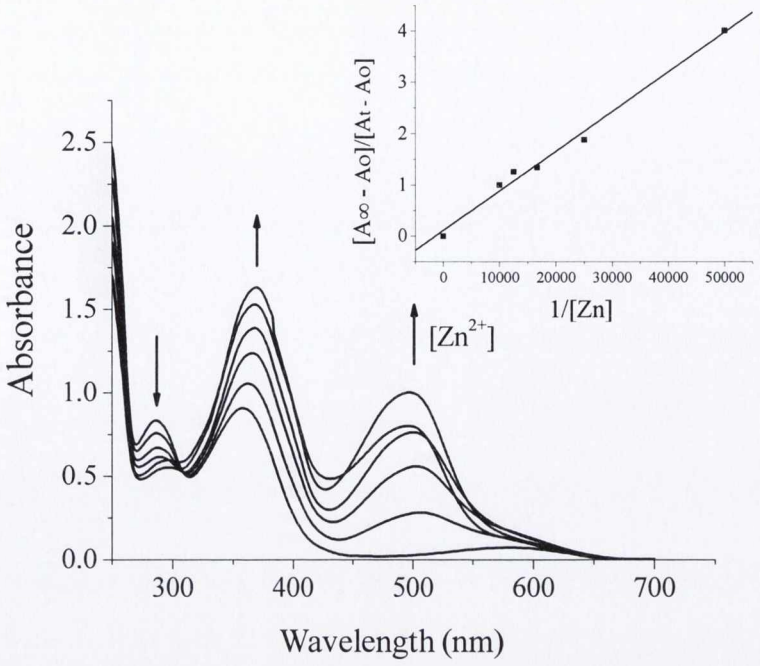


Figure 2.21 The absorption spectra of solutions of **SP7** (1.0 x 10^{-4} M, acetonitrile, 293 K) after 20 min from the addition of 0.2, 0.4, 0.6, 0.8 and 1 equivalent of $ZnCl_2$; (Inset) Plot of $(A_\infty - A_x)/(A_x - A_0)$ against 1/[*C*].

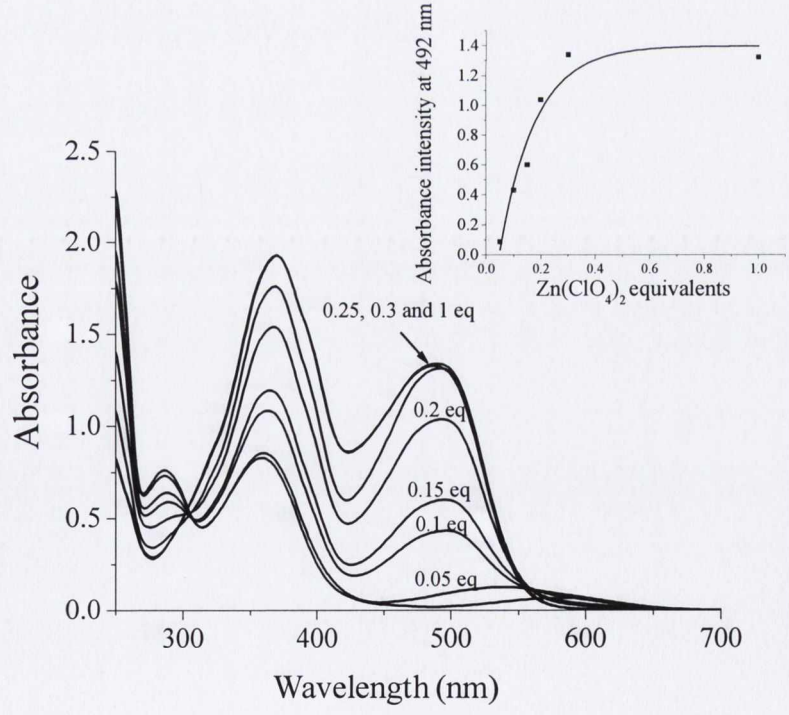


Figure 2.22 Absorption spectra of **SP7** (1.0 x 10^{-4} M, acetonitrile, 293 K) after increasing the concentration of $Zn(ClO_4)_2$; (Inset) Absorption intensities at 492 nm of the same solution of **SP7**. The plateau of the maximum absorption intensity at 492 nm is reached after the addition of 0.3 eq of the zinc perchlorate.

equivalents of zinc perchlorate are sufficient to produce the maximum response of the spiropyran (figure 2.22).

In order to characterize the spiropyran-metal complexes, the complexation kinetics were studied in acetonitrile after addition of 1 eq of zinc and copper chlorides and perchlorates. The coordination of the different cations follows first order kinetic and the observed rate constant can be determined using eqn (1), where A_∞, A_t and A_0 are the absorbance of the complex at time infinity, t and 0 respectively, k_{ob} is the observed rate constant and t is the time.

$$\ln \frac{(A\infty - At)}{(A\infty - Ao)} = k_{ob}t \qquad \textbf{equation 1}$$

The rate constants values of each complex can be extrapolated from the slope of the plot of $(A\infty - At)/(A\infty - Ao)$ versus t as its falloff is linear (inset Figure 2.23). Thus the k_{ob} values of all complexes were calculated and they are 1.3 x 10^{-2} s^{-1} for copper perchlorate, 1.5 x10^{-1} s^{-1} for copper chloride while, in the presence of zinc, 1.8 x 10^{-2} s^{-1}

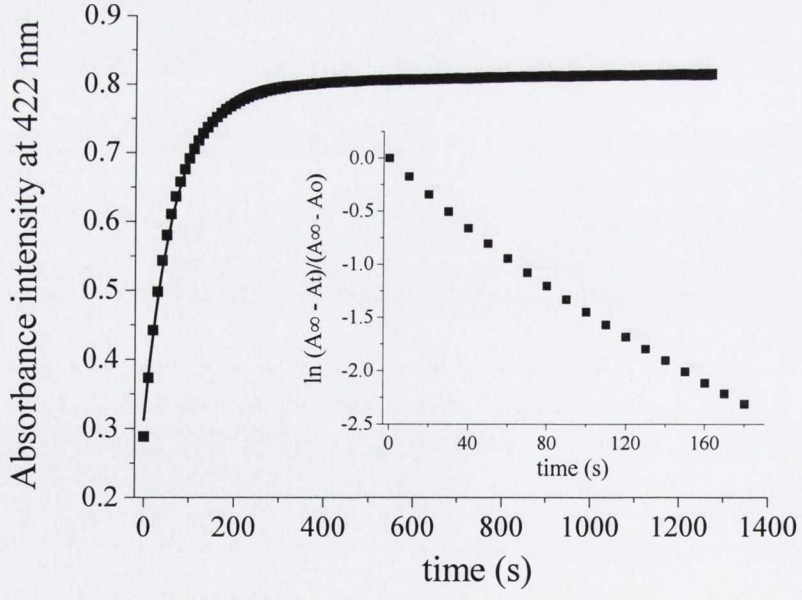


Figure 2.23 The increase in absorption at 422 nm of a solution of **SP7** ($1.0x10^{-4}$ M, acetonitrile, 293K) after the addition of 1 equivalent of $Cu(ClO_4)_2$; (Inset) Plot of $(A_\infty - A_t)/(A_\infty - A_0)$ versus time.

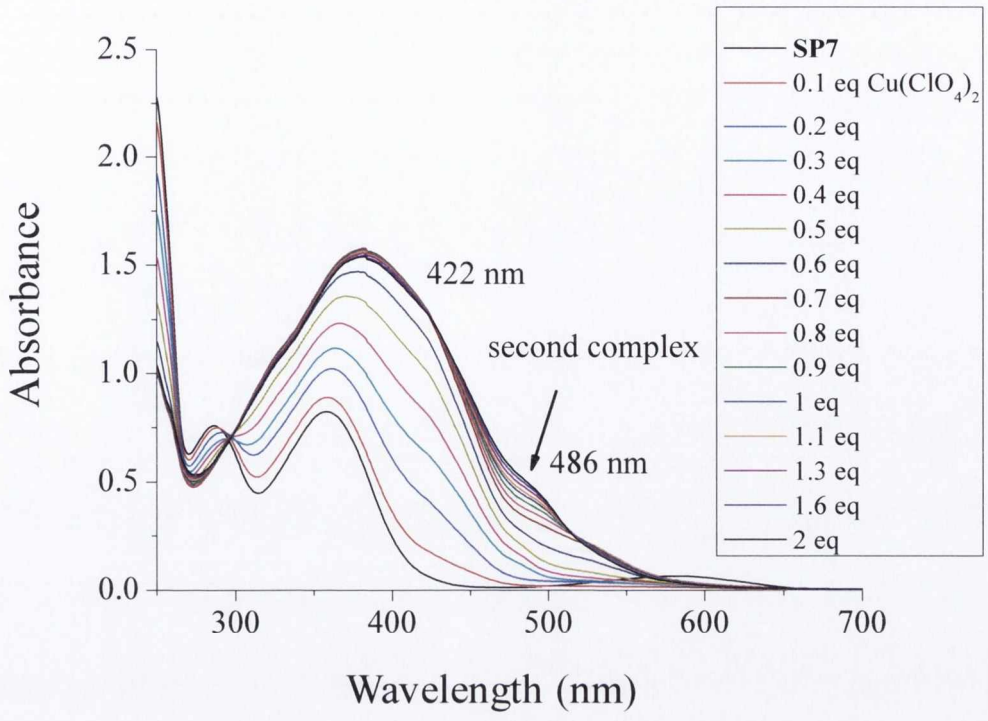


Figure 2.24 Absorption spectra of a solution of **SP7** ($1.0x10^{-4}$ M, acetonitrile, 293 K) after the addition of more than 1 equivalent of $Cu(ClO_4)_2$; the formation of a new species is observable at 486 nm as the concentration of copper is higher than 1 equivalent.

and 6.4×10^{-2} s^{-1} were found for perchlorate and chloride respectively. In the presence of $Zn(ClO_4)_2$, $ZnCl_2$ and $CuCl_2$ the coordination process is slow. The maximum absorptions of the three complexes were reached after the solutions containing **SP7** and metal salts had been stored in the dark for 120, 60 and 50 min respectively. A very fast response was observed upon addition of $Cu(ClO_4)_2$ with a full complexation time that ranges between 2.5-3 min. The absorbance increase versus time at 422 nm upon addition of 1 eq of $Cu(ClO_4)_2$ to a spiropyran solution (10^{-4} M in acetonitrile) is displayed in figure 2.23. The fast coloration rate allows a naked eye real-time detection of the cation as the solution containing the spirochromene and copper turns from colourless into orange-yellow immediately after the addition of the cation.

By analyzing and comparing the different effects of cations and counterions on the behaviour of **SP7**, a curious result was obtained when the concentration of copper perchlorate was higher than 1 equivalent. As shown in figure 2.24, a shoulder at 422 nm proved the formation of the spiropyran-metal complex. Its corresponding intensity reached the maximum as the concentration of copper was equimolar to the molecule

concentration. If the concentration of metal rises above the equimolarity, a new shoulder appears at 486 nm, indicating probably the formation of a different complex.

2.4.9 Emission Measurements and Zinc Detection Limit

The ring opening of spiropyrans by means of UV irradiation produces the open merocyanines. The latter are known to be emitting species due to the conjugation through the molecule skeleton, which is instead disrupted in the closed form.[12] Upon excitation of the solutions of our spiropyran in the presence of different cations at λ_{exc} = 481 nm, the emission spectra revealed high intensity bands in the ranging between 633 and 644 nm only in the presence of zinc. No response was observed in the presence of copper (II) (figure 2.25). The effect of the counterion was observed in the emission experiment as the addition of either zinc chloride or perchlorate produced two slightly different responses.

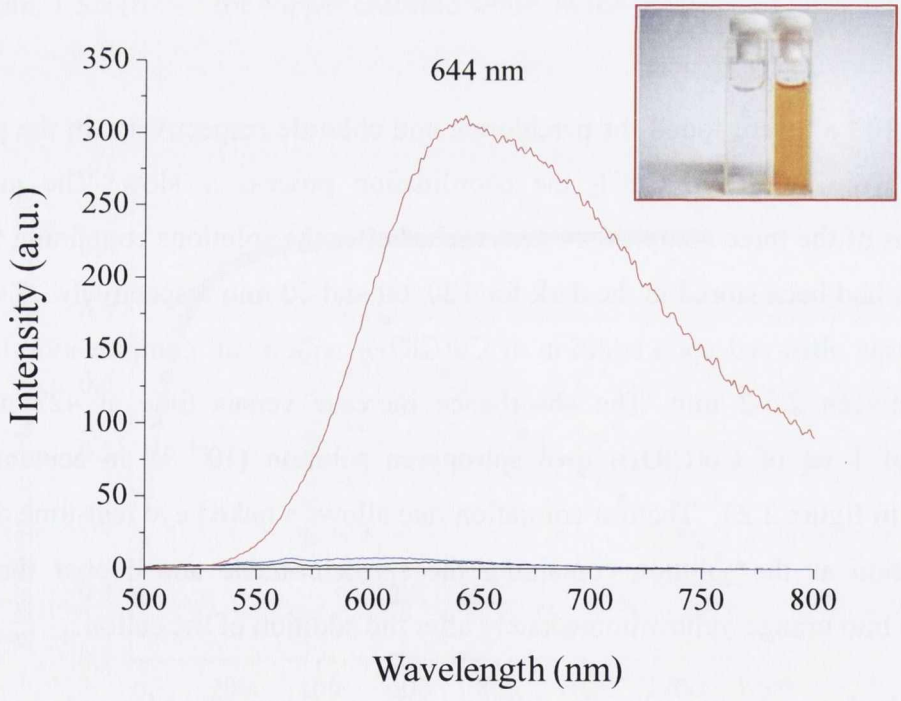


Figure 2.25 Emission spectra of a **SP7** solution ($1.0x10^{-5}$ M, acetonitrile, 293K) before (black), after the addition of 1 equivalent of $ZnCl_2$ (red) and after the addition of 1 equivalent of $CuCl_2$ (blue), λ_{exc} = 481 nm; (Picture) coloration of a **SP7** solution ($1.0x10^{-5}$ M, acetonitrile, 293K) after addition of $ZnCl_2$.

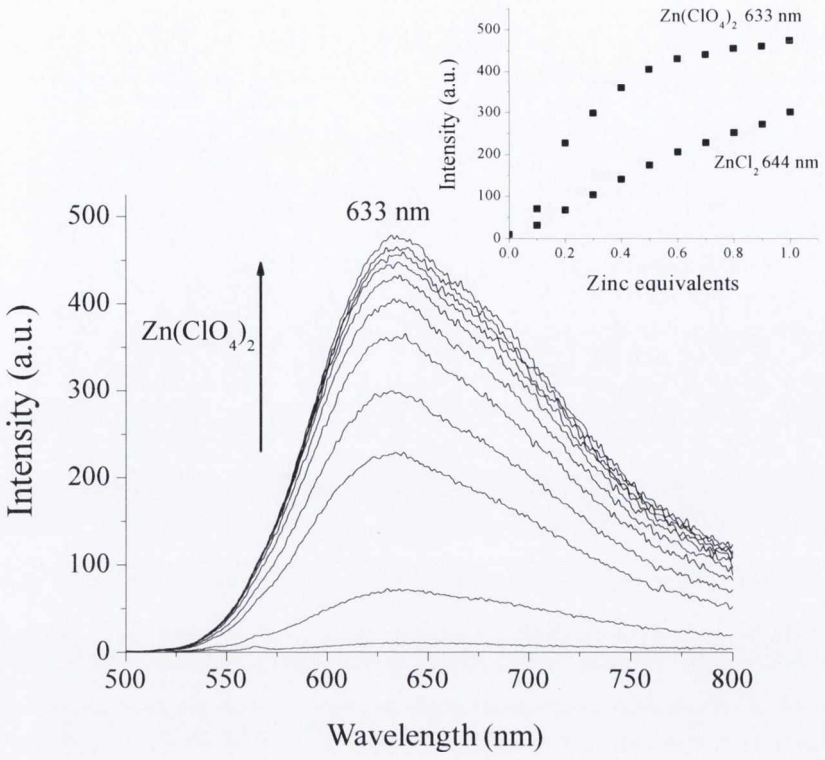


Figure 2.26 Emission spectra of a **SP7** solution ($1.0x10^{-5}$ M, acetonitrile, 293 K) after varying the concentration of $Zn(ClO_4)_2$, λ_{exc} = 481 nm; (Inset) counterion effect on the emission response of a solution of **SP7**.

The emission intensity of the spiropyran-metal complex after the addition of zinc perchlorate was approximately double the emission in the presence of zinc chloride (inset figure 2.26). Additionally, going from perchlorate to chloride produced abathochromic shift from 633 nm to 644 nm. The dramatic response of **SP7** to the addition of zinc perchlorate allowed the investigation of the corresponding detection limit. As shown in figure 2.24, an increased concentration of zinc perchlorate produced an increase in the emission at 633 nm. The maximum intensity was reached after the addition of 1 eq of $Zn(ClO_4)_2$. The LOD method was used to find the detection limit. The lowest concentration of zinc detected was 3×10^{-7} M.

2.4.10 Single-crystal X-ray Diffraction

Numerous attempts were made to grow crystals of a **ME–M** complex and we were finally successful when thin plates (dec. 270°C) of (*E*)-4-(2-(3-methoxy-5-nitro-2-

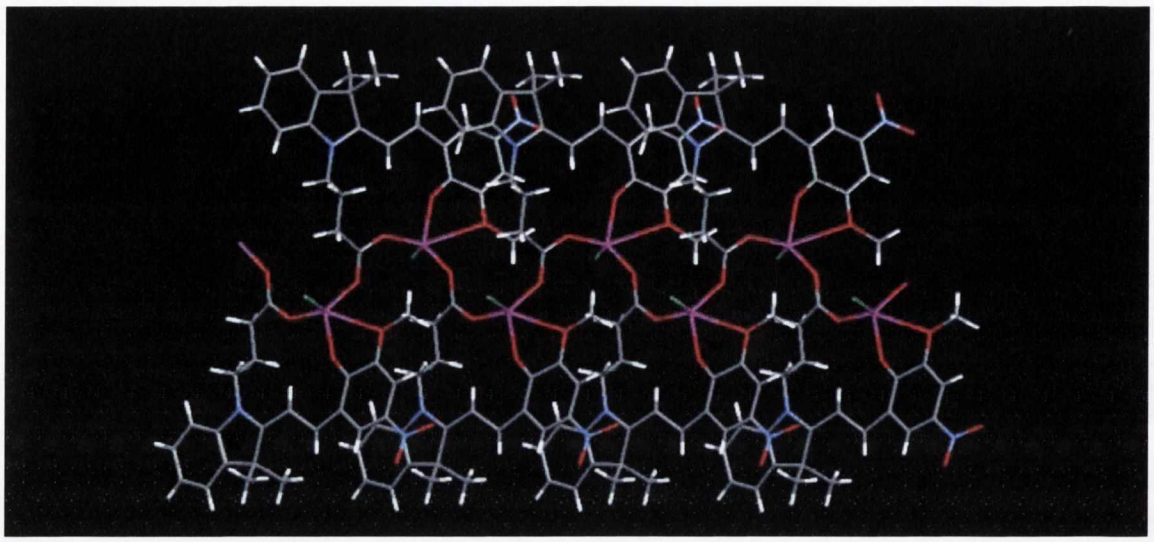


Figure 2.27 An extended core of metal ions (Zn^{2+} ions in pink, chloride ions in green) surrounded by a hydrophobic cladding.

oxidostyryl)-3,3-dimethyl-3*H*-indolium-1-yl)butanoate zinc(II) chloride were obtained in an NMR tube (see experimental ^{1}H-NMR section). The crystal structure determination of Zn(II)–MC–Cl shows that the merocyanine is a monovalent anion, as the carboxylic acid moiety has been deprotonated. The Zn(II) displays a somewhat unusual distorted square-pyramidal arrangement, where each metal ion is coordinated to one chloride ion and three different MC's simultaneously. The four Zn···O distances within each complex ion are in the range of 2.01–2.83 Å, with the longest distance involving the methoxy oxygen atom. The structure is split into a distinctly hydrophilic core, an extended 1-D chain composed of metal ions, chloride ions and the coordinating sites of the ligand, surrounded by a hydrophobic "cladding" composed of the relatively non-polar and aromatic components of the merocyanine ligand (figure 2.27). The segregated and low-dimensional nature of the crystal structure of this compound is likely a strong contributor to the poor crystallinity of the sample. It is also likely that the reversible nature of the molecular geometry of the ligand produces a solution with both the closed and the open form of the **SP7** from which crystal growth is exceedingly difficult. Nevertheless, this is an extremely rare example of a crystal structure of a metal complex of a functionalised spiropyran. A comparison of the results obtained from ^{1}H-NMR and single crystal X-ray diffraction on the spiropyran-zinc (II) chloride complex

shows that the triad of binding sites that was intended to interact directly with the metal ion was indeed fully engaged in both solution and in the solid state.

2.4.11 MALDI-TOF Mass Spectrometry

Matrix-assisted laser desorption/ionization or MALDI is a soft ionization technique that allows the detection of molecules that tend to be fragile when ionized with other techniques. Therefore we decided to employ this tool in order to gather additional information about spiropyran-metal ion complexation in solution. Acetonitrile solutions of **SP** containing equimolar amounts of $Zn(ClO_4)_2$, $ZnCl_2$, $CuCl_2$ and $Cu(ClO_4)_2$ were equilibrated overnight and the corresponding spectra were recorded. In previously reported ESI-MS experiments, spiropyran-metal complexes with stoichiometry 1:1 and 2:1 were identified,[19,22-24] and counterions were often included in the pseudo molecular ions signals confirming their contribution to the coordination. In our case, we did observe several **MCM** complexes with different ratios, but we did not detect any signal due to the presence of coordinated counterions. However, peaks corresponding to **MCM** complexes with coordinated solvent molecules were found. In the **SP7**−$Zn(ClO_4)_2$ solution, two peaks indicating the presence of a 2**SP7**−Zn and 3**SP7**−2Zn complexes were found at 911 *m/z* and 1401 *m/z* respectively (figure 2.28a). Three additional peaks can be assigned to **MCM** complexes with varying number of coordinated solvent molecules; 568 *m/z* for the molecular ion $[\mathbf{SP}+2CH_3CN+Zn]^+$, 675 *m/z* for $[\mathbf{SP}+3CH_3CN+2Zn]^+$ and 1013 *m/z* for $[2\mathbf{SP}+H_2O+2\ CH_3CN+Zn]^+$. A very similar situation was observed in the presence of $ZnCl_2$ (figure 2.28b). The peaks at 568 m/z, 911 m/z and 1401 m/z are analogous to the ones observed in the presence of zinc perchlorate. Additionally the signal at 668 m/z was given to the molecular ion $[\mathbf{SP}+2CH_3CN+3H_2O+2Zn]^+$ which has same stoichiometry found in the X-ray crystallography experiments and in the Job's analysis, while the peak at 1011 m/z was attributed to $[2\mathbf{SP}+H_2O+2\ CH_3CN+Zn]^+$. The difference between the values of 1013 m/z in the presence of zinc perchlorate and 1011 m/z in the presence of zinc chloride are due to the different state of protonation of the carboxy group of **SP7**.

The addition of $CuCl_2$ to a solution of **SP7** produced the formation of similar complexes and the contribution of the solvents in the coordination was confirmed also

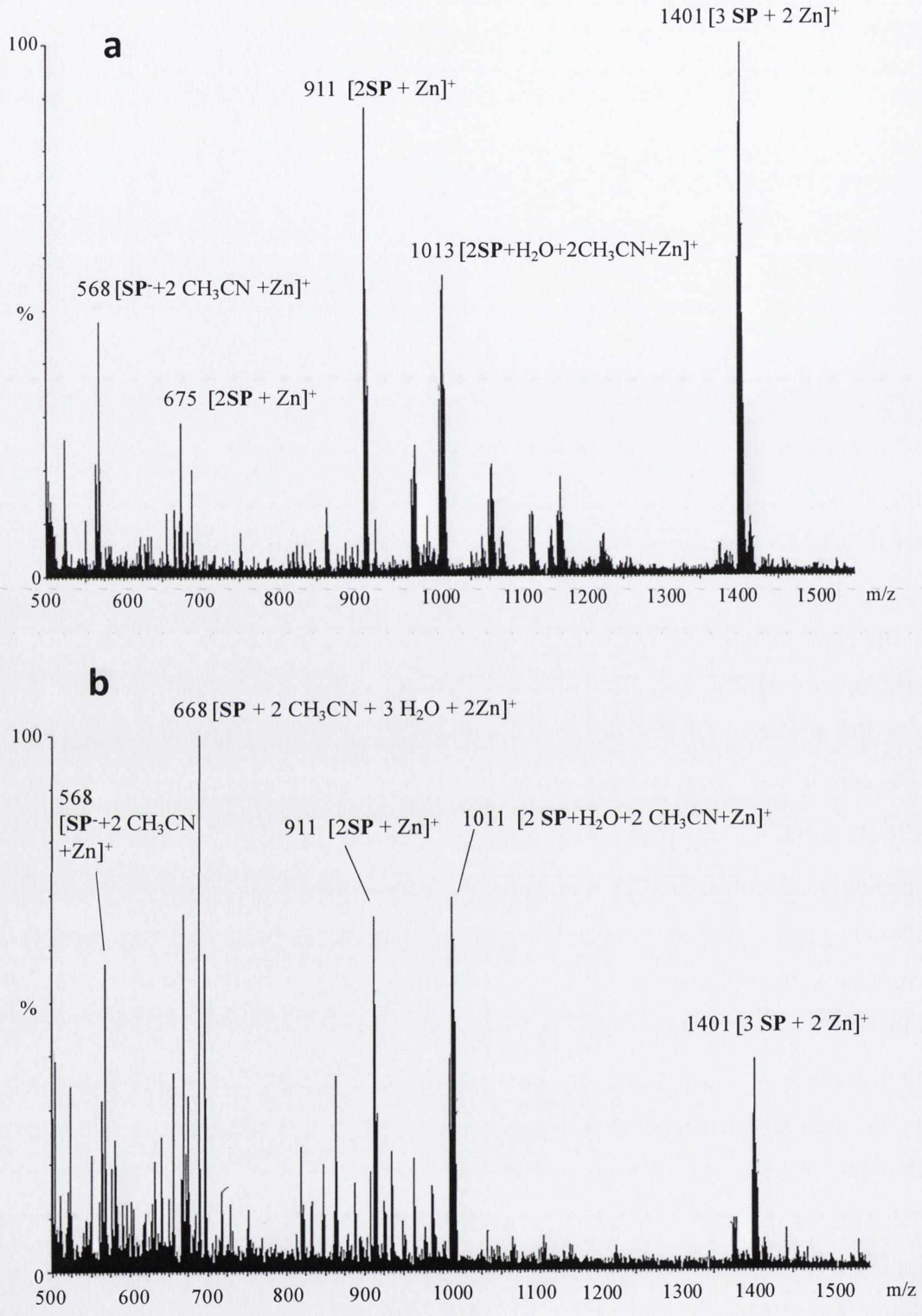


Figure 2.28 MALDI-TOF mass spectrum of an acetonitrile solution of **SP7** containing (**a**) $[Zn(ClO_4)_2]$=[**SP7**]=$1x10^{-3}$M and (**b**) $[ZnCl_2]$=[**SP7**]=$1x10^{-3}$M.

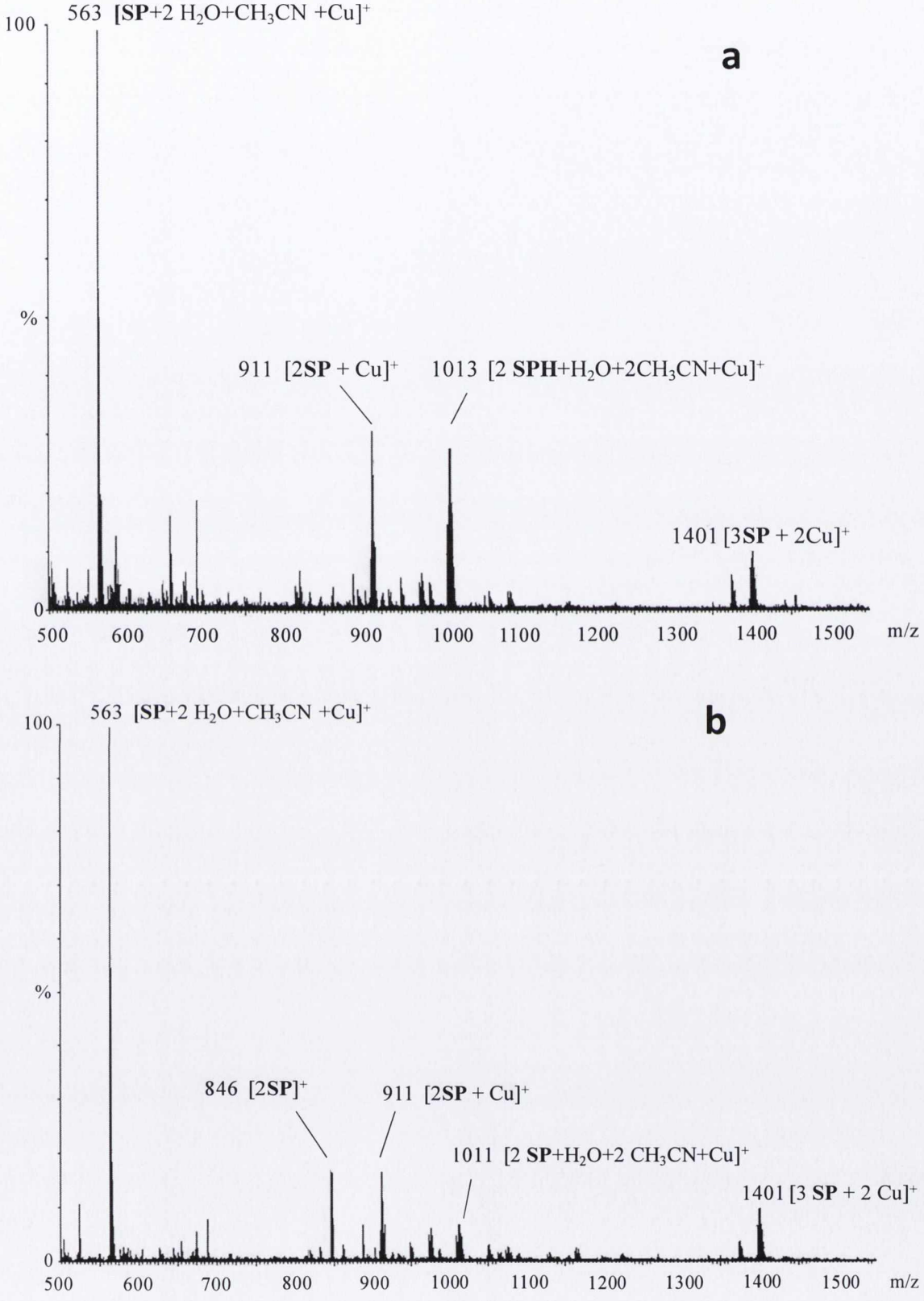


Figure 2.29 MALDI-TOF mass spectrum of acetonitrile solutions of **SP7** containing (**a**) $[CuCl_2]$=[**SP7**]=1x10^{-3}M and (**b**) $[Cu(ClO_4)_2]$=[**SP7**]=1x10^{-3}M.

in this instance. The following peaks were observed and assigned to their corresponding molecular ions (figure 2.29a): 563 m/z for [**SP**+2H_2O+CH_3CN+Cu]$^+$, 911 m/z [2**SP**+Cu]$^+$, 1013 m/z [2 **SP**+H_2O+2CH_3CN+Cu]+, 1401 m/z [3**SP**+2Cu]$^+$. Also the coordination of copper perchlorate followed the same patterns and the peaks at 563, 911, 1011 and 1401 m/z were assigned to [**SP**+2H_2O+CH_3CN +Cu]$^+$, [2**SP**+Cu]$^+$, [2**SP**+H_2O+2 CH_3CN+Cu]$^+$ and [3**SP**+2 Cu]$^+$ respectively. An unusual signal at 846 m/z was noticed and it corresponds to a dimer [2**SP**]$^+$ with no copper (figure 2.29b). We are currently investigating this result as we found this unexpected species only in the presence of $Cu(ClO_4)_2$. In summary we have been able to detect the presence 2:1 and 1:1 spiropyran-metal complexes in the presence of both copper and zinc with different counter ions. Additionally, the peak indicating a 1:2 SP:Zn complex was detected in the presence of $ZnCl_2$ and this result matches perfectly with the spectroscopic and crystallographic data.

2.4.12 Conclusions on Group 2

This group of spiropyrans showed interesting responses to eleven biologically important metal cations. The formation of complexes was observed *via* UV-vis absorption spectroscopy. All spirochromene-metal chelates absorbed light in the visible region of the electromagnetic spectrum while metal free spiropyran solutions are generally colourless and absorb in the UV region. Significantly different absorption patterns were found for all compounds of group 2 in the coordination of copper and iron that gave wide absorptions, blueshifted with respect to those of the other complexes. The latter are in fact narrower with sharper peaks localized between 500 nm and 580 nm. All complexes are reversible as the metal guest is ejected upon irradiation with visible light. Remarkably higher intensity peaks were observed for zinc complexes. These results pushed us to analyze the zinc complexes formed with **SP4** and **SP7** by means of ^{1}H-NMR spectroscopy in order to establish if the carboxylated tether on **SP7** participate effectively to the coordination a metal guest. The spectra obtained confirmed successfully this hypothesis as **SP4** forms partially a bidentate complex with zinc (II) while all three binding sites on the ligand **SP7** are actively coordinating to the metal ion, and the dominating species n solutions seems to be, in this case, a discrete dinuclear 1 : 2 spiropyran-zinc complex. Additionally we studied extensively the effect of two

different counterions, chloride and perchlorate, on the coordination process. Changing counterion from $ZnCl_2$ and $Zn(ClO_4)_2$, only a slight shift in the complex absorption maxima from 494 to 492 nm was observed while a drastic increase in the sensitivity for the bivalent cation was noticed in the presence of perchlorate. Since the zinc complexes are highly emitting, this last result was further investigated by fluorescence spectroscopy which is a more sensitive technique with respect to UV-vis absorption spectroscopy, in order to estimate the detection limit which was found to be 3×10^{-7} M for $Zn(ClO_4)_2$. Going from $Cu(ClO_4)_2$ to $CuCl_2$ a dramatic drop in the affinity for the cation was observed as the binding constant falls from K=3.37x10^4 M^{-1} to K=2.04x10^3 M^{-1} respectively. Additionally, in the presence of perchlorate, the spiropyran-copper complex formation is the fastest of the series, allowing the real-time naked eye detection of the cation in less than 3 min from the addition while the other complexes are fully formed in a time ranging between 50 min to 2 h. Upon nucleation, a coordination polymer is favoured kinetically, as shown by single-crystal X-ray diffraction. The crystal structure of the **SP7**-zinc chloride complex contains a coordination polymer with a stoichiometry of 1:1:1 (**SP7**/Zn/Cl). Finally, we were able to detect 2:1 and 1:1 spiropyran-metal complexes in the presence of both copper and zinc with different counterions using MALDI-TOF MS. Additionally, a peak indicating a 1:2 **SP7**:Zn complex was detected in the presence of $ZnCl_2$ and this result matches very well with the data obtained from spectroscopic and crystallographic data.

2.4.13 Binding Studies on Compounds of Group 3

Members of this group of compounds are designed to retain the capability of forming reversible complexes with bivalent cations as the nitro group present in all these structures should have the same effect observed on spiropyrans of group 2. Compound **SP8** is the only derivative that has only one potential binding site which is represented by the phenolate in its corresponding open isomer. Molecules **SP9**, **SP10**, and **SP11** can form bidentate receptors that bind the guest between the phenolate in the open isomer and the terminal functional group on the indolic nitrogen tethers.

2.4.14 UV-vis Absorption Studies

The addition of eleven monovalent and bivalent biologically important cations to spiropyrans solutions in acetonitrile gave unexpected results. The first compound analysed was **SP8**. The absorption spectrum of this derivative shows three maxima in the ultraviolet region at 263 nm, 293 nm, and 341 nm respectively. The presence of 1 equivalent of ten of the eleven metals did not produce any variation of the spiropyran spectrum. However, addition of 1 equivalent of copper perchlorate caused a sudden colour change from slightly pink to deeply orange in few seconds. This event was accompanied by the appearance of an intense absorption band localized in the visible region with maximum intensity at 496 nm. Other two maxima of the same intensity were visible in the UV region at 263 nm and 305 nm respectively (figure 2.30a).

Despite the structural difference between **SP8** and the other members of this group, the addition of the same amount of $Cu(ClO_4)_2$ caused the same colour changes in acetonitrile solutions of **SP9**, **SP10**, and **SP11**. The absorption spectrum of a **SP9** shows bands in the UV region at 266 nm, 301 nm, and 340 nm. After addition of copper (II), the UV-vis spectrum of the same solution showed an intense absorption band, flat on its top with maximum intensity at 515 nm and a shoulder at 493 nm. Weak absorption shoulders were observed at 410-414 nm in the spectra of solutions containing the same molecule and either iron (II) or zinc (II) indicating little interactions with these two cations as well (figure 2.30b). The absorption maxima recorded at 269 nm, 299 nm, and 340 nm for a metal free solution of compound **SP10** were similar to those of **SP8** and **SP9**. Addition of zinc (II) perchlorate and iron perchlorate (II) caused the appearance of two shoulders in the spiropyran spectra at 410 nm and 400 nm respectively (figure 2.30c). Addition of copper (II) perchlorate caused an intense absorption band to appear in the range of 450-600 nm with maximum intensity at 517 nm (figure 2.30c). Even compound **SP11** which is functionalized with a carboxylated tether did not show any interaction with any of the tested metal salts except for a copper (II) perchlorate. The presence of this metal in fact caused analogous changes in the compound absorption spectra which resemble the changes observed for the other compounds in this group. The absorption band risen from addition of copper had its maximum localized at 514 nm.

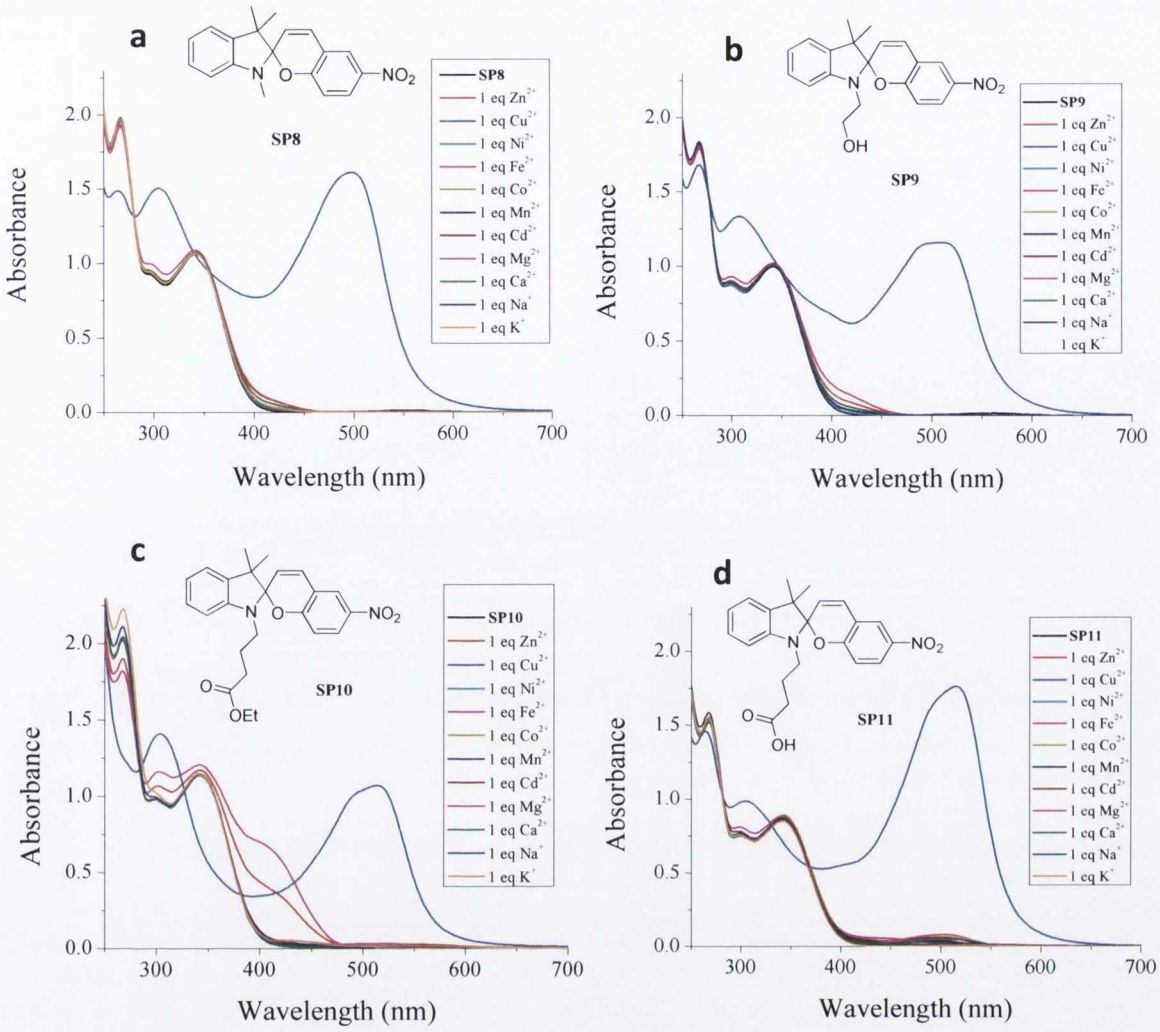


Figure 2.30 Absorption spectra of **SP8** (**a**), **SP9** (**b**), **SP10** (**c**), and **SP11** (**d**) ($1.0x10^{-4}$ M, acetonitrile, 293 K) before and after the addition of 1 eq of different metal perchlorates and chlorides.

The response of the four spiropyrans to different concentrations of $Cu(ClO_4)_2$ was investigated. In all experiment similar events were observed. The sequential addition from 0.1 to 1 equivalent of copper (II) caused different bands to appear at different wavelengths which resolved eventually in those reported in figure 2.30. However, in all cases different isosbestic points were observed. These results are shown in figure 2.31. Addition of 0.4 equivalents of copper (II) to a solution of **SP8** caused the appearance of two bands with maxima at 481 nm and 503 nm which coalesced into a broad absorption with maximum at 496 nm in the presence of higher concentrations of the metal (figure 2.31a). In the same spectra two isosbestic points are localized at 277 nm and 348 nm. Increasing the concentration of copper (II) in a solution of **SP9** caused two similar

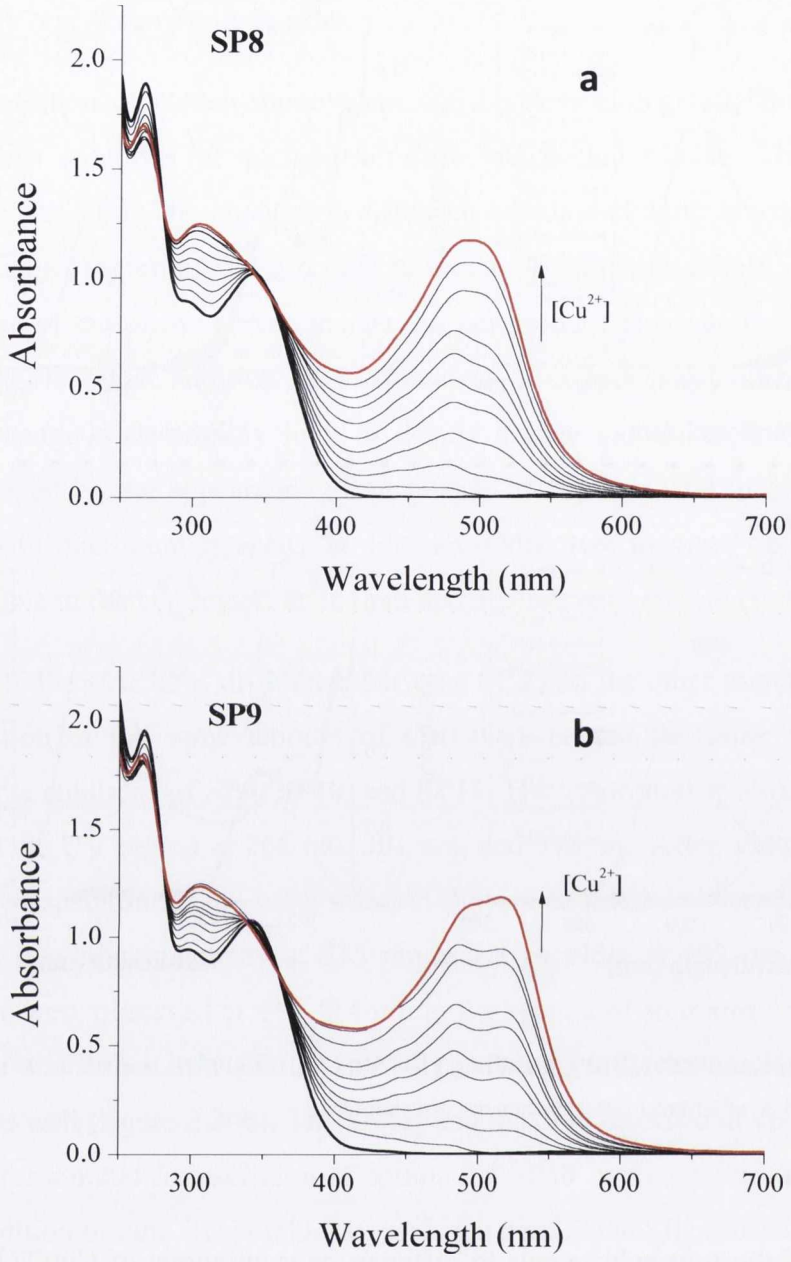


Figure 2.31 Absorption spectra of **SP8** (**a**) and **SP9** (**b**) (1.0 x 10^{-4} M, acetonitrile, 293 K) after increasing the concentration of $Cu(ClO_4)_2$.

bands to appear in the visible region with maximum intensity at 488 nm and 515 nm. Three isosbestic points were observed at 279, 338, and 361 nm (figure 2.31b). The same number of isosbestic points was observed for the solutions containing either **SP10** and **SP11**. In the first case they were localized at 277, 335, and 360 nm (figure 2.32a) while in the second case at 278, 332, and 365 nm (figure 2.32b). Two bands with maxima at 481 nm and 515 nm were observed in the spectra of compound **SP10** at low

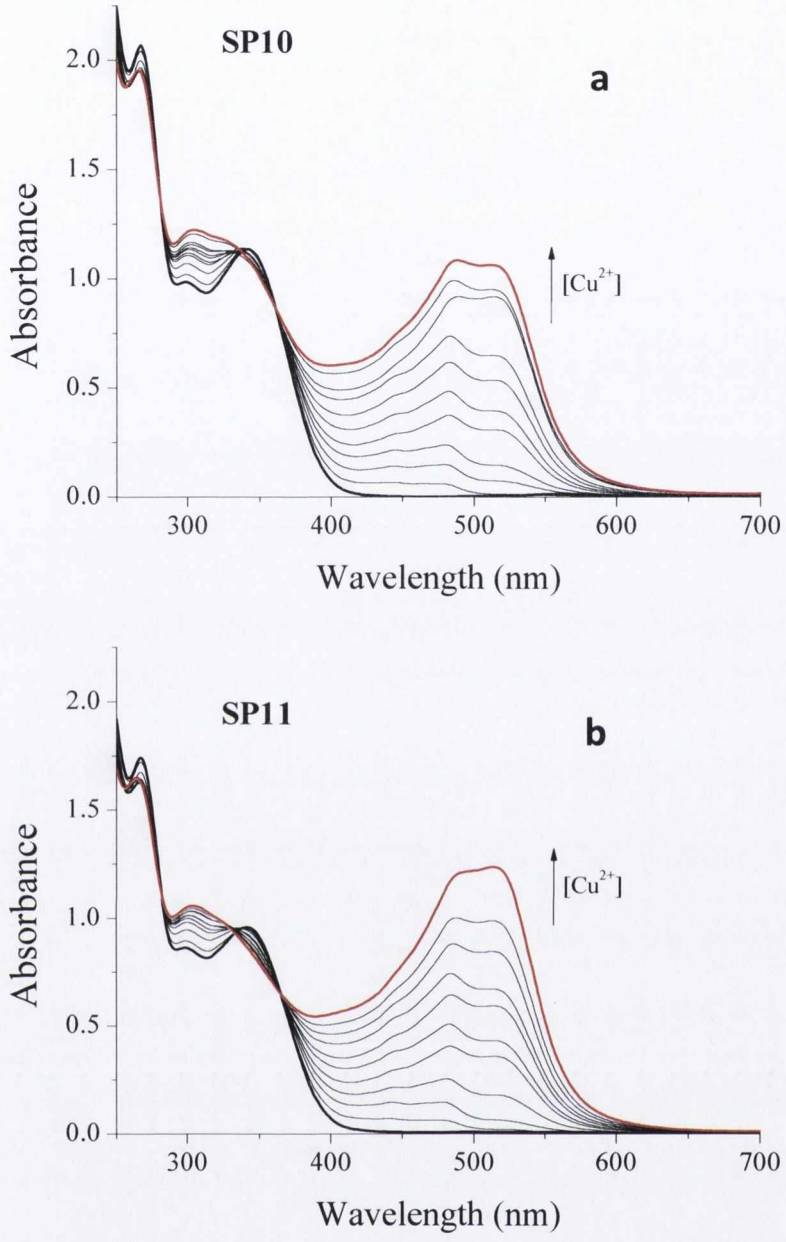


Figure 2.32 Absorption spectra of **SP10** (**a**) and **SP11** (**b**) (1.0×10^{-4} M, acetonitrile, 293 K) after increasing the concentration of $Cu(ClO_4)_2$.

concentration of copper (II). These two bands coalesced partially at higher concentrations of the metal evolving in two absorptions at 491 nm and 517 nm observed after the addition of 1 equivalent of copper (figure 2.32a). Analogously, compound **SP11** responded to low concentrations of copper (II) with two absorption maxima at 482 nm and 517 nm in the visible region that shifted at 491 nm and 512 nm respectively (figure 2.32b).

2.4.15 Reversibility of the Spiropyran-Copper Interactions

The solutions containing the four spiropyrans and 1 equivalent of copper were irradiated with visible light for 10 min and the corresponding UV-vis spectra were recorded. The absorption maxima in the spectrum of **SP8** underwent remarkable changes in its features after irradiation. First the two absorption maxima in the ultraviolet region at 263 nm and 305 nm shifted bathochromically to 271 nm and 308 nm and their intensity increased after irradiation with visible light. The broad absorption in the visible region decreased in intensity and shifted hypsochromically from 496 nm to 452 nm. A small shoulder was barely visible at 378 nm (figure 2.28a). The changes that took place in the absorption of a solution of **SP9** and copper perchlorate after irradiation with visible light resembled those observed for **SP8**. The maximum at 347 nm redshifted slightly to 352 nm retaining its intensity while the peak at 414 nm redshifted to 417 nm and underwent a significant intensity decrease. The maximum absorption located at 504 nm dropped to an intensity value which was 1/3 of the non-irradiated solution one and blueshifted to 472 nm (figure 2.28b). Analogously, the absorption maximum at 517 nm of a solution of **SP10**-$Cu(ClO_4)_2$ decreased in intensity and blueshifted to 478 nm. The peak 266 nm of non irradiated solution moved upward after irradiation with visible light and shifted to 271 nm while the two smooth absorption bands at 302 nm and 329 nm coalesced in one unique absorption band higher in intensity whose maximum was located at 310 nm (figure 2.28c). Finally, a solution containing **SP11** and $Cu(ClO_4)_2$ responded to visible light irradiation with a blueshift of the maximum at 514 nm to a new absorption band appeared at 480 nm concomitant with a loss of intensity of the 50%. Additionally a new absorption band was observed at 391 nm while the two peaks at 264 and 306 nm redshifted to 271 and 311 nm respectively. The maximum at 271 nm was lower in intensity with respect to that at 264 nm while the appearance of the new peak at 311 nm was accompanied by an intensity increase (figure 2.28d). The interaction between the members of this group of spiropyran based receptors and copper (II) perchlorate underwent visible changes upon irradiation with visible light. If a complex was actually formed between the spirochromenes and copper (II), these results would indicate only a partial release of the metal guest from the receptors sites as the original spectra of metal free solutions of spiropyrans were not recovered after irradiation with visible light. Overall, a very selective response to

copper (II) was observed with all the members of this group regardless to the substituent present on the indolic half of the molecules.

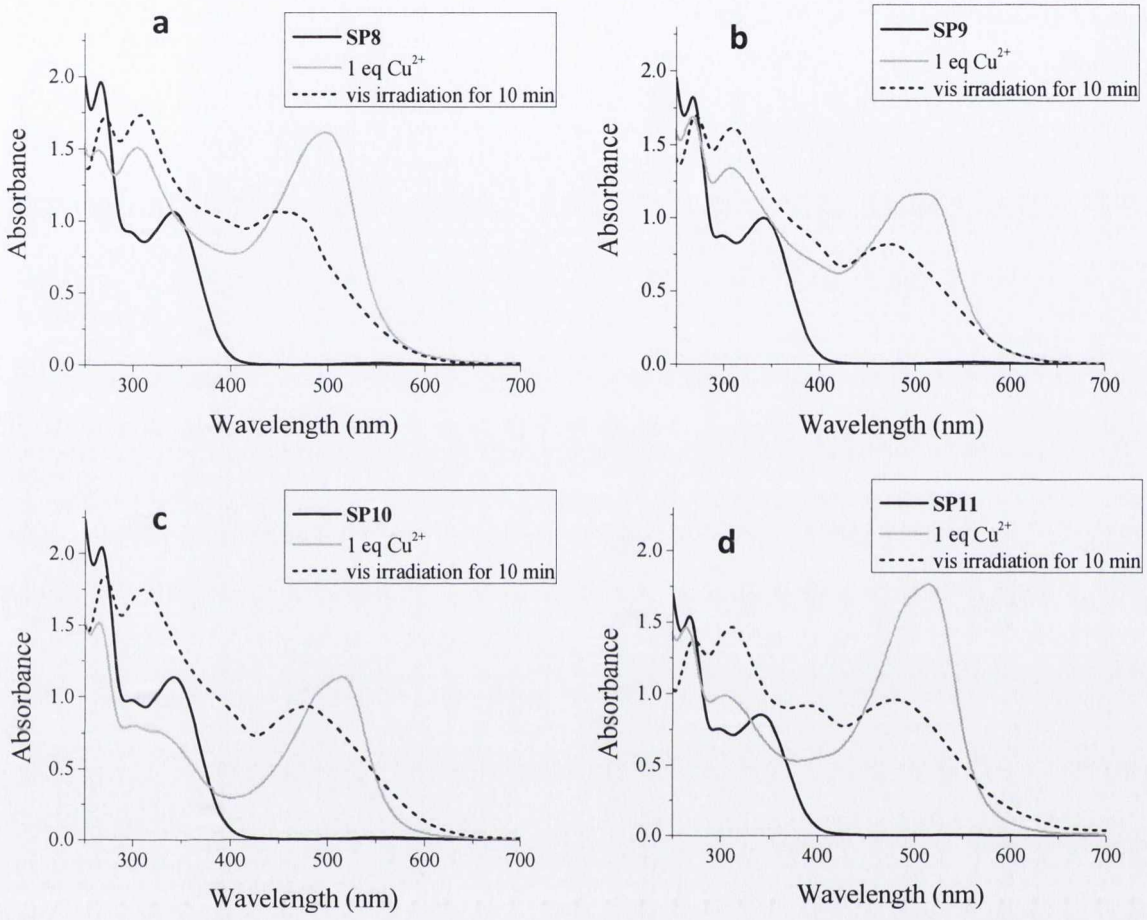


Figure 2.33 Absorption spectra of **SP8** (**a**), **SP9** (**b**), **SP10**(**c**), and **SP11** (**d**) ($1.0x10^{-4}$ M, acetonitrile, 293 K) before (black curves), after the addition of 1 eq of copper perchlorates (grey curves), and irradiation with visible light for 10 min (dotted curves).

2.4.16 Mass Spectroscopy Analysis

As mentioned above, spiropyrans can form complexes with transition metals whose composition can vary depending on the structure of the switchable molecule. Complexes were the ratio SP-M^{2+} is either 2:1 or 1:1 are often observed. When the ratio is 2:1, two open merocyanines usually cooperate in the coordination of a metal cation by means of their phenolate anions. Thus, sandwich like complexes are formed and the metal guest is trapped between the two molecules. Considering the unusual results

observed with all the spiropyrans belonging to group 3, a similar explanation would be plausible. Since all compounds responded to the presence of copper (II) perchlorate in the same manner regardless to the substituent on the indolic moiety, we thought that sandwich like complexes formed between to molecular switches and the metal guests where the interaction between the three parts was only due by the coordination between two phenolate and the metal while the substituent on N is completely extraneous to the binding. In order to confirm this hypothesis we carried out MALDI-TOF MS studies on the solutions containing **SP8**, **SP9**, **SP10**, and **SP11** in the presence of an equimolar amount of $Cu(ClO_4)_2$. Calculation of the theoretical mass of spiropyran-copper complex 1:1 affords a value of 385 m/z for the molecular ion [**SP8**-Cu^{2+}]$^+$. If two molecules of compound **SP8** form a sandwich like complex with one Cu^{2+} cation the resulting molecular ion [2**SP8**-Cu^{2+}]$^+$ mass would be 707 m/z. In figure 2.34a the spectrum of **SP8** in the presence of copper shows a peak whose value of 643 m/z corresponds exactly to a [2**SP8**]$^+$ dimer with no copper in it and a weight loss of two protons. The small peak at 322 mz correspond to monomer [**SP8**]$^+$. A peak indicating the molecular ion [2**SP9**]$^+$ at 703 m/z was found in mass spectroscopy analysis carried out on the **SP9** solution containing copper (figure 2.34b). In this experiment other peaks were found at 330, 352, and 423 m/z. That at 352 corresponds to the molecular ion [**SP9**]$^+$ Also in this case is seems that the metal does not form a complex. In the analysis of the solution containing **SP10** and the same cation, the presence of a spiropyran-spiropyran dimer was confirmed by its molecular ion peak [2**SP10**]$^+$ at 843 m/z (figure 2.35a) while a peak at 422 mz indicated the a single molecule of **SP10**. The carboxylated compound **SP11** formed apparently a dimer as well, whose molecular ion [2**SP11**]$^+$ peak is the one shown in figure 2.35b at 787 m/z. Also in this case a small peak at 393 m/z revealed the presence of the monomer **SP11**. All these experiment showed the formation of new species that apparently were not complexes.

2.4.17 Purification and Identification of SP-dimers

The MALDI-TOF mass spectra suggested the possible formation of dimers with no trace of copper (II). In order to investigate if copper (II) could be involved in a process different from a chelation, namely a redox reaction, and to characterize the dimers observed *via* mass spectroscopy, we scaled up the process by reacting amounts of the

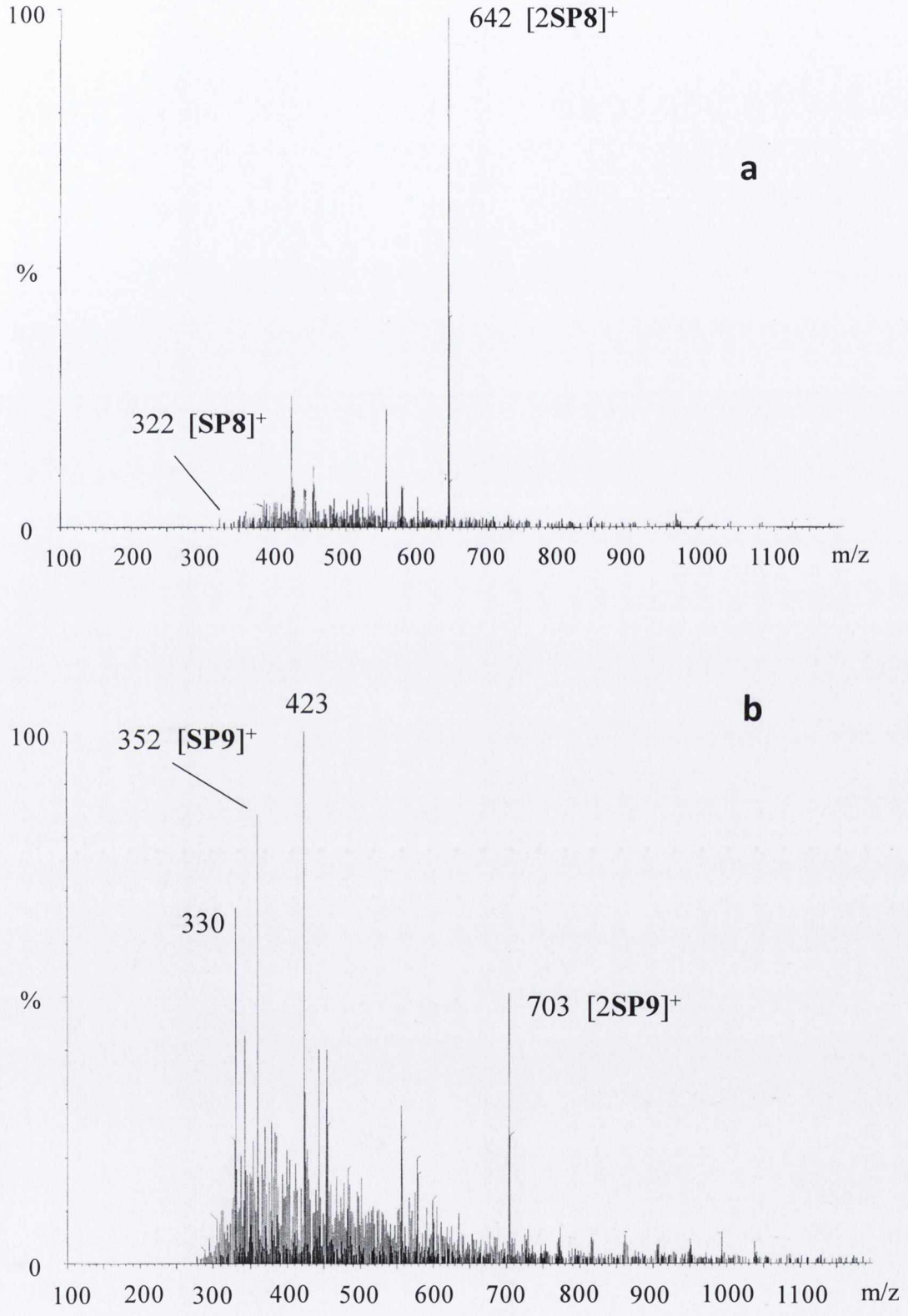


Figure 2.34 MALDI-TOF mass spectrum of acetonitrile solutions of **SP8** (**a**) and **SP9** (**b**) containing $[Cu(ClO_4)_2]$=[**SP**]=1x10^{-3}M.

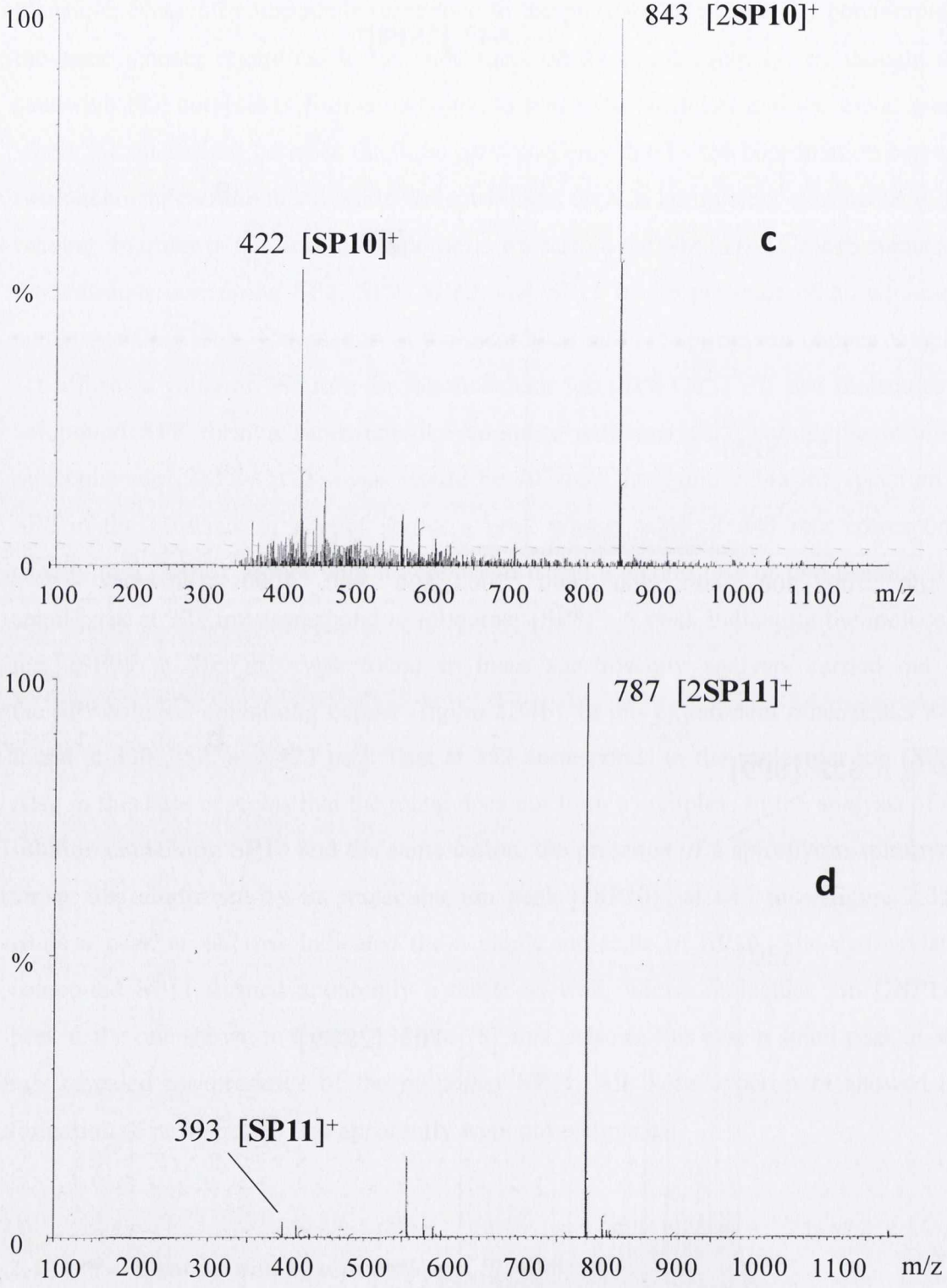


Figure 2.35 MALDI-TOF mass spectrum of acetonitrile solutions of **SP10** (**a**) and **SP11** (**b**) containing $[Cu(ClO_4)_2]$=[**SP**]=1x10^{-3}M.

four spiropyrans with equimolar amount of copper perchlorate in the same condition used in the UV-vis experiments.

Approximately 10 mmol of each spirochromene were dissolved in 5 ml of acetonitrile and an equimolar amount of copper perchlorate dissolved in 100 µl of deionised water was added to each spiropyran solution which was stirred at r.t. for 24h. The solvent was evaporated and each crude was redissolved in dichloromethane and washed with an aqueous solution of $NaHCO_3$ containing the 5% of EDTA. The latter is a well known chelating agent that should bind all the copper (II) cations in solution leaving any spiropyran derivative as metal free compounds. In each solution a red precipitate was observed an filtered off. Each organic phase was collected and the solvent was evaporated under reduced pressure. A first thin layer chromatography analysis of compounds **SP8** and **SP10** reaction mixtures revealed after 24h the appearance of one new spot each, whose retention factor (0.4 in hexane/ethylacetate 6:4) was lower than that of the corresponding spiropyran derivative (0.8 in hexane/ethylacetate 6:4). In both cases, these new species were purified *via* flash chromatography on silica gel and successively characterized by means of both mass spectroscopy and ^{1}H-NMR analysis. Reaction yields were calculated to be 46% and 43% for **SP8** and **SP10** respectively.

MALDI-TOF MS analysis of the compound purified from the reaction of **SP8** revealed the same peak observed in the previous experiment whose value correspond to a molecular ion of mass equal to 742 Da. Analogously, the purification of the compound obtained during the reaction of **SP10** with copper perchlorate had a mass of 842 Da. In both cases these molecular masses are double of the corresponding spiropyrans mass, less two protons each. This implies that two spiropyrans reacted with each other forming probably a C-C bond with the loss of two protons. If this hypothesis was true, the ^{1}H-NMR of each spiropyran should lack of two protons. To confirm this, both mono and bidimensional ^{1}H-NMR analysis were carried out on the two compounds obtained from these purifications. The ^{1}H-NMR spectrum of **2SP8** is shown in figure 2.36a. It is very interesting to observe that this spectrum resembles perfectly that of a single molecule of SP. Seventeen protons are counted in this spectrum while a single molecule of **SP8** has 18 protons. Considering a mass that is equal to the double of that of **SP8** minus two protons, the structure of **2SP8** must have a plane of symmetry. Overall, the spectrum found correspond to molecule **2SP8** (figure 2.36) which is the

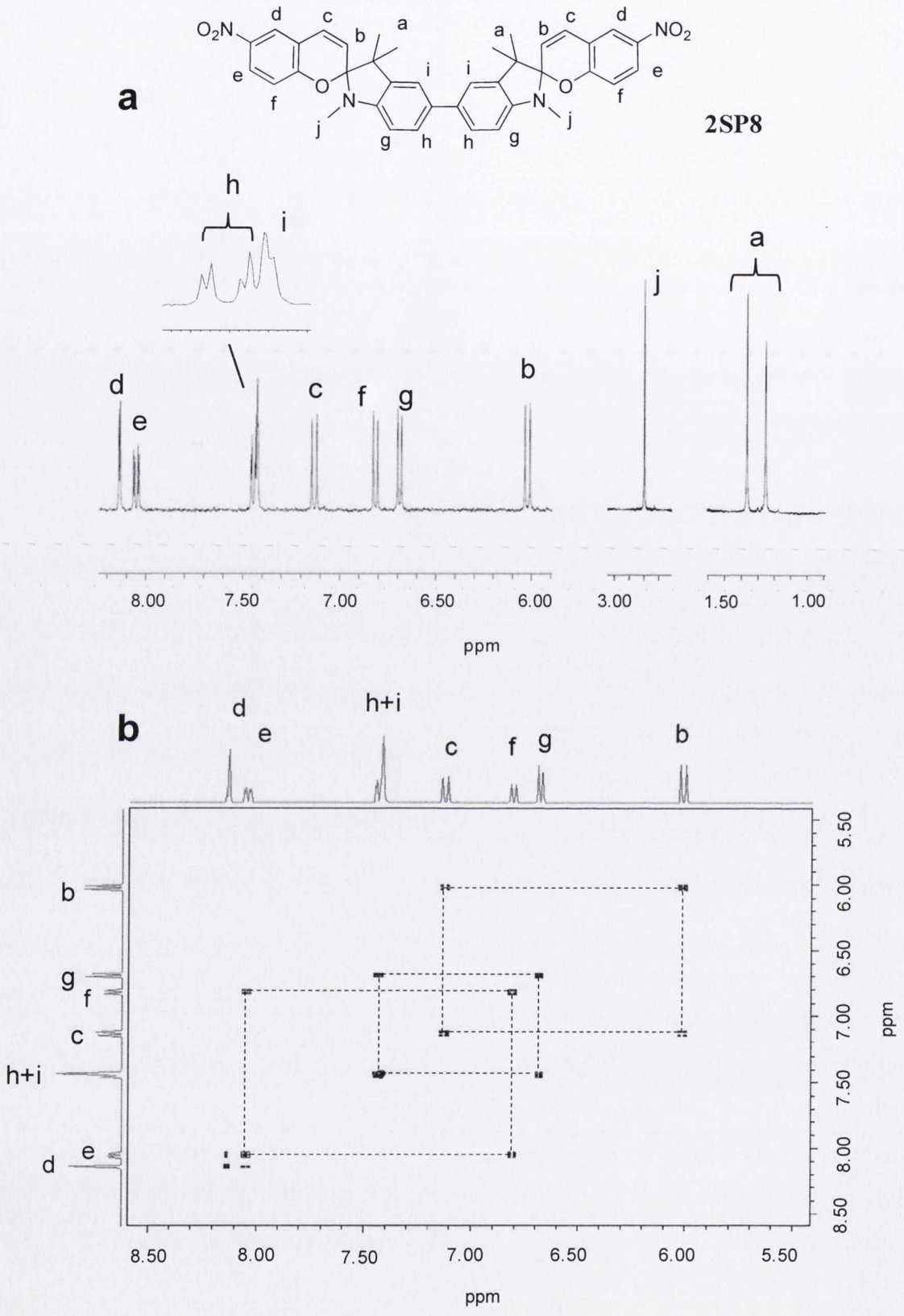


Figure 2.36 (**a**) ^{1}H-NMR and (**b**) ^{1}H-^{1}H COSY NMR partial spectra of **2SP8** ($1x10^{-2}$ M in acetonitrile, 293K).

dimer of two spiropyrans linked to each other through a C-C bond located in 5-position of their indolic system. The typical peaks of the *gem* methyl groups are visible as two singlets that integrate for 6 protons each at 1.25 and 1.36 ppm (*a* in figure 2.36a). These values indicates that the two methyl groups are not magnetically equivalent and the spiropyran is in its closed form. This hypothesis is confirmed by the shift of the indolic methyl groups *j*, which are observed as a singlet that integrates for six protons at 2.79 ppm, and by the coupling constant of the two vinylic protons *b* and *c,* located at 6.02 ppm and 7.14 ppm respectively, that is equal to 10.4 Hz. This value is typical for a *cis* configuration. The aromatic protons *f* are observable as a doublet at 6.82 ppm while protons *e* and *d* are shifted to a lower field at 8.05 (double doublet) and 8.13 (doublet) ppm respectively. The fact that these two signals are not a doublet for *e*, and a singlet for *d*, indicates a long range coupling between the two protons, confirmed by their coupling constant of 2.8 Hz. Protons *g* give a doublet at 6.68 ppm whose coupling constant is equal to 8.0 Hz. The same value is observed for the double doublet located at 7.45 ppm which correspond to protons *h*. A non symmetric doublet at 7.42 ppm indicates protons *i*. Also in this case long range coupling between *h* and *i* was observed. The coupling between *d-e-f* and *h-i-j* are underlined in the ^{1}H-^{1}H COSY of the compound aromatic region depicted in figure 2.36b.

Purification by column flash chromatography of the crude obtained from reacting compound **SP10** with $Cu(ClO_4)_2$ afforded the pure compound **2SP10** whose ^{1}H-NMR and ^{1}H-^{1}H COSY NMR spectra are reported in figure 2.37a and 2.37b respectively. The presence of a symmetry plane is deduced from its ^{1}H-NMR that shows the proton shifts of one single molecule, minus one aromatic proton. Thus the spectra obtained correspond to a spiropyran dimer like the one depicted in figure 2.37 with two dyes attached to each other through a C-C bond located in *para* position with respect to the indolic nitrogen. Analogously to compound **2SP8**, the *gem* methyl groups are not magnetically equivalent and they can be identified as two singlets at 1.27 and 1.33 ppm that integrate for six protons each (*a* in figure 2.37a). The triplet at 1.19 ppm was assigned to the CH_3 protons *n* of the ethyl ester while the corresponding CH_2 *m* were identified in the quadruplet at 4.07 ppm. The aliphatic protons attached to the indolic nitrogen gives three groups of signals: a multiplet in the range 1.84-1.89 ppm for protons *k*, a triplet at 2.35 ppm assigned to protons *l*, and another multiplet between 3.21 and 3.29 ppm corresponding to protons *j* which are directly attached to the nitrogen.

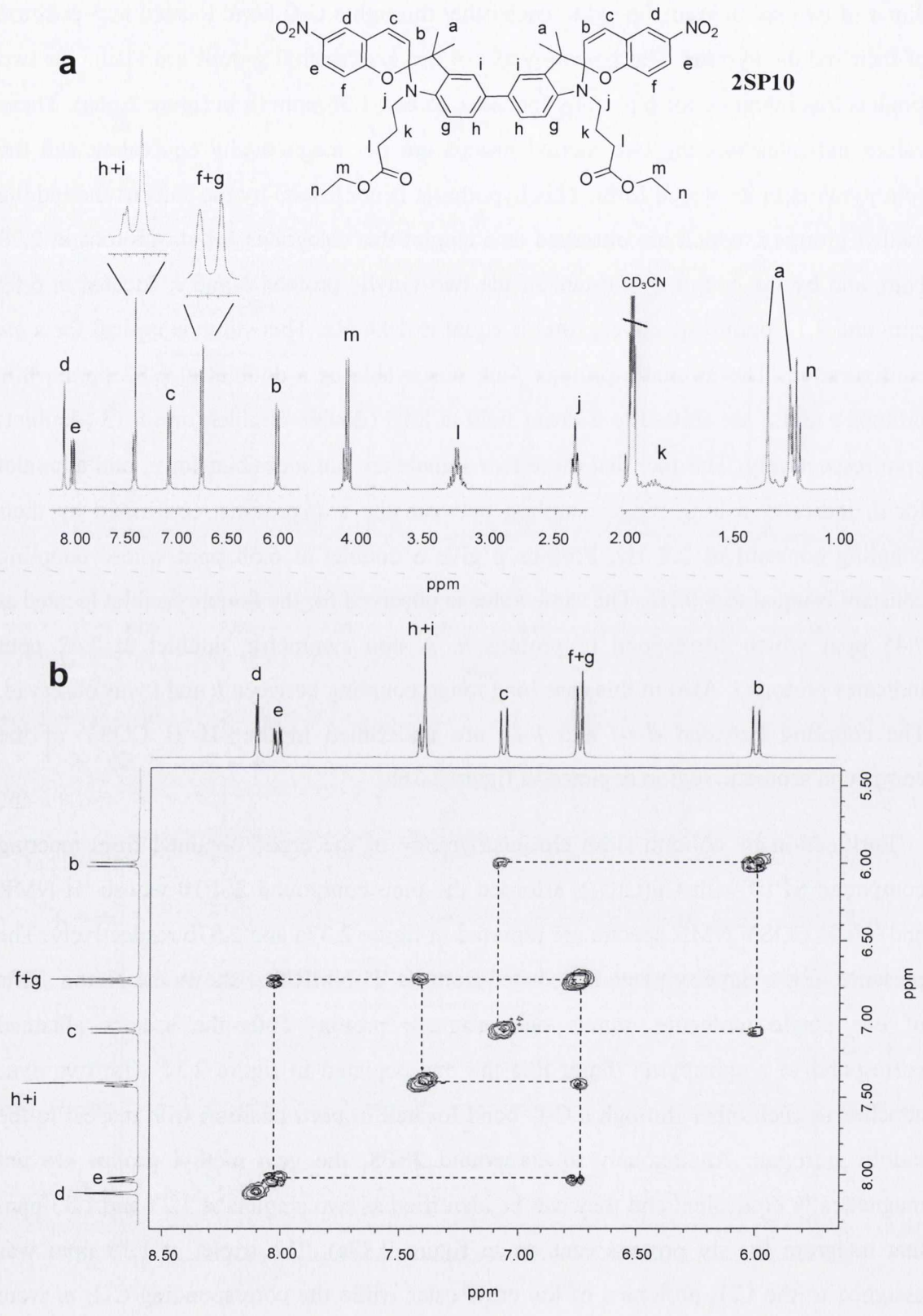


Figure 2.37 (**a**) ^{1}H-NMR and (**b**) ^{1}H-^{1}H COSY NMR partial spectra of **2SP10** ($1x10^{-2}$ M in acetonitrile, 293K).

The vinylic protons *b* and *c* are identified by two doublets at 6.01 ppm for *b* and 8.81 ppm respectively and their coupling constant of 10.4 Hz confirms their *cis* configuration. Long range coupling was observed for the two aromatic protons on the benzopyran ring *d* and *e* that are identified as a doublet and a double doublet at 8.13 and 8.02 ppm. The doublet at 6.75 ppm integrates for four protons and it correspond to the overlapping of two distinct doublets that identify protons *f* and *g*. The signals at 7.42 ppm integrate for four protons and correspond to protons *h* and *i*. The correlation between protons *e-f*, *g-i*, and *h-i* can be clearly seen in the aromatic region ^{1}H-^{1}H COSY NMR spectra of **2SP10** reported in figure 2.37b. Here, the doublet at 6.75 ppm is interrelated with signals at 7.42 ppm because of the interaction between protons *g* and *h*. The same doublet at 6.75 ppm interrelates with the shifts of protons at 8.02 ppm because of the interactions between protons *f* at 6.75 ppm and *e* at 8.02 ppm.

Reaction of spiropyran **SP9** with equimolar amount of $Cu(ClO_4)_2$ in larger scale produced several by-products. The purification of these compounds by flash chromatography resulted to be particularly difficult. Several attempts were made changing conditions and eluent polarity but they were all unsuccessful. However, a sufficient amount of compound **2SP9**, depicted in figure 2.38, was purified *via* preparative thin layer chromatography by using a mixture 1:1 of ethyl acetate and hexane as eluent ($Rf = 0.4$), and eventually characterized. The ^{1}H-NMR **2SP9**, reported in figure 2.38a, shows similar patterns observed in the spectrum of the analogous **2SP8**, confirming compound **2SP9** to be a symmetric dimer. The four *gem* methyl groups *a* are magnetically equivalent and they are identified by two singlets integrating for six protons each at 1.25 and 1.30 ppm. The two tethers functionalized with a terminal OH group pending from each indolic nitrogen, give very characteristic signals. The multiplet in the region from 3.26 ppm to 3.40 ppm was attributed to the four protons *j* while the multiplet shifted to a lower field, in the range of 3.59-3.82 ppm corresponds to methylene protons *k* Those of the two OH groups, namely protons *l*, are two triplets located at 3.69 ppm and 3.82 ppm. The aromatic region was studied also by ^{1}H-^{1}H COSY NMR and it is shown in figure 2.38b. The two doublets corresponding to the vinylic protons are localized at 6.03 for proton *b*, and 7.08 ppm for proton *c*. Their coupling constant value is equal to 10.4 Hz and is typical for a *cis* configuration. This confirms the fact that both units are in their closed forms and not in the merocyanine ones. Two overlapped doublets are observable at 6.76 and 6.78 ppm and the whole

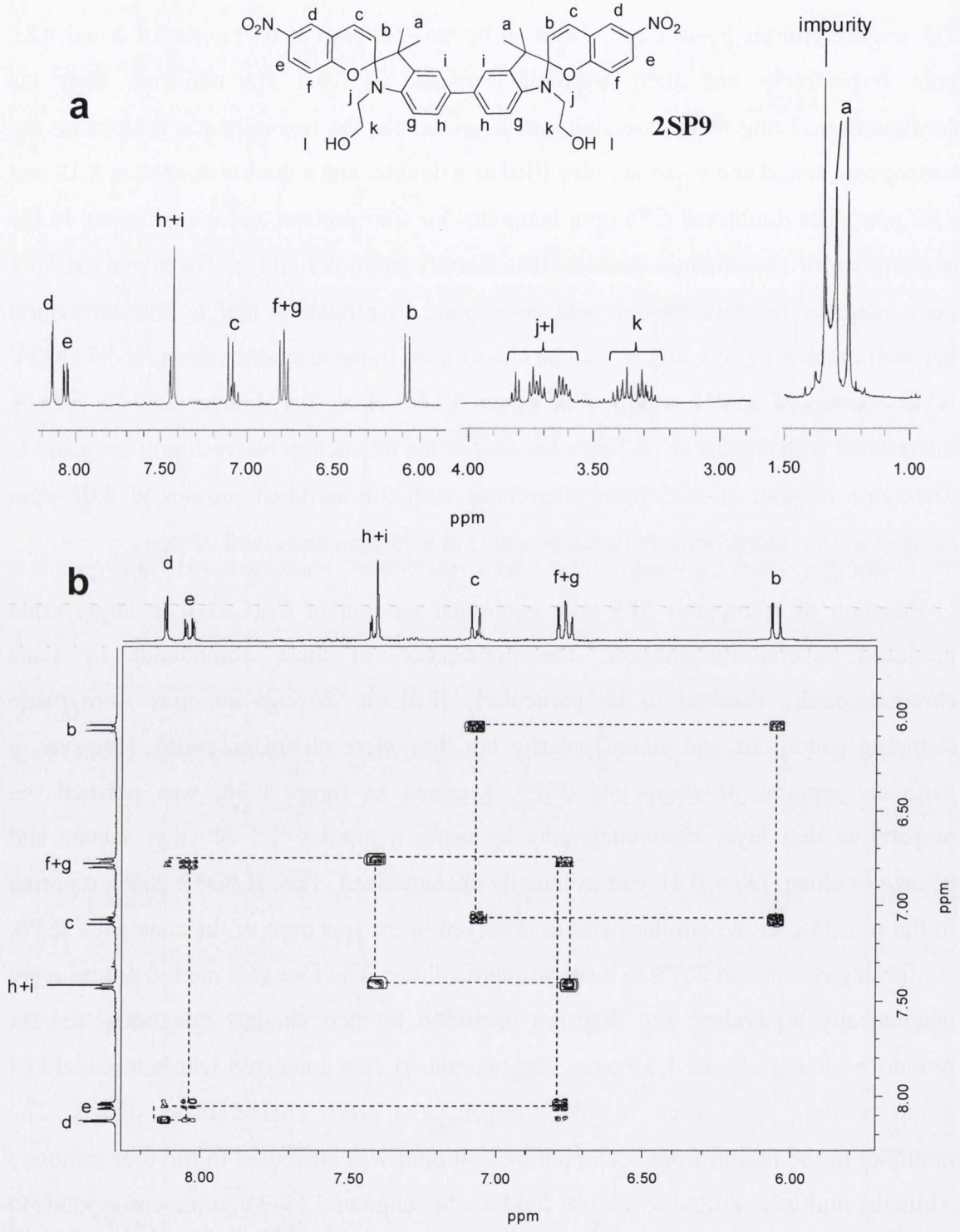


Figure 2.38 (**a**) ^{1}H-NMR and (**b**) ^{1}H-^{1}H COSY NMR partial spectra of **2SP9** ($1x10^{-2}$ M in acetonitrile, 293K).

integration is four protons. The first signal at 6.76 ppm corresponds to proton *g* as it correlates with the multiplet at 7.40-7.42 ppm. The latter integrates for four protons which correspond to *h* and *i*. The second doublet at 6.78 ppm corresponds to proton *f* in

the benzopyran part of the molecule and its correlation with the double doublet at 8.02 ppm, assigned to proton *e*, can be clearly seen in the spectrum. Long range coupling was observed between the doublet 8.12 ppm, assigned to proton *d*, and the double doublet corresponding to *e*, as confirmed by their coupling constant of 2.8 Hz. Although it was not possible to carry out any UV-visible experiment on this molecule since it was not pure, we identified in its ^{1}H-NMR very similar patterns to those observed for **2SP8** and **2SP10** and both magnetic resonance and mass spectroscopy analysis suggested that a dimerization took place.

Reaction of $Cu(ClO_4)_2$ with **SP11** was carried out but the purification of any side product failed. The MALDI-TOF MS analysis reported above is the only data we have and no speculations are allowed on the hypothetical structures of compounds generated during the reaction.

2.4.18 SP Dimers' Photoswitchability and Response to Cu(II)

The binding capability of the spiropyran dimers obtained by addition of $Cu(ClO_4)_2$ their corresponding monomers was investigated by UV-vis absorption spectroscopy. Spectra of colourless acetonitrile solutions containing **2SP8** and **2SP10** are showed in figure 2.39 and 2.40. Spiropyran **2SP8** absorbs in the UV region with two distinctive bands with maxima at 275 nm and 303 nm. It is interesting to observe that its molar absorption coefficient of $\varepsilon = 3.5x10^{5}\ M^{-1}cm^{-1}$ is an order of magnitude higher than $\varepsilon = 1.1x10^{4}\ M^{-1}cm^{-1}$ observed for the corresponding monomer **SP8**. This increased capability of absorbing light of compound **2SP8** is probably due by its extended conjugation between the two indolic moieties. Irradiation with UV light at 254 nm caused the appearance of a new band in the visible region at 579 nm (figure 2.39a) accompanied by blue colouration of the solution. This band indicates more likely the photoisomerization of the spiropyran units in their corresponding merocyanines. At this stage it is not clear if one or both units are involved in the photoisomerization. The band in the visible region disappeared after 10 minutes of storage in the dark and the spiropyran spectrum was fully recovered. Addition from 0.4 to 3 equivalent of $Cu(ClO_4)_2$ to the same spiropyran solution produced the appearance of new bands in the visible region with the highest intensity peak at 475 nm that reached its maximum value after the addition of 3 equivalent of salt. Concomitantly the two absorption maxima in

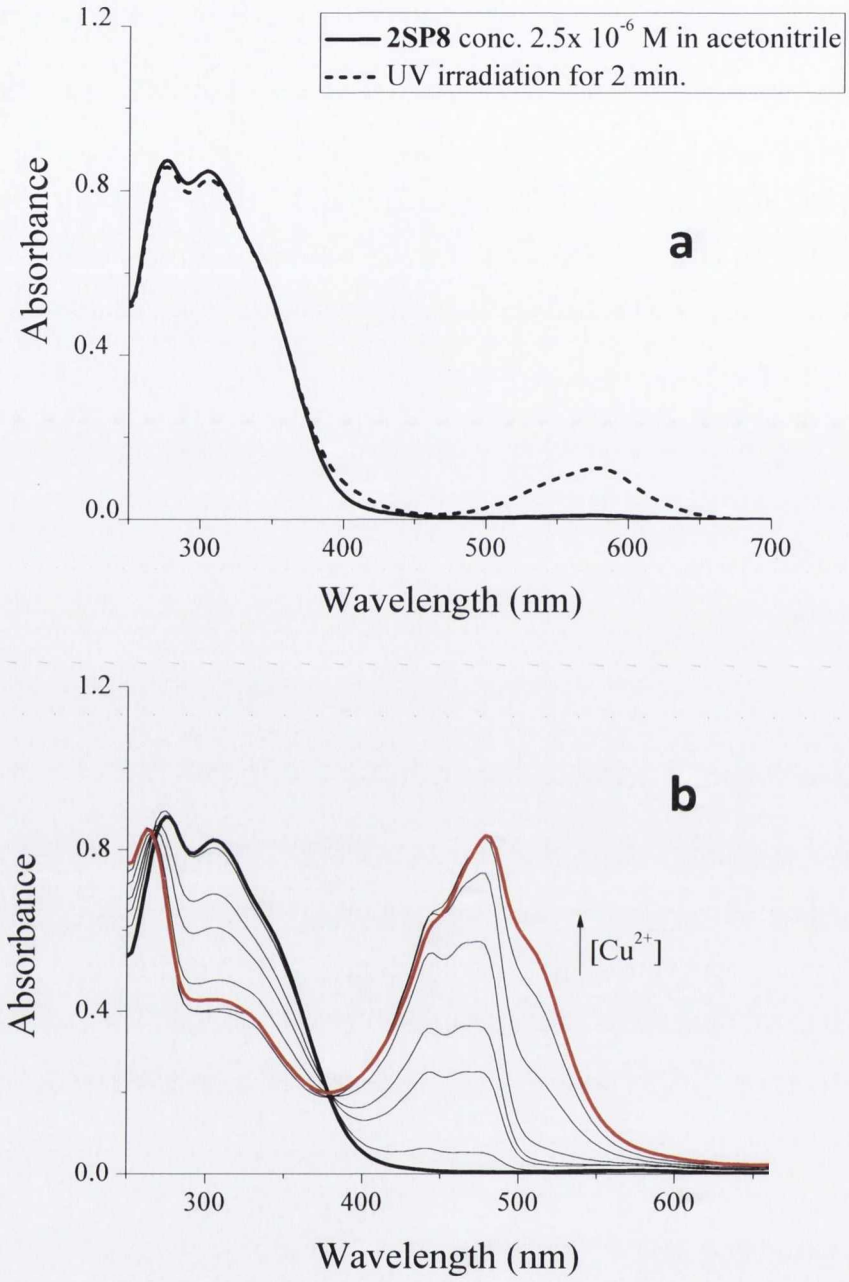


Figure 2.39 (**a**) UV-vis spectra of a solution of **2SP8** ($2.5x10^{-6}$ M in acetonitrile, 293K) before (black curve) and after (dotted curve) irradiation with UV light; (**b**) UV-vis absorption spectra of **2SP8** ($2.5x10^{-6}$ M, acetonitrile, 293 K) after increasing the concentration (0.4-3 equivalents) of $Cu(ClO_4)_2$.

the UV region decreased asymmetrically and two isosbestic points were noticed at 264 nm and 368 nm (figure 2.39b). The appearance of the new bands is probably due to ring opening of both spiropyran units and the following formation of a copper complex where the metal is trapped between the two phenolates.

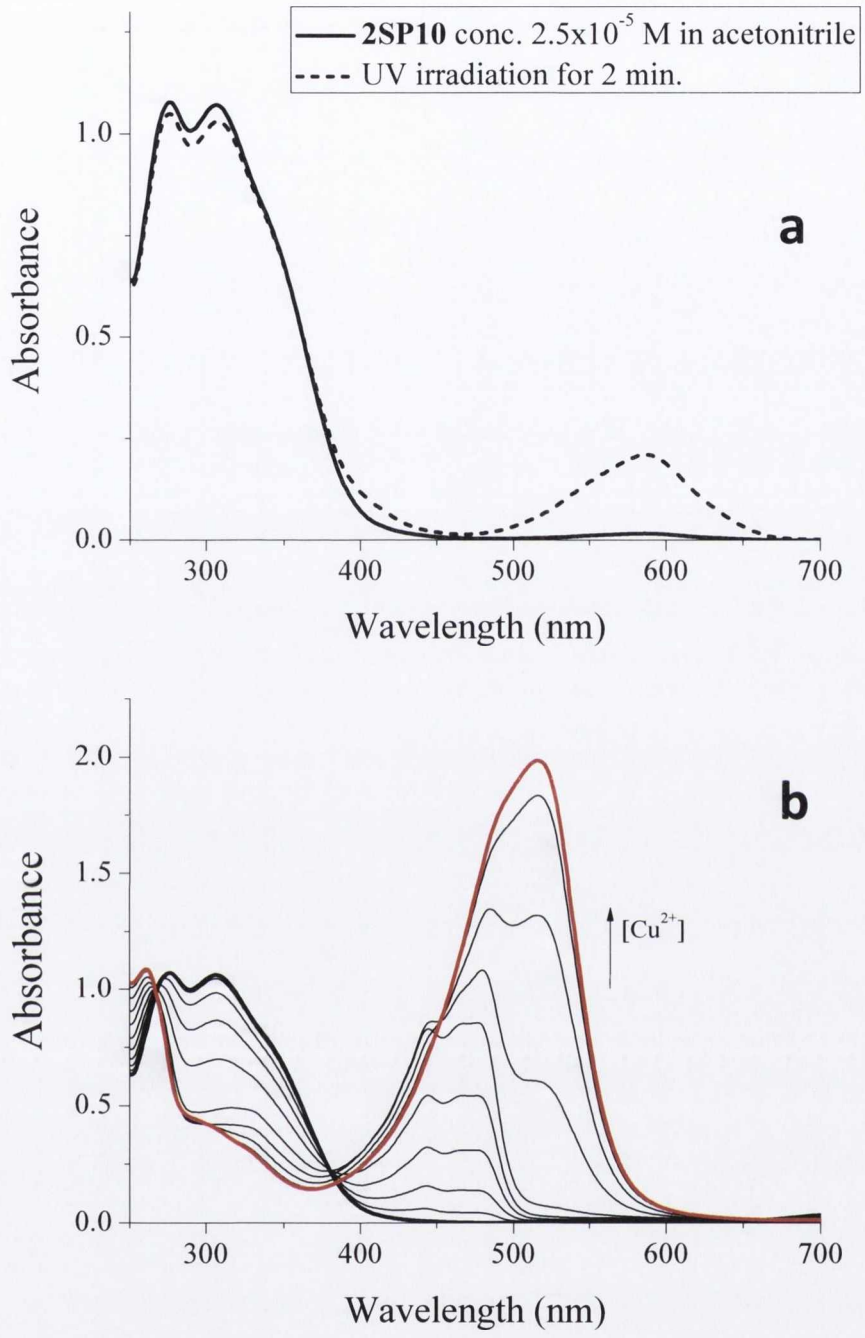


Figure 2.40 (**a**) UV-vis spectra of a solution of **2SP10** ($2.5x10^{-5}$ M in acetonitrile, 293K) before (black curve) and after (dotted curve) irradiation with UV light; (**b**) UV-vis absorption spectra of **2SP10** ($2.5x10^{-5}$ M, acetonitrile, 293 K) after increasing the concentration (0.1-1 equivalents) of $Cu(ClO_4)_2$.

Compound **2SP10** responded to photostimulation with UV light as well. Its spectra before and after irradiation are shown in figure 2.40a. Analogously to compound **2SP8**,

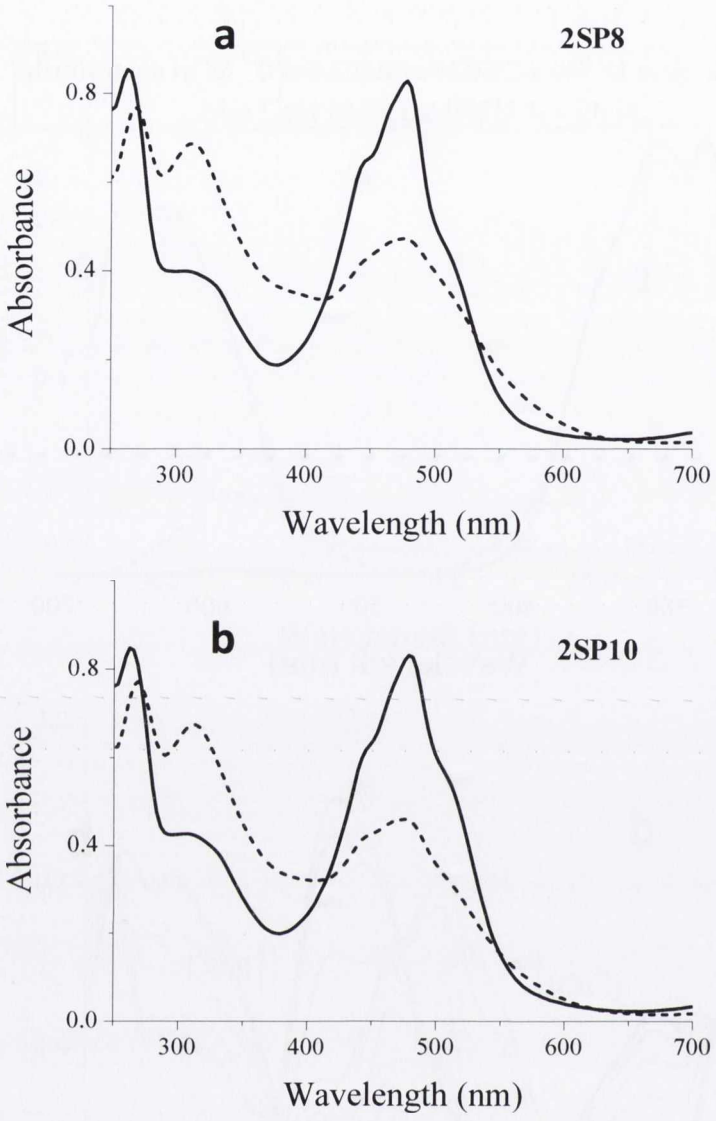


Figure 2.41 (**a**) UV-vis spectra of a solution of **2SP8** ($2.5x10^{-6}$ M in acetonitrile, 293K) in the presence of 3 equivalents of $Cu(ClO_4)_2$ before (black curve) and after (dotted curve) irradiation with visible light; (**b**)) UV-vis spectra of a solution of **2SP10** ($2.5x10^{-5}$ M in acetonitrile, 293K) in the presence of 1 equivalent of $Cu(ClO_4)_2$ before (black curve) and after (dotted curve) irradiation with visible light.

an acetonitrile solution of **2SP10** is colourless and absorbs in the UV region with maxima at 275 nm and 308 nm. Its molar absorption coefficient of $\varepsilon = 4.2x10^4\ M^{-1}cm^{-1}$ four times higher than $\varepsilon = 1.0x10^4\ M^{-1}cm^{-1}$ observed for the corresponding monomer **SP10**. Irradiation with UV light triggers the photoisomerization of the spiropyran subunits to the open merocyanines accompanied by the appearance of a visible band with maximum intensity at 586 nm. This new absorption band disappeared shortly after storage in the dark. The addition of $Cu(ClO_4)_2$ caused dramatic changes in the molecule

absorption profile, similar to those observed for **2SP8**. The absorption maximum at 275 nm blueshifted to 261 nm while that at 308 nm decreased in intensity (figure 2.40b). A strong intensity band evolved in the visible region reaching it maximum absorption intensity at 515 nm after the addition of 1 equivalent of Cu (II). This band indicates probably the formation of a complex with a copper ion coordinated by the phenolate units of an isomer with two merocyanines. The two tethers present on each SP subunits can participate at the chelation as well; this offers alternative coordination geometries that still need more comprehensive investigations.

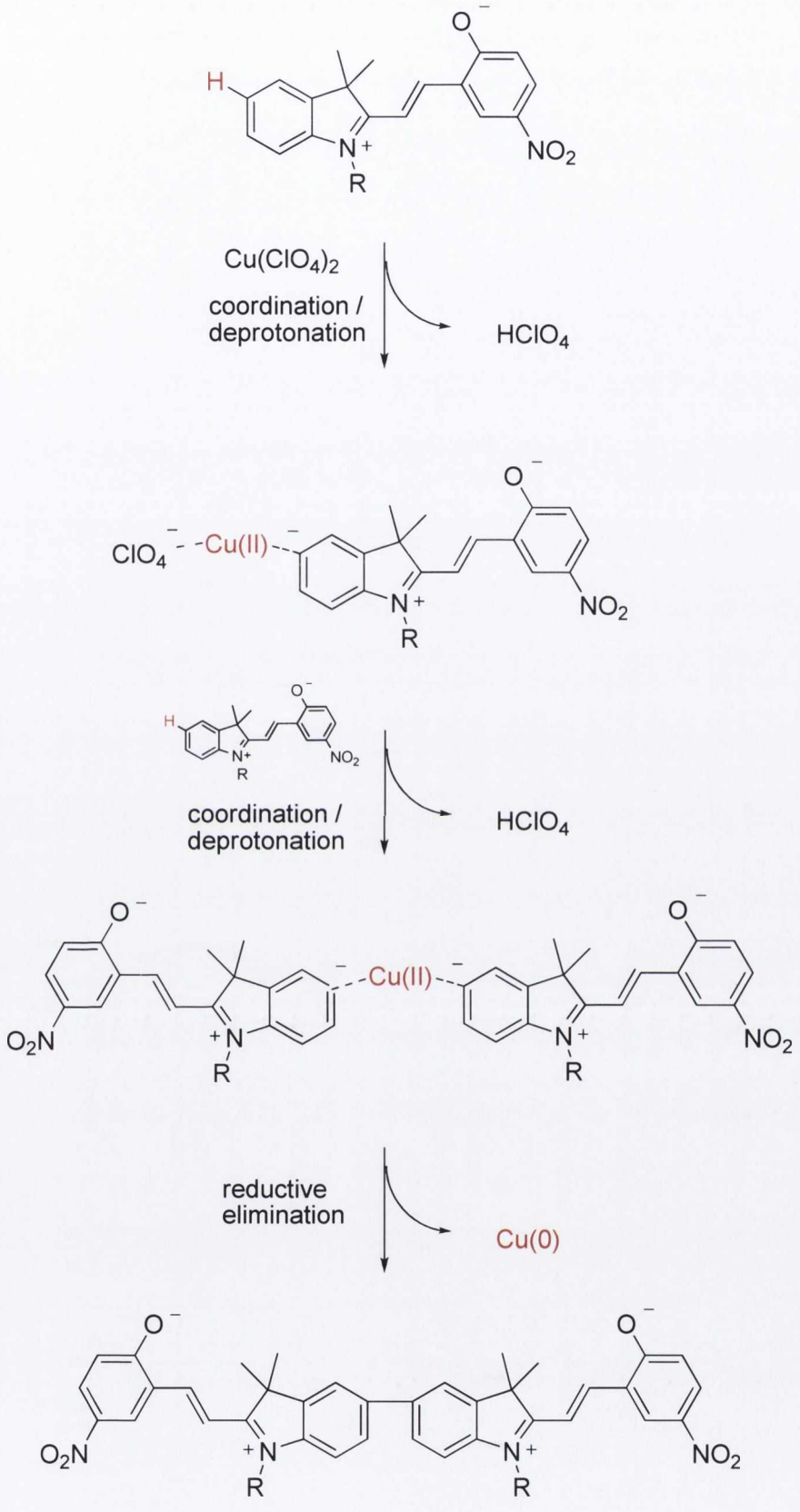
The reversibility of copper complexation was investigated by irradiating with visible light the spiropyran solutions **2SP8** and **2SP10** containing the metal. Interestingly, the phenomena observed were very similar to those observed after shining visible light on the solutions containing spiropyrans **SP8** and **SP10** in the presence of copper (II). In both cases the bands in the visible region of their spectra decreased in intensity and blueshifted but the spectra of the spirochromenes in the absence of copper (II) was not recovered (figure 2.41a and 2.41b) This indicates probably just a partial release of the metal cation from the photochromic system. Additionally these changes were completely irreversible as neither storage in the dark nor irradiation with UV light recovered the spectra observed before irradiation with visible light. These unexpected results need to be further investigated.

2.4.19 Possible Mechanism of Dimerization

The dimerization observed consists in an aryl carbon-carbon bond formation *via* a regioselective oxidative coupling between two identical molecules. The reaction is likely to be induced by the stoichiometric amount of copper (II) which is probably oxidized to copper (0) (the red precipitate we observed) during the process. We found a mechanistic explanation to such a process in two well known coupling reactions: the Cham-Lam coupling and the Ullmann coupling. The Chan-Lam coupling allows aryl carbon-heteroatom bond formation *via* an oxidative coupling of arylboronic acids, stannanes or siloxanes with NH or OH containing compounds in air. Substrates include phenols, amines, anilines, amides, imides, ureas, carbamates, and sulfonamides. The reaction is induced by either a stoichiometric amount of copper (II) (generally $Cu(OAc)_2$) or a catalytic amount of copper catalyst which is reoxidized by atmospheric

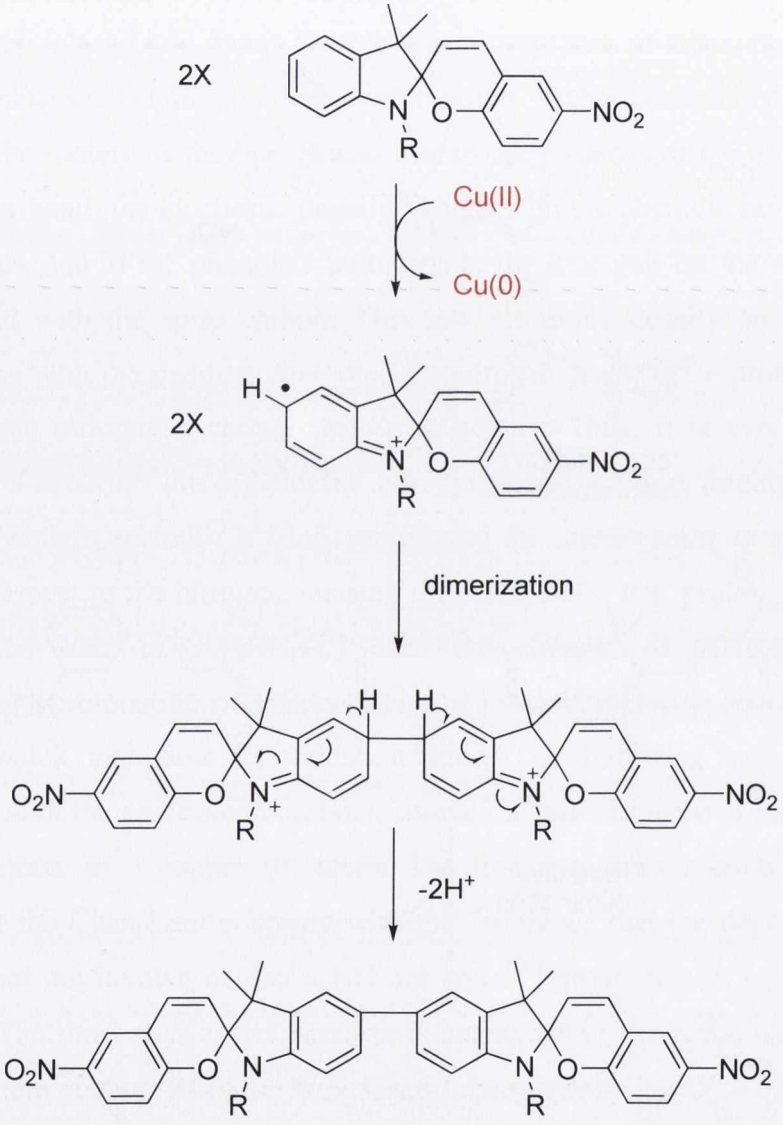
oxygen.[25-33] On the other hand, the Ullman coupling involves the formation of biaryls through coupling of aryl halides with an excess of copper at elevated temperatures (200°C). The active species is a copper (I)-compound which undergoes oxidative addition with the second equivalent of halide, followed by reductive elimination and the formation of the aryl-aryl carbon bond.[34, 35] The process involving the dimerization of our spiropyrans seems to follow the Chan-Lam reaction path but leading to the formation of a biaryl product like in the Ullmann coupling. We suggest the mechanism depicted in scheme 2.9. First, it is known that spiropyrans may exist in two different forms, namely closed and open. The electronic properties of these molecules undergo dramatic changes depending on their conformation. Higher electronic density is present on the indolic moiety of the open forms due to the presence of the nitrogen lone pair. On the other hand, the electronic density is higher on the phenolic moiety of the open merocyanines due to the phenolate anion while the lone pair on the nitrogen forms a double bond with the spiro carbon. This low electronic density on the open forms indole, along with the positive charge on its nitrogen gives to the proton in *para* with respect to the nitrogen a certain degree of acidity. Thus, it is very likely that the presence of a first Cu^{2+} ion triggers the spiropyran ring opening, forcing it to stay in its open form while a second Cu^{2+} ion coordinates the merocyanine in its 5-position, in *para* with respect to the nitrogen, causing the release of a first proton. In this first step the oxidation state of copper (II) does not change. At this stage, a second coordination/deprotonation step takes place and a second molecule coordinates the same Cu^{2+} ion which maintains its oxidation state. The following step is a reductive elimination with the carbon-carbon bond formation between the two molecules and the reduction/release of a copper (0) atom. The first two steps resemble the first step reported for the Chan-Lam coupling with the difference that the deprotonation of the substrate does not involve neither a NH nor and OH group present on the aryl but the aryl itself. The third step in our reaction is analogous to the reductive elimination of copper (0) from copper (II) in the same Chan-Lam reaction.

There is a second proton on the indolic part of a merocyanine that may be acidic: this proton is located in 7-position, in close proximity of the merocyanine nitrogen. In theory, the carbon atom in 7-position could be prone to undergo the same sequence of events with a first deprotonation/coordination to a Cu^{2+} ion followed by coupling with a second molecule. The reason why we observed regioselectivity for the 5-position is



Scheme 2.9 Mechanism of dimerization of our spiropyrans.

probably due by both sterical and electronic effect of the indolic moiety. First, the indolic nitrogen of our molecules, bears an aliphatic chains which may create an obstacle to the coordination of a copper atom by the very close carbon in 7-position. Additionally, if our hypothesis is correct and the molecular switches are in their open form, the indolic nitrogen would be positively charged. The repulsion between the nitrogen and the copper ion positive charges would impede the coordination of copper as well.



Scheme 2.10 Mechanism of dimerization of our spiropyrans *via* radical formation.

An alternative route for the dimerization of our compounds considers the formation of radical species. In this case the Cu(II) is reduced to Cu(0) triggering the formation of two SP radicals (scheme 2.10). In this case the molecules do not need to be in their open form. The dimerization follows the reduction of copper. Abstraction of two protons from the indolic aromatic regions allows the conjugation to be fully restored and the dimer to be formed. The ability of copper (II) to trigger radical reactions on similar systems was reported and discussed extensively by Pragst and his collaborators.[36]

These results would explain the odd peak observed when the compound **SP7**, functionalized with a methoxy group in 8'-position was mixed with an equimolar amount of $Cu(ClO_4)_2$. Its MALDI-TOF MS spectrum in figure 2.26b shows clearly a peak at 846 m/z corresponding to the double of compound **SP7** mass. However, it seems that the presence of a binding site like the methoxy group in 8'-position prevent partially the dimerization since peaks of 2:1 and 1:1 spiropyran-copper (II) complexes are predominant in compound **SP7** mass analysis while these peaks were not observed at all in for the analogues with no binding group on the benzopyran part of their skeletons. Additionally, the addition of $CuCl_2$ to **SP7** did not produce any mass peak that could be related to the presence of a dimer, thus the counter ion seems to play a crucial role in the oxidative coupling of our group 3 molecules.

2.4.20 Conclusions on Group 3

This group of spiropyrans bearing different substituents only on the indolic part of their skeleton showed selective responses only to the presence of copper (II) ions. However the interaction with copper (II) appeared to be only partially reversible as irradiation with visible light was not capable to produce the complete release of the metal cation. By deepening our studies on these unusual interactions with copper (II) we discovered that the binding of this metal is accompanied by a dimerization of our molecules. Indeed, we purified two compounds, namely **2SP8** and **2SP10**, that are the products of a regioselective oxidative cross-coupling mediated by copper (II). A third compound, **2SP9**, was identified *via* MALDI-TOF MS and mono and bidimensional ^{1}H-NMR spectroscopies any purification attempt failed. The pure dimers **2SP8** and **2SP10** retained their capability of chelating copper (II) ions but irradiation of the formed complexes with visible light produced irreversible changes that are currently under

investigation. It is interesting to observe that compounds **2SP8** and **2SP10** were produced in very mild conditions with yields ranging around 45%. At the best of our knowledge this is the first example of cross coupling mediated by copper (II) in such mild conditions causing the symmetric dimerization of spiropyran dyes. We are currently verifying if the scope of this reaction can be broadened.

2.4.21 Binding Studies on Compounds of Compounds of Group 4

The choice of a structurally rigid substituent able to bind transition metal cations in **SP12** and **SP13** was not made randomly but it is the result of a rational design which came from the knowledge we reached by studying the members of the other three groups of molecules. For example, the choice of the three different substituents on group 1 compounds produced receptors able to form stable complexes with bivalent metal cations that cause deep coloration changes in of the metal free spiropyran solutions. However, one of our aims was creating photoreversible sensor in order to overcome the problem of one time use sensors These structures first did not offer the chance of photocontrol on the binding process and second they did not display selectivity for any particular cation. The selectivity was achieved indeed with compounds of group 3 that responded only to the presence of copper but the photocontrol of the spiropyran-metal interaction was still not achieved. Finally compounds belonging to group 2 formed photoreversible complexes but with poor selectivity for the metal guests. However, the presence of a methoxy group in all members of group 2 seems to promote a sensitive response to the presence of zinc. At this point we envisaged the possibility to further optimize structures of group 2 in order to narrow the spectrum of transition metals they could interact with, leading this preference towards zinc (II) cation. Additionally, the new structures should retain the capability to interact reversibly with the metal. To achieve the required selectivity towards zinc, it is necessary to complement the optical properties of the spiropyran backbone with appropriate functional groups that, collectively, provide a binding site that matches the specific coordination requirements of the targeted ion. With this in mind, we decided to keep the methoxy group in 8'-position of the spiropyran backbone since as well as the nitro group in 6'-position since it allows to achieve the control on the coordination process. For choosing a suitable functional group on the indolic

moiety, we needed to carry out some research on the already known zinc receptors in order to spot the best candidate.

2.4.22 Zinc Detection and Known Zinc Sensors

The importance of zinc for maintaining the structural integrity of proteins, and for regulating gene expression are well known.[37] Although at low levels zinc is an essential mineral used by plants and animals, at higher levels, zinc pollution is suspected of causing cardiovascular, reproductive, immune and respiratory problems.[38] The detrimental effects of zinc contamination on plants and fish may be even greater due to their increased sensitivity to low aqueous Zn(II) concentrations.[39] Ever increasing concerns for ecological issues such as the potential toxicity of zinc pollutants have driven the need for more effective detection methods and selective and versatile sensors. Noteworthy examples of such compounds have been reported.The synthesis and activity evaluation of two fluorescent water soluble PET sensors **108** and **109** (figure 2.42) for the sensing of Zn(II) was reported by Gunnlaugsson and his collaborators.[40] The two molecules incorporate a receptor site that consists aryl based iminodiacetate moiety,

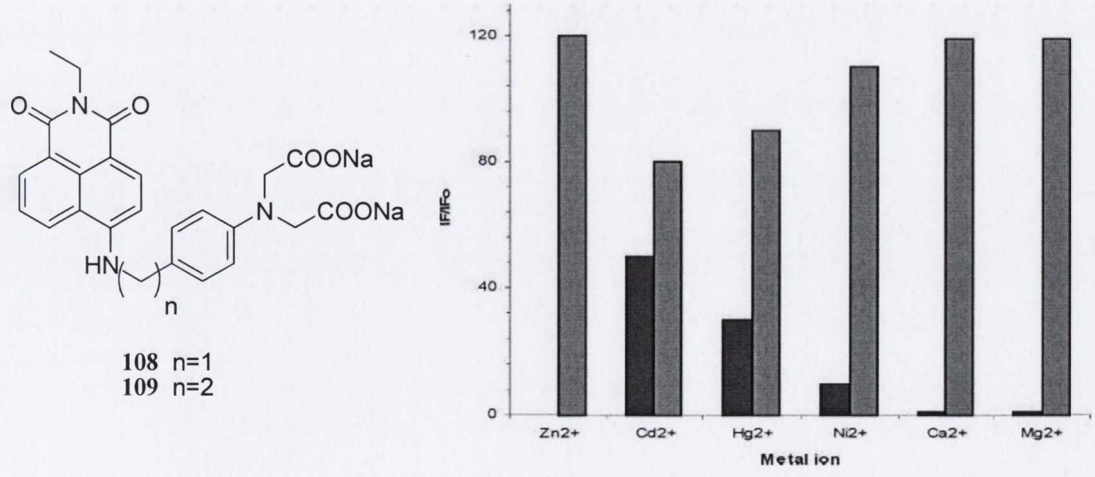


Figure 2.42 Relative fluorescence intensity responses of **108** to various metal ions. Dark grey bars represent emission without Zn(II) for a particular metal ion. Light grey bars represent the emissions upon addition of Zn(II) to respective metal ion. The first bar shows the response to Zn(II) in the absence of any competitive ions.[40]

linked *via* a methylene or an ethylene spacer to 4-amino-1,8-naphthalimide fluorophore. The sensor fluorescence is quenched by photoinduced electron transfer from the electron rich receptor to the electron deficient fluorophore but it is systematically "switched on" upon addition of zinc (II). The latter is coordinated by the two carboxylated groups and the amino group of the receptor impeding the electron transfer to the fluorophore. The high selectivity to zinc (II) was observed at physiological pH of 7.4 even in the presence of competitive metal cations (histogram in figure 2.42).

Two iminodiacetate groups were incorporated in the two selective zinc sensors **110** and **111** synthesized by Ngwendson and Banerjee (figure 2.43).[41] The sensitivity for zinc (II) is higher for compound **111** than compound **110**. This was explained by theoretical studies which suggested that the four chelating carboxylates on **110** do not participate at the binding of zinc (II) at the same time introducing a degree of fluxionality in the sensor-metal complex. However, the three binding moieties of **111** coordinate zinc at the same time resulting in a more rigid and stable complex. Both compounds shows remarkable fluorescence enhancements in the presence of zinc even in mixture with competitive cations (plot in figure 2.43).

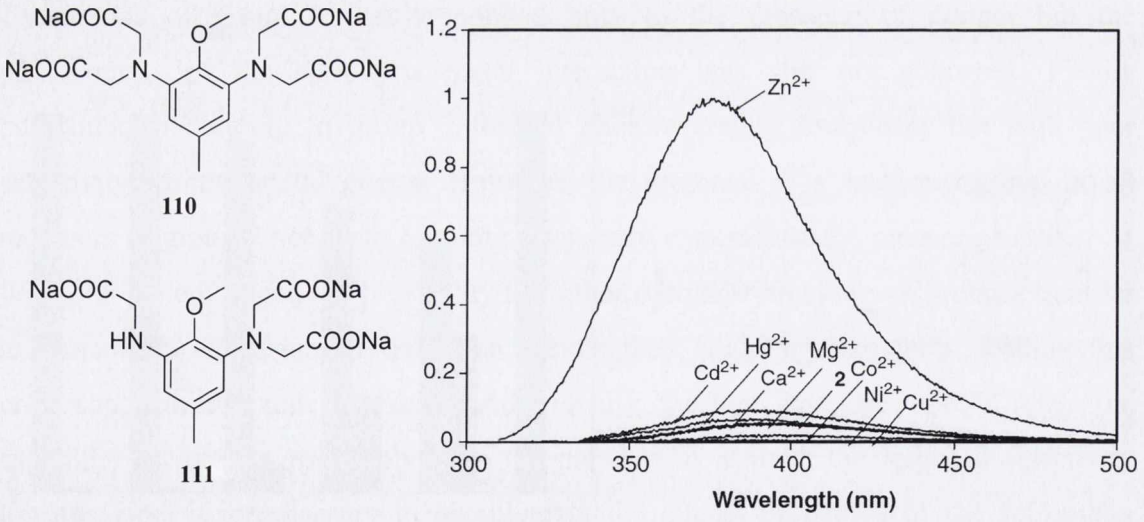
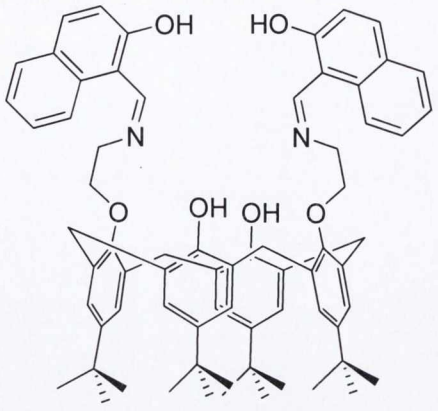


Figure 2.43 Fluorescence spectrum of **111** in the presence of various metal ions in 0.1 M HEPES buffer at pH 7 (λ_{exc}=300 nm).[41]

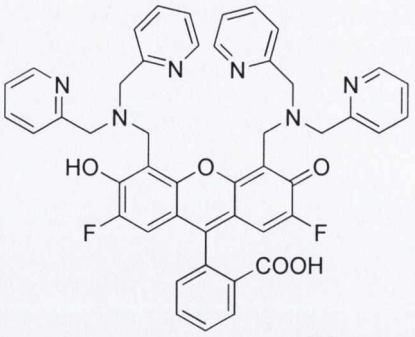


112

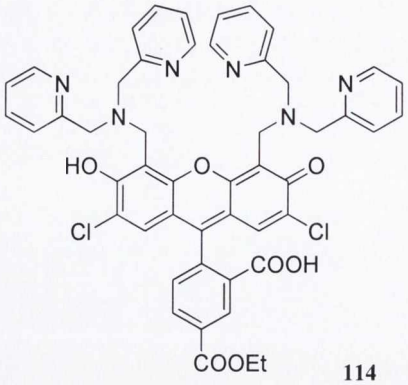
Scheme 2.11 Selective zinc (II) sensor synthesized by Dessingou and co-workers.

Dessingou and co-workers reported on the synthesis and the selective fluorescence enhancement caused by the binding with zinc of compound **112** (scheme 2.11) that incorporate in its calyx[4]arene ring two N-(2-hydroxynaphthyl-1-methylimine units as additional binding sites. Fluorescence of the naphthyl units are quenched by photoinduced electron transfer from the electron rich methylimines. Upon addition of zinc(II) the fluorescence intensity underwent a dramatic increase due to caging of the cation in the calixarene cavity and additional coordination by the two hydroxy groups and the two methylimine units. Thus, the lone pairs in the latter are involved in the metal chelation and cannot produce the PET effect anymore. No fluorescence enhancement was observed after the addition of Ti^{4+}, VO^{2+}, Cr^{3+}, Mn^{2+}, Fe^{2+}, Co^{2+}, Ni^{2+}, Cu^{2+}, Mg^{2+}, Cd^{2+} and Hg^{2+}.[42]

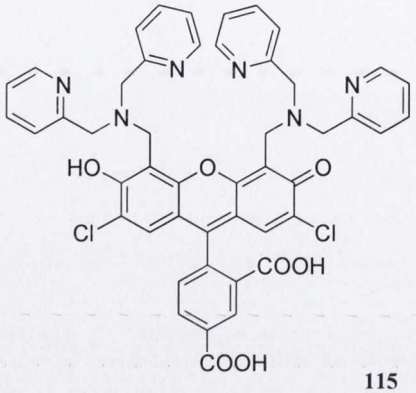
Lippard and his collaborators delved into studying zinc detection and developed numerous fluorescent probes which are at the same time non toxic, water soluble, and highly selective for this metal in *in vivo* studies. Few examples will be reported hereafter (scheme 2.12). Most of these probes are PET (photoinduced electron transfer) based system with fluorescein units functionalized with suitable binding sites that are electron donor and quench the fluorescein emission when they are not ligating zinc (II). Upon binding, the fluorescein emission undergoes dramatic enhancement whose entity depends on the whole molecular structures and substituents present on its skeleton. Compound **113**, which bears two DPA (di(2-picolyl)amine) receptor sites and it is



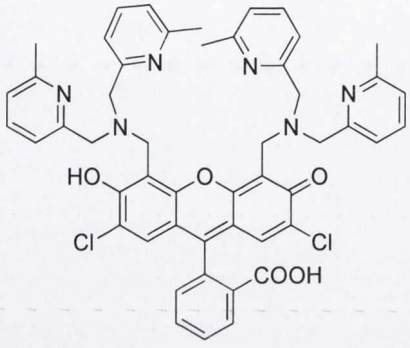
113



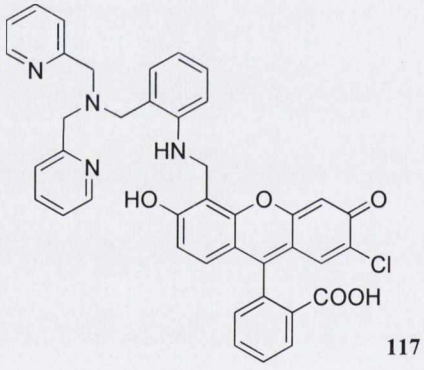
114



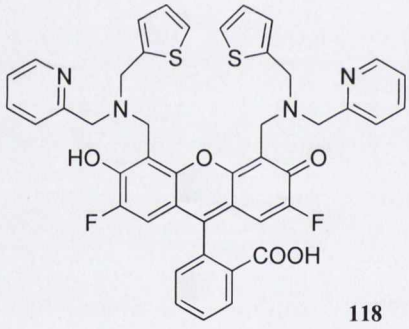
115



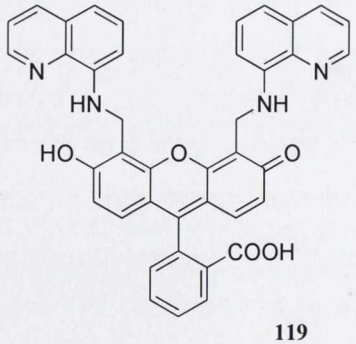
116



117



118



119

Scheme 2.12 Selective zinc (II) sensor synthesized by Lippard and co-workers.

fluorinated at 2' and 7'-positions of its fluorophore offers low background fluorescence with great enhancement upon ligation.[43] It was proven by X-Ray analysis that the two pyridine nitrogens and the hydroxy group on the fluorophore bind a zinc cation. The carboxy group on compound **114** impedes the internalization in cells because of its hydrophilic character. This feature allows the quantification of extracellular zinc (II) while the substitution with an ester group permits the cell membrane permeation of **115** followed by hydrolysis by esterases. Thus the quantification of intracellular levels of zinc (II) is achieved.[44] Methylation of pyr residues on the DPA receptors afforded structure **116** with high selectivity of Zn(II) over Fe(II).[45] The loss of one pyridinyl arm in both DPA units of compound **117** produced a dramatic increase of the fluorescence background with no fluorescence enhancement upon zinc ligation.[46] Substitution of pyr unit with the thiophene derivative **118** lowered the background fluorescence in concomitantly to a slight decrease for zinc affinity.[47] Quinoline containing derivative **119** affords 150 folds enhancement fluorescence upon zinc ligation with small interference with Ni (II) and Cu (II).[48]

2.4.23 A Novel Spiropyran Based Photoswitchable Zinc (II) Receptor

In all Lippard's molecules the zinc cation is caged between the three nitrogens of a DPA moiety and the hydroxy group located in close proximity, on the fluorophore skeleton. However, considering the interference with other metal ions that often affects zinc sensors,[48,49] the presence of a functional group with relatively low conformational flexibility would be desirable. In the light this, the choice of the substituent for our molecules was directed to a 2-methylpyridine. Thus, our sensor **SP13** should be able mimic the coordination observed in the DPA for some extent, with relatively higher rigidity that would overcome the problem of interference with other competitive cations. Additionally, binding process is expected to be controllable at will as the affinity for zinc can be modulated by irradiation with visible light. Analogue **SP12** was synthesized as a reference molecule[50] to evaluate the real effect of the methoxy group in driving the selectivity towards zinc (II).

2.4.24 Binding Studies

In order to establish whether the combination of the three functional groups were, in fact, capable of offering selective metal ion recognition, systematic binding studies were performed via UV-vis absorption spectroscopy on **SP12** and **SP13** with the same eleven metal ions utilized in the previous studies. The absorption spectra of SPs were taken before and after the addition of 1 equiv of each metal salt. The absorption spectrum of a colourless solution of **SP13** does not show bands in the visible region of the spectrum (black curve in figure 2.44). Upon addition of Zn(II) the colourless spiropyran switches to the orange merocyanine metal complex **MCZn13**. The appearance of an absorption band at 504 nm accompanies this process (grey curve in figure 2.44). This band disappears when the solution is irradiated with visible light, as **MCZn13** switches back

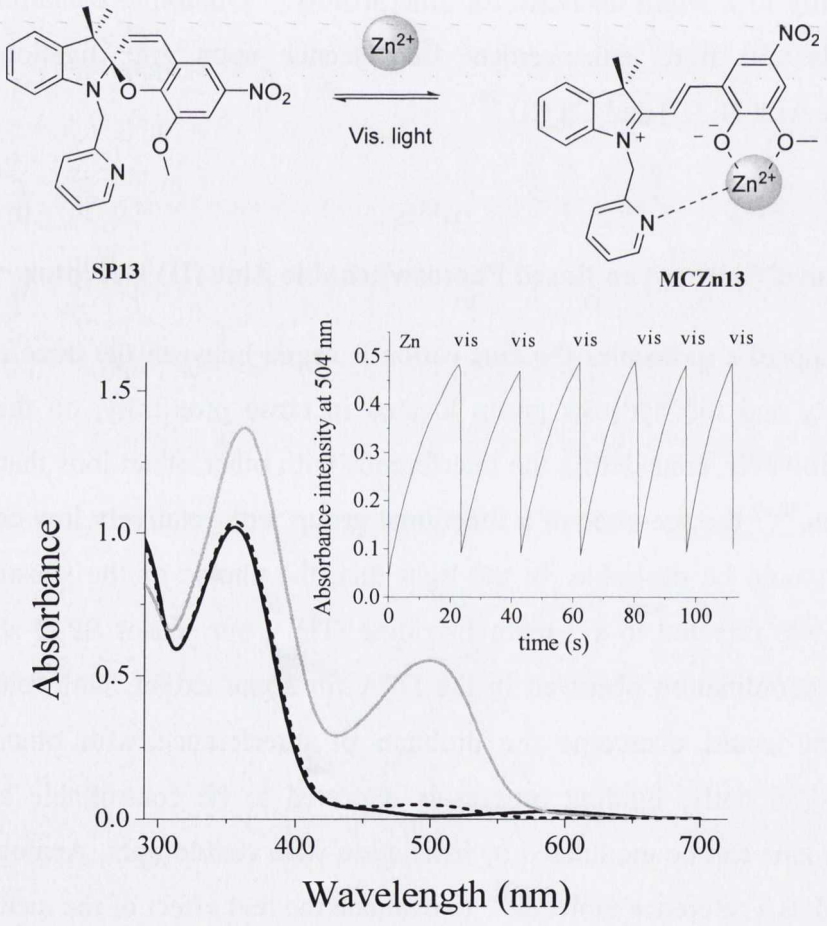


Figure 2.44 Reversible interconversion between the closed spiropyran **SP13** and a hypothetical merocyanine-zinc complex **MCZn13**. Absorption spectra of **SP13** ($1.0x10^{-4}$ M, acetonitrile, 293 K) (black line) before, (grey line) after the addition of 1 equiv of $Zn(ClO_4)_2$ and (dotted line) after the subsequent irradiation with visible light for 1 min; (Inset) sequential cycles of conversion between **SP13** and **MCZn13** controlled by visible light.

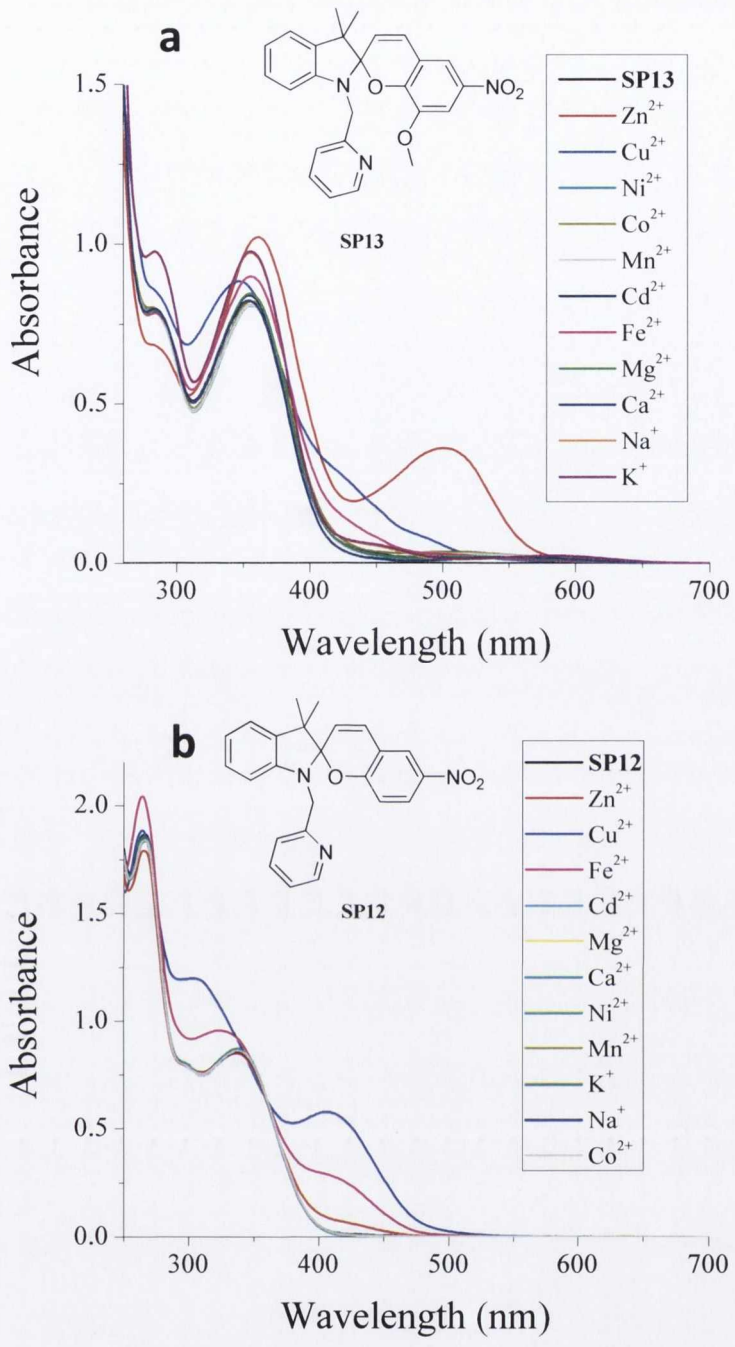


Figure 2.45 Absorption spectra of spiropyran **SP13** ($1.0x10^{-4}$ M, acetonitrile, 293 K) (**a**) and spiropyran **SP12** ($1.0x10^{-4}$ M, acetonitrile, 293 K) (**b**) after 20 min from the addition of 1 equiv of different metal perchlorates and chlorides.

to **SP13** (dotted curve in figure 2.44). Several cycles of irradiation were carried out confirming the reproducibility of the process as shown in the inset of figure 2.44.

No absorption changes were observed after the addition of other metal cations, such as Ni(II), Co(II), Mn(II), Cd(II), Mg(II), Ca(II), Na, K and only a shoulder appeared

around 400-460 nm after the addition of Cu(II), Fe(II) and Cr(III) (figure 2.45a). Particularly impressive is the selectivity to Zn(II) over Cd(II) since these cations may compete in the coordination and produce undesirable interference.[41,51] The same metal solutions were tested on the reference molecule **SP12**, which differs from **SP13** for the presence of a hydrogen instead of the methoxy group in 8'-position. As shown in figure 2.45b, **SP12** responded to the presence of iron (II), and copper (II) with intense bands in the range of 400-450 nm while the presence of zinc produced a negligible response. Additionally all the absorption bands in the presence of these metals are located in the same range making discrimination between the different cations impossible. Thus the choice of a methoxy group as an additional chelating site in **SP13** is confirmed. The absorbance intensities at 504 nm of a solution of **SP13** before and after the addition of the metal cations tested are reported in the histogram of figure 2.46. The ion selectivity can be quantified in terms of the relative responses based on the absorbance intensities. The ratio of the intensity of absorbance of Zn(II):Cu(II):Co(II):Cd(II):Cr(III) is 100:12:10:6:1.

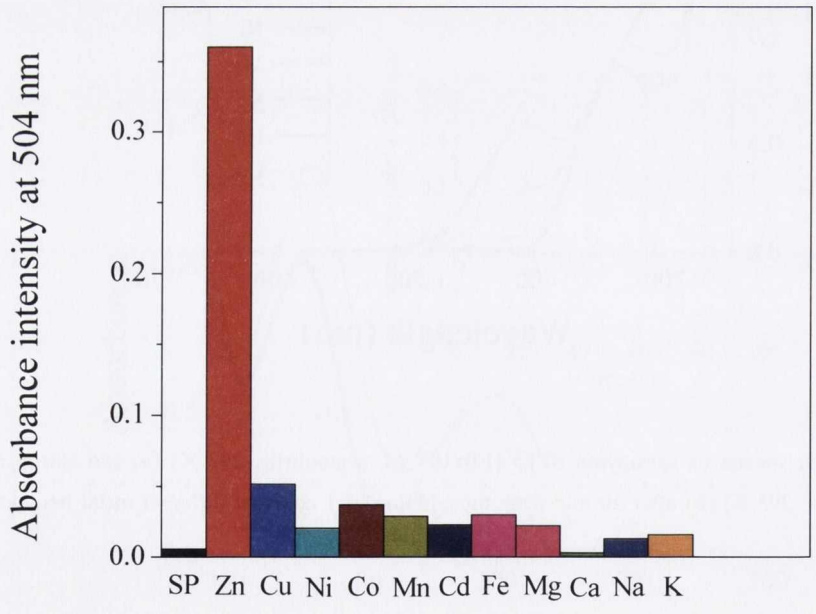


Figure 2.46 Absorption intensity at 504 nm of solutions of spiropyran **SP13** ($1.0x10^{-4}$ M, acetonitrile, 293 K) before and after the addition of 1 equiv of $Zn(ClO_4)_2$, $Cu(ClO_4)_2$, $Ni(ClO_4)_2$, $Co(ClO_4)_2$, $Mn(ClO4)_2$, $Cd(ClO_4)_2$, $Fe(ClO_4)_2$, $Mg(ClO4)2$, $CaCl_2$, NaCl and KCl.

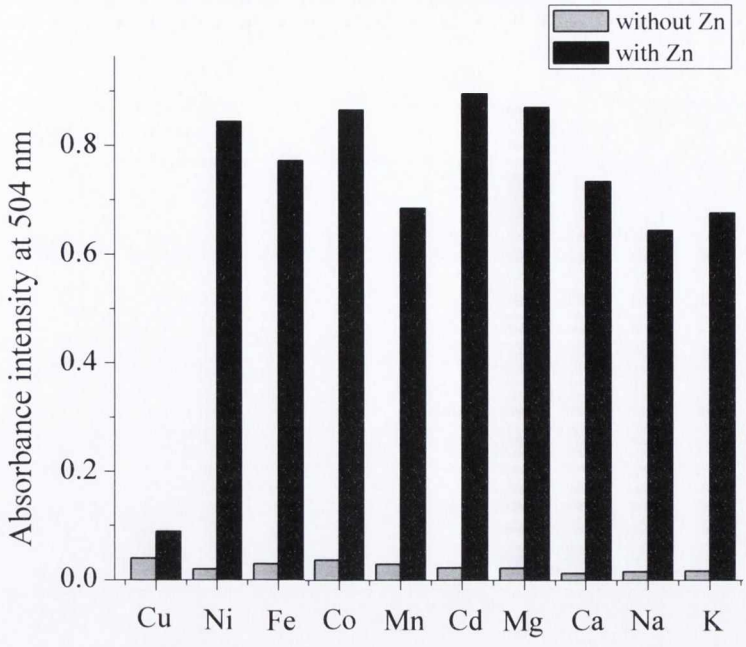


Figure 2.47 Absorbance intensity responses of **SP13** ($1.0x10^{-4}$ M, acetonitrile, 293 K) to various metal ion. Grey bars represent the absorption of **SP13** at 504 nm in the presence of 1 equiv of a selected metal ion. Black bars represent the absorption of **SP13** at 504 nm in the presence of a binary mixture of Zn(II) and a competitive metal ion (1 equiv each).

To further probe the selectivity of **SP13** we also examined the response of our sensor when presented with two different metal ions simultaneously. Eleven such experiments were carried out, and the results are displayed in figure 2.47. The observed absorption intensities of the binary mixtures at 504 nm, indicative of the presence of a **MCZn13** complex, range between 0.6 and 0.8 a.u. while no absorption is observed at the same wavelength in the absence of zinc. In ten of the eleven competitive experiments, **SP13** displays a strong preference for Zn(II) ions, and the only anomalous result was obtained when the **SP13** was presented with a solution containing a mixture of Zn(II) and Cu(II). It is not clear, at this point, what the reason is for the solution behaviour of **SP13** in the latter case, but we are currently carrying out an in-depth study (involving both solution- and solid-state based techniques) in order to elucidate the exact nature of the binding (stoichiometry, binding strength, possible kinetic factors), which may shed more light on this result. Overall, however, it is clear that the **SP13** sensor presented herein, is very effective at distinguishing between Zn(II) and a large number of other, potentially competing metal ions.

2.4.25 Emission Studies

The emission spectra of **SP13** were taken before and after the addition of 1 equivalents of Zn(II), Cu(II), and Fe(II). Only the complex **MCZn13** shows an intense band at 624 nm figure 2.48, while no emission was observed in all other cases.

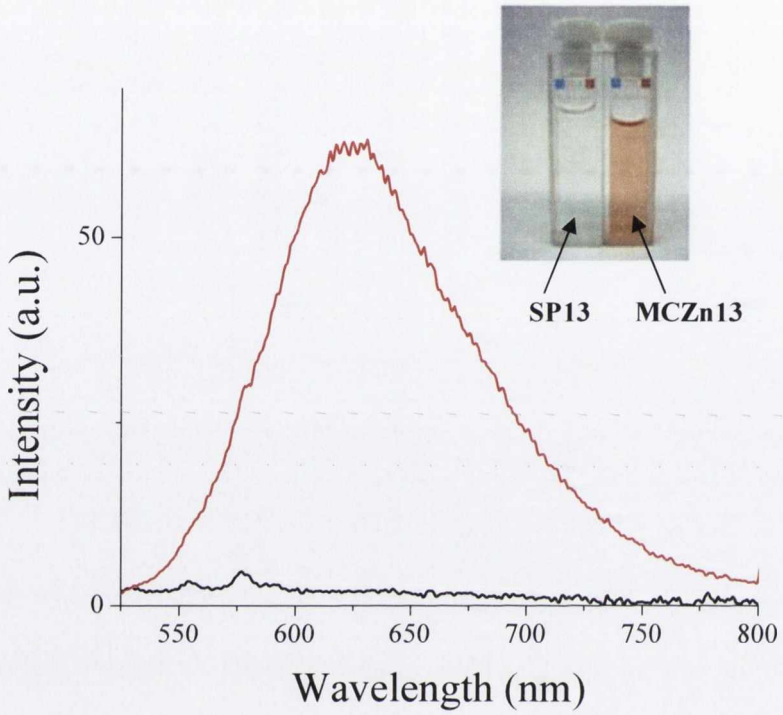


Figure 2.48 Emission spectra of a solution of **SP13** ($1.0x10^{-5}$ M, acetonitrile, 293 K, λ_{exc}=492 nm) before (black) and after the addition of 1 equiv of $Zn(ClO_4)_2$ (red). The picture shows the spiropyran solutions in the absence and in the presence of zinc.

The dependence of the absorbance on the concentration of metal salt was examined to investigate the composition of the complex **MCZn13**. The absorbance at 504 nm reached a plateau when an equivalent amount of Zn(II) was added to a solution of **SP13** (figure 2.49). This suggested a stoichiometry for the zinc-spiropyran complex of 1:1. In order to confirm this result, the composition of the complex was determined spectrophotometrically by means of the isomolar solutions technique (Job's method of continuous variations). The plot of the absorbance values measured at the absorption maximum of the complex **MCZn13** versus the zinc molar ratio of isomolar solutions is featured in the inset of figure 8. As shown, the apex is located at a zinc molar ratio of 0.5, which corresponds to a spiropyran-metal stoichiometry of 1:1.

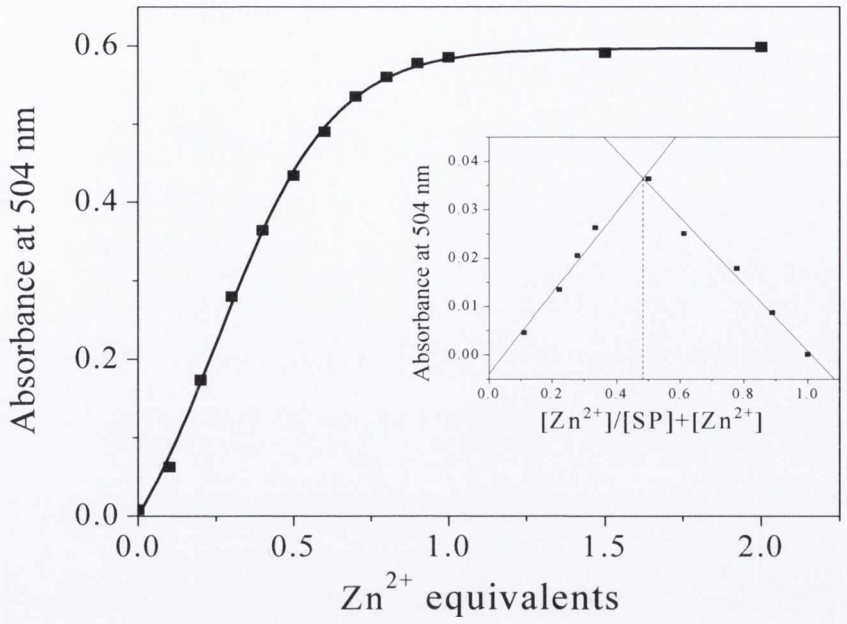


Figure 2.49 Absorption intensities at 504 nm of a solution of spiropyran **SP13** ($1.0x10^{-4}$ M, acetonitrile, 293 K) after increasing the concentration of $Zn(ClO_4)_2$; (Inset) Job's analysis of **MCZn13** complex ($[SP]+[Zn^{2+}] = 3.0x10^{-5}$ M, acetonitrile, 293 K).

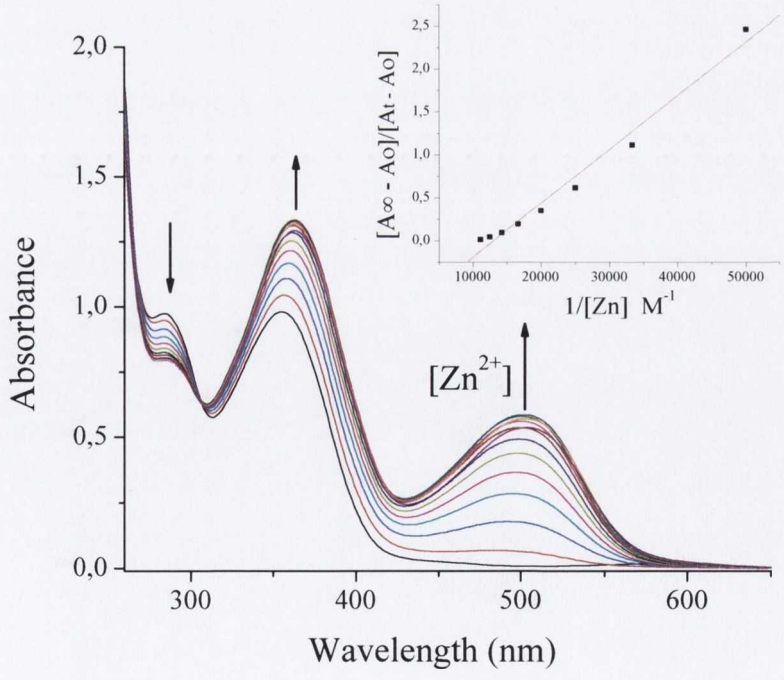


Figure 2.50 The absorption spectra of a solution of **SP13** ($1.0x10^{-4}$ M, acetonitrile, 293 K) after 20 minutes from the addition of 0.1, 0.2, 0.3, 0.4, 0.5, 0.6, 0.7, 0.8, 0.9, 1, 1.5, 2 equivalent of $(Zn(ClO_4)_2$; (Inset) Plot of $(A_\infty - A_x)/(A_x - A_0)$ against 1/[C], binding constant $k = 1.6x10^4$ M^{-1}.

The binding constant *k* value for the **MCZn13** complex was determined from the absorbance intensities recorded at different zinc concentrations (figure 2.50) following the modified Benesi-Hildebrand equation $1/\Delta A = 1\Delta A_{max} + (1/k[C])(1/\Delta A_{max})$. Here $\Delta A = A_x - A_0$ and $\Delta A_{max} = A_\infty - A_0$ where A_0, A_x and A_∞ are the intensities of the SP-Zn complex at 504 nm considered in the absence of zinc, at a certain concentration of zinc and at a concentration of complete interaction respectively; *k* is the binding constant and [C] is the concentration of zinc. The *k* value of 1.6×10^4 M^{-1} was extrapolated from the slope of the plot $(A_\infty - A_x)/ (A_x - A_0)$ against 1/[C] shown in the inset of figure 2.50.

2.4.26 ^{1}H-NMR Studies

^{1}H-NMR studies of the complexation of Zn(II) by **SP13** suggested that all three components of the phenoxy-methoxy-pyridine triad participated in metal binding (figure 2.51). The ^{1}H-NMR spectrum of spiropyran **SP13** (**SP13**in figure 2.51) changed dramatically after the addition of 1 equivalent of zinc (**MCZn13** in figure 2.51). The characteristic signals for the pyridyl protons (n) and (l) shifted significantly downfield, from 7.67 ppm and 8.48 ppm to 7.91 ppm (n') and 8.87 ppm (l') respectively due to the opening of the molecule and the formation of the complex. Additionally, the appearance of a new series of peaks in the range of 7.5-7.8 ppm was attributed to the aromatic protons of the **MCZn13** complex (See Table 2.3). The singlet of the methoxy group in 8'-position at 3.80 ppm (f) ppm shifted to 3.68 ppm and a new singlet appeared for the methoxy group of the complex form at 3.54 ppm (f') This new signal is quite broad suggesting coordination with the metal. The typical singlets attributed to the *gem*-methyl groups (a) in the closed form were located at 1.26 ppm and 1.32 ppm. In the metal complex they are magnetically equivalent due to the *quasi* planar structure of the merocyanine and they appear as a singlet at 1.84 ppm (a'). The doublet for one of the olefinic protons of *trans*-**MCZn13** can be identified at 8.29 ppm (c'). Its large coupling constant (J=16 Hz) confirms the trans configuration of the associated double bond. The ratio between **SP13** and the **MCZn13** complex is ca. 60:40 after the addition 1 equivalent of $ZnCl_2$.

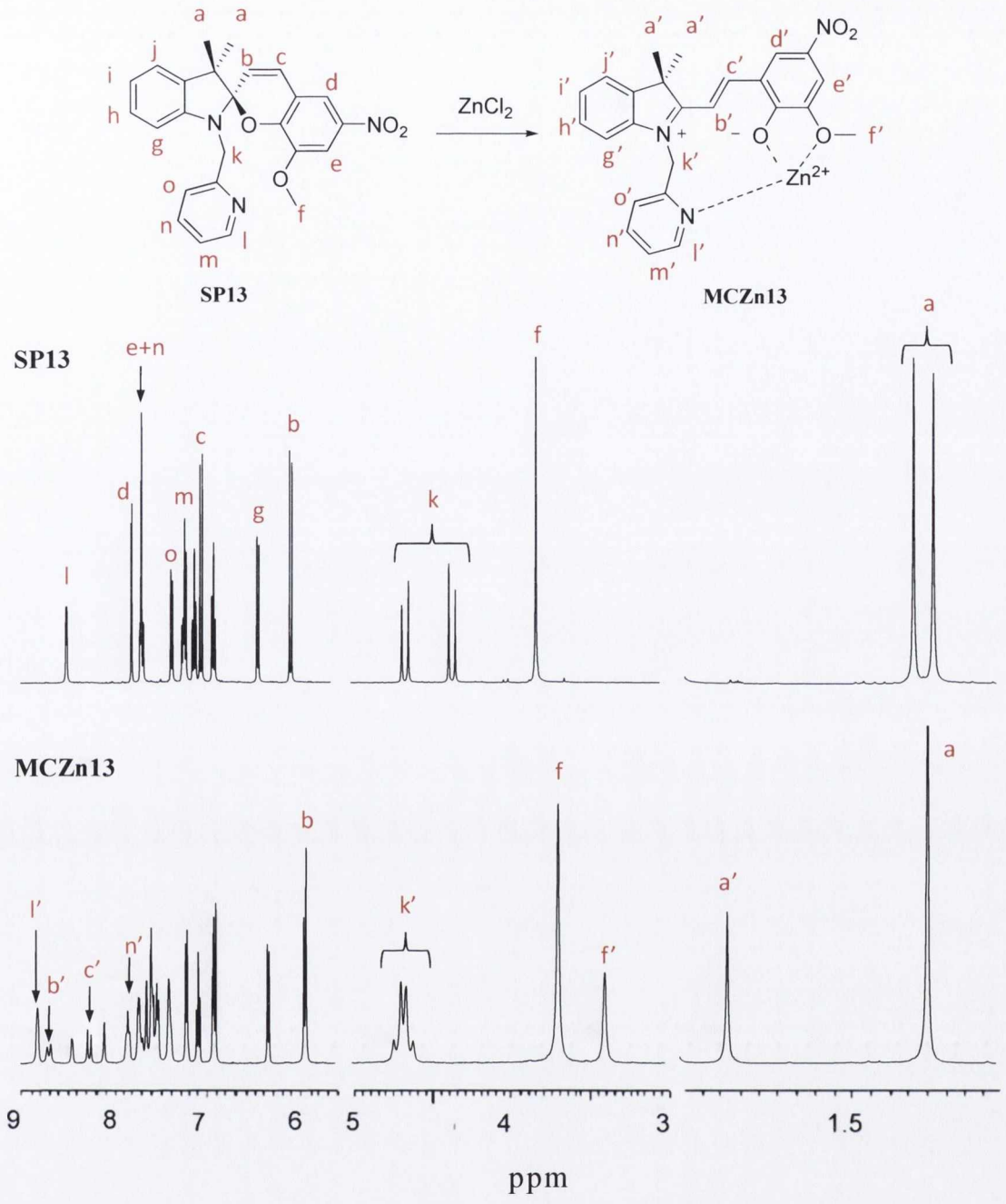


Figure 2.51 ^{1}H-NMR partial spectra of 1 ($2x10^{-2}$ M in acetonitrile, 293 K) prior to (**SP13**) and after the addition of 1 eq of $ZnCl_2$ (**MCZn13**).

2.4.27 Conclusions on Group 4

Although the Job's analysis suggests that there is a 1:1 metal ion/spiropyran stoichiometry in solution, it is not possible at this stage to determine if the complex is mono or polynuclear. It is possible that the phenolate-methoxy site acts as a chelate for one metal ion, whereas the pyridine moiety binds to a neighbouring metal ion.

SP13					MCZn13				
protons	δ (ppm)	no. of protons	multiplicity	*J* (Hz)	protons	δ (ppm)	no. of protons	multiplicity	*J* (Hz)
a	1.26 and 1.32	6	s		a'	1.84	3	s	
b	6.03	1	d	10.36	b'	8.62	1	d	15.4
c	7.01	1	d	10.36	c'	8.29	1	d	16
d	7.77	1	d	2.56	d'	8.16	1	s	
e	7.68	1	d	2.6	e'	7.48	1	s	
f	3.8	3	s		f'	3.54	3	s	
g	6.4	1	d	7.8	g'	7.8-7.5	1	m	
h	7.09	1	td	7.6 and 1.2	h'	7.8-7.5	1	m	
i	6.88	1	t	7.3	i'	7.8-7.5	1	m	
j	7.21	1	d	7.6	j'	7.8-7.5	1	m	
k	4.34 and 4.64	2	d	16.96 and 17	k'	5.88	2	s	
l	8.48	1	d	4.8	l'	8.87	1	d	4.76
m	7.19	1	m		m'	7.46	1	t	6.08
n	7.67	1	ddd	5.04 and 1.8	n'	7.91	1	t	7.6
o	7.33	1	d	8	o'	7.5-7.7	1	m	

Table 2.3 ^{1}H-NMR spectroscopy data (400 MHz, CD_3CN, 298 K) for **SP13** before (**SP13**) and after the aditon in mixture with **MCZn13** (1 equiv of Zn)

Nevertheless, the nature and the orientation of the three binding sites have created a ligand that offers an effective complement to the requirements of Zn(II) ions.

Reference List

(1) Shao, N.; Zhang, Y.; Cheung, S. M.; Yang, R. H.; Chan, W. H.; Mo, T.; Li, K. A.; Liu, F. *Analytical Chemistry* **2005**, *77*, 7294-7303.

(2) Shao, N.; Gao, X.; Wang, H.; Yang, R. H.; Chan, W. H. *Analytica Chimica Acta* **2009**, *655*, 1-7.

(3) Chibisov, A. K.; Gorner, H. *Chemical Physics* **1998**, *237*, 425-442.

(4) Gorner, H.; Chibisov, A. K. *Journal of the Chemical Society-Faraday Transactions* **1998**, *94*, 2557-2564.

(5) Gorner, H.; Atabekyan, L. S.; Chibisov, A. K. *Chemical Physics Letters* **1996**, *260*, 59-64.

(6) Chibisov, A. K.; Gorner, H. *Physical Chemistry Chemical Physics* **2001**, *3*, 424-431.

(7) Keum, S. R.; Lee, K. B.; Kazmaier, P. M.; Buncel, E. *Tetrahedron Letters* **1994**, *35*, 1015-1018.

(8) Swansburg, S.; Buncel, E.; Lemieux, R. P. *Journal of the American Chemical Society* **2000**, *122*, 6594-6600.

(9) Shao, N.; Jin, J. Y.; Cheung, S. M.; Yang, R. H.; Chan, W. H.; Mo, T. *Angewandte Chemie-International Edition* **2006**, *45*, 4944-4948.

(10) Shao, N.; Jin, J. Y.; Wang, H.; Zhang, Y.; Yang, R. H.; Chan, W. H. *Analytical Chemistry* **2008**, *80*, 3466-3475.

(11) Scherer, D.; Dorfler, R.; Feldner, A.; Vogtmann, T.; Schwoerer, M.; Lawrentz, U.; Grahn, W.; Lambert, C. *Chemical Physics* **2002**, *279*, 179-207.

(12) Raymo, F. M.; Giordani, S. *Journal of the American Chemical Society* **2001**, *123*, 4651-4652.

(13) Raymo, F. M.; Giordani, S.; White, A. J. P.; Williams, D. J. *Journal of Organic Chemistry* **2003**, *68*, 4158-4169.

(14) Wojtyk, J. T. C.; Wasey, A.; Xiao, N. N.; Kazmaier, P. M.; Hoz, S.; Yu, C.; Lemieux, R. P.; Buncel, E. *Journal of Physical Chemistry A* **2007**, *111*, 2511-2516.

(15) Shiraishi, Y.; Adachi, K.; Itoh, M.; Hirai, T. *Organic Letters* **2009**, *11*, 3482-3485.

(16) Shao, N.; Wang, H.; Gao, X. D.; Yang, R. H.; Chan, W. H. *Analytical Chemistry* **2010**, *82*, 4628-4636.

(17) Stauffer, M. T.; Weber, S. G. *Analytical Chemistry* **1999**, *71*, 1146-1151.

(18) Salhin, A. M. A.; Tanaka, M.; Kamada, K.; Ando, H.; Ikeda, T.; Shibutani, Y.; Yajima, S.; Nakamura, M.; Kimura, K. *European Journal of Organic Chemistry* **2002**, 655-662.

(19) Chernyshev, A. V.; Metelitsa, A. V.; Gaeva, E. B.; Voloshin, N. A.; Borodkin, G. S.; Minkin, V. I. *Journal of Physical Organic Chemistry* **2007**, *20*, 908-916.

(20) Yagi, S.; Nakamura, S.; Watanabe, D.; Nakazumi, H. *Dyes and Pigments* **2009**, *80*, 98-105.

(21) Benesi, H. A.; Hildebrand, J. H. *Journal of the American Chemical Society* **1949**, *71*, 2703-2707.

(22) Nakamura, M.; Takahashi, K.; Fujioka, T.; Kado, S.; Sakamoto, H.; Kimura, K. *Journal of the American Society for Mass Spectrometry* **2003**, *14*, 1110-1115.

(23) Nakamura, M.; Fujioka, T.; Sakamoto, H.; Kimura, K. *New Journal of Chemistry* **2002**, *26*, 554-559.

(24) Kimura, K.; Sakamoto, H.; Kado, S.; Arakawa, R.; Yokoyama, M. *Analyst* **2000**, *125*, 1091-1095.
(25) Quach, T. D.; Batey, R. A. *Organic Letters* **2003**, *5*, 4397-4400.
(26) Quach, T. D.; Batey, R. A. *Organic Letters* **2003**, *5*, 1381-1384.
(27) Kantam, M. L.; Venkanna, G. T.; Sridhar, C.; Sreedhar, B.; Choudary, B. M. *Journal of Organic Chemistry* **2006**, *71*, 9522-9524.
(28) Evans, D. A.; Katz, J. L.; West, T. R. *Tetrahedron Letters* **1998**, *39*, 2937-2940.
(29) Chan, D. M. T.; Monaco, K. L.; Wang, R. P.; Winters, M. P. *Tetrahedron Letters* **1998**, *39*, 2933-2936.
(30) Gonzalez, I.; Mosquera, J.; Guerrero, C.; Rodriguez, R.; Cruces, J. *Organic Letters* **2009**, *11*, 1677-1680.
(31) Sreedhar, B.; Venkanna, G. T.; Kumar, K. B. S.; Balasubrahmanyarn, V. *Synthesis-Stuttgart* **2008**, 795-799.
(32) Lam, P. Y. S.; Clark, C. G.; Saubern, S.; Adams, J.; Winters, M. P.; Chan, D. M. T.; Combs, A. *Tetrahedron Letters* **1998**, *39*, 2941-2944.
(33) Hugel, H. M.; Rix, C. J.; Fleck, K. *Synlett* **2006**, 2290-2292.
(34) Fanta, P. E. *Chemical Reviews* **1946**, *38*, 139-196.
(35) Fanta, P. E. *Chemical Reviews* **1964**, *64*, 613-632.
(36) Pragst, F.; Ziebig, R.; Kunze, J.; Jugelt, W.; Krause, M. *Zeitschrift Fur Physikalische Chemie-Leipzig* **1976**, *257*, 465-481.
(37) Trumbo, P.; Yates, A. A.; Schlicker, S.; Poos, M. *Journal of the American Dietetic Association* **2001**, *101*, 294-301.
(38) Fosmire, G. J. *American Journal of Clinical Nutrition* **1990**, *51*, 225-227.
(39) Ronald, E. *"Zinc Hazard to Fish, Wildlife and Invertebrates: A Synoptic Review"* **1993**, Contaminant Hazard Reviews; U.S. Department of the Interior, Fish and Wildlife Service: Laurel, Maryland.
(40) Parkesh, R.; Lee, T. C.; Gunnlaugsson, T. *Organic & Biomolecular Chemistry* **2007**, *5*, 310-317.
(41) Ngwendson, J. N.; Banerjee, A. *Tetrahedron Letters* **2007**, *48*, 7316-7319.
(42) Dessingou, J.; Joseph, R.; Rao, C. P. *Tetrahedron Letters* **2005**, *46*, 7967-7971.
(43) Chang, C. J.; Nolan, E. M.; Jaworski, J.; Burdette, S. C.; Sheng, M.; Lippard, S. J. *Chemistry & Biology* **2004**, *11*, 203-210.
(44) Woodroofe, C. C.; Masalha, R.; Barnes, K. R.; Frederickson, C. J.; Lippard, S. J. *Chemistry & Biology* **2004**, *11*, 1659-1666.
(45) Goldsmith, C. R.; Lippard, S. J. *Inorganic Chemistry* **2006**, *45*, 555-561.
(46) Burdette, S. C.; Frederickson, C. J.; Bu, W. M.; Lippard, S. J. *Journal of the American Chemical Society* **2003**, *125*, 1778-1787.
(47) Nolan, E. M.; Ryu, J. W.; Jaworski, J.; Feazell, R. P.; Sheng, M.; Lippard, S. J. *Journal of the American Chemical Society* **2006**, *128*, 15517-15528.
(48) Nolan, E. M.; Jaworski, J.; Okamoto, K. I.; Hayashi, Y.; Sheng, M.; Lippard, S. J. *Journal of the American Chemical Society* **2005**, *127*, 16812-16823.
(49) Gholivand, M. B.; Mozaffari, Y. *Talanta* **2003**, *59*, 399-407.
(50) Ren, J. Q.; Tian, H. *Sensors* **2007**, *7*, 3166-3178.
(51) Xue, L.; Liu, C.; Jiang, H. *Organic Letters* **2009**, *11*, 1655-1658.

CHAPTER 3

CONCLUSIONS AND FUTURE WORK

3.1 Conclusions

In this project we synthesized novel spiropyrans and explored the possibilities of using already known compounds as potential ion sensors. Indeed, we synthesized and studied the interaction with biologically important monovalent and bivalent cations of thirteen spiropyrans. The most important achievements in these studies have been the following:

- we have synthesized and characterized the first spiropyran-based photoreversible zinc (II) selective sensor;
- we have evaluated the counter ion effects on the metal binding;
- we have obtained one of the very few spiropyran-metal crystal structure reported so far in literature;
- we have reported the first copper (II) mediated oxidative cross-coupling causing the dimerization of spiropyrans in extremely mild conditions.

3.2 Future Work

Locklin and co-workers reported in 2008 the synthesis of MMA based photochromic polymers attached to glass supports.[1] The photochromic properties were given by spiropyrans attached to the MMA chains which could cause dramatic changes in the glass wettability after irradiation with UV light. These changes were reversible upon irradiation with visible light. Interestingly they observed that the glass colour was susceptible to change when the same supports were dipped into solutions containing bivalent cations. These changes reflected the reversible formation of spiropyran-cation complexes where the metal release could be actuated *via* irradiation with a visible light source. Although no selectivity to a particular cation was claimed, this approach is the basis for developing analytical tools for detecting metal ions in solution, overcoming the limitations of one-time use sensors.

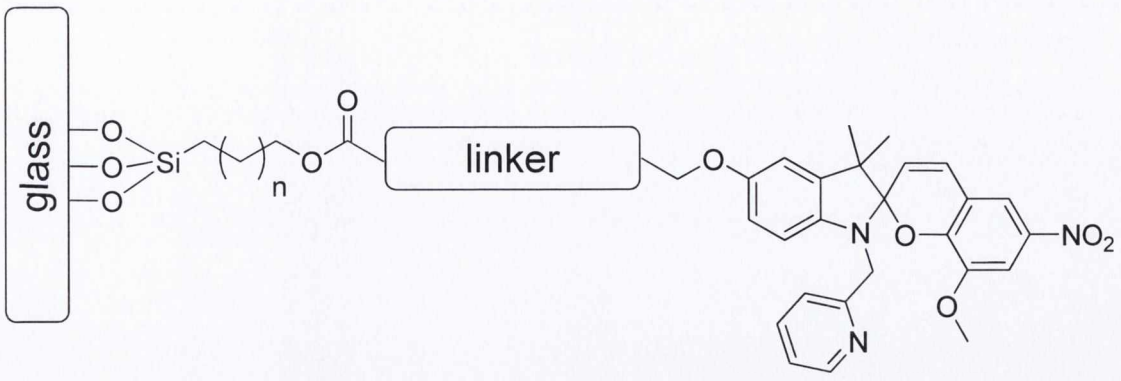


Figure 3.1 Schematic representation of the deepstick constituents.

Our idea is to use the same approach in order to develop dipsticks as useful and practical tools for the detection of zinc (II) in solution. These tools may contain three different parts as shown in figure 3.1, namely a glass support, a linker, and a zinc (II) selective spiropyran. It is important that the molecular switch retains its binding capability, hence the linker should be attached for instance *via* ether bond to the spiropyran 5-position. This should guarantee its ionochromic properties. The linker should be of an appropriate length and chemically compatible with both glass and spiropyran in order to permit the interaction between sensor and metal. Glass is a good support since it is inert and easily functionalized. Such a system would offer several advantages:

- the detection can be conducted at the location where the sample is collected or, for environmental monitoring purposes, where the sample is found;
- since the metal presence is detected also by naked eye, there is no need of sophisticated technical support;
- the solutions containing zinc (II) ions will result in the colour change of the solid support where the presence of intense colour will indicate high level of the analyte and a faint colour will indicate lower concentrations of it.

Overall, we believe that this research should contribute to further development of new versatile and reversible metal receptors that may find potential applications in metal sensing.

Reference List

(1) Fries, K.; Samanta, S.; Orski, S.; Locklin, J. *Chemical Communications* **2008**, 6288-6290.

CHAPTER 4

EXPERIMENTAL

4.1 General

Chemicals were purchased from Acros Organics or Aldrich and were used as received. Chloroform was distilled over CaH_2. Otherwise stated, all chemicals were obtained from commercial sources and used as received. All melting points were determined with a Stuart SMP3 instrument. Infrared spectra were obtained on a Perkin Elmer Paragon 1000 Fourier Transform spectrometer. Flash chromatography was carried out using silica gel, particle size 0.04-0.063 mm. TLC analysis was performed on precoated $60F_{254}$ slides, and visualised by either UV irradiation or $KMnO_4$ staining.

4.2 UV-vis Absorption and Emission Studies

UV-Vis absorption measurement were carried out with a Perkin Elmer Lambda 35 UV-Vis Spectrometer. The spiropyrans solutions of concentration $1x10^{-4}$ M were prepared by dilution starting from mother solutions of spiropyrans $1x10^{-3}$ M in spectroscopic grade methanol and acetonitrile. The trifluoroacetic acid and triethylamine solutions were prepared in water and they had concentration of $1x10^{-2}$ M. The metal perchlorates and chlorides solutions were prepared in distilled water and they had a concentration of $1x10^{-2}$ M. Quartz cuvettes of 1 cm path length were used. The solutions were irradiated in custom built cabinet by means of a UVGL-58 Handheld UV Lamp at 254 nm and a Schott KL 1500 LCD visible lamp.

In the UV-vis absorption studies on the protonation, 1 ml of spiropyran solutions were placed in a quartz cuvette of 1 cm path length and 1 μl (1 eq) of either trifluoroacetic acid or triethylamine solutions were added by means of a micropipette.

In the UV-vis absorption studies on the complexation, 1 ml of spiropyran solutions were placed in a quartz cuvette of 1 cm path length and 1 μl (1 eq) of the metal solutions was added by means of a micropipette.

In the experiments of sequential cycles of conversion between spiropyrans and their metal complexes controlled by visible light the solutions were irradiated by means of the visible light source when they reached the thermal equilibrium.

In the emission studies standard solution of spiropyrans ($1.0x10^{-5}$ M) in spectroscopic grade acetonitrile were prepared and equilibrated overnight at 293 K in the dark. The spiropyran solutions (3 ml) was placed into a 1 cm path length cuvette and the emission spectra were recorded; 1 equivalent (3 μl) of standard solutions of metal perchlorates ($1.0x10^{-3}$ M) were added and the resulting solutions were equilibrated in the dark for 20 min and the emission spectra were taken.

4.3 ^{1}H-NMR studies

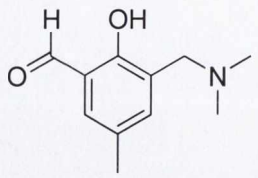
Proton Nuclear Magnetic Resonance spectra were recorded on a Bruker DPX 400 MHz spectrometer in $CDCl_3$, CD_3CN and d-DMSO. All the solvents were standardised with respect to TMS. Chemical shifts are reported in ppm and coupling constants in Hertz. Carbon NMR spectra were recorded Bruker DPX 100 MHz with total proton decoupling. Standard solutions of zinc chloride (2 M) were prepared in D_2O. An aliquot of this solution (10 μl) was added to 800 μl of spiropyran solution $2x10^{-2}$ M in CD_3CN. The samples were stored in the dark for 24 h and the spectra were collected.

4.4 Mass Spectrometry

MALDI-TOF MS spectra were acquired with a Waters MALDI-Q TOF Premier spectrometer. The instrument was operated in positive reflectron mode. The matrix used in the experiments was *trans*-2[3(4-*tert*-Butylphenyl)-2-methyl-2-propenylidene]malononitrile dissolved in DCM (2 mg/ml). Acetonitrile solution of the complexes were prepared by adding 10 μl of a $1x10^{-1}$ M solution of the desired metal chloride or perchlorate to a $1x10^{-3}$M solution of spiropyrans. The resulting mixtures were equilibrated overnight at 20°C in the dark. Matrix solutions were mixed with complex solutions with ratio 1:1 and 1 μl of the resulting mixture was spotted on the MALDI plate. The compound [Glu^{1}] Fibrinopeptide B, 1570.6774 m/z $(M+H)^{+}$ was used as reference.

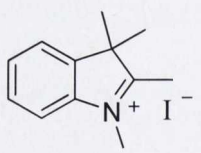
4.5 Compounds

3-((Dimethylamino)methyl)-2-hydroxy-5-methylbenzaldehyde (99)



To a suspension containing 400 mg (2.94 mmol) of 5-methylsalicylaldehyde and 0.358 ml (4.41 mmol) of formaldehyde (37% solution in H_2O) in 20 ml of absolute ethanol, 0.4 ml (4.41 mmol) of dimethylamine (solution 60% in H_2O) were added. The reaction was carried out for 48h and the solution was then concentrated and the residue was dissolved in dichloromethane and dried over Na_2SO_4. The product was purified via flash chromatography using a mixture of DCM/MeOH 9:1. 453 mg of a yellow oil were obtained, yield 80%. **^{1}H-NMR** (400 MHz, $CDCl_3$): δ = 2.29 (s, 3H, CH_3), 2.36 (s, 6H, $(CH_3)_2$), 3.64 (s, 2H, CH_2), 7.11 (s, 1H, arom.), 7.44 (s, 1H, arom.), 10.32 (s,1H, CHO). **^{13}C-NMR** (100 MHz, $CDCl_3$): δ= 19.8 (CH_3), 44.2 (NCH_3), 44.3 (NCH_3), 60.4 (CH_2), 121.9, 123.6, 127.6,128.0, 135.9 (arom.), 159.1 (COH), 191.4 (CHO). **HRMS (*m/z* - ES) :** Found: 193.1108 ($(M+H)^+$, Requires: 193.1103).

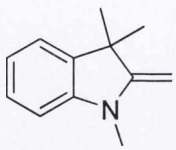
1,2,3,3-Tetramethyl-3H-indolium iodide (100)



A solution of 2,3,3-trimethylindolenine (1.6ml, 10 mmol) in 20 ml of CH_3I was stirred at 60°C under N_2 for 1h. The solution was then cooled to r.t. and a white precipitate was filtered off and washed with Et_2O to afford 2.45 gr of the product as a pink powder, yield = 81%. **^{1}H-NMR** (400 MHz, DMSO): δ= 1.52 (s, 6H, $(CH_3)_2$), 2.76 (s, 3H, CH_3), 3.91 (s, 3H, CH_3N), 7.58-7.66 (m, 2H, arom.), 7.82-7.86 (s, 1H, arom.), 7.88-7.94 (s, 1H, arom.). **^{13}C-NMR** (100 MHz, DMSO): δ= 14.0 (CH_3), 21.7 (CH_3), 34.6 (CH_3 salt), 53.9 ($C(CH_3)_2$), 115.7, 123.2, 128.8, 129.3, 141.6, 142.1, (arom.), 195.9 (C=N). **HRMS**

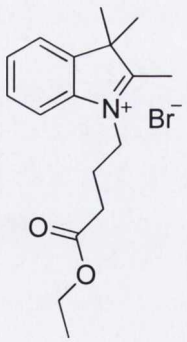
(*m/z* -ES) : Found: 300.0261 ($(M+H)^+$, Requires: 300.0249). **υ (cm^{-1}) :** 3025, 1695, 1510, 1465, 1202, 991. **mp :** 258 °C.

1,3,3-Trimethyl-2-methyleneindoline (101)



Compound **100** (729 mg, 2.12 mmol) was stirred in 40 ml of a 1:3 mixture of Et_2O/NaOH aq 2M for 30 minutes. The organic phase was collected, dried over Na_2SO_4 and the solvent was evaporated to afford 368 mg of a pink oil, yield = 71%. **^{1}H-NMR** (400 MHz, DMSO): δ= 1.37 (s, 6H, $(CH_3)_2$), 3.06 (s, 3H, CH_3N), 3.861 (s, 2H, ethylene), 6.56 (d, 1H, *J*=7.8 Hz, arom.), 6.78 (t, 1H, *J*=7.4 Hz, arom.), 7.12 (d, 1H, *J*=7.2 Hz, arom.), 7.15 (t, 1H, *J*=8.00 Hz, arom.), 7.28 (s, 1H, arom.). **^{13}C-NMR** (100 MHz, DMSO): δ= 28.3 (CH_3N), 29.5 (2 x CH_3), 43.6 ($C(CH_3)_2$), 72.5 (C ethylene), 104.4, 117.8, 121.3, 127.1, 137.1, 145.9 (arom.), 162.4 (C=CH_2). **HRMS (*m/z* -ES) :** Found: 174.1290 ($(M+H)^+$, Requires: 174.1283).

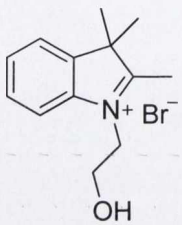
1-(4-Ethoxy-4-oxobutyl)-2,3,3-trimethyl-3H-indolium bromide (102)



A solution of 2,3,3-trimethylindolenine (8.49 mmol, 1.36 ml) and 4-bromobutyrate (12.7 mmol, 1.81 ml) in 20 ml of chloroform was stirred under reflux for 24h. The solution was cooled to room temperature and the solvent was then evaporated. To the purple residue 1 ml of methanol was added and the product was crystallized from 20-30 ml of diethyl ether affording 1.22 g of a pink powder, yield 43%. **^{1}H-NMR** (400 MHz, $CDCl_3$): δ= 1.19 (t, 3H, *J*=7.0 Hz, CH_3), 1.62 (s, 6H, $(CH_3)_2$), 2.21-2.27 (m, 2H, CH_2),

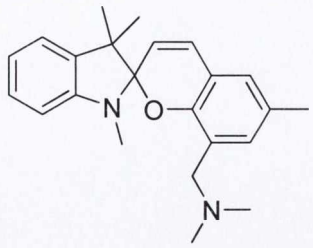
2.70 (t, 2H, J=5.8 Hz, CH_2), 3.17 (s, 3H, CH_3), 4.02 (q, 2H, J_1=7.6 Hz, J_2=14.6 Hz, CH_2), 4.86 (t, 2H, J=8.0 Hz, CH_2), 7.53-7.60 (m, 3H, arom.), 8.01-8.10 (m, 1H, arom.). **^{13}C-NMR** (100 MHz, $CDCl_3$): δ=13.6 (CH_3), 15.7 (CH_3), 22.2 (CH_2), 22.4, 22.6 ((CH_3)$_2$), 29.9 (CH_2), 48.0 (C(CH_3)$_2$), 54.1 (NCH_2), 60.5 (OCH_2CH_3),, 115.4, 122.6, 129.1, 129.5, 140.7, 141.1 (arom.), 172.3 (COOEt), 195.9 ($NCCH_3$). **HRMS (*m/z* -ES) :** Found: ((M^+-Br) 274.1810, $C_{17}H_{24}NO_2$ Requires: 274.1807). **υ (cm^{-1}) :** 2999, 1722, 1468, 1371, 1206, 768. **mp :** 187°C.

1-(2-Hydroxyethyl)-2,3,3-trimethyl-3H-indolium bromide (103)



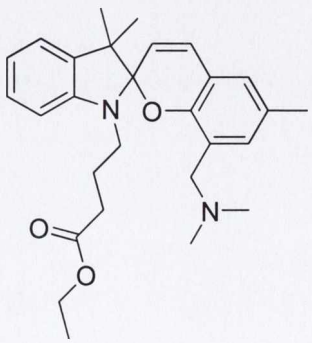
A solution of 2,3,3-trimethyl-3H-indole (1.40 g, 8.8 mmol) and 2-bromoethanol (1.37 g, 10.9 mmol) in MeCN (20 ml) was heated for 24 h under reflux and N_2. After cooling down to ambient temperature, the solvent was distilled off under reduced pressure. The residue was suspended in hexane (25 ml) and the mixture was sonicated and filtered. The resulting solid was crystallized from $CHCl_3$ (35 ml) to afford **1** (1.14 g, 46%) as a pink solid. **^{1}H-NMR** (400 MHz, CD_3CN): δ = 1.61 (6H, s, (CH_3)$_2$), 2.81 (3H, s, CH_3), 4.02–3.94 (2H, m, CH_2OH), 4.54 (2H, t, J=5.0 Hz, CH_2N), 4.82 (1H, t, J=6.0 Hz, OH), 7.65–7.54 (2H, m, arom.), 7.74–7.72 (1H, m, arom.), 7.83–7.75 (1H, m, arom.); **^{13}C-NMR** (100 MHz, CD_3CN): δ = 14.61 (CH_3), 21.93 (CH_3+CH_3), 50.86 (C(CH_3)$_2$), 54.67 (CH_2N), 57.80 (CH_2OH), 115.54, 123.33, 129.03, 129.71, 141.42, 141.99, 198.84 (arom.); **HRMS (*m/z* -ES)**: Found: ((M^+-Br) 204.1381, $C_{13}H_{18}NO$ Requires: 204.1388)**υ (cm^{-1}) :** 3251, 1611, 1606, 1465, 1093, 1058. **mp :** 195°C.

N,N-Dimethyl-1-(1',3',3',6-tetramethylspiro[chromene-2,2'-indoline]-8-yl)methanamine (SP1)



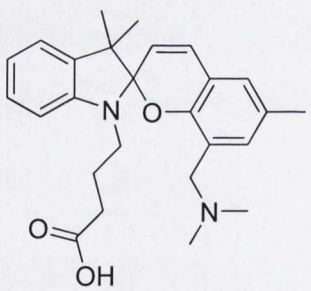
A solution containing compounds **101** (368 mg, 2.12 mmol) and **99** (410 mg, 2.12 mmol) were stirred in EtOH at reflux for 12h. The solution was concentrated at reduced pressure and the crude was purified via flash chromatography on silica gel using a mixture of ethyl acetate and diethyl ether 8:2. The product was obtained as a pink powder, 560 mg, yield=56%. **^{1}H-NMR** (400 MHz, $CDCl_3$): δ= 1.16 (s, 3H, CH_3), 1.28 (s, 3H, CH_3), 2.01 (s, 6H, $N(CH_3)_2$), 2.25 (s, 3H, CH_3 Ph), 2.65 (s, 3H, CH_3N), 5.77 (d, 1H, *J*=10.2 Hz, ethylene), 6.54 (d, 1H, *J*=7.7 Hz, arom.), 6.83 (t, 1H, *J*=7.4 Hz, arom.), 6.86 (s, 1H, arom.), 6.91 (d, 1H, *J*=10.2 Hz, ethylene), 7.11 (d, 1H, *J*=7.2 Hz, arom.), 7.17 (t, 1H, *J*=7.7 Hz, arom.). **^{13}C-NMR** (100 MHz, CD_3CN): δ= 20.3, 20.6 (CH_3), 26.0 (CH_3 arom.), 29.0 (NCH_3), 45.5 ($N(CH_3)_2$), 51.3 ($C(CH3)_2$), 55.9 (CH_2), 103.9 (C spiro.), 107.1, 118.5, 119.5, 119.7, 121.5, 124.6, 126.3, 127.8, 128.8, 130.3, 131.4, 136.9 (arom.), 148.9 (CNO_2), 149.8 (arom.). **HRMS (*m/z* -ES) :** Found: 349.2282 ($(M+H)^+$, $C_{23}H_{28}N_2O$ Requires: 349.2280). **υ (cm^{-1}) :** 2816, 1605, 1455, 1360, 1247, 927. **mp :** 70°C.

Ethyl 4-(8-((dimethylamino)methyl)-3',3'-dimethyl-6-nitrospiro[chromene-2,2'-indoline]-1'-yl)butanoate (SP2)



A solution containing 1.02 g (2.89 mmol) of **102** and 0.670 g (3.47 mmol) of 3-((dimethylamino)methyl) -2-hydroxy-5-methylbenzaldehyde **19** in 20 ml of absolute ethanol was refluxed for 24h. The solvent was removed under reduced pressure and the crude was purified by silica gel column chromatography using DCM/MeOH 9:1. A violet-purple oil was obtained, 1.1 g, yield 55%. **^{1}H-NMR** (400 MHz, $CDCl_3$): δ= 1.15, (s, 3H, CH_3), 1.20 (t, 3H, *J*= 7.1 Hz), 1.25, (s, 3H, CH_3), 1.87 (m, 2H, CH_2), 2.18-2.30 (m, 11H, $N(CH_3)_2$, CH_3 arom., CH_2), 3.10 (m, 2H, CH_2), 3.80 (s, 2H, $CH_2N(CH_3)_2$), 4.08 (q, 2H, 7.1 Hz, OCH_2CH_3), 5.68 (d, 1H, *J*=10.3 Hz, CH), 6.56 (d, 1H, *J*=7.6 Hz), 6.73-6.80 (m, 3H, arom+vinyl.), 6.98-7.06 (m, 4H, arom.). **^{13}C-NMR** (100 MHz, CD_3CN): δ= 13.7 (CH_3), 19.3 (CH_3), 19.4 (CH_3), 24.1 (CH_2), 25.5 (CH_3), 31.3 (CH_2), 41.6 ($N(CH_3)_2$), 42.5 (NCH_2), 51.5 ($C(CH_3)_2$), 53.4 ($CH_2N(CH_3)_2$), 60.0 (OCH_2CH_3), 105.6 (spiro.), 106.3, 115.1 (arom.), 119.1, 119.2, 119.7, 121.6, 127.5 129.1, 129.3, 129.5, 133.8, 136.4, 147.0 (arom.), 150.6 (CO), 172.9 (COOEt). **HRMS (*m/z* -ES) :** Found: 449.2797 ($(M+H)^+$, $C_{28}H_{36}N_2O_3$ Requires: 449.2804). **υ (cm^{-1}) :** 3423, 2963, 2461, 1727, 1606, 1456.

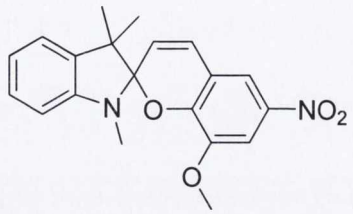
4-(8-((Dimethylamino)methyl)-3',3',6-trimethylspiro[chromene-2,2'-indoline]-1'-yl)butanoic acid (SP3)



A solution containing 512 mg (1.14 mmol) of **SP2** was stirred for 48h in a mixture 2:1 of THF and an aqueous solution of NaOH (2N). The product was extracted with chloroform and dried over Na_2SO_4. The product was purified *via* flash chromatography using a mixture of DCM/MeOH 9:1 which afforded 320 mg of a blue solid, yield 66%. **^{1}H-NMR** (400 MHz, CD_3CN): δ= 1.15, (s, 3H, CH_3), 1.25 (s, 3H, CH_3), 1.87 (m, 2H, CH_2), 2.18-2.30 (m, 11H, $N(CH_3)_2$, CH_3 arom., CH_2), 3.10 (m, 2H, CH_2), 3.65 (s, 2H, $CH_2N(CH_3)_2$), 5.68 (d, 1H, *J*=10.3 Hz, CH), 6.56 (d, 1H, *J*=7.6 Hz), 6.73-6.80 (m, 3H, arom+vinyl.), 6.98-7.06 (m, 4H, arom.). **^{13}C-NMR** (100 MHz, CD_3CN): δ = 19.3 (CH_3), 19.4 (CH_3), 24.1 (CH_2), 25.5 (CH_3), 31.3 (CH_2), 41.6 ($N(CH_3)_2$), 42.5 (NCH_2),

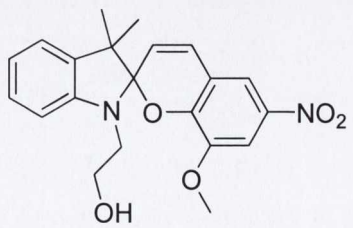
51.5 ($C(CH_3)_2$), 53.4 ($CH_2N(CH_3)_2$), 105.6 (spiro.), 106.3, 115.1 (arom.), 119.1, 119.2, 119.7, 121.6, 127.5 129.1, 129.3, 129.5, 133.8, 136.4, 147.0 (arom.), 150.6 (CO), 172.9 (COOH). **HRMS (*m/z* -ES) :** Found: 421.2501 ($(M+H)^+$, $C_{26}H_{32}N_2O_3$ Requires: 421.2491). **υ (cm^{-1}) :** 2961, 1748, 1605, 1456, 1134. **mp :** 105°C.

8-Methoxy-1',3',3'-trimethyl-6-nitrospiro[chromene-2,2'-indoline] (SP4)



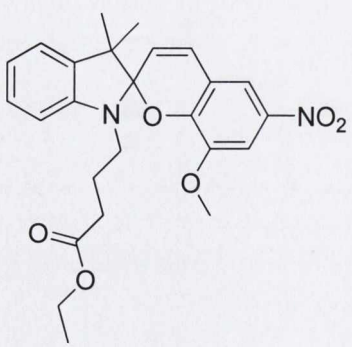
A solution containing 0.857 g (2.83 mmol) of **101** and 0.473 g (2.83 mmol) of 3-methoxy-5-nitrosalicylaldehyde in 20 ml of ethanol was stirred at reflux for 24h. The solution was then concentrated and kept in the freezer for 24h. A yellow powder was filtered off from the chilled solution and washed with cold ethanol. It was then dissolved in 30 ml of dichloromethane, washed with a 10 % aqueous solution of Na_2CO_3 , dried over $NaSO_4$. The solvent was then distilled at reduced pressure affording 540 mg of a grey solid, yield 54%. **^{1}H-NMR** (400 MHz, CD_3CN): δ= 1.16 (s, 3H, CH_3), 1.26 (s, 3H, CH_3), 2.75 (s, 3H, NCH_3), 3.79 (s, 3H, OCH_3), 5.96 (d, 1H, *J*=10.4 Hz, CH ethylene), 6.61 (d, 1H, *J*=7.7 Hz, arom.), 6.85 (d, 1H, *J*=7.6 Hz, arom), 7.03 (d, 1H, *J*=10.4 Hz, H ethylene), 7.13 (d, 1H, *J*=7.0 Hz, arom.), 7.19 (t, 1H, *J*=7.6 Hz, arom.), 8.02 (d, 1H, *J*=2.7 Hz, arom.), 8.11 (d, 1H, *J*=2.7 Hz, arom.). **HRMS (*m/z* -ES) :** Found: 353.1505 ($(M+H)^+$, $C_{20}H_{20}N_2O_4$ Requires: 353.1501). **υ (cm^{-1}) :** 2965, 1609, 1515, 1467, 1338, 1270. **mp :** 160°C.

2-(3',3'-Dimethyl-6-nitro-3'H-spiro[chromene-2,2'-indol]-1'-yl)ethanol (SP5)



A solution of **103** (1.14 g, 4 mmol) in KOH aq 5% (20 ml) was stirred at ambient temperature for 30 min. Then, it was extracted with Et_2O (3x20 ml). The organic phase was dried over Na_2SO_4, filtered, and concentrated under reduced pressure to afford a yellow oil. The oil was then dissolved in 20 ml of EtOH and 3-methoxy-2-hydroxy-5-nitrobenzaldehyde (0.87 g, 4 mmol) was added to the solution which was heated for 6 h under reflux and N_2. After cooling down to ambient temperature, the mixture was filtered. The resulting solid was dissolved in DCM , washed with a Na_2CO_3 solution in water (10%) and the organic phase was dried over Na_2SO_4. After evaporation of solvent 520 mg, 83% of product were obtained as a golden solid. **^{1}H-NMR** (400 MHz, CD_3CN): δ = 1.16 (3H, s, CH_3), 1.25 (3H, s, CH_3), 2.84 (1H, bs, OH), 3.39-3.22 (2H, m, CH_2N), 3.67-3.41 (2H, m, CH_2OH), 3.79 (3H, s, OCH_3), 6.01 (1H, d, *J*=10.4, ethylene), 6.69 (1H, d, *J*=7.8, arom.), 6.88 (1H, d, *J*=7.36, arom.), 7.01 (1H, d, *J*=10.4, ethylene), 7.14 (2H, d, *J*=7.60 Hz, arom.), 7.17 (1H, t, *J*=7.60, arom.), 7.69 (1H, d, *J*=2.56 Hz, arom.), 7.79 (1H, d, *J*=2.56 Hz, arom.); **^{13}C-NMR** (100 MHz, CD_3CN): δ= 18.5 (CH_3), 24.8 (CH_3), 45.3 ($C(CH_3)_2$), 52.1 (CH_2N), 55.5 (CH_3O), 59.3 (CH_2OH), 106.2, 106.6, 106.9 (arom.), 114.8 (spiro C), 118.3, 118.9, 121.3, 121.8, 127.3, 127.4, 135.4, 140.1, 146.6, 146.8, 148.5 (arom.). **HRMS (*m/z* -ES)**: Found: 383.1608 $(M+H)^+$, $C_{25}H_{23}N_3O_4$ Requires: 383.1607). **υ (cm^{-1}) :** 3188, 1584, 1559, 1500, 1274, 1227, 1086. **mp :** 178°C.

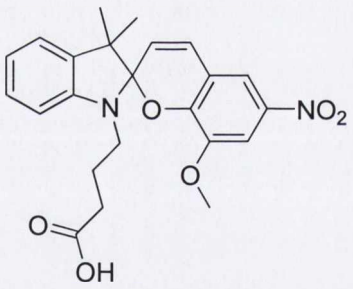
Ethyl 4-(8-methoxy-3',3'-dimethyl-6-nitrospiro[chromene-2,2'-indoline]-1'-yl)butanoate (SP6)



A solution containing 0.783 g (2.21 mmol) of **102** and 0.653 g (3.32 mmol) of 3-methoxy-5-nitrosalicylaldehyde in 20 ml of ethanol was stirred at reflux for 24h. The solution was then concentrated and kept in the freezer for 24h. A yellow powder was filtered off from the chilled solution and washed with cold ethanol. It was then

dissolved in 30 ml of dichloromethane, washed with a 10 % aqueous solution of Na_2CO_3 , dried over Na_2SO_4. The solvent was then distilled at reduced pressure affording 351 mg of a blue solid, yield 35%. **^{1}H-NMR** (400 MHz, $CDCl_3$): δ= 1.19 (s, 3H, CH_3), 1.24 (t, 3H, *J*=4.3 Hz, CH_3), 1.29, (s, 3H, CH_3), 1.90-2.00 (m, 2H, CH_2), 2.34-2.38 (m, 2H, CH_2), 3.25-3.27 (m, 2H, CH_2), 3.77 (s, 3H, OCH_3), 4.08-4.13 (m, 2H, CH_2), 5.85 (d, 1H, *J*=10.3 Hz, CH), 6.64 (d, 1H, *J*=7.8 Hz, arom.), 6.85 (d, 1H, , *J*=10.3 Hz, CH), 6.88 (m, H, arom.), 7.08 (d, 1H, *J*=7.2 Hz, arom.), 7.20-7.28 (m, 1H, arom.), 7.63-7.70 (m, 2H, arom.). **^{13}C-NMR** (100 MHz, $CDCl_3$): δ= 13.7 (CH_3), 19.5 (CH_3), 23.5 (CH_3), 25.5 (CH_2), 31.3 (CH_2), 42.5 (NCH_2), 52.2 ($C(CH_3)_2$), 55.8 (OCH_3), 59.9 (OCH_2CH_3), 106, 106.3, 107.4 (arom.), 114.9 (C spiro.), 117.7, 118.9,121.2, 121.5, 127.2, 127.7, 135.5 (arom.), 139.9 (CNO_2), 146.5 (arom.), 146.9 (COMe), 148.9 (CO), 172.7 (COOEt). **HRMS (*m/z* -ES) :** Found: 453.2036 ($(M+H)^+$, $C_{25}H_{28}N_2O_6$ Requires: 453.2026). **υ (cm^{-1}) :** 2932, 1733, 1519, 1479, 1333, 1270. **mp :** 123°C.

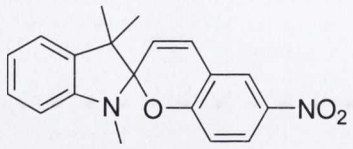
4-(8-Methoxy-3',3'-dimethyl-6-nitrospiro[chromene-2,2'-indoline]-1'-yl)butanoic acid (SP7)



A solution containing 180 mg (0.398 mmol) of **SP6** was stirred in a solution 2:1 of THF and aqueous NaOH 10% for 48h. The reaction was quenched with 40 ml of an acqueous solution of citric acid 10%, the product was then extracted with chloroform and dried over $MgSO_4$. The solvent was evaporated to afford 150 mg of a blue powder, yield 88.8%. **^{1}H-NMR** (400 MHz, $CDCl_3$): δ= 1.19 (s, 3H, CH_3), 1.29, (s, 3H, CH_3), 1.72-1.78 (m, 2H, CH_2), 2.24-2.26 (m, 2H, CH_2), 3.09-3.16 (m, 2H, CH_2), 3.77 (s, 3H, OCH_3), 5.76 (d, 1H, *J*=10.3 Hz, CH), 6.53 (d, 1H, *J*=7.8 Hz, arom.), 6.73 (d, 1H, *J*=10.3 Hz, CH), 6.82 (m, 1H, arom.), 6.98-7.10 (m, 2H, arom.), 7.52-7.63 (m, 2H, arom.), 9.95 (s, 1H, COOH). **^{13}C-NMR** (100 MHz, $CDCl_3$): δ= 18.7 (CH_3), 23.5 (CH_2), 25.3 (CH_3), 31.3 (CH_2), 42.5 (NCH_2), 52.2 ($C(CH_3)_2$), 55.9 (OCH_3), 106.0, 106.3, 107.2 (arom.),

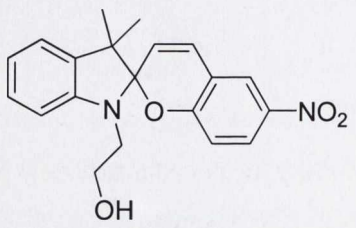
115.2 (C spiro.), 117.7, 118.5, 121.1, 121.5, 127.2, 127.7, 135.5 (arom.), 130.0 (CNO_2), 147.1 (arom.), 147.1 (COMe), 148.9 (CO), 172.7 (COOH). **HRMS (*m/z* -ES) :** Found: 425.1713 ($(M+H)^+$, $C_{23}H_{24}N_2O_6$ Requires: 425.1713). **υ (cm^{-1}) :** 2962, 1707, 1583, 1513, 1232, 1166, 1088. **mp :** 178°C

1',3',3'-Trimethyl-6-nitrospiro[chromene-2,2'-indoline] (SP8)



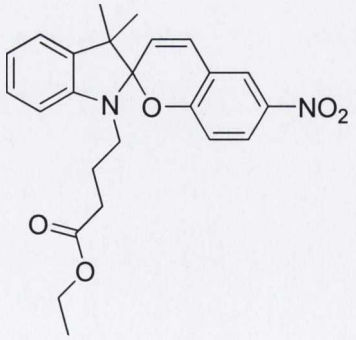
A solution containing 0.3 g (1 mmol) of **101** and 0.167 g (1 mmol) of 5-nitrosalicylaldehyde in 20 ml of ethanol was stirred at reflux for 24h. The solution was then concentrated and kept in the freezer for 24h. A yellow powder was filtered off from the chilled solution and washed with cold ethanol. It was then dissolved in 30 ml of dichloromethane, washed with a 10 % aqueous solution of Na_2CO_3 , dried over Na_2SO_4. The solvent was then distilled at reduced pressure affording 200 mg of a grey solid, yield 62%. **^{1}H-NMR** (400 MHz, CD_3CN): δ= 1.22 (s, 3H, CH_3), 1.32 (s, 3H, CH_3), 2.77 (s, 3H, NCH_3), 5.90 (d, 1H, *J*=10.4 Hz, CH ethylene), 6.60 (d, 1H, *J*=7.7 Hz, arom.), 6.79 (d, 1H, *J*=8.4 Hz, arom), 6.90 (d, 1H, *J*=7.3 Hz, arom), 6.97 (d, 1H, *J*=10.4 Hz, H ethylene), 7.13 (d, 1H, *J*=7.2 Hz, arom.), 7.19 (t, 1H, *J*=7.7 Hz, arom.), 8.03 (s, 1H, arom.), 8.11 (d, 1H, *J*=2.8 Hz, arom.). **^{13}C-NMR** (100 MHz, CD_3CN): δ= 19.9 (CH_3), 25.9 (NCH_3), 28.8 (CH_3), 52.2 ($C(CH_3)_2$), 106.3 (C spiro.), 107.1, 115.5, 118.7, 119.7, 121.5, 121.6, 122.6, 125.8, 127.8,128.3 (arom.), 136.1 (arom.), 140.9 (CNO_2), 147.7, 159.8 (arom.). **HRMS (*m/z* -ES) :** Found: 323.1395 ($(M+H)^+$, $C_{19}H_{18}N_2O_3$ Requires: 323.1396). **υ (cm^{-1}) :** 1609, 1487, 1330, 1269. **mp :** 179°C.

2-(3',3'-Dimethyl-6-nitrospiro[chromene-2,2'-indoline]-1'-yl)ethanol (SP9)



A solution of **103** (0.5 g, 1.8 mmol) in KOH (aq 5%) (20 ml) was stirred at ambient temperature for 30 min. Then, it was extracted with Et_2O (3x20 ml). The organic phase was dried over Na_2SO_4, filtered, and concentrated under reduced pressure to afford a yellow oil. The oil was then dissolved in 20 ml of EtOH and 2-hydroxy-5-nitrobenzaldehyde (0.35 g, 2.1 mmol) was added to the solution which was heated for 6 h under reflux and N_2. After cooling down to ambient temperature, the mixture was filtered. The resulting solid was dissolved in DCM , washed with a Na_2CO_3 solution in water (10%) and the organic phase was dried over Na_2SO_4. After evaporation of solvent 520 mg, 83% of product were obtained as a purple solid. **^{1}H-NMR** (400 MHz, CD_3CN): δ = 1.19 (3H, s, CH_3), 1.28 (3H, s, CH_3), 3.86 (1H, t, *J*=6.0, OH), 3.39-3.23 (2H, m, CH_2N), 3.69-3.58 (2H, m, CH_2OH), 6.03 (1H, d, *J*=10.4, ethylene), 6.71 (1H, d, *J*=8.0, arom.), 6.76 (1H, d, *J*=9.2, arom.), 6.88 (1H, t, *J*=7.6, arom.), 7.07 (1H, d, *J*=10.4, ethylene), 7.15 (2H, d, *J*=7.2, arom.), 7.19 (1H, t, *J*=7.6, arom.), 8.04 (1H, dd, J_1=9.2 Hz, J_2=2.8 Hz, arom.), 8.11 (1H, d, *J*=2.4 Hz, arom.); **^{13}C-NMR** (100 MHz, CD_3CN): δ= 19.10 (CH_3), 25.17 (CH_3), 45.93 ($C(CH_3)_2$), 52.52 (CH_2N), 59.90 (CH_2OH), 106.80, 107.06, 115.27, 119.39, 121.73, 122.28, 122.73, 125.59, 127.69, 127.82, 133.94, 135.99, 147.37, 159.46 (arom.). **HRMS (*m/z* -ES)**: Found: 353.1512 $(M+H)^+$, $C_{20}H_{21}N_2O_4$ Requires: 353.1501). **υ (cm^{-1}) :** 3363, 1608, 1577, 1508, 1478, 1331, 1270, 948, 745. **mp :** 170°C.

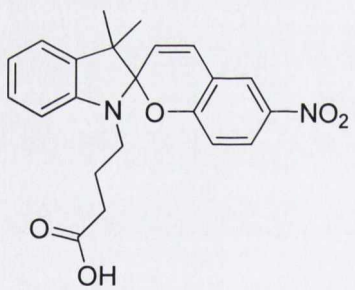
Ethyl 4-(3',3'-dimethyl-6-nitrospiro[chromene-2,2'-indoline]-1'-yl)butanoate (SP10)



A solution containing 0.6 g (1.69 mmol) of the indolium bromide salt **102** and 0.34 g (2.03 mmol) of 5-nitrosalicylaldehyde were added in 20 ml of absolute ethanol and refluxed for 24h. The solution was then cooled to r.t. and the dark purple mixture was further cooled in an ice bath and filtered. The filter cake was washed with cold ethanol

yielding an orange solid which was dissolved in dichloromethane and washed with an aqueous solution of Na_2CO_3. The organic layer was dried over Na_2SO_4 and the solvent was distilled at reduced pressure. Recrystallization from ethanol afforded 170 mg of a pale yellow powder, yield 23%. **^{1}H-NMR** (400 MHz, $CDCl_3$): δ = 1.21 (s, 3H, CH_3), 1.25, (t, 3H, *J*=7.3 Hz, CH_3), 1.31 (s, 3H, CH_3), 1.90-2.02 (m, 2H, CH_2), 2.35-2.40 (m, 2H, CH_2), 3.21-3.26 (m, 2H, CH_2), 4.11-4.14 (m, 2H, CH_2), 5.89 (d, 1H, *J*=10.5 Hz, CH), 6.67 (d, 1H, *J*=7.8 Hz, arom.), 6.76 (d, 1H, *J*=8.7 Hz, arom.), 6.92 (d, 1H, *J*=10.5 Hz, CH), 6.93 (m, 1H, arom.) 7.12 (d, 1H, *J*=6.8 Hz, arom.), 7.20-7.25 (m, 1H, arom.), 8.01-8.05 (m, 2H, arom.). **^{13}C-NMR** (100 MHz, $CDCl_3$): δ=14.2 (CH_3), 19.9 (CH_3), 24.1 (CH_3), 25.9 (CH_2), 31.7 (CH_2), 43.1 (NCH_2), 52.6 ($C(CH_3)_2$), 60.5 (OCH_2CH_3), 106.7, 106.8 (arom.), 115.6 (C spiro.), 118.4, 119.6, 121.7, 121.8, 122.7, 125.9, 127.8, 128.2, 135.9 (arom.), 140.9 (CNO_2), 147.0 (arom.), 159.5 (CO), 173.1 (COOEt). **HRMS (*m/z* -ES) :** Found: 423.1919 ($(M+H)^+$, $C_{24}H_{26}N_2O_5$ Requires: 422.1920). **υ (cm^{-1}) :** 2962, 1732, 1510, 1479, 1332,1274, 1089, 952. **mp :** 116°C.

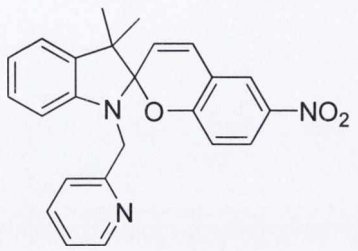
4-(3',3'-Dimethyl-6-nitrospiro[chromene-2,2'-indoline]-1'-yl)butanoic acid (SP11)



A solution containing 151.1 mg (3.58 mmol) of **SP10** were stirred in a solution 2:1 of THF and aqueous NaOH 10% for 48h. The reaction was quenched with 40 ml of an aqueous solution of citric acid 10%, the product was then extracted with chloroform and dried over $MgSO_4$. The solvent was finally evaporated affording 129.4 mg of a wine red solid, yield 91%. **^{1}H-NMR** (400 MHz, CD_3CN): δ = 1.21 (s, 3H, CH_3), 1.30 (s, 3H, CH_3), 1.93-2.02 (m, 2H, CH_2), 2.41-2.45 (m, 2H, CH_2), 3.21-3.26 (m, 2H, CH_2), 5.88 (d, 1H, *J*=10.4 Hz, CH), 6.67 (d, 1H, *J*=7.8 Hz, arom.), 6.76 (d, 1H, *J*=8.7 Hz), 6.90 (d, 2H, *J*=10.4 Hz, CH), 6.93 (m, 1H, arom.), 7.10-7.22 (m, 2H, arom.), 7.99-8.01 (m, 2H, arom.), 10.02 (s, 1H, COOH). **^{13}C-NMR** (100 MHz, CD_3CN): δ=19.0 (CH_3), 25.9 (CH_2), 25.3 (CH_3), 30.5 (CH_2), 42.6 (NCH_2), 52.6 ($C(CH_3)_2$), 106.7, 106.8 (arom.), 115.2 (C spiro.), 118.5, 119.4, 121.7, 121.8, 122.7, 125.6, 127.7, 128.1, 136.1 (arom.),

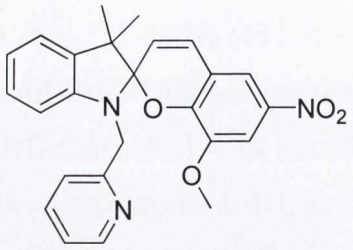
140.9 (CNO_2), 147.0 (arom.), 159.5 (CO), 196.1 (COOH). **HRMS (*m/z* -ES) :** Found: 395.1607 ($(M+H)^+$, $C_{22}H_{22}N_2O_5$ Requires: 395.1607). **υ (cm^{-1}) :** 2965, 1731, 1661, 1578, 1477, 1333, 1274. **mp :** 99°C.

4.2.2.3',3'-Dimethyl-6-nitro-1'-(pyridin-2-ylmethyl)spiro [chromene-2,2'-indoline] (SP12)



A solution containing 2-(Bromomethyl)pyridine hydrobromide (1.15 g, 6.8 mmol) and 2,3,3-trimethylindolinine (0.723 ml, 6.8 mmol) was stirred at 120°C in 1,2-dichlorobenzene for 24 h. The slurry was filtered off and washed with diethyl ether to afford a brown solid. This was dissolved in dichloromethane and 10 ml of 1M NaOH solution were added. After the mixture was stirred for 24 h, the organic layer was collected, dried over Na_2SO_4 and the solvent was evaporated. The resulting solid was dissolved in ethanol and 4-nitrosalicylaldehyde (0.74 g, 4.4 mmol) was added to the solution which was stirred for 24 h. The solvent was evaporated and the crude was purified *via* chromatography using a mixture of hexane/ethyl acetate 8:2 as eluent. The purification afforded 109 mg of a pink powder, yield 6%. **^{1}H-NMR** (400 MHz, $CDCl_3$): δ= 1.34 (s, 3H, CH_3), 1.38 (s, 3H, CH_3), 4. 46 (d, 1H, *J*=17.0 Hz, CH_2 Pyr.), 4. 68 (d, 1H, *J*=17.0 Hz, CH_2 Pyr.), 5.98 (d, 1H, *J*=10.3 Hz, ethylene), 6.37 (d, 1H, *J*=7.7 Hz, arom.), 6.81 (d, 1H, *J*=8.9 Hz, arom.), 6.91 (d, 1H, *J*=10.3 Hz, ethylene), 6.94 (t, 1H, *J*=7.6 Hz, arom.), 7.13 (t, 1H, *J*=7.7 Hz, Pyr.), 7.18 (d, 1H, *J*=7.2 Hz, arom.), 7.26 (m, 1H, arom.), 7.42 (d, 1H, *J*=7.6 Hz, Pyr.), 7.59 (t, 1H, *J*=7.1 Hz Pyr), 8.01 (d, 1H, *J*=2.7 Hz, arom.), 8.06 (dd, 1H, *J*=8.9 Hz, arom.), 8.59 (d, 1H, *J*=4.6 Hz, CHN Pyr.). **^{13}C-NMR** (100 MHz, $CDCl_3$): δ= 20.0 (CH_3), 26.2 (CH_3), 49.0 (NCH_2), 52.7 ($C(CH_3)_2$), 106.4, 107.7, 115.6, 118.4, 120.4, 121.1, 121.5, 121.9, 122.5, 122.8, 126.0, 127.8, 128.9, 136.0, 138.1, 141.1, 146.5, 148.2, 158.1, 159.2 (arom.). **HRMS (*m/z* -ES)**: Found: 400.1675 ($(M+H)^+$, $C_{24}H_{21}N_3O_3$ Requires: 400.1661). **υ (cm^{-1}) :** 2964, 1649, 1609, 1514, 1478, 1334, 1270, 1088, 946. **mp :** 136°C.

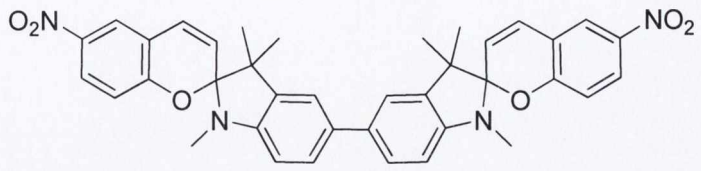
8-Methoxy-3',3'-dimethyl-6-nitro-1'-(pyridin-2-ylmethyl)spiro[chromene-2,2'-indoline] (SP13)



2-(Bromomethyl)pyridine hydrobromide (3.9 mmol, 1 g) was dissolved in water (4 ml) and cooled in an ice-bath. A solution of K_2CO_3 (1M) was added dropwise to the solution under vigorous stirring until the solution pH was adjusted to 7. The mixture was stirred for 1h at room temperature and then was extracted with ethyl acetate (20 ml) and dried over Na_2SO_4. After evaporation of the solvent, the red solid obtained (0.46 g) was reacted with 2,3,3-trimethylindolinine (2.1 mmol) in CH_3CN (15 ml) at 70°C for 24h. The solution was cooled to room temperature, the solvent was evaporated under reduced pressure and the viscous residue obtained was stirred in 20 ml of NaOH aq 0.1M for 2h at r.t. The mixture was then extracted with ethyl acetate (20x2 ml) dried over Na_2SO_4 and the solvent was removed under reduced pressure. The brown oil obtained (1 equivalent) was reacted with 3-methoxy-5-nitrosalicylaldehyde (1 equivalent, 1.73 mmol) in 20 ml of ethanol at reflux for 15h. The solvent was distilled under reduced pressure and the product was purified *via* flash chromatography using a mixture of hexane/ethyl acetate 8:2 as eluent. The reaction afforded 400 mg of a green powder with an overall yield of 40%. **^{1}H-NMR** (400 MHz, CD_3CN): δ= 1.27 (s, 3H, CH_3), 1.32 (s, 3H, CH_3), 3.79 (s, 3H, OCH_3), 4. 34 (d, 1H, *J*=17.0 Hz, CH_2 Pyr.), 4. 64 (d, 1H, *J*=17.0 Hz, CH_2 Pyr.), 6.04 (d, 1H, *J*=10.4 Hz, ethylene), 6.40 (d, 1H, *J*=7.8 Hz, arom.), 6.87 (t, 1H, *J*=7.3 Hz, arom.), 7.01 (d, 1H, *J*=10.4 Hz, ethylene), 7.09 (t, 1H, *J*=7.6 Hz, arom.), 7.19 (t, 1H, *J*=6.8 Hz, Pyr.), 7.21 (d, 1H, *J*=7.6 Hz, arom.), 7.33 (d, 1H, *J*=8.0 Hz, Pyr.), 7.66 (t, 1H, *J1*=8.0 Hz, Pyr), 7.75 (d, 1H, *J*=2.4 Hz, arom.), 7.77 (d, 1H, *J*=2.4 Hz, arom.), 8.48 (d, 1H, *J*=4.8 Hz, CHN Pyr.). **^{13}C-NMR** (100 MHz, CD_3CN): δ= 18.9 (CH_3), 25.6 (CH_3), 49.0 (CH_2N), 52.5 ($C(CH_3)_2$), 55.9 (OCH_3), 106.6, 107.3, 107.4, 115.3, 118.7, 119.8, 121.2, 121.3, 121.9, 122.1, 127.7, 128.7, 136.1, 136.6, 140.6, 146.8, 147.1, 148.7, 149.2, 158.6 (arom.). **HRMS (*m/z* -ES)**: Found: 430.1774

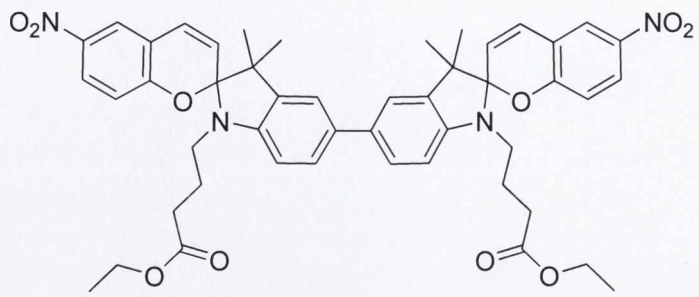
($(M+H)^+$, $C_{25}H_{23}N_3O_4$ Requires: 430.1767). **υ (cm^{-1}) :** 1592, 1515, 1477, 1331, 1272, 1088, 910. **mp :** 124°C.

1,1',3,3,3',3'-hexamethyl-5,5'-bi[6,6'-nitrospiro[chromene-2,2'-indoline]] (2SP8)



Compound **SP8** (100 mg, 0.31 mmol) was dissolved in 10 ml of acetonitrile and $Cu(ClO_4)_2$ $6H_2O$ (117 mg, 0.31 mmol) was dissolved in 200 µl of distilled water. The aqueous solution containing copper (II) was added to the organic solution containing compound **SP8** which was stirred for 24 h at room temperature. The solvent was evaporated under reduced pressure and the crude was dissolved in 10 ml of DCM and filtered. The filtrate was washed with a saturated solution of $NaHCO_3$ (3 x 5 ml) containing the 5% of EDTA. The organic phase was then dried over Na_2SO_4 and the solvent was distilled under reduced pressure affording a brown solid which was purified *via* flash chromatography on silica gel using a mixture of hexane/ethyl acetate 9:1 as eluent (*Rf* = 0.5). The procedure afforded 45 mg of a yellow solid, yield 43%. **^{1}H-NMR** (400 MHz, CD_3CN): δ = 1.25 (s, 6H, CH_3), 1.36 (s, 6H, CH_3), 2.79 (s, 6H, NCH_3), 6.02 (d, 2H, *J*=10.4 Hz, CH ethylene), 6.68 (d, 2H, *J*=8.0 Hz, arom.), 6.82 (d, 2H, *J*=9.2 Hz, arom.), 7.14 (d, 2H, *J*=10.4 Hz, H ethylene), 7.42 (d, 2H, *J*=2.0 Hz), 7.45 (dd, 2H, *J1*=8.0 Hz, *J2*=2.0 Hz, arom.), 8.05 (dd, 2H, *J1*=9.2 Hz, *J2*=2.8 Hz, arom.), 8.13 (d, 2H, *J*=2.8 Hz, arom.). **^{13}C-NMR** (100 MHz, CD_3CN): δ = 19.1 (CH_3), 25.2 (CH_3), 28.2 (NCH_3), 52.2 ($C(CH_3)_2$), 106.8 (C spiro.), 107.3, 115.2, 119.1, 120.2, 121.5 (arom.), 122.7 (vinylic), 125.6, 125.9 (arom.), 128.2 (vinylic), 133.5, 137.1, 141.1, 146.8, 159.7 (arom.). **HRMS (*m/z* -ES) :** Found: 643.2561 ($(M+H)^+$, $C_{19}H_{18}N_2O_3$ Requires: 643.2557). **υ (cm^{-1}) :** 2961, 1613, 1515, 1477, 1332, 1267,1086, 947. **mp :**163°C.

5,5'-bi[ethyl 4,4'-(3',3'-dimethyl-6-nitrospiro[chromene-2,2'-indoline]-1'-yl)butanoate] (2SP10)



Compound **SP10** (100 mg, 0.24 mmol) was dissolved in 10 ml of acetonitrile and $Cu(ClO_4)_2$ $6H_2O$ (87 mg, 0.24 mmol) was dissolved in 200 µl of distilled water. The aqueous solution containing copper (II) was added to the organic solution containing compound **SP10** which was stirred for 24 h at room temperature. The solvent was evaporated under reduced pressure and the crude was dissolved in 10 ml of DCM and filtered. The filtrate was washed with a saturated solution of $NaHCO_3$ (3 x 5 ml) containing the 5% of EDTA. The organic phase was then dried over Na_2SO_4 and the solvent was distilled under reduced pressure affording a brown solid which was purified *via* flash chromatography on silica gel using a mixture of hexane/ethyl acetate 7:3 as eluent (*Rf* = 0.38). The procedure afforded 48 mg of a green solid, yield 46%. **^{1}H-NMR** (400 MHz, CD_3CN): δ = 1.25 (s, 6H, CH_3), 1.36 (s, 6H, CH_3), 2.79 (s, 6H, NCH_3), 6.02 (d, 2H, *J*=10.4 Hz, CH ethylene), 6.68 (d, 2H, *J*=8.0 Hz, arom.), 6.82 (d, 2H, *J*=9.2 Hz, arom.), 7.14 (d, 2H, *J*=10.4 Hz, H ethylene), 7.42 (d, 2H, *J*=2.0 Hz), 7.45 (dd, 2H, *J1*=8.0 Hz, *J2*=2.0 Hz, arom.), 8.05 (dd, 2H, *J1*=9.2 Hz, *J2*=2.8 Hz, arom.), 8.13 (d, 2H, *J*=2.8 Hz, arom.). **^{13}C-NMR** (100 MHz, CD_3CN): δ = 13.1 (CH_3CH_2O), 18.6 (CH_3), 23.4 (CH_2), 24.8 (CH_3), 30.6 (CH_2COO), 42.2 (CH_2N), 52.1 ($C(CH_3)_2$), 59.6 (CH_3CH_2O), 106.6, 106.7, 118.5, 119.9 (arom.), 121.3 (vinylic), 122.3, 125.1, 125.4, 125.5 (arom.), 127.7 (vinylic), 132.8, 136.4, 140.6, 145.6, 158.9 arom.), 172.5 (COO). **HRMS (*m/z* -ES) :** Found: 643.2561 ($(M+H)^+$, $C_{19}H_{18}N_2O_3$ Requires: 643.2557). **υ (cm^{-1}) :** 2965, 1728, 1612, 1516, 1476, 1332, 1266, 1086, 949. **mp :**198°C.